INVESTIGATING THE FUNCTION OF MAKORIN 1 IN *DROSOPHILA* OOGENESIS

Dissertation

zur Erlangung des Grades

Doktor der Naturwissenschaften

Am Fachbereich Biologie

Der Johannes Gutenberg-Universität Mainz

Vorgelegt von

Annabelle Cynthia Elisabeth Dold

Geboren am 30.11.1989 in Tuttlingen, Deutschland

Mainz, November 2019

Dekan:

Berichterstatter 1:

Berichterstatter 2:

Tag der mündlichen Prüfung:

Hiermit versichere ich gemäß § 12, (2) der Promotionsordnung vom 01.04.2018:

Für die Anfertigung der vorgelegten Arbeit wurde keine entgeltliche Hilfe Dritter, insbesondere eine Promotionsberatung oder -vermittlung in Anspruch genommen.

Mainz, den _____ _____

(Unterschrift)

PREFACE

Publications that are partially based on the work presented here are:

Dold A, Han H, Liu N et al. 2019. Makorin 1 controls embryonic patterning by alleviating Bruno1-mediated repression of *oskar* translation.
bioRxiv, DOI: 10.1101/501643

Hildebrandt A, Brüggemann M, Rücklé C, Boerner S, Heidelberger JB, Busch A, Hänel H, Voigt A, Möckel MM, Ebersberger S, Scholz A, **Dold A**, Schmid T, Ebersberger I, Roignant JY, Zarnack K, König J and Beli, P. 2019. The RNA-binding ubiquitin ligase MKRN1 functions in ribosome-associated quality control of poly(A) translation. *Genome Biol* 20:216.

The study I present here was supervised by Prof. Jean-Yves Roignant (CIG Lausanne, Switzerland). Furthermore, I was supported by a collaboration among different research groups. These include the groups of Prof. Paul Lasko (McGill University, Montreal, Canada), Dr. Julian König (IMB Mainz, Germany), Dr. Petra Beli (IMB Mainz, Germany), Dr. Kathi Zarnack (BMLS Frankfurt, Germany) and Prof. René Ketting (IMB Mainz, Germany). Moreover, the IMB core facilities supported my work by allowing me to use their instruments (Genomics, Microscopy and Flow Cytometry), produced reagents for me (Media Lab and Protein Production) and analyzed my data (Bioinformatics).

The experiments described here were designed, conducted and analyzed by me with the following exceptions: Hong Han and Niankun Liu (McGill University) constructed the $Mkrn1^{W}$ and $Mkrn1^{S}$ alleles as well as the *UAS-FLAG-Mkrn1* transgene. Production of these fly strains was supervised by Paul Lasko (McGill University). Andrea Hildebrandt (IMB) performed the mass spectrometry experiments and prepared the iCLIP libraries described in this study. The mass spectrometry experiments were supervised by Petra Beli (IMB) while the iCLIP experiments were supervised by Julian König (IMB).
Anke Busch (IMB) analyzed the Mkrn1 interactome and iCLIP data. Nastasja Kreim (IMB) analyzed the RNA-seq data. Mirko Brüggemann (BMLS) further analyzed the iCLIP data for a global overview on targets and binding sites. Cornelia Rücklé (BMLS) identified the PAM2 and PAM2L motif in *Drosophila* Makorin proteins. The bioinformatic analysis of the iCLIP binding sites and PAM2 motifs was supervised by Kathi Zarnack (BMLS).

Everyone mentioned above also supported me with valuable feedback and discussions.

TABLE OF CONTENTS

ABBREVIATIONS

5’TOP	5’ terminal oligopyrimidine
A	Alanine
A site	Amino acid site
ABCE1	ATP-binding cassette sub-family E member 1
AMPK	AMP-activated protein kinase
AR	Adenosine-rich
Arg	Arginine
bcd	Bicoid
Bic-D	Bicaudal D
bp	Base pairs
BRE	Bruno response elements
Bru1	Bruno
BSF	Bicoid stability factor
C3H	Cyc_3His
CAA	2-chloracetamide
Cas	CRISPR-associated
cDNA	Reversely transcribed RNA
CPE	Cytoplasmic polyadenylation element
ctrl	Control
CRISPR	Clustered regularly interspaced short palindromic repeats
CycA	Cyclin A
Cys	Cysteine
D	Aspartic acid
DAPI	4′,6-diamidino-2-phenylindole
Dcp1	Decapping protein 1
Dcp1, cleaved	Death caspase-1
DNA	Deoxyribonucleic acid
dsRNA	Double stranded RNA
DTT	Dithiothreitol
E	Glutamic acid
E site	Exit site
E1	Ubiquitin-activating enzyme
E2	Ubiquitin-conjugating enzyme
E3	Ubiquitin-ligating enzyme

EDEN	Embryonic deadenylation element
eEF	Eukaryotic translation elongation factor
Egfr	Epidermal growth factor receptor
Egl	Egalitarian
eIF	Eukaryotic translation initiation factor
eRF	Eukaryotic translation release factor
Enc	Encore
ESC	Embryonic stem cell
F	Phenylalanine
FLAG	DYKDDDDK-peptide
FISH	Fluorescent ISH
FMRP	Fragile X Mental Retardation Protein
G	Glycine
gDNA	Genomic DNA
GDP	Guanosine-diphosphate
GFP	Green fluorescent protein
Glu	Glutamic acid
Grk	Gurken
gRNA	Guide RNA
GSK-3β	Glycogen synthase kinase-3β
GTP	Guanosine-triphosphate
h	Hour
HECT	Homologous to E6-AP carboxy terminus
HELZ	Helicase with zinc finger
His	Histidine
hnRNP	Heterogeneous Nuclear Ribonucleoprotein
Hrb27C	Heterogeneous nuclear ribonucleoprotein at 27C
hrg	Hiiragi
HRP	Horse radish peroxidase
hTERT	Human telomerase reverse transcriptase
I	Isoleucine
IBE	IMP-binding element
iCLIP	Individual-nucleotide resolution UV crosslinking and IP
IGF2BP	Insulin-like growth factor 2 mRNA-binding protein

Imp	IGF-II mRNA-binding protein
IP	Immunoprecipitation
K	Lysine
LC-MS/MS	Liquid chromatography-tandem mass spectrometry
LRRK2	Leucine-rich repeat kinase 2
Lys	Lysine
m^6A	N^6-methyladenosine
MAPK	Mitogen-activated protein kinase
Me31B	Maternal expression at 31B
Met	Methionine
min	Minute
Mkrn	Makorin RING Finger Protein
MLLE	Mademoiselle
Mnk1	MAP kinase-interacting protein kinase 1
mRNA	Messenger RNA
mRNP	Messenger ribonucleoprotein
MTOC	Microtubule organizing center
Myc	Myelocytoma
N	Asparagine
n.s.	Not significant
NF-κB	Nuclear factor kappa-light-chain-enhancer of activated B cells
nos	Nanos
nt	Nucleotide
O/N	Over night
Orb	oo18 RNA-binding protein
Osk	Oskar
P	Proline
P bodies	Processing bodies
P site	Polypeptide site
PABP	poly(A) binding protein
PAGE	Polyacrylamide gel electrophoresis
PAM2	PABP-interacting motif 2
PBS	Phosphate-buffered saline
PCR	Polymerase chain reaction

pgc	Polar granule component
PIC	Preinitiation complex
polyA	Poly adenosine
PTM	Post-translational modification
PTP	Polypyrimidine tract binding protein
Pum	Pumilio
Q	Glutamine
qPCR	Quantitative PCR
R	Arginine
Rack1	Receptor of activated protein kinase C 1
RBP	RNA-binding protein
RBR	RING-between-RING
RFP	Red fluorescent protein
RING	Really interesting new gene
RNA	Ribonucleic acid
rpm	Rotations per minute
RT	Room temperature (~22-23°C)
RT-qPCR	Reverse transcriptase with subsequent qPCR
S	Serine
sec	Second
Seq	Sequencing
SILAC	Stable isotope labeling by amino acids in cell culture
SOLE	Spliced oskar localization element
Sqd	Squid
SR	Stalling reporter
Stau	Staufen
TGFα	Transforming growth factor alpha
Tm1	Tropomyosin
TRAF	Tumor necrosis factor receptor-associated factor
TRITC	Tetramethylrhodamine
tRNA	Transfer RNA
UAS	Upstream activation sequence
Ub	Ubiquitin
UPF	UP-Frameshift

UTR	Untranslated region
V	Valine
Val	Valine
W	Tryptophan
WB	Western blot
Wisp	Wispy
YBX1	Y-box-binding protein 1
Yps	Ypsilon schachtel
ZnF	Zinc finger

SUMMARY

Axis formation of the *Drosophila* embryo is determined by the localized expression of specific mRNAs and proteins. This asymmetric distribution is already established during oogenesis in the mother. Oskar (Osk), which induces the formation of the posterior axis is among the first determinants to localize to the posterior pole of the egg-to-be, the oocyte. Translation of *osk* mRNA is repressed during its transport by several factors, including the RNA-binding protein Bruno1 (Bru1). When reaching the posterior pole, the translational repression is relieved by a yet unknown signal.

In this study, we identified the highly conserved E3 ligase Makorin 1 (Mkrn1) as a novel activator of *osk* translation. Apart from its RING E3 ligase domain, Mkrn1 possesses C3H-type zinc finger (ZnF) domains that have been proposed to mediate the binding to RNA. Indeed, we show that Mkrn1 localizes to the posterior pole where it specifically interacts with osk 3' UTR via its first ZnF domain. The binding is enhanced by the polyA binding protein (pAbp) that interacts with Mkrn1 via a non-consensus PAM2 motif. Furthermore, Mkrn1 interacts with several other RNA-binding proteins that regulate *osk* expression during oogenesis.

Mechanistically, we found that Mkrn1 activates osk translation by competing with Bru1 for binding to *osk* 3' UTR. Thus, we characterized *Drosophila* Mkrn1 as a novel and essential regulator of oogenesis. The fact that Mkrn1 shares several features with its mammalian ortholog, such as the identity of interaction partners and the dependency of pAbp for binding to RNA, suggests that the function of Mkrn1 during oogenesis might be conserved.

ZUSAMMENFASSUNG

In *Drosophila* bilden sich die embryonalen Körperachsen durch die lokale Expression bestimmter mRNAs und Proteine. Die asymmetrische Verteilung dieser Faktoren etabliert sich bereits in der Mutter während der Oogenese. Oskar (Osk) ist eines der ersten Proteine, das sich am posterioren Abschnitt der Eizelle – oder Oozyte – anlagert. Diese Positionierung ist von großer Bedeutung, da Osk die posteriore Orientierung in der Oozyte einleitet. Um die präzise Verteilung von Osk zu gewährleisten, wird die Translation während des Transports der mRNA gehemmt. Bruno (Bru1) spielt dabei eine entscheidende Rolle: das Protein bindet *osk* mRNA und unterdrückt dabei die Translation. Am posterioren Teil der Oozyte wird diese Hemmung allerdings aufgehoben, um die Translation zu ermöglichen. Wie es zu diesem Wechsel kommt, ist jedoch nicht bekannt.

In der folgenden Arbeit wurde die E3 Ligase Makorin 1 (Mkrn1) als neuer Faktor, der *osk* mRNA reguliert, charakterisiert. Mkrn1 ist evolutionär stark konserviert und regt die Translation von *osk* am posterioren Ende der Oozyte an. Neben einer RING Domäne besitzt Mkrn1 zwei Zink Finger (ZnF) Domänen. Es wurde postuliert, dass die ZnF Domänen in Mkrn1 benötigt werden, um RNA zu binden. Mit meiner Studie wurde diese Theorie bestätigt: *Drosophila* Mkrn1 bindet *osk* mRNA über die ZnF1 Domäne. Die spezifische Interaktion mit dem 3’ UTR von *osk* wird über die Bindung mit dem polyA Bindeprotein (pAbp) gestärkt. Mkrn1 interagiert mit pAbp über ein nicht konserviertes PAM2 Motiv. Neben pAbp bindet Mkrn1 weitere RNA-Bindeproteine, die die Expression von *osk* während der Oogenese regulieren.

Zusammenfassend aktiviert Mkrn1 die Translation von *osk*, indem es mit Bru1 um dieselbe Bindestelle an der mRNA konkurriert. Damit charakterisiert diese Arbeit Mkrn1 als neuen und essentiellen Regulator der Oogenese. Interessanterweise bestehen viele Gemeinsamkeiten zwischen Mkrn1 in *Drosophila* und Säugetieren. Beispielsweise interagieren beide orthologen Proteine mit den gleichen Proteinen und binden RNA mit der gleichen Abhängigkeit zu pAbp. Diese Erkenntnisse deuten darauf hin, dass Mkrn1 in Säugetieren eine ähnliche Funktion während der Oogenese besitzen könnte.

INTRODUCTION

1.1. Translation

Since the 1950s, the idea of proteins being produced from messenger RNAs (mRNAs) has fascinated many researchers. Today, the genetic code through which RNA can be read and converted into proteins is deciphered [1]. In addition, translation, the process of protein production is well-understood. Translation is usually divided into different phases: initiation, elongation, termination and recycling.

During translation initiation, the ribosome assembles and positions itself at the start codon of the bound mRNA [2, 3]. Since the ribosome is a highly structured multi-subunit complex, its assembly is a tightly regulated process. Initially, an intermediate complex builds up, the so-called 43S preinitiation complex (PIC). The PIC is composed of the 40S small subunit and the translation initiation factors eIF3, eIF1 and eIF1A, which are associated with the 5’ cap of the target mRNA. Binding of these factors prevents premature assembly with the 60S subunit. Therefore, eIF3, eIF1 and eIF1A are also recruited during translation termination and stay associated with the ribosome to enhance the efficiency of recycling [3].

Association of the 43S PIC with the 5’ end of the mRNA is mediated by the eIF4F complex (Fig. 1A). The eIF4F complex itself consists of the cap-binding protein eIF4E, the RNA helicase eIF4A and the scaffolding protein eIF4G [3, 4]. The interaction among the complex subunits is extremely stable and supports the individual functions. For example, the interaction between eIF4E and the 5’ cap is stabilized by eIF4G [5, 6]. The eIF4E protein in turn recruits the small ribosomal subunit to the 5’ end of the mRNA. Simultaneously, eIF4E and eIF4G enhance the helicase activity of eIF4A [7-10]. The activation of eIF4A is required to unwind secondary structures in the 5’ UTR of the bound mRNA.

Apart from components of the eIF4F complex, eIF4G is known to interact with various other factors to enhance efficiency of the initiation process. For instance, binding to eIF3 enhances the recruitment of the PIC to eIF4F and the 5’ cap [11, 12]. In addition, eIF4G interacts with the polyA binding protein (PABPC1, hereinafter referred to as PABP or pAbp for mammals and *Drosophila*, respectively). As the name suggests, PABP binds to the polyadenosine (polyA) tail at the 3’ UTR of mRNAs [13, 14]. The interaction of eIF4G to eIF4E is independent of the binding to PABP allowing a closed-loop formation of the mRNA (Fig. 1A) [15]. By connecting the 5’ and 3’ UTR of the mRNA with each other, initiation is further strengthened as ribosomes

that finish translation can immediately associate with the eIF4F complex again [16, 17]. Consequently, the eIF4F complex remains associated with the mRNA's 5' UTR during the whole process of translation.

After binding of the 43S complex, scanning for the start codon (ATG) at the mRNA begins [18]. This is supported by eIF1 and eIF1A which induce conformational changes in the 40S subunit [19]. With opening of the mRNA binding channel, the 43S PIC is thus able to scan the mRNA for the start codon. The start codon itself is recognized by the initiator tRNA encoding for methionine (Met-$tRNA_i^{Met}$) that is bound to eIF2-GTP. Within the ribosomal mRNA binding channel, three distinct sites lie adjacent to each other that each bind to a nucleotide triplet: the amino acid (A), polypeptide (P) and exit (E) site. The initiator Met-$tRNA_i^{Met}$ binds to the start codon within the P site of the 40S subunit and with this determines the first amino acid of the polypeptide chain [18]. Recognition of the start codon mediates another conformational change of the PIC that locks the binding channel to the mRNA [19-21]. Moreover, start codon recognition induces the recruitment of eIF5 which binds to GTP-eIF2 and induces GTP hydrolysis. Since the resulting GDP-eIF2 has a reduced affinity to Met-$tRNA_i^{Met}$, it dissociates from the PIC [22, 23]. The GTPase eIF5B eventually mediates the release of the residual initiation factors [24, 25].

The dissociation of the initiation factors enables the full assembly of the 80S ribosome by 60S subunit joining [20, 26]. After the positioning of the translation-competent ribosome, the initiator tRNA at the P site sets the phase of translation elongation. In this phase, the ribosome moves along the mRNA from 5' to 3'. While scanning, different amino acid-loaded tRNAs bind to the A site. Their interaction with the ribosome is dynamic until correct base pairing between a tRNA anticodon and the mRNA triplet occurs. Stable binding of the correct tRNA is supported by elongation factor eEF1A and hydrolysis of GTP [27]. The tRNA at the A site is subsequently relocated to the P site and its amino acid transferred to the growing polypeptide chain. This transfer is achieved via a peptidyl transferase reaction conducted by rRNAs of the large ribosomal subunit [27].

After the peptidyl transfer, GTP hydrolysis by eEF2 promotes translocation of the ribosome [28]. Thus, the deacetylated tRNA occupies now the E site where it is released from the ribosome together with eEF2. In addition, the unbound A site is free for binding to the next tRNA. Recognition of the anticodon tRNA is a major rate-limiting step of translation. It is also

the tRNA abundance as well as the accurate usage of the codon that has a great impact on the elongation rate [29-32].

While the ribosome moves along the mRNA, the produced polypeptide chain grows. However, the nascent protein first needs to acquire its correct folding before exiting the ribosome. None or incorrect folded proteins are otherwise recognized and degraded by the proteasome [33]. Therefore, the polypeptide is first protected from its environment by passing through the exit tunnel of the ribosome. While passing through this tunnel, the nascent polypeptide chain acquires its secondary structure [34, 35]. The exit tunnel is mainly composed of rRNAs of the 60S subunit and isolates the immature protein [36]. Due to the RNAs, the tunnel exhibits a negative charge. Thus, depending on the charge of the amino acids, the chain interacts differently with the tunnel influencing the rate of elongation [37]. In contrast to the tunnel, the exit site consists mainly of ribosomal proteins. These proteins interact with chaperones, which ensure protection of the secreted polypeptide chain and allow folding to the tertiary structure [36, 38, 39].

Different stop codons exist determining the end of the polypeptide chain and termination of translation. In contrast to the other codons, termination codons are not recognized by tRNAs but proteins: release factor eRF1 mimics the anticodon stem-loop and binds to the A site. Successively, binding induces hydrolysis of the peptidyl tRNA at the P position [40, 41]. The peptide chain is subsequently released by the GTPase eRF3 that induces translocation of eRF1 to the P site. Subsequently, eRF3 dissociates while the ATPase ABCE1 binds and promotes dissociation of the 60S subunit from the mRNA [42]. Release of the 40S subunit is realized by dissociation of the mRNA and the remaining deacetylated tRNA at the P position. To enhance the process of translation reinitiation the split ribosome subunits are further recycled. Various proteins can mediate recycling of the small subunit. These factors include eIF1, eIF1A and eIF3 as well as the ABCE1 complex [42]. Binding of the initiation factors to the 40S subunit consequently results in a competent PIC that can reinitiate translation.

1.1.1. Regulation of translation

Translation is one of the most regulated processes within the cell ensuring a temporal and spatial control of gene expression. Since translational regulation is extremely fast and can be composed for specific mRNAs, quick responses to external stimuli are achieved. For instance, when iron levels within a cell decrease, translation of the transferrin receptor is enhanced to ensure efficient intake of iron molecules [43]. On the other hand, translation of ferritin, a protein that binds to and stores iron, is repressed. Also, many genes are expressed according to the circadian rhythm although their mRNAs are constantly present. This discrepancy is accomplished by a tight translational regulation of mRNAs [44, 45]. Additionally, in neurons and other polarized cells, mRNAs are transported to specific sites and locally translated. A well-studied mRNA that is regulated in this manner is *β-actin*. It encodes a protein inducing axonal growth in neurons [46, 47]. To achieve a distinct localization of the protein, *β-actin* mRNA is localized to the axons and only translated upon demand. Local translation is mediated by RNA-binding proteins (RBPs) including insulin-like growth factor 2 mRNA-binding protein (IGF2BP). IGF2BP binds to the 3' UTR of *β-actin* mRNA and prevents its premature translation [48-50].

Although regulation occurs during all phases of translation, the initiation phase is the main target ensuring a rapid and flexible control of gene expression [3]. Among others, eIF4E is heavily controlled by its expression pattern, stability and function due to its critical role in translation initiation. For instance, post-translational modifications (PTMs) of eIF4E affect its binding to the 5' cap as well as the eIF4F complex. Phosphorylation is such a PTM that influences the function of eIF4E on initiation [51]. Ubiquitination of eIF4E is another PTM resulting in decreased phosphorylation and reduced association with eIF4G [52]. Moreover, several proteins have been identified that bind to eIF4E and thereby weaken its affinity to subunits of the eIF4F complex. One well-known class of proteins that modulates translation in this manner are eIF4E-binding proteins (4E-BPs). Since 4E-BPs bind to the same domain of eIF4E as eIF4G does, the small proteins compete for binding to eIF4E [53, 54]. Interestingly, the binding affinity of 4E-BPs to eIF4E is regulated by their phosphorylation state as well [55, 56].

One main field of activity for many 4E-BPs is the regulation of maternal mRNAs in oocytes and embryos. In these cell systems, mRNAs need to be translationally silent until present at specific sites or at distinct developmental stages. For instance, the highly conserved 4E-

transporter (4E-T) protein was identified as negative regulator of translation initiation in *Xenopus laevis* (hereinafter referred to as *Xenopus*) oocytes [57, 58]. In *Drosophila* oocytes and embryos, the 4E-BP protein Cup acts in a similar manner competing with eIF4G for eIF4E (Fig. 1B) [59-61].

Apart from 4E-BPs, other proteins are known to regulate initiation by affecting the eIF4F complex. The eIF4E homologous protein (4EHP) can bind directly to the 5' cap. Although the protein structure of 4EHP is very similar to eIF4E, it does not possess the binding motif for eIF4G. Thus, association of 4EHP to the cap results in translational repression [62]. Also, 4EHP is an important regulator of translation during oogenesis and embryogenesis in *Drosophila* and mice, respectively [63-65]. The protein GIGYF further binds and stabilizes 4EHP [66, 67]. Moreover, GIGYF sequesters maternal expression at 31B (Me31B) that recruits the decapping complex [66-69]. Therefore, 4EHP does not only repress translation but also mediates the degradation of bound mRNAs (Fig. 1C).

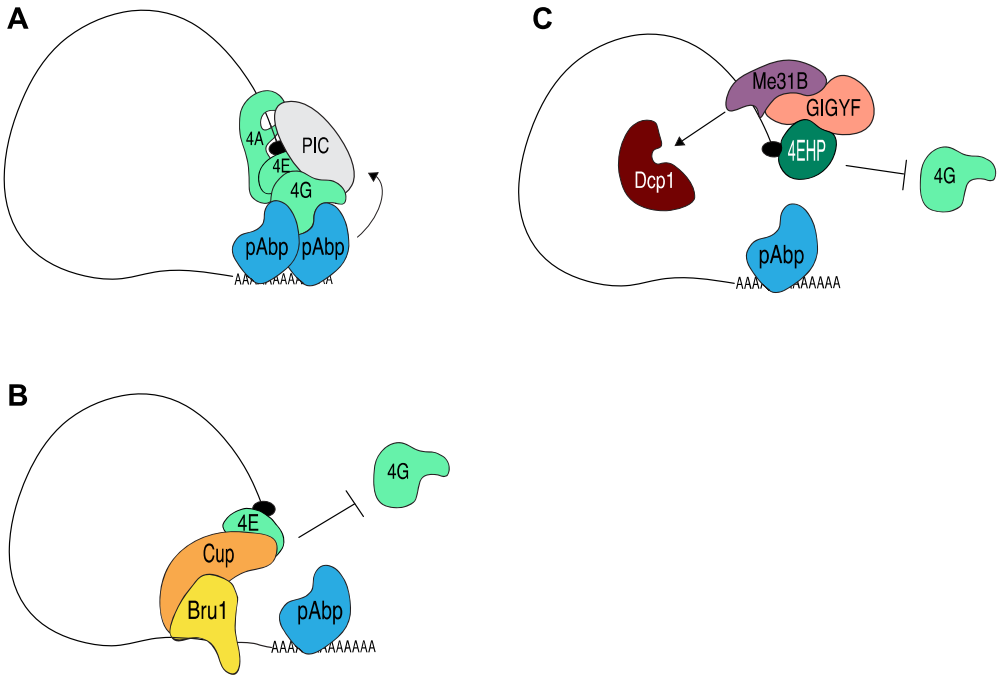

Figure 1. Translation initiation is regulated by different factors.
(A) During translation initiation, the eIF4F complex (light green) binds to the 5' UTR and recruits the PIC (grey). The cap binding protein eIF4E (light green) enables association of the PIC with the mRNA. The RNA helicase eIF4A (light green) unwinds the 5' UTR allowing the 40S subunit to scan for the start codon. eIF4G (light green) enhances the interactions among the eIF4F subunits with the PIC. Translation initiation is further supported by the interaction of the eIF4G with the 3' UTR, which is mediated by the binding to pAbp (blue). **(B)** In *Drosophila*, binding of the repressor Bru1 (yellow) recruits the 4E-BP Cup (orange). Cup competes with eIF4G (light green) for the interaction with eIF4E (light green), thus repressing translation initiation. **(C)** The eIF4E homologous protein (4EHP, dark green) binds to the 5' cap and represses translation. As 4EHP lacks the binding motif for eIF4G (light green), the closed-loop formation cannot form. In addition, 4EHP is stabilized by its interaction partner GIGYF (orange) that sequesters additional factors like Me31B (purple). Me31B promotes destabilization of the bound mRNA by recruiting Dcp1 (dark red) and other factors of the decapping complex.

LARP1 is another protein that regulates translation by modulating the interaction of eIF4F with the cap structure [70, 71]. LARP1 belongs to a complex family of La-related proteins (LARP) that evolved specific functions within the cell [72]. It binds to mRNAs possessing so-called 5' terminal oligopyrimidine (5'TOP) sequences and competes with eIF4E to the cap [73]. The 5'TOP motif is especially enriched in transcripts encoding ribosomal proteins and other factors involved in translation [71]. On the other hand, LARP1 was shown to interact with PABP and stimulate translation [73, 74]. Overall, the regulatory role of LARP1 differs depending on its target mRNAs as well as its interaction partners [72].

In addition to eIF4E, eIF4G is another member of the eIF4F complex that is frequently targeted by regulatory factors. Similar to eIF4E, different kinases mediate phosphorylation of eIF4G, which has an impact on its function [75-78]. Phosphorylation of eIF4G by Pak2 for instance reduces the affinity to eIF4E [79]. Consequently, binding of eIF4E to the 5' cap is decreased

leading to suppression of translation. On the other hand, the protein kinase PKCα influences translation by enhancing the interaction of eIF4G with the eIF4E kinase Mnk1 [80]. Binding to eIF4G brings Mnk1 in close proximity to eIF4E resulting in its phosphorylation [81].

Apart from manipulation of initiation factors, translation can also be regulated by other means. For instance, error-prone mRNAs need to be distinguished together with their aberrant polypeptides and degraded. These include mRNAs that contain a premature stop codon resulting from mutations within the coding sequence. Such mRNAs are recognized and degraded by a mechanism referred to as nonsense-mediated mRNA decay (NMD). One important player of the NMD is the exon junction complex (EJC). Upon splicing, it is deposited upstream of exon-exon junctions [82]. Since the EJC stays associated with the transcript, it is an indicator of properly processed mRNAs. If a premature stop codon is present upstream of an exon-exon junction, the EJC recruits the NMD factor UP Frameshift 3 (UPF3) to the ribosome [82]. Subsequently, the ATPase UPF1, another core factor of the NMD pathway, binds inducing translation termination [83, 84].

1.1.1.1. The role of the polyA tail in translational regulation

In the cytoplasm, PABP coats the polyA tail of an mRNA. PABP is known to bind a minimum of 12 adenosines with a preference for the polyA tail compared to internal adenosine stretches [13, 14, 85]. Moreover, PABP mainly binds to polyadenylated mRNA via its RRM1 and RRM2 domains [86]. When bound, one PABP molecule covers around 27 nucleotides. Thus, with an average length of 50-100 adenosines in metazoans, the polyA tail can be bound by several PABP molecules [87].
Due to its role in mRNA circularization during translation, it does not come as a surprise that the polyA tail plays a crucial role in translational regulation. In fact, a shorter length of the polyA tail has been linked to translational repression. This is probably due to a reduced interaction between pAbp and the eIF4F complex. Especially in ovaries and embryos, shortening of the polyA tail is used to repress translation of maternal mRNAs [88-90].

The length of the polyA tail is regulated by the CCR4-NOT1 deadenylase complex. This complex is composed of different proteins and highly conserved in eukaryotes [91]. Apart from

shortening of the polyA tail to modify the rate of translation, deadenylation can also lead to complete degradation of the mRNA. In fact, deadenylation is the main mechanism for mRNA decay used in cells [92, 93]. Shortening of the polyA tail to less than 25 nucleotides initiates decapping of the 5' end and subsequently exonucleolytic degradation [94-96].

Controlling the polyA tail length is an important mean to modulate translation in response to environmental stimuli. However, to ensure specificity of the CCR4-NOT1 complex, additional proteins that bind to the 3' UTR of target mRNAs are required. In line with this, distinct *cis*-regulatory elements are known to mediate deadenylation. For instance, recognition of the embryonic deadenylation element (EDEN) in *Xenopus* embryos induces deadenylation of the bound mRNA [97]. For other *cis*-acting elements, the effect is not as clear and depends on the proteins that bind to the mRNA as well as on their interactions with other factors. For example, the RBP Smaug regulates maternal mRNAs in *Drosophila* oocytes and embryos by recruiting the CCR4-NOT1 complex [98, 99]. When binding to the mRNA, Smaug induces deadenylation and destabilization of localized transcripts. Another protein that represses translation via inducing deadenylation is Pumilio (Pum). It binds to the 3' UTR of mRNAs in oocytes and embryos of various species and interacts directly with PABP [85, 100-105]. Due to its conserved role in recruiting the deadenylase complex, Pum is a global effector of mRNA stability [106, 107].

Interestingly, PABP itself not only blocks but also promotes deadenylation by recruiting CCR4 [108, 109]. This interaction allows a precise regulation of mRNA stability and translation. Also, *Drosophila* pAbp plays an important role in regulating the stability of maternal mRNAs [110]. Consequently, PABP is another target to regulate translation. Several proteins are known to directly modulate the function of PABP including PABP interacting proteins (Paip). Paip1 for instance binds to PABP and other initiation factors, which enhances translation [111, 112]. On the other hand, Paip2 binds PABP in competition with Paip1 thereby reducing the binding of PABP to the polyA tail [113, 114].

Apart from deadenylation, mRNAs can undergo polyadenylation by cytoplasmic polyA polymerases. Especially in ovaries and embryos where mRNAs need to be stored and can only be post-transcriptionally regulated, polyA polymerases are powerful regulators of translation [97]. Interestingly, 15-20% of vertebrate mRNAs contain a cytoplasmic polyadenylation

element (CPE) [115]. The CPE is recognized by distinct proteins that recruit cytoplasmic polymerases [116].

Moreover, not all mRNAs need to be activated for translation at the same time, which requires specific RBP that ensure different waves of activation and silencing [97]. In *Drosophila* for instance, two different cytoplasmic polyadenylases are expressed at distinct stages of oogenesis: in the early phases of oogenesis, a canonical polyA polymerase called hiiragi (hrg) induces translation of mRNAs while in the late phase of oogenesis and oocyte-to-embryo transition this process is carried out by the atypical polyA polymerase wispy (wisp) to ensure expression of maternal mRNAs [117-120].

1.2. Ubiquitination

Apart from translation, protein levels and activities are regulated by other mechanism. One layer of post-translational regulation is the modification of specific amino acids within proteins. PTMs occurring on proteins include phosphorylation, acetylation, methylation and ubiquitination. These modifications are of extreme importance as they can affect structure, binding, localization and stability of the protein [121]. Ubiquitination has emerged as one PTM with high conservation as well as tremendous effects on various signaling pathways within the cell. During this reversible process, ubiquitin (Ub) is covalently attached to its substrate by the formation of an isopeptide bond between the glycine at the Ub C-terminus and a lysine of the targeted protein. Since the attachment of Ub requires high energy, three different classes of enzymes act in synergy to deposit Ub: the ubiquitin-activating (E1), ubiquitin-conjugating (E2) and ubiquitin-ligating (E3) enzymes (Fig. 2A) [122, 123].

In the first step of the ubiquitination cascade, Ub is activated with the help of ATP and bound to E1 via a thioester bond [124, 125]. Next, by a transthioesterification, Ub is transferred to an E2 enzyme resulting in an E2-Ub complex [126]. Subsequently, an E3 enzyme mediates the attachment of ubiquitin to the substrate by an isopeptide bond [126]. For this final ubiquitination step, the E3 ligase needs to bind both, the substrate as well as the E2-Ub enzyme. Since E3 enzymes need to interact with substrate as well as E2-Ub, the binding ensures the controlled and specific ubiquitination of target proteins. Indeed - compared to only two E1s and less than 40 E2s – it is estimated that around 700 different E3 ligases exist in humans [127-131]. The

high number of E3 ligases highlights the complexity of the ubiquitin system that relies on specific interactions with the target protein.

In eukaryotes, mainly three types of E3 ligases exist that are defined by the presence of their domain structure: HECT (homologous to E6-AP carboxy terminus), RING (really interesting new gene) and RBR (RING-between-RING) E3 ligases [123]. Whereas HECT ligases transfer Ub from E2-Ub to the substrate via an E3-Ub thioester intermediate, RING enzymes catalyze a direct attachment of Ub to the substrate (Fig 2A). RBR ligases on the other hand possess a RING domain but transfer Ub by an E3-Ub intermediate similar to HECT ligases [132]. Given that E3 ligases act by bringing E2-Ub enzymes and target proteins in close proximity, their binding specificity to the substrate is of great importance. To accomplish this specificity, RING ligases often act together with an adaptor protein that binds to the substrate [133]. RING ligases compose the biggest class of E3 ligases with around 600 proteins predicted to be expressed in humans [134]. Moreover, computational analysis of RING E3s demonstrated that around three quarter contain additional domains that might regulate the binding to E2-Ub, substrates or other components like RNA and DNA [134].
Although the RING domain was identified in 1991, the functional relevance of this domain remained unknown for many years [135]. In 1999, several groups demonstrated that the RING domain promotes transfer of Ub to specific substrates by binding to E2-Ub enzymes [136-140]. Interestingly, the pathway RING ligases are involved in greatly varies depending on the enzyme and the ubiquitinated substrate.

In addition, the manner in which Ub is attached to the substrate determines the substrate's fate [141]. This attachment can result in the deposition of a single Ub or several Ubs arranged in a chain, referred to as mono- or polyubiquitination, respectively (Fig. 2B). The structure and position of the PTM in turn is recognized by different effector proteins. For instance, deposition of a single Ub can be a signal for DNA repair or induce chromatin remodeling [142-144]. Moreover, different lysines on one substrate can be targeted for monoubiquitination. The effect of multi-monoubiquitination, however, remains still elusive. Recent studies suggest that this modification is involved in trafficking and degradation [145, 146].

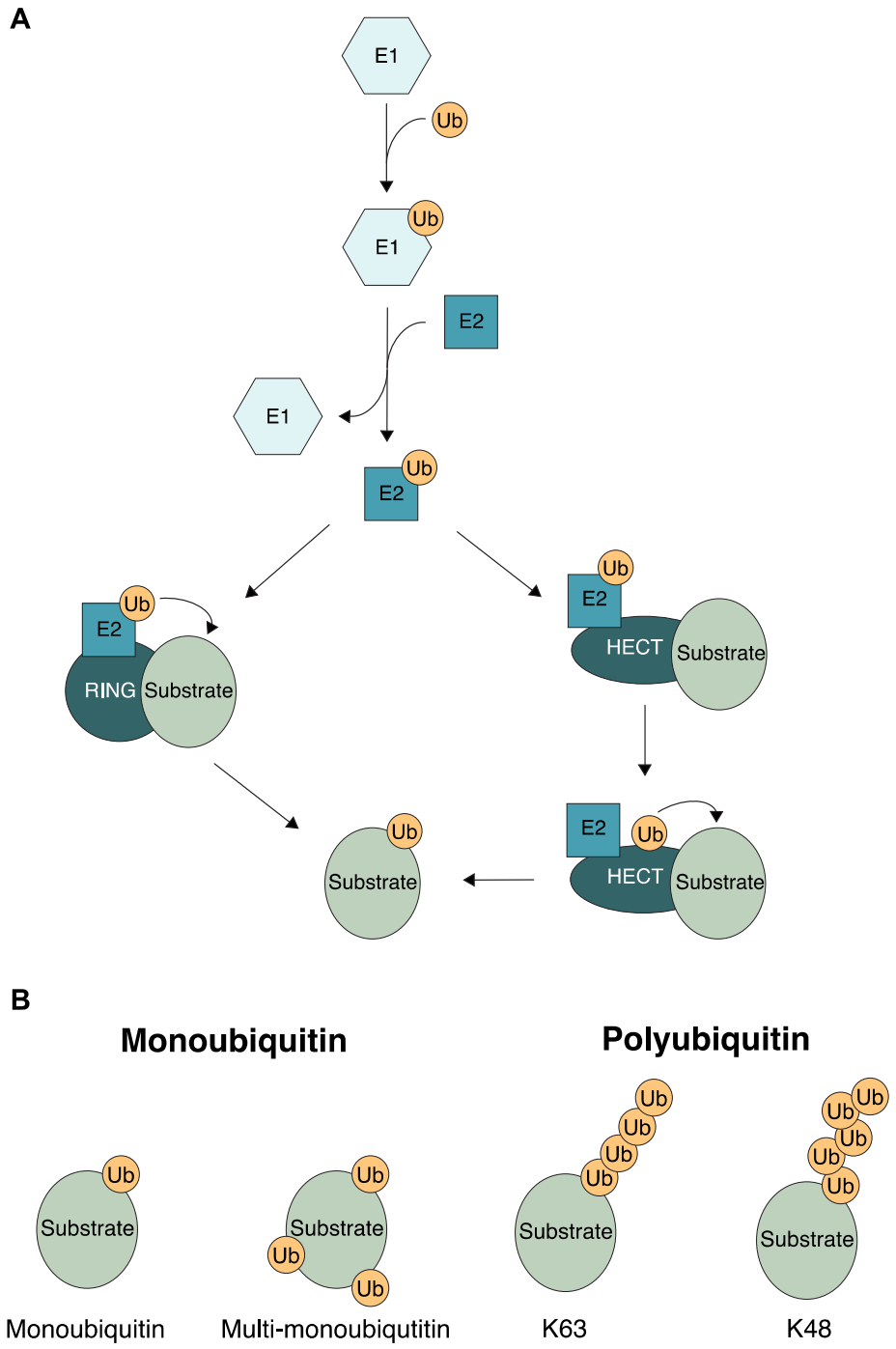

Figure 2. Ubiquitination processes differ depending on the E3 ligase.
(A) Schematic representation of the ubiquitination cascade. Ub (yellow) is first activated and loaded on the E1 enzyme (light blue) using a thioester bond. Ub is further transferred to an E2 (blue) by a transthioesterification. To ubiquitinate the substrate, an E3 enzyme (dark green) mediates the attachment of Ub. The E3 ligase can act in different ways to attach Ub on the target protein. For instance, HECT and RBR ligases transfer Ub from the E2 enzyme to the substrate via an E3-Ub thioester intermediate. Ub is then attached to the substrate directly from the HECT enzyme. On the other hand, RING domain E3 ligases transfer Ub to the substrate without an intermediate step. **(B)** Ub can be attached in different manners to the substrate. One distinguishes mono- and polyubiquitination dependent on chains of Ub present at the substrate. Among others, monoubiquitin signals chromatin remodeling and DNA repair. Using a distinct lysine within Ub for the polyubiquitin chain results in different conformations that are recognized by distinct effector proteins. Polyubiquitination via K48 for instance signals degradation of the modified protein by the proteasome while K63 linkages activate the NF-κB pathway.

Similarly, polyubiquitination can mediate different effects on the substrate as well, depending on the linkage type [147]. As mentioned above, Ub is covalently bound to the lysine of a substrate protein. Interestingly, Ub itself harbors seven lysines that can serve as ubiquitination targets themselves. Moreover, the N-terminal methionine of Ub is a target for ubiquitination as well. Depending on the modified amino acid of Ub, various functions of the PTM arise [148]. The chains are recognized by different Ub-binding proteins, which possess different binding domains. The major signal for protein degradation, for instance are polyubiquitin chains via K48 [149]. In contrast, ubiquitination chains of Lys63 on TRAF E3 ligase activate expression of NF-κB upon external stimuli [150-152]. Compared to these polyubiquitin chains, others including Lys27 and Lys29 linkages are not as abundant. These modifications are now on the verge of being studied as they need more sensitive methods. For instance, when the erroneous protein LRRK2 is modified with these chains, it aggregates, which prevents its neuronal toxicity [153]. Moreover, combinations of different lysines used to attach Ub are possible resulting in branched polyubiquitin chains [154].

Another field gaining more interest is the deubiquitination of substrate proteins [155]. Deubiquitinases can alter Ub signaling pathways and rescue substrates from degradation by removing K48 linkages.

1.2.1. The role of E3 ligases in regulation of translation

Apart from the above-mentioned examples on how Ub affects cellular processes, translation is also heavily regulated by E3 ligases. RING ligases are powerful mediators of this process allowing fast responses to various incidents.

The most logical implementation of the Ub system during translation is based on the successful degradation of incomplete or aberrant polypeptide chains. Several quality control pathways have been identified that secure proper protein production within the cell. For instance, mRNAs consisting of a premature stop codon are recognized by the NMD pathway (1.1.1). Recruitment of the NMD complex leads to degradation of the mRNA and ubiquitination of the aberrant protein by the E3 ligase UPF1 [156, 157]. Moreover, read-through translation of an mRNA lacking a stop codon induces degradation of the nascent polypeptide [158]. Detection of such

error-prone mRNAs is mediated by the ribosome-associated quality control (RQC) pathway. RQC results in the degradation of the aberrant polypeptide via K48-linked polyubiquitination mediated by the RING ligase Listerin [159, 160].
Another RING E3 ligase, ZNF598, has been reported to initiate RQC in human cell culture upon translation of adenosine rich transcripts [161, 162]. RQC is activated by stalling of the ribosome during translation elongation [158]. When stalling, ZNF598 binds to the ribosome and ubiquitinates components of the 40S subunit including RPS10 and RPS20 [161]. Ubiquitination of ribosomal proteins further results in abrogation of translation and disassembly of the ribosome.

Interestingly, many RING ligases have evolved distinct functions including additional binding specificities. In fact, around 300 of these enzymes are predicted to bind to RNA [163]. This ability brings another layer of specificity, as the sequestration of an E3 ligase to its target might depend on a certain RNA [164]. As such, binding of the RING E3 ligase Roquin to mRNAs regulates mRNA stability [165, 166]. In macrophages, Roquin interacts witch a stem-loop structure of the *TNF-α* mRNA and recruits the CCR4-NOT1 complex resulting in degradation of the bound mRNA [167]. Interestingly, the RING E3 ligase MEX3C regulates the stability of its target RNA by another mechanism. MEX3C localizes to processing bodies (P bodies) and ubiquitinates a subunit of the CCR4-NOT1 complex [168, 169]. This ubiquitination does not induce degradation but stimulates the deadenylation activity of the complex [169].

1.2.2. The Makorin protein family has broad functions during development

1.2.2.1. Structural domains of Makorin proteins

Another RING E3 ligase that possesses the ability to bind RNA is the Makorin RING finger protein (Mkrn). Proteins belonging to the Mkrn family are characterized by their domain structure consisting of several Cys_3His (C3H) zinc fingers (ZnF) and a RING domain [170]. The arrangement of cysteines and histidines within the ZnF plays a critical role in the interaction

with nucleic acids as well as in their sequence preference [171, 172]. However, the relevance of this RNA binding activity in Mkrn proteins has not been described yet.

In addition, other motifs present in different Mkrn paralogs have been annotated: whereas only MKRN1 and MKRN3 comprise a PABP-interacting motif 2 (PAM2), a PAM2-like (PAM2L) motif is present in MKRN1, MKRN2 and MKRN3 [173]. The two motifs share similar binding specificities to the Mademoiselle (MLLE) domain present in PABP and other proteins [111, 174, 175]. While the consensus sequence of the PAM2 motif comprises the core sequence EFxP (x being any hydrophobic or aromatic residue), the PAM2L motif consists of the core (D/E)FxxP sequence [174, 175]. The PAM2 motif has been extensively studied due to its role in the interaction with PABP [111, 174]. On the other hand, the PAM2L motif was only recently identified mediating the interaction with the MLLE-containing protein Rrm4 in *Ustilago maydis [175]*. It is likely that the PAM2 and PAM2L motif support distinct cellular functions of the Mkrn proteins by mediating binding to specific factors.

1.2.2.2. The Makorin family consists of different paralogs with potential functions during development

Altogether, the Mkrn family of proteins is highly conserved throughout animal kingdom with up to four family members existing in vertebrates (Fig. 3) [170, 172]. Additionally, many intronless genes evolved by gene duplication from the *Mkrn* genes [170, 172, 176]. As the Mkrn family depicts a high evolutionary conservation and many gene duplications, it has been suggested that the gene family has important functions during development. Interestingly, the members of the family are highly enriched in oocytes and maternally deposited in fish [170]. Also, in rice (*Oryza sativa* L. var. Nipponbare), MKRN displays a prominent expression in ovaries and embryos [177].

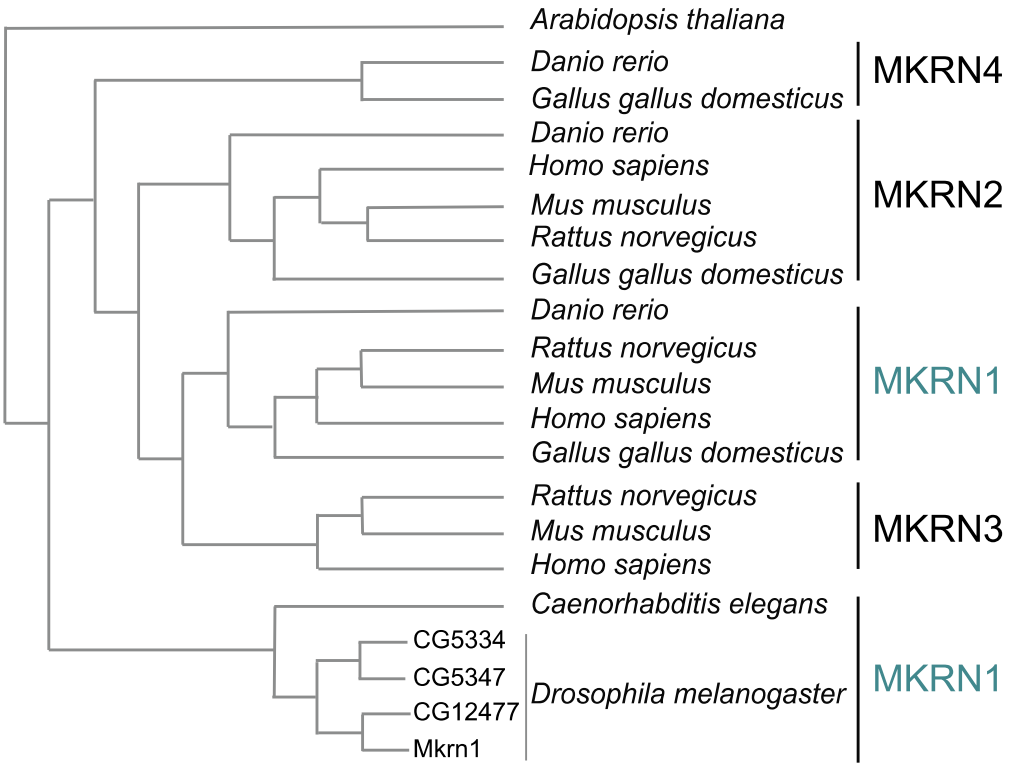

Figure 3 Species tree of the Mkrn family.
The Mkrn family consists of four paralogs with MKRN1 (highlighted in turquois) being the common ancestor. Four *MKRN1*-related genes are present in *Drosophila*. Tree adopted from TreeFam [178, 179].

Within the Makorin protein family, *MKRN1* and *MKRN2* are the only intron-containing genes expressed in vertebrates [172, 180]. Among the many retrocopies, *MKRN1* has been proposed to be the common ancestor. This is also why it is referred to as "the source" ("makor") of the family [172]. In line with this, Mkrn1 is the most studied family member. For instance, several reports identified ubiquitination targets of human MKRN1 [181-184]. Due to the different targets, MKRN1 has been implicated in diverse functions within the cell including tumorigenesis, maintenance of pluripotency and metabolism [181, 183-188].

For instance, MKRN1 ubiquitinates human telomerase reverse transcriptase (hTERT) and therefore negatively affects telomere length [181]. The E3 ligase also has been implicated in the ubiquitination-dependent degradation of the tumor suppressors p53 and p21 [183]. Additionally, MKRN1 promotes degradation of AMP-activated protein kinase (AMPK) [184]. This in turn results in suppression of mTOR signaling and contributes to insulin resistance in mice. Since the substrates of MKRN1 undergo degradation, it is not surprising that MKRN1 induces polyubiquitination via Lys48, a mark for proteasomal degradation [184].

Compared to a rather ubiquitous expression of human *MKRN1*, the mouse ortholog is highly enriched in testis [172, 189, 190]. Furthermore, murine embryonic stem cells (ECSs) and induced pluripotent cells display strong MKRN1 expression that decreases upon differentiation

[185, 188]. In contrast, mutation of *MKRN1* does not lead to embryonic defects in mice [189]. Interestingly, studies in *Drosophila* revealed a crucial role of *Mkrn1* during oogenesis: its knockout impairs oocyte development while its knockdown leads to malformation of embryos, indicating a critical role in axis polarity [191].

Compared to MKRN1, the function of MKRN2 remains more elusive. In mammals, MKRN2 consists of a similar protein structure like MKRN1 containing four ZnFs and a RING domain [180]. However, human MKRN2 is only 46% identical to MKRN1 (BLASTP [192, 193]). Due to the evolutionary divergence, it was suggested that MKRN1 and MKRN2 are involved in distinct cellular processes [180]. This is supported by the high homology of MKRN2 among different species. In humans, MKRN2 is expressed in various tissues including CD34+ hematopoietic cells, leukemic cell lines, thymus and testis [194-196]. This relatively broad expression suggests various biological functions.

Interestingly, *MKRN2* is essential for male fertility in mice [195, 197]. Furthermore, a reduced expression of *MKRN2* in sperm correlates with infertility in human men [195]. Mutations in the *Mkrn* ortholog *lep-2* in *Caenorhabditis elegans* (herein after referred to as *C. elegans*) led to male sterility as well [198].

In *Xenopus*, *mkrn2* depicts high expression levels in testis [199]. Moreover, *mkrn2* is required for neurogenesis and axis formation during early embryogenesis. Interestingly, the ZnF3 and RING domains of mkrn2 are necessary for stimulating the glycogen synthase kinase-3β (GSK-3β) expression [199, 200]. The mechanism of mkrn2 in this process however is unclear. In line with reports for MKRN1, ubiquitination substrates of MKRN2 were identified including the NF-κB subunit p65 [201]. Therefore, these observations highlight the importance of the conserved RING domain.

In contrast to the two paralogs described above, the intronless *MKRN3* gene evolved later in evolution and is only present in therian mammals [170, 202]. *MKRN3* is paternally imprinted and displays high expression in testis [172, 202]. Furthermore, the human *MKRN3* gene is located in the genomic region associated with the Prader-Willi syndrome. However, *MKRN3* does not have a direct implication as mutations within the gene alone do not cause the disease [203]. Intriguingly, SNPs in *MKRN3* as well as reduced expression levels have been associated with central precocious puberty [204-207]. In mice, MKRN3 was suggested to have a similar function in the onset of puberty due to its specific expression pattern in the hypothalamus prior

to puberty [204]. Accordingly, mouse MKRN3 negatively regulates Nptx1, a neuronal protein involved in the timing of puberty [208].

The tight association of *Mkrn* expression and juvenile-to-adult transition was also examined in *C. elegans as* well as *Drosophila*, suggesting a conserved function [186, 198, 209]. The *Mkrn* ortholog of *C. elegans*, *lep-2*, has a critical role in juvenile-to-adult transition by degrading the developmental regulator LIN-28B [198, 209]. Also, a recent study in *Drosophila* observed a similar relevance in the transition to adulthood: *Mkrn1* mutant larvae display a delayed instar to pupariation time [186].

The paralog *Mkrn4* has evolved different functions during evolution: although *MKRN4* is annotated as pseudogene in humans and not expressed in mammals, in fish and amphibians it has a specific expression pattern in gonads and early embryogenesis [170, 210]. Nevertheless, elucidation of its function awaits further investigations.

Collectively, the distinct functions and expression patterns of the Makorin proteins highlight the important and conserved roles of this family during development. However, as the mechanism by which Mkrn proteins mediate these different cellular processes remains largely elusive, further research is needed to uncover these functions and their degree of conservation.

1.2.2.3. MKRN1 has an impact on translational regulation

Although all Makorin paralogs possess a similar protein structure, so far only MKRN1 and MKRN2 have been shown to ubiquitinate target proteins [181-184, 201]. While the reports on MKRN2 are limited, many studies focused on the E3 ligase activity of mammalian MKRN1. Similarly, the ability to interact with RNA was only observed for mammalian MKRN1 and MKRN2 [173, 185, 211]. Intriguingly, E3 ligases that have the ability to bind to RNA were implicated in post-transcriptional gene regulation [163, 164].

Curiously, in mouse ESCs, many mRNAs that are locally translated at the ER are bound by MKRN1 [185]. Hence, a possible role of MKRN1 in the transport or translational control of mRNAs in undifferentiated cells has been suggested. However, the regulatory function of

MKRN1 in this process remains elusive. Recently, another study proposed specific binding of human MKRN1 upstream of A-rich sequences on mRNA [173]. The finding supports the conserved RNA-binding ability of MKRN1. Nevertheless, the question remains whether the observed interaction with RNA can be assigned to one or more ZnF domains.

Due to the reported interaction with RNA, it not surprising that MKRN1 associates with other RNA binding proteins (RBPs): mass spectrometry approaches identified interactors of mammalian MKRN1 including PABP, IGF2BP1, LARP1, LARP4B, heterogeneous nuclear Ribonucleoprotein D (hnRNP D), UPF1 and Y-box-binding protein 1 (YBX1) among others [173, 185]. Moreover, the interaction with PABP is the best-studied one and is conserved in human, mouse and rat [173, 185, 212]. The binding to PABP occurs via the PAM2 domain of MKRN1 [212]. Strikingly, interaction of a short MKRN1 isoform to PABP stimulates translation of the bound mRNA in rat neurons [212]. More recently, human MKRN1 was shown to act in synergy with ZNF598 on ribosome-associated quality control. Upon translation of adenosine-rich stretches, MKRN1 ubiquitinates RPS10 and PABP to prevent translation of the error-prone mRNA [173]. These findings reveal miscellaneous functions of MKRN1 being able to promote and abrogate translation. Therefore, the precise mechanism by which MKRN1 exerts this function and how the E3 ligase is regulated needs further investigation.

1.3. Oogenesis

One well-established model system to study the interplay of mRNA localization and translation is oogenesis. Especially in *Drosophila*, this process is under investigation since the 1980s. Due to the extensive research, the individual regulatory processes can be deciphered in great detail using advanced methods [213, 214].

Drosophila females possesses two reproductive organs called ovaries. The ovaries themselves consist of 16 to 20 stretches of autonomous egg chambers, so-called ovarioles [214]. At the anterior of every ovariole are the germline stem cells located in a structure called the germarium (Fig. 4A). One germline stem cell divides in an asymmetrically manner, resulting in one stem cell and one cystoblast. The cystoblast further divides four times with incomplete cytokinesis producing a 16-cell cyst. The manner of the divisions results in germ cells being interconnected

with each other via ring canals. One cell located at the posterior of the cyst will receive signals inducing the oocyte fate. The other 15 cells become nurse cells, which produce maternal factors that are transported to the oocyte during oogenesis. In the germarium, a monolayer of somatic cells, called follicular cells, encloses the cyst to form a separated egg chamber [215]. The egg chamber further matures in 14 defined developmental stages, with stages 1-6 referred to as early oogenesis, stage 7-10A as mid-oogenesis and stages 10B-14 as late oogenesis (Fig. 4A).

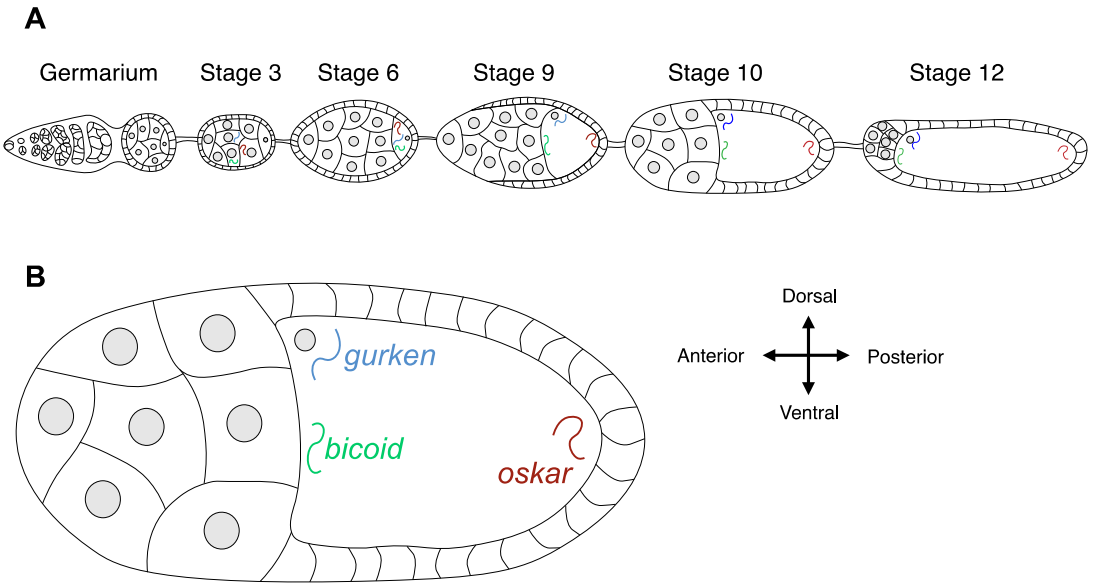

Figure 4. Schematic representation of *Drosophila* oogenesis.
(A) Within the ovariole, the germ cells are present at the anterior site of the germarium. Asymmetric division of the stem cell results in a cystoblast that further divides four times. Due to incomplete cytokinesis during these divisions, a 16-cell cyst is formed interconnected by ring canals. One cell in the cyst, positioned at the posterior, is determined as oocyte. The cyst separates from the germarium and forms an egg chamber. A layer of follicle cells surrounds every egg chamber enabling a permanent connection to the germarium. The egg chamber subsequently develops in 14 distinct stages with the oocyte taking up factors produced by the other so-called nurse cells. The uptake of factors like mRNAs and proteins results in growth of the oocyte. Beginning with stage 11, the nurse cells undergo apoptosis leading to the oocyte being the only remaining cell of the cyst. The oocyte, still surrounded by follicle cells, matures into an egg and awaits fertilization. **(B)** With maturation of the oocyte, a set of factors positions at distinct sites to induce axis specification. This localization promotes axis polarity of the oocyte and is crucial for embryogenesis. The mRNAs *oskar* (red), *gurken* (blue) and *bicoid* (green) are critical players of axis formation inducing the posterior, antero-dorsal and anterior sites, respectively.

Since the oocyte is the only cell that will develop into the egg, it is also the only one that undergoes meiosis. Progression of meiosis first arrests during prophase I and remains in this stage most of the time during oogenesis [216].

During early oogenesis, factors required for oocyte maturation and embryogenesis that are produced by the nurse cells are transported to the oocyte. This transport is mediated via the actin-dependent motor protein Myosin along the ring canals [217-219]. In addition, a microtubule network organizes through the ring canals with a microtubule organizing center

(MTOC) directed at the posterior of the oocyte [217, 220]. The transport within the oocyte itself is mainly restricted to this microtubule network [217, 221]. During stage 5, the oocyte nucleus and additional maternal factors, including *gurken* (*grk*) mRNA, are localized to the posterior pole of the oocyte. Bicaudal D (Bic-D) and Egalitarian(Egl) are necessary for this early stage directed transport [222, 223]. Both, Bic-D and Egl bind to the microtubule motor protein complex [224, 225]. Upon binding to mRNA, the Bic-D/Egl-complex is activated and transports messenger ribonucleoproteins (mRNPs) across the microtubule network [226, 227].

A distinct population of follicle cells, termed polar cells, establishes at the anterior and posterior sites of the egg chamber [214]. Together with Grk protein, they determine the posterior identity of the oocyte [228-230]. Grk is a TGFα homolog that is secreted to the posterior polar cells [231]. The Egfr ligand Grk binds to the Torpedo receptor and activates the MAPK signaling cascade [231, 232]. The polar cells signal back to the oocyte which leads to the relocalization of the oocyte nucleus and Grk to the antero-dorsal site at stage 8/9 [233, 234].

At the antero-dorsal site, Grk signaling occurs again determining the dorsal fate of adjacent follicle cells [235, 236]. Repositioning of the nucleus at stage 8 is accompanied by dramatic changes of the oocyte's microtubule network: the microtubule minus ends spread throughout the oocyte cortex with a density gradient to the anterior [237-240]. The microtubule plus ends on the other hand focus towards the posterior pole. Therefore, transport to the posterior now requires the plus end-directed motor protein Kinesin 1 [241, 242]. Transport of mRNAs like *bicoid* (*bcd*) to the anterior, however, is minus end-directed and mediated by the motor protein Dynein [238, 243, 244].

Since the microtubule network is only weakly polarized, transport of maternal factors is relatively slow and random [245]. Thus, factors like *oskar* (*osk*) mRNA are additionally anchored at the posterior pole by the actin cytoskeleton and RBPs [237, 246-249]. At the posterior, the germ plasm is formed that will later define the germ cells during embryogenesis. The germ plasm is a specialized compartment of the oocyte cytoplasm containing mRNAs, proteins, ribosomes and rRNAs [214]. Among others, the germ plasm-specific components include *osk* and *nanos* (*nos*) mRNAs as well as the proteins Osk, Aubergine (Aub) and Vasa.

By stage 10B, cytoplasmic streaming within the oocyte becomes fast and coordinated [245]. Actin filaments redistribute and orient in a random manner around the oocyte cortex [250]. As

a consequence, the microtubule network, which is anchored by actin bundles, rearranges as well and becomes more loose. The microtubules further align parallel to the oocyte cortex and redistribute to subcortical regions [250]. At stage 11, the so-called dumping of the nurse cell cytoplasm occurs. The cytoplasm of the nurse cells is transported via the ring canals to the oocyte and released [245]. Fast streaming further supports mixing of the dumped components within the oocyte cytoplasm [251]. At around the same time the nurse cells start to degenerate [252]. Meiosis of the oocyte continues by stage 13 and arrests again in metaphase I during stage 14. At this stage, the egg is completed and awaits egg activation to finish meiosis. Interestingly, egg activation is not dependent on fertilization as in mammals but relies on mechanical stress during transit to the oviduct [253].

1.3.1. Regulation of localization and translation during oogenesis

The asymmetry within egg chambers mainly depends on different signaling pathways that are crucial for oogenesis. Within the oocyte, this asymmetry further establishes axis specification of the embryo, which is accomplished by local gradients of mRNAs and proteins. These gradients are generated via localization of maternal mRNAs that are primarily transcribed in the nurse cells, transported to their destination in the oocyte, and translated only at the specific time needed [116]. Localization and translation of individual maternal mRNAs is highly regulated and extremely complex. It involves diverse RBPs and interactions of proteins with mRNAs in dynamic mRNP complexes. Moreover, the mRNP composition highly varies in different tissues and developmental stages [211, 254, 255]. The same protein can bind various targets and depending on the mRNP composition, the regulatory function might differ [256]. This tight regulation is necessary to achieve temporal and localized expression of proteins, which ensures axis specification needed for embryonic development.

The genes essential for embryonic patterning are a focus of research since many years and referred to as maternal effect genes. Mutations of these genes lead to defects in axis polarity and segmentation in the oocyte resulting in embryonic lethality [257-259]. Among those genes are *bcd*, *grk* and *osk* that establish the embryonic axes [260-262]. *bcd*, *grk* and *osk* mRNAs are localized during mid-oogenesis to the anterior, antero-dorsal and posterior of the oocyte,

respectively (Fig. 4B). Local translation of the mRNAs creates a protein gradient inducing antero-posterior and dorsal-ventral axis formation in the embryo [116].

Localization of *bcd* mRNA is required for patterning of the head and thorax [261]. Therefore, the mRNA is localized to the anterior at stage 8 but only translated upon egg fertilization [116]. In the embryo, Bcd protein induces transcription of developmental genes and regulates translation of bound mRNAs [263-265]. Grk protein on the other hand is already present during oogenesis as it is necessary to induce both, the antero-posterior and dorsal-ventral axis [228, 231, 235]. For this purpose, the mRNA is first transported to the posterior at stage 1 and relocalized to the antero-dorsal site at stage 8/9 [266]. Although transport and translation of *grk* are tightly coupled, the two processes are independent of each other [267, 268]. The gene *osk* encodes an mRNA that is transported to the oocyte in early oogenesis and localized to the posterior pole at stage 8 [248, 269]. Localization of *osk* mRNA is crucial for the pole plasm definition at the posterior [270]. Similar to *bcd*, *osk* retains the same localization throughout oogenesis. However, immediately after reaching the posterior, *osk* is translated [249, 271]. Interestingly, *osk* mRNA as well as Osk protein have distinct functions during oogenesis. The mRNA associates with various proteins and its noncoding function is thought to sequester these proteins in tight mRNP complexes to the posterior pole [272, 273]. Osk protein on the other hand regulates the polarity of the microtubule network in mid-oogenesis and anchors *osk* mRNA to the posterior cortex [274, 275]. During embryogenesis, it nucleates the components of the germ plasm by binding to distinct mRNAs and proteins [276-278].

In conclusion, the regulatory mRNPs that form during oogenesis are highly complex to achieve a stage-dependent localization and translation of key transcripts.

1.3.1.1. Regulation of *grk* expression by different RBPs

As mentioned above, *grk* is initially transported to the posterior site by the minus end-directed motor protein Dynein and Bic-D/Egl. The accumulation of *grk* during early oogenesis depends on *cis* elements present in its 5’ UTR and 5’ CDS [268]. At the posterior, translation is activated by the DEAD box mRNA helicase Vasa [279, 280]. Vasa activates translation of *grk* by interacting with the initiation factor eIF5B [281, 282].

Localization of *grk* to the antero-dorsal site during mid-oogenesis is a stepwise process beginning with transport to the anterior cortex at stage 7/8 [233, 281, 282]. With dorsal positioning of the nucleus at stage 9, *grk* further localizes to the location of the nucleus [266]. The transport of *grk* to the antero-dorsal site depends on the microtubule network and Dynein [233, 266]. Similarly, this localization is mediated via Bic-D/Egl and requires *cis* elements within the *grk* 3' UTR [268, 283, 284]. The importance of different *cis* elements reveals that distinct RBPs are involved in the localization process. Additionally, from stage 9 onwards, *grk* is transcribed in the oocyte nucleus, which enhances its accumulation at the antero-dorsal site [283, 285].

Localization and anchoring to the antero-dorsal site depends on Dynein and Squid (Sqd) [266, 286]. Interestingly, the *Sqd* gene produces three different isoforms that are either localized in the oocyte nucleus or cytoplasm [285]. Thus, Sqd regulates different processes of *grk* including export from the oocyte nucleus, cytoplasmic localization and translation. In addition, Sqd is required in the nurse cells to repress the translation of *grk* during its transport to and within the oocyte [267]. The accumulation of Sqd in the oocyte nucleus depends on K10, which has been implicated in the regulation of *grk* localization and translation as well [266, 267, 283, 285]. K10 binds directly to Sqd and mutants of *Sqd* and *K10* display similar defects with Grk accumulating along the anterior cortex [285, 287].

Moreover, additional proteins are required to achieve the specific expression of *grk*. For instance, Sqd interacts with Bruno (Bru1) that binds to the *grk* 3' UTR as well [285, 288]. Interestingly, the 3' UTR is required for both, the relocalization of *grk* mRNA to the anterior site and for translational repression implicating a role for Bru1 in these processes [283]. Sqd also associates with other factors including heterogeneous nuclear ribonucleoprotein at 27C (Hrb27C) and the human ortholog of IGF2BP1, IGF-II mRNA-binding protein (Imp) [289, 290]. However, these interactions depend on RNA, indicating that the proteins might function independently of another. Although Hrb27C and Imp associate both with *grk* mRNA, their regulatory role differs. Hrb27C is involved in the localization of *grk* to the antero-dorsal site by binding to its 3' UTR [289]. In contrast, Imp has only a mild effect on *grk* expression during mid-oogenesis. It binds to *grk* 5' UTR and localizes with the mRNA in the oocyte [290].

Translational activation of *grk* during mid-oogenesis is mediated by lengthening of the polyA tail. Properly localized *grk* mRNA undergoes polyadenylation via oo18 RNA-binding protein

(Orb) [291, 292]. Orb recognizes the CPE in the 3' UTR of *grk* and recruits the polyA polymerase wisp. At the antero-dorsal site, translational activation depends on pAbp and Encore (Enc), which interact physically and genetically with each other [293, 294]. Enc is thought to act as a scaffolding protein recruiting different proteins that are required for *grk* translation [294, 295].

1.3.1.2. Regulation of *osk* expression by different RBPs

Similar to *grk* mRNA, *osk* remains translationally silent during its transport and is only activated from stage 9 onwards at the posterior [249, 271]. Localization of *osk* mRNA occurs in three different phases: transport to the oocyte, localization to the posterior pole and anchoring at the posterior [269, 296]. The steps are distinct from each other and require the interplay of different proteins.

Already in the cyst stage, *osk* mRNA is transcribed and transported to the oocyte [248, 269]. The initial transport to the oocyte, similar to *grk* mRNA, depends on the microtubule network, Dynein and Bic-D/Egl [224, 248, 269, 297]. Furthermore, the transport to the oocyte requires the 3' UTR of *osk* [272, 273]. Among others, a stem-loop structure within the 3' UTR is needed for the Dynein-mediated transport of *osk* [298]. However, the localization also depends on additional sequences. Interestingly, the individual *cis*-acting elements present within the 3' UTR are weak localization signals on their own [299]. The sequences might facilitate the exchange with transport factors mediating posterior localization of *osk* mRNA. Cooperated transport between different proteins ensures a dynamic control that can be easily modified depending on the oocyte's needs.

After transport to the oocyte, *osk* needs to localize to the posterior pole. This is first observed at stage 8 and requires the polarized microtubule network [221, 242]. As mentioned above, the plus end-directed transport is mediated by Kinesin 1 [241, 300]. Interestingly, the minus end-directed cargo protein dynactin is also transported to the posterior. Upon localization, it induces growth of the microtubule network [301]. This in turn is important for the stabilization and polarization of the microtubules as well as for the proper localization of *osk* at the posterior cortex.

Several *cis*-elements in *osk* mRNA are essential for its localization to the posterior. For example, the group of Anne Ephrussi demonstrated that splicing of the first intron is required for its transport [302, 303]. Splicing produces the spliced *oskar* localization element (SOLE) that arranges in a stem-loop structure [303]. Disruption of this stem-loop affects *osk* mRNP motility along the microtubule network and consequently its localization. A second function of splicing is the deposition of the EJC at the exon-exon junction, which is another crucial player in the localization of *osk* to the posterior [302-306].

Different dissections of the 3' UTR revealed the presence of diverse regulatory elements that facilitate the localization to the posterior [249, 270, 296]. In fact, the *osk* 3' UTR alone is sufficient for posterior localization [249, 296]. In the background of wild-type *osk*, the 3' UTR induces posterior positioning of a reporter mRNA. Strikingly, this transport is accomplished due to base pairing with the wild-type *osk* containing SOLE and EJC. *osk* molecules can base pair via stem-loop structure located in the 3' half of *osk* 3' UTR [307]. As a result, the molecules associate in multi-copy mRNP complexes and localize to the posterior by a hitchhiking mechanism [277, 307].
The protein Sqd, an important regulator of *grk*, is also required for localization of *osk* [292, 308]. Sqd binds to the *osk* 3' UTR and *Sqd* null mutants affect the microtubule organization. Thus, Sqd is directly involved in the localization of *osk* to the posterior pole [292, 308].

Although the microtubule network is necessary for the posterior transport of *osk*, the actin filament has an important role in this process as well [221, 309]. The actin-related protein Tropomyosin (Tm1) binds directly to *osk* 3' UTR and is required for its posterior accumulation [310, 311]. Tm1 does not interfere with the cytoskeleton network but recruits Kinesin 1, hence modulating *osk* mRNP motility [311, 312].

As described before, anchoring of localized mRNAs is extremely important to enhance mRNA and protein gradients. Transport of *osk* mRNA within the oocyte is only weakly biased towards the posterior. Therefore, accumulation of *osk* requires its tight association with the posterior cortex. This anchoring process is accomplished by the actin filament [237, 246, 247]. Moreover, translation of *osk* mRNA initiates a positive feedback loop as Osk protein binds and anchors its own mRNA [248, 249].

Two protein isoforms are produced by the *osk* gene: Short Osk and Long Osk. Short Osk is essential for germ plasm assembly by recruiting distinct germ plasm components including Vasa [248, 269, 271, 313, 314]. Long Osk on the other hand associates with membranous structures at the posterior and anchors its own mRNA during cytoplasmic streaming [275]. Interestingly, Osk not only binds to its own mRNA but also to others like *nos*, indicating that anchoring of mRNAs by Osk is a common process to restrict posterior localization [313, 315].

To increase the efficiency of posterior localization, mislocalized Osk protein is targeted for degradation by the proteasome [316]. The degradation of Osk requires multi-phosphorylation of the mislocalized protein.

Apart from degradation, the main mechanism to prevent mislocalization of Osk protein is by translational repression. During its transport, Cup travels with *osk* mRNA and silences it through competition with eIF4G for binding to eIF4E (Fig. 1B, 1.1.1). Another mechanism by which Cup can repress translation of target mRNAs is by recruiting the CCR4-NOT1 complex that will lead to deadenylation [317]. In addition, Cup has been implicated to mediate the posterior localization of *osk* by binding to different localization factors [59]. These include a subunit of the EJC complex that is recruited to the *osk* mRNP via Cup.

However, Cup does not only suppress *osk* but also other maternal mRNAs [61]. Its binding specificity is mediated through the RBP Bru1 that recruits Cup to *osk* [60]. Bru1 binds to the *osk* 3’ UTR at distinct sites called Bru1 responsive elements (BREs) [318, 319]. At the *osk* 3’ UTR, three distinct BREs are present that play a crucial role in the regulation of *osk* translation [318, 320]. While two of them (the AB region) are positioned at the proximal 5’ end, the C region is located at the distal end of the 3’ UTR. If all three BRE sites are deleted, *osk* is prematurely translated at stage 5 onwards [318]. However, although Bru1 associates more strongly with the AB region, deletion of the BRE-C alone prevents *osk* translation and embryos display severe patterning defects leading to lethality [318, 320]. Thus, the BRE-C region is not only involved in translational repression but also activation of *osk* [320].

Mutation studies within the C region identified nucleotides 977 to 988 of the *osk* 3’ UTR to be essential for the function of *osk* [273]. This was surprising as Bru1 binding to *osk* was not affected indicating that another protein might mediate the translational activation. Bicoid stability factor (BSF) was suggested to be such a factor of *osk* as it binds to the identified

sequence [321]. Interestingly, while knockdown of *BSF* did neither affect the stability nor the polyA tail length of *osk* mRNA, translation was strongly reduced in late oogenesis. However, since *osk* expression was normal during mid-oogenesis, it was suggested that an additional factor might be needed for early activation of *osk* translation [321].

Although the translational silencing of *osk* by Bru1 depends on Cup, Bru1 can also act independently [322, 323]. When binding to several *osk* transcripts at once Bru1 sequesters the molecules in large mRNPs [322]. The association of multiple *osk* mRNAs in one complex was assumed to prevent the association of translation factors with these transcripts. Such higher order complexes containing translationally repressed *osk* mRNAs have been also proposed to involve the polypyrimidine tract binding protein (PTB) [324]. Nevertheless, the regulatory role of *osk* dimerization and hitchhiking is still under debate, as mutations within the regulatory sequences do not interfere with translation activation [325].

Bru1 also interacts with other regulatory factors including Me31B [60]. In *Me31B* mutants, *osk* is prematurely expressed in the nurse cells, demonstrating that it represses *osk* translation [326]. In addition, Me31B interacts with Cup in an RNA-dependent manner [60]. Both, Bru1 and Me31B colocalize with Cup in the germ plasm. Together, these findings indicates that although the function of Me31B is most prominent during transport to the oocyte and early oogenesis, the protein still associates with *osk* in later stages probably to repress its translation. This hypothesis is in line with the fact that Bru1 alone is not sufficient to repress *osk* translation [327].

Translational activation of *osk* occurs at the posterior pole and involves a set of different proteins as well as *cis* elements. Hrb27C for instance has a dual function in regulation of *osk* translation. On the one hand, it can bind a *cis*-regulatory element in the 5’ UTR activating *osk* translation [289, 327]. On the other hand, Hrb27C interacts with Bru-1 and binds to the BRE-AB region to repress translation [300, 328, 329]. Another protein that influences *osk* translation is Imp. The RBP was shown to bind to the *osk* 3’ UTR at distinct sequences called IMP-binding elements (IBEs) [330]. Mutations within these sequences affect translational activation and anchoring of *osk* but mutations in *Imp* itself did not. These observations imply that another unknown factor binds to the IBEs and acts as translational activator [325, 330].

In addition, Staufen (Stau), a dsRNA-binding protein, has a distinct role in *osk* translational activation as well. The protein associates with *osk* during early stages in the oocyte, travels with the mRNA to the posterior pole and remains associated with it throughout oogenesis [272, 300, 331, 332]. Localization of Stau and *osk* depends on each other, implicating that they are transported together in the same mRNP complex [332, 333]. When Stau is absent, *osk* is not translated and remains at the anterior site of the oocyte [248]. Two distinct domains within the Stau protein are required to transport *osk* to the posterior and to activate its translation [331]. Currently, it is unknown how Stau activates *osk* translation, although this process was shown to be independent of Bru1 [318].

Orb is another well-studied protein that mediates translational activation of mRNAs including *osk*. The RBP associates with *osk* during mid-oogenesis and binds to the CPE located in its 3' UTR [334]. As for *grk*, Orb induces lengthening of the polyA tail [334, 335]. Orb performs this function by interacting with the cytoplasmic polyA polymerases hrg and wisp [117, 118].

In summary, the interplay of the factors mentioned above highlight the complex regulation of *osk*. Many of them have dual functions, including regulation of mRNA stability, transport and translation. While there are numerous information regarding their activity towards *osk*, more work remains to be done to investigate the precise molecular mechanisms underlying these processes.

AIMS OF THIS STUDY

Over the past decades, researchers shed light on the regulatory processes during oogenesis in *Drosophila*. Especially the regulation of *osk* expression has been the focus of many groups. These studies highlight the complex interaction among proteins to safeguard *osk* mRNA to the posterior of the oocyte and regulate its translation. Translational activation of *osk*, however, is a process that remains largely elusive. One main obstacle is the small fraction of mRNAs within the oocyte that is actively translated. Indeed, most mRNAs remain repressed within the oocyte, while only a minor fraction is localized to its destination [336].

To distinguish between *osk* mRNP complexes at the posterior from mislocalized ones and analyze the effect of specific proteins only on actively translated mRNAs is a bottleneck that researchers are still trying to bypass. Given that the composition of mRNP complexes is extremely dynamic, new methods are now established to study them in more detail [337-339]. Although our understanding of *osk* regulation is growing, many questions remain unanswered. Among them is the bivalent role of the BRE-C region in translational repression and activation. Moreover, what happens at the posterior pole to actively derepress translation is not clear yet. Work by the Macdonald lab helped to understand the regulation of *osk* translation and suggested the involvement of a still unknown factor in this process [273, 321].

A recent study by the group of Paul Lasko highlighted the importance of the protein Mkrn1 in *Drosophila* development: depletion of Mkrn1 in early embryogenesis results in defects of segmentation and axis polarity similar to the phenotype observed when *osk* is mutated [191]. Due to these observations, a new regulator of *osk* expression was suggested. Interestingly, knockout of *Mkrn1* displays female sterility highlighting an essential role of the E3 ligase during oogenesis [186]. Although Mkrn1 belongs to a highly conserved family of proteins, little is known about its function and biological relevance.

This study aims to decipher the function of *Drosophila* Mkrn1 and its biological importance during oogenesis. As a new regulator of *osk* mRNA, its role in translational activation was assessed. Also, the specificity of Mkrn1 to interact with the *osk* 3' UTR and the regulatory function of its binding were investigated.

RESULTS

3.1. Identification of Mkrn1 as a new regulator of *Drosophila* oogenesis

3.1.1. Four *Mkrn1*-related genes are present in *Drosophila*

Through the animal kingdom, *Mkrn* genes are present and show a high conservation (Fig. 3) [170, 172]. Overall, the Mkrn protein family shares a common structure consisting of a RING domain and up to four ZnFs. While the RING domain has been shown to ubiquitinate target proteins in human cells, the function of the ZnFs remains more elusive [173, 181, 183, 340]. For instance, it has been proposed that the ZnF domains enable the interaction with RNA due to their structure and indeed mammalian MKRN1 can bind directly to RNA [172, 173, 185]. However, whether the interaction of Mkrn proteins with RNA is mediated via one or a combination of several ZnF domains is still unclear.
In mammals, up to four *Mkrn* family members are present while *Drosophila* and other invertebrates like *C. elegans* comprise only one gene encoding *Mkrn1* (Fig. 3) [170, 172, 173]. In *Drosophila*, three related genes diverged from *Mkrn1* which are not characterized yet: *CG12477*, *CG5334* and *CG5347*. Compared to *Mkrn1*, these genes are intronless with the exception for *CG12477* harboring an intron in its 3' UTR. The gene structure and similarity to *Mkrn1* suggests that these genes might have evolved as retrocopies from *Mkrn1*. Thus, the question emerges whether the encoding proteins have a similar or redundant function to Mkrn1.

Recent studies highlighted an important role of *Mkrn1* during oogenesis and axis polarity in *Drosophila* [186, 191]. To assess whether all four genes have a role in oogenesis or solely *Mkrn1*, we first analyzed the expression pattern of the four individual genes throughout *Drosophila* development by quantitative PCR (RT-qPCR, Fig. 5). As expected, *Mkrn1* mRNA is highly expressed in ovaries and during early embryogenesis. The levels of *Mkrn1* mRNA decreased dramatically after 2.5 h post egg laying which marks the maternal-to-zygotic transition [341, 342]. Together with the high mRNA levels in ovaries, this expression pattern indicates that *Mkrn1* is maternally deposited and degraded upon gastrulation. Compared to *Mkrn1*, the levels of *CG12477*, *CG5334* and *CG5347* peak in pupae and males (Fig. 5). Interestingly, the expression of the three *Mkrn1*-related genes are very similar among each other

with low transcript levels detected in females and embryos. From this observation we conclude that *Mkrn1* has a distinct biological role in *Drosophila* females, especially during oogenesis and early embryogenesis. In contrast, *CG12477*, *CG5334* and *CG5347* seem to have evolved a distinct function that might be needed during spermatogenesis.

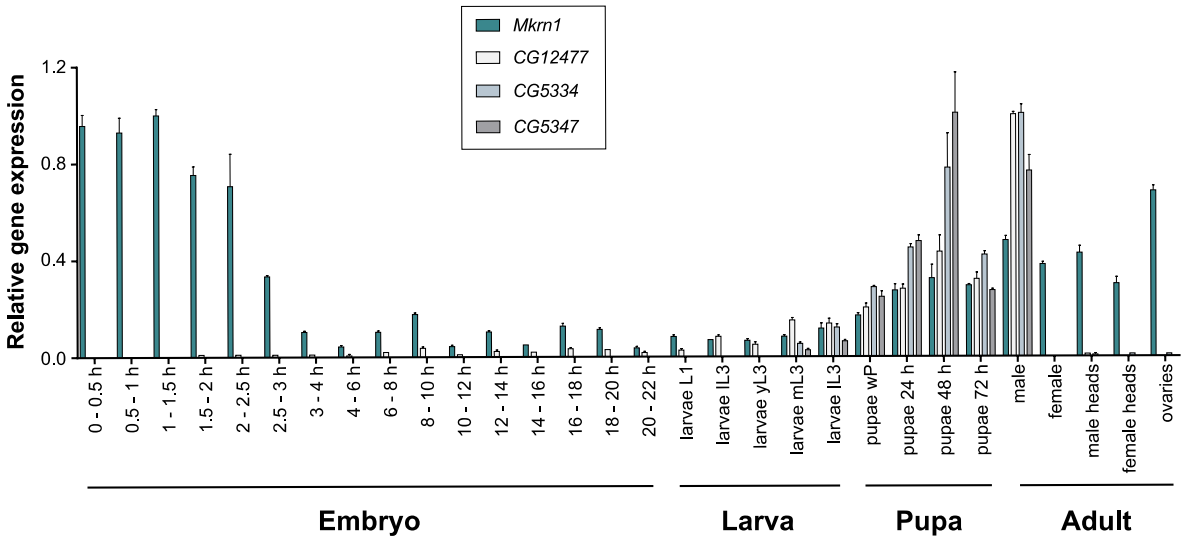

Figure 5. Expression of the four *Mkrn1*-related genes during *Drosophila* development.
RNA was isolated from different developmental stages including embryogenesis, larval stages, pupation and adulthood. *Mkrn1* mRNA levels (turquois) were compared to the transcript levels of *CG12477* (light grey), *CG5334* (gray) and *CG5347* (dark gray). mRNA levels were measured by RT-qPCR and normalized to *Rpl15* mRNA. Error bars depict Stdev, n = 3.

3.1.2. *Mkrn1* mutants display female sterility due to defects during oogenesis

To gain further insights into possible functions of *Mkrn1* genes in *Drosophila*, we applied the CRISPR/ Cas9 system to generate knockout alleles [343]. This well-established system uses the ability of a CRISPR-associated (Cas) endonuclease to cleave DNA. The specificity of the Cas activity relies on a guide RNA (gRNA) that was initially found to be transcribed from the so-called clustered regularly interspaced short palindromic repeats (CRISPR) locus. To utilize this method, the gRNA is specifically designed to contain a homologous region to the target sequence. When binding together with the gRNA to this sequence, Cas9 induces a double-strand break. The induced DNA lesion will subsequently be repaired by non-homologous end

joining introducing mutations within the sequence [344, 345]. We aimed to generate knockouts of *Mkrn1* and *CG12477*. To produce a gene deletion, two gRNAs were designed targeting the genomic locus of *Mkrn1* or *CG12477* (5.2.2.3).

In both cases, the method led to successful deletions of 1854 and 747 nucleotides of the genomic regions of *Mkrn1* and *CG12477*, respectively. Since the deletion in the *Mkrn1* gene comprises the complete coding sequence leading to a molecular null allele, we further refer to it as $Mkrn1^{N}$ (Fig. 6A). For *CG12477*, the induced deletion resulted in a truncated protein including the 18 N-terminal amino acids that we assume to be non-functional (Fig. 6B). For simplicity, I will refer to this mutant as a null allele, $CG12477^{N}$. In addition, we analyzed different mutants of the *Mkrn1* gene generated by our collaborator (Paul Lasko, McGill University, Montreal) comprising either a premature stop codon upstream of the RING domain ($Mkrn1^{S}$) or an 8 amino acid deletion in the ZnF1 ($Mkrn1^{W}$, Fig. 6A) [346]. To exclude off-target effects produced by CRISPR/ Cas9, all mutants were crossed over a respective deficiency line (referred to as $Mkrn1^{Def}$ and $CG12477^{Def}$).

In all cases, mutant flies were viable and did not show any obvious phenotype (data not shown). However, females of all *Mkrn1* mutants depicted sterility defects (Fig. 6C): neither $Mkrn1^{N}$ nor $Mkrn1^{S}$ females produced eggs while the eggs laid by $Mkrn1^{W}$ females did not develop further into larvae. In comparison, *Mkrn1* mutant males were not compromised in their fertility (Fig. 6C). Moreover, $CG12477^{N}$ females and males did not show any fertility defect. Thus, Mkrn1 has an essential role on female fertility. As $Mkrn1^{N}$ and $Mkrn1^{S}$ mutant females did not produce any eggs, we assume that the function of Mkrn1 is essential during oogenesis. On the other hand, CG12477 may act redundant with the two other Mkrn-related proteins expressed in a similar fashion during pupation and in males (Fig. 5). For my PhD, I further focused on Mkrn1 and its role during oogenesis.

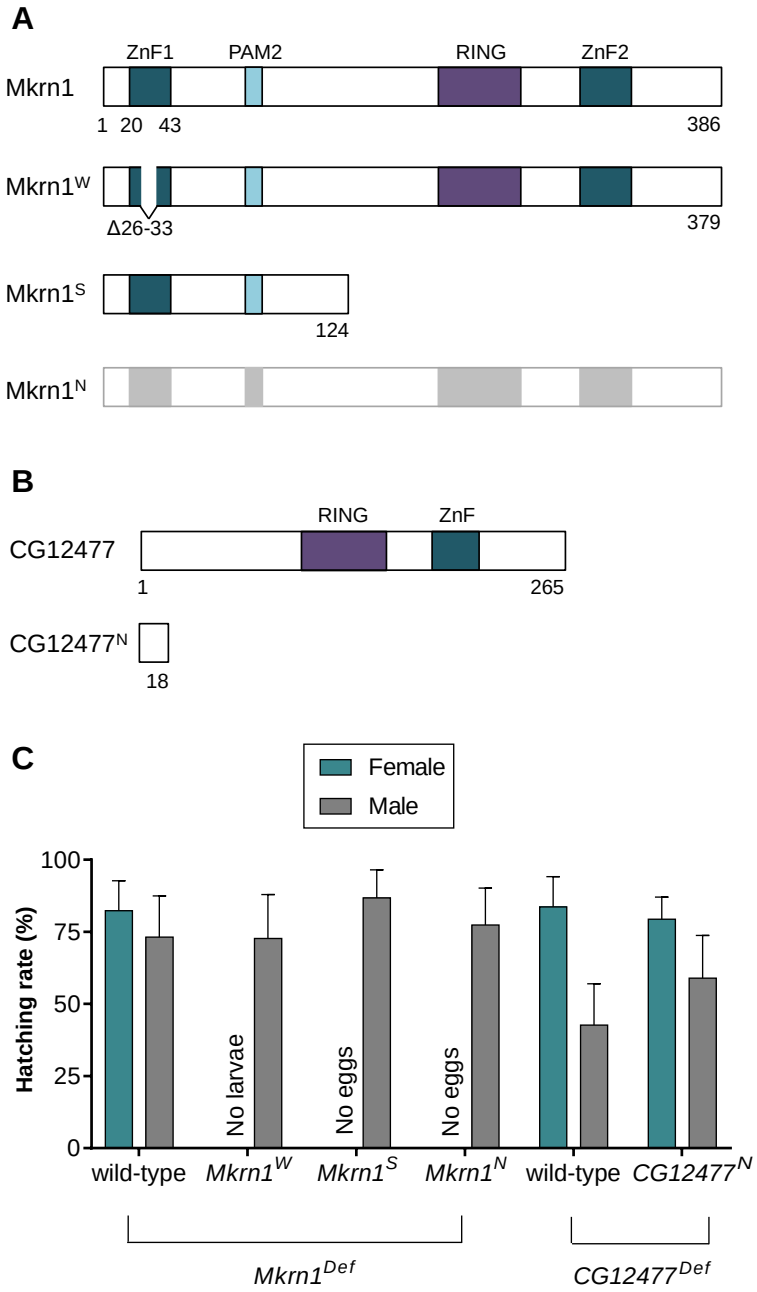

Figure 6. Mutations within the *Mkrn1* gene affect female fertility.
(A) Schematic diagram of the proteins encoded by *Mkrn1* and *CG12477* alleles used to analyze their function *in vivo*. $Mkrn1^{N}$ is a null allele and produces no protein. $Mkrn1^{W}$ comprises a small deletion in the ZnF1 domain while the $Mkrn1^{S}$ allele produces a truncated protein. **(B)** $CG12477^{N}$ leads to a truncated peptide comprising the 18 N-terminal amino acids. **(C)** Hatching rates of *Mkrn1* and *CG12477* mutant flies. Either mutant females or males over the respective deficiency were crossed with wild-type flies of the opposite sex. For males, individual crosses with single males and three to four females were performed. Embryos were collected and the ratio of larvae compared to laid eggs (hatching rate) was determined. At least 3 different biological experiments were performed for females. For males, at least 7 different biological experiments were performed.

Due to the essential role of Mkrn1 during oogenesis, we aimed to examine ovaries in more detail. To this end, immunostainings against the oocyte-specific protein Orb were conducted either in wild-type or *Mkrn1* mutant ovaries. For all alleles analyzed, flies were crossed over

Mkrn1^{Def}. In wild-type as well as *Mkrn1* mutants, the oocyte is determined, which is illustrated by an accumulation of Orb (Fig. 7A). However, compared to wild-type ovarioles, the oocyte is not properly positioned at the posterior pole. Moreover, *Mkrn1*^{N} and *Mkrn1*^{S} egg chambers do not develop further than stage 9. In contrast, a fraction of the *Mkrn1*^{W} mutant ovaries developed into mature eggs. In many *Mkrn1*^{N} and *Mkrn1*^{S} mutant ovaries, egg chambers display condensed DNA and are positive for the apoptotic marker cleaved death caspase-1 (Dcp-1, Fig. 7B).

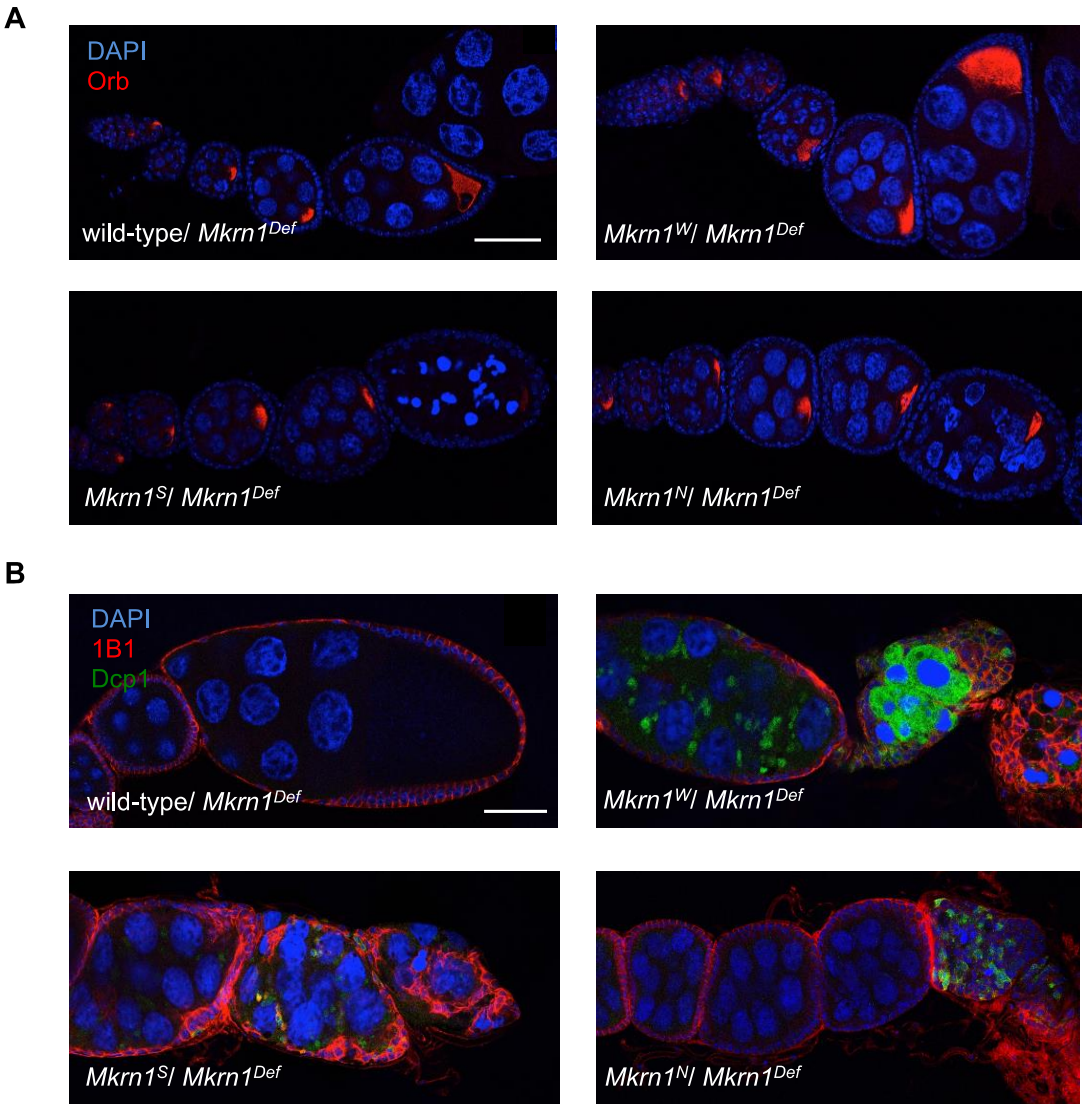

Figure 7. Mutations of the *Mkrn1* gene affect oogenesis.
Ovaries of different *Mkrn1* alleles over *Mkrn1* deficiency were immunostained with (A) α-Orb (oocyte-specific; red) or (B) α-1B1 (cytoskeleton-specific; red) and α-Dcp1, cleaved (apoptotic marker; green). To stain the nuclei, DAPI (blue) was used. Scale bars indicate 50 µm.

To confirm the specificity of *Mkrn1* mutations, rescue experiments were conducted. Therefore, the UAS-Gal4 system was employed. This system uses a yeast regulatory promoter region (UAS), which is targeted by the transcriptional activator GAL4 [347-349]. By applying a tissue-

specific promoter for GAL4, this system is used to drive overexpression of a target sequence. However, as the conventional *UASt* enhancer sequence is not able to promote expression in the germline the *UASp* promoter was used [347, 350]. GAL4 was expressed via the promoter of the *nanos* gene (in the later referred to as *nos>GAL4* driver).

To perform rescue experiments, transgenic flies carrying a FLAG-tagged *Mkrn1* coding sequence under the control of a *UASp* enhancer sequence were utilized [346]. Using a *nos>GAL4* driver, Mkrn1 was specifically overexpressed in ovaries which led to a complete rescue of the $Mkrn1^{N}$ phenotype (Fig. S1A). The rescue flies were also able to lay eggs that further developed into larvae (Fig. S1C). On the other hand, overexpression of Mkrn1 in follicle cells using a *Tj>GAL4* driver did not lead to a rescue (Fig. S1B, S1C). Therefore, we conclude that the tagged *Mkrn1* transgene is functional and Mkrn1 is specifically required in the germline.

3.2. Mkrn1 regulates translation of *osk* mRNA

3.2.1. Mkrn1 ensures correct expression of *osk* during oogenesis

An earlier study performed by the Lasko group suggested that Mkrn1 has a role in embryonic segmentation and axis polarity [191]. Together with the results obtained above, this suggests that deposition of factors involved in axis specification is impaired in *Mkrn1* mutant ovaries. To test this hypothesis, immunostainings of different proteins involved in embryonic patterning were conducted [346]. Although the phenotype of $Mkrn1^{W}$ flies is relatively mild compared to $Mkrn1^{S}$ and $Mkrn1^{N}$, the small deletion in the ZnF1 domain was sufficient to disrupt localization of Osk and Stau proteins [346]. The positioning of Osk at the posterior cortex is a main determinant of pole cell establishment and accomplished via transport of *osk* mRNA during oogenesis [116]. During its localization, *osk* mRNA stays translationally silent. Upon localization to the posterior pole, however, translation of *osk* is activated. This results in a positive feedback loop of Osk anchoring its own mRNA [248, 249].

By western blotting (Fig. 8A), we found a profound reduction of Osk protein in all *Mkrn1* ovary lysates. Compared to the reduced protein levels, stability of *osk* mRNA was hardly affected in the tested mutants (Fig. 8B). Furthermore, in the early stages, we could hardly observe a staining for Osk protein while *osk* mRNA was correctly localized, indicating that translation rather than localization is the primary defect in *Mkrn1* mutant ovaries [346].

To analyze a potential role of Mkrn1 on mRNA stability on a global scale, we further performed RNA-sequencing (RNA-seq) experiments in $Mkrn1^{W}$ ovaries. This analysis was performed only in $Mkrn1^{W}$ mutants as the ovaries comprise mature egg chambers and is thus directly comparable with control ovaries. RNA-seq analysis revealed only a mild change in gene expression compared to heterozygous $Mkrn1^{W}$ ovaries that were used as control (Fig. S2). Moreover, the patterning genes *grk, bcd* and *nos* were not differentially expressed neither. Collectively, these experiments indicate that Mkrn1 has an important role in regulating *osk* translation at the posterior pole but is dispensable for *osk* mRNA localization or stability.

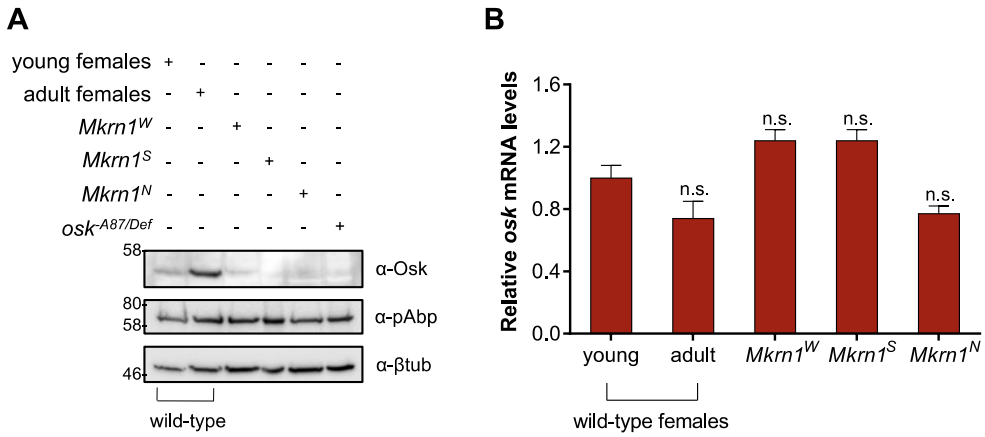

Figure 8. *Mkrn1* mutant ovaries display reduced levels of Osk protein.
(A) Western blot analysis from lysates of $Mkrn1^{W}$, $Mkrn1^{S}$ and $Mkrn1^{N}$ ovaries. Proteins were compared to 1 day-old (young) or 7 day-old (adult) wild-type females. The protein levels of endogenous Osk and pAbp were analyzed. β-Tubulin was used as loading control. Ovary lysates from osk^{A87} females over deficiency were analyzed as control for the α-Osk antibody. **(B)** RT-qPCR analysis of the genotypes examined in (A). The level of *osk* mRNA was normalized to *Rpl15* mRNA. Error bars depict Stedv, n = 2.

3.2.2. Mkrn1 interacts with factors involved in *osk* expression

In order to further examine the function of Mkrn1, we created different mutations in the protein sequence (Fig. S3A). For instance, a point mutation within the RING domain was introduced (H239E, Mkrn1^{RING}) resembling the mutation that has been used for human MKRN1 [181, 183]. Moreover, we deleted the ZnF1 domain in the same manner as present in the *Mkrn1^{W}* allele (deletion of amino acids 26-33, Mkrn1$^{\Delta ZnF1}$) and introduced three point mutations within the ZnF2 domain (C302A, C312A and C318A, Mkrn1^{ZnF2}). Using immunofluorescence, we could observe a cytoplasmic localization of all tested Mkrn1 mutants in *Drosophila* S2R+ cultured cells (Fig. S3B), consistent with previous findings for MKRN1 orthologs [185, 198, 212]. Overexpression of the different Mkrn1 mutant constructs in cells revealed a high stability of Mkrn1^{RING} compared to the others (Fig. S3C). The strong protein stability upon mutation of the RING domain is consistent with reports for mammalian MKRN1, which found that the E3 ligase autoregulates its own protein stability via ubiquitination [181].

Intrigued by the similarities we observed for Mkrn1 compared to the mammalian protein, we asked if Mkrn1 also binds to similar interaction partners. To this end, we overexpressed either Myc-tagged GFP, Mkrn1 or Mkrn1^{RING} in S2R+ cells and isolated the proteins via immunoprecipitation (IP) against the Myc tag. The co-purified proteins were identified using liquid chromatography-tandem mass spectrometry (LC-MS/MS) by label-free quantification (5.2.6.2). Proteins enriched in the Mkrn1 or Mkrn1^{RING} IP were subsequently compared to GFP pulldown. While we could identify 26 significantly enriched interactors of Mkrn1, Mkrn1^{RING} associated with more than 300 proteins compared to the GFP control (Fig. 9). This difference is likely due to the increased stability of the RING mutant. Nevertheless, we observed an overlap of enriched proteins in both IPs including pAbp, Imp, Sqd Hrb27C, larp and Larp4B (Fig. 9) [346]. Moreover, eIF4G, Me31B and Upf1 were enriched as well in the Mkrn1^{RING} interactome (Fig. 9B).

The mentioned proteins are all RBPs with known roles on *osk* expression during *Drosophila* oogenesis (pAbp, Squid, Me31B, Hrb27C) or translation in general (Imp, larp, eIF4G and Larp4B). For instance, mutation of *pAbp* leads to arrest in early oogenesis due to destabilization of *osk* mRNA [110]. Squid on the other hand is required for proper localization of *osk* mRNA by binding directly to its 3’ UTR [292, 308]. Interestingly, mutation of the *Me31B* gene results

in premature translation of *osk* mRNA [326]. In addition, Hrb27C has been implicated in localization and translation of *osk* mRNA by binding to its 3' UTR [327-329].

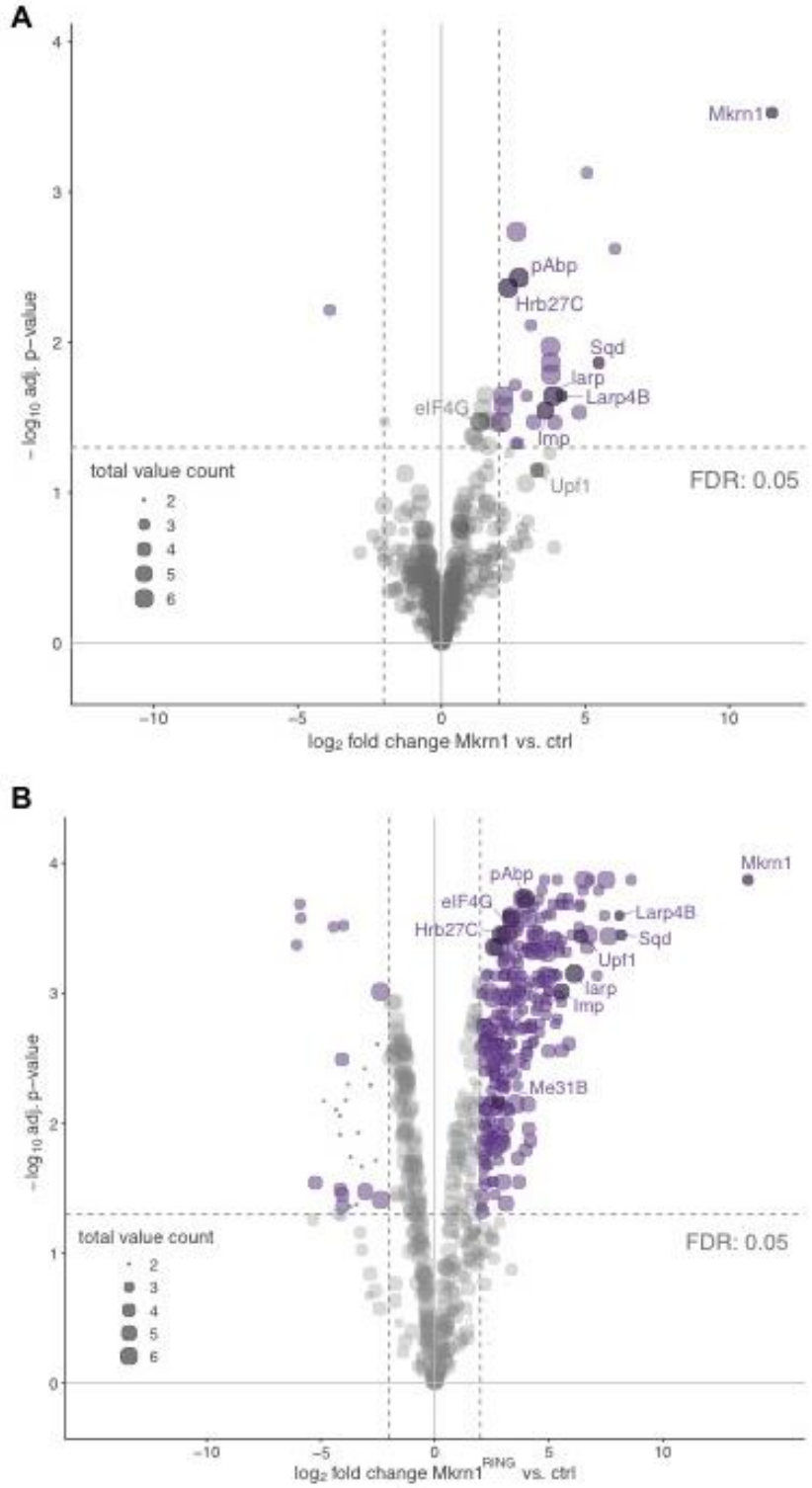

Figure 9. Interactome of Mkrn1 in S2R+ cells.
Either Myc-tagged (A) Mkrn1 or (B) Mkrn1^{RING} was overexpressed in cultured cells and isolated by IP. Interactors of Mkrn1 were identified using LC-MS/MS and label-free quantification. The enrichment of proteins compared to the control (Myc-GFP, ctrl) is depicted in a volcano plot using a combined cutoff of $\log_2$ fold change of 2 and an FDR of 0.05. For both experiments, 3 technical replicates of the ctrl and Myc-Mkrn1 IP were prepared and compared with each other.

To verify the interactome data, we performed reciprocal co-IP experiments of selected proteins with Mkrn1. We overexpressed either GFP- or Myc-tagged pAbp, Imp, Sqd, eIF4G or Me31B in cultured cells and analyzed the binding to co-transfected Mkrn1^{RING}. We used the Mkrn1^{RING} mutant due to its higher stability. With these experiments, we could confirm the interaction between Mkrn1^{RING} and the above-mentioned proteins by western blot analysis (Fig. S4). Furthermore, the binding of Mkrn1^{RING} to its interaction partners did not change when samples were treated with RNase T1, indicating that the interactions are RNA-independent. However, it might still be possible that an intact polyA tail that persisted the RNase treatment might mediate the interactions. We also tested the binding of Mkrn1 to the decapping enzyme Dcp1 and eIF4E that were enriched in the interactome. By co-IP experiments, we could not recapitulate these interactions (Fig. S4F, S4G).

3.2.3. Mkrn1 is stabilized by its interaction with pAbp

Interestingly, the interaction of MKRN1 with pAbp has been shown to be conserved for mammals [173, 185, 212]. Given that we also identified pAbp in the mass spectrometry analysis as one of the main binders of Mkrn1 (Fig. 9), we further focused on this interaction. To confirm a functional association of Mkrn1 and pAbp, we performed co-IP experiments in *Drosophila* ovaries. To do so, FLAG-Mkrn1 was overexpressed via a *nos>Gal4* driver and immunoprecipitated using an antibody against the FLAG tag. As control, protein extracts of *nos>Gal4* driver ovaries were processed in a similar manner. Western blot analysis confirmed our cell culture finding showing a strong association of Mkrn1 with pAbp (Fig. 10A).

Interestingly, many of the proteins identified in the Mkrn1 interactome (Fig. 9) are known to interact with pAbp. Apart from its well-studied interaction with eIF4G, pAbp has been shown to interact with Sqd, Hrb27C, Imp, Me31B, larp and Upf1 [15, 74, 83, 294, 351-353]. Thus, we wondered whether Mkrn1 binds to its identified interactors indirectly via pAbp. To address this question, we increased the stringency of the Myc-based IP using higher amount of salt for the washing steps. Performing an IP with Mkrn1^{RING} as bait, we analyzed the interacting proteins by mass spectrometry compared to GFP. For a more quantitative result that will allow comparison among the different conditions, we used stable isotope labeling by amino acids in

cell culture (SILAC, 5.2.6.2). Due to the different molecular weights of arginine and lysine supplemented in the medium, the cells express proteins labelled with either “heavy” or “light” amino acids [354]. This allows a direct comparison between different conditions, and in this case, different wash stringencies.

Our results were very similar compared to the label-free mass spectrometry method described above (Fig. 9) confirming the reproducibility of the different approaches. As seen before, pAbp was among the strongest interactors of $Mkrn1^{RING}$ and persisted the high salt wash (Fig. 10B). In contrast, the binding of $Mkrn1^{RING}$ to the other strong interactors Sqd and Imp was compromised. Interestingly, although other interactors displayed only a moderate enrichment in the IP, the binding was hardly affected using a higher salt wash. We confirmed the finding by co-IP experiments with a similar salt gradient (150 mM, 300 mM and 500 mM NaCl, Fig. S5A). Together, the data highlight the stable interaction between Mkrn1 and pAbp. Also, Mkrn1 might be part of a complex containing pAbp, Sqd, Imp, eIF4G, Me31B and other proteins.

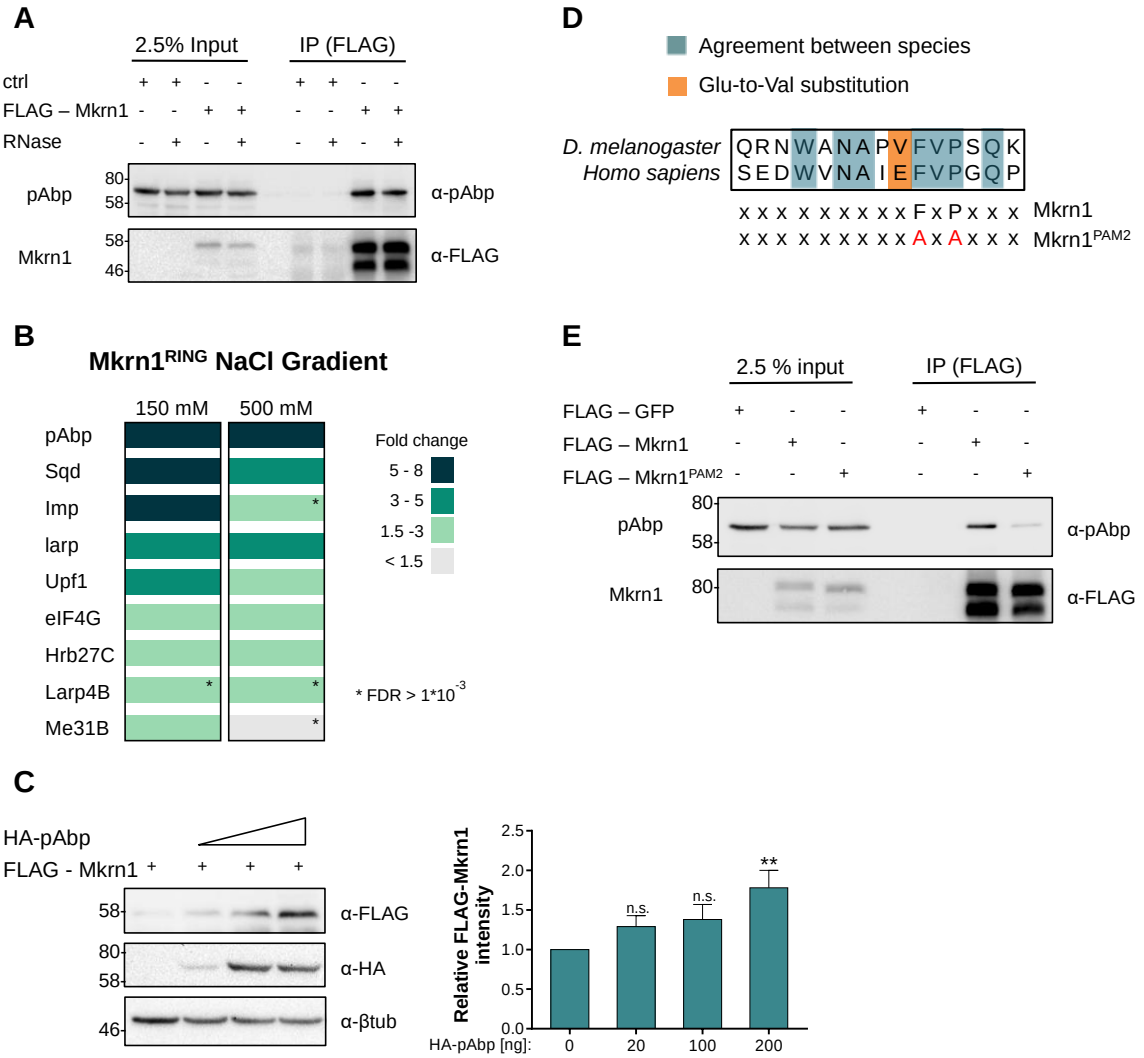

Figure 10. Mkrn1 interacts with pAbp via the PAM2 motif.
(A) pAbp interacts with Mkrn1 in ovaries. co-IP experiments were performed in ovaries and analyzed by western blotting. FLAG-Mkrn1 was overexpressed in ovaries using a *nos>Gal4* driver. To analyze if the interaction with pAbp is mediated by RNA, the IP was performed in the absence or presence of RNase T1. **(B)** The interactome of Mkrn1^{RING} in S2R+ cells was measured by SILAC-based mass spectrometry analysis. Myc-GFP or Myc-Mkrn1^{RING} were immunoprecipitated in the presence of RNase T1 using either 150 mM or 500 mM NaCl for washing. The fold change in the IP of Mkrn1^{RING} over GFP is indicated for the selected proteins. The interaction with pAbp persisted the high salt washes. **(C)** Co-expression of pAbp stabilizes Mkrn1. FLAG-Mkrn1 was co-transfected with increasing levels of HA-pAbp in S2R+ cells. Left: proteins were examined using western blotting. Right: intensities of FLAG-Mkrn1 levels analyzed by western blots were quantified and normalized to intensities of β-tubulin. The relative intensity was further normalized to *Mkrn1* mRNA levels (normalized to *Rpl15* mRNA), which was analyzed by RT-qPCR. Error bars depict SEM, n = 9, n.s. $p > 0.05$, ** $p \leq 0.01$ (one sample t-test). **(D)** Comparison of the PAM2 motif in *Drosophila* and humans. In *Drosophila*, a Glu to Val substitution (orange) is present in the consensus sequence. The PAM2 motif was mutated using two amino acid substitutions at positions 90 and 92 to alanine (F90A and P92A, Mkrn1^{PAM2}). **(E)** Western blot analysis of co-IP experiments between FLAG-Mkrn1 and endogenous pAbp in S2R+ cells. The interaction of pAbp and Mkrn1 is reduced when the PAM2 motif is mutated.

To further examine the link between Mkrn1 and pAbp, Mkrn1 was co-transfected with increasing amounts of pAbp in S2R+ cultured cells. Interestingly, we found that the protein levels of Mkrn1 were elevated in the presence of pAbp in a dose-dependent manner (Fig. 10C).

This observation suggests that pAbp has a positive effect on the stability of Mkrn1. The same effect was seen when using cycloheximide, an inhibitor of translation: when co-transfecting pAbp, Mkrn1 was stabilized compared to GFP used as control (Fig. S5B). Additionally, the cycloheximide treatment displayed degradation kinetics of the proteins detected by western blotting. Compared to GFP, GFP-pAbp and the loading control β-tubulin, Mkrn1 was quickly degraded. As this degradation was observed in the presence of GFP-pAbp, we conclude that Mkrn1 is stabilized by its interaction with pAbp but not protected from degradation.

For mammalian MKRN1, the interaction with PABP has been analyzed in more detail. The PAM2 motif, which is known to mediate the binding of several proteins to PABP, is present in mammalian MKRN1 and mutation of this motif impair the interaction with PABP [111, 174, 212]. In *Drosophila*, the PAM2 motif of Mkrn1 contains an amino acid substitution of glutamic acid to valine (Fig. 10D), raising the question whether the motif is still functional. To analyze whether Mkrn1 can interact with pAbp via this motif in *Drosophila*, we introduced mutations within the PAM2 motif: The phenylalanine at position 10 was shown to be essential for the binding of the PAM2 motif to the MLLE domain [174, 355]. Furthermore, the proline at position 12 is also highly conserved and plays an important role in the binding to MLLE [174]. Therefore, we mutated both amino acids to alanine ($Mkrn1^{PAM2}$, Fig. 10D).
The association with pAbp was analyzed using co-IPs of either Flag-tagged GFP (as control), Mkrn1 or $Mkrn1^{PAM2}$ overexpressed in S2R+ cells. Strikingly, this experiment revealed that the interaction between Mkrn1 and pAbp was compromised when the PAM2 motif is mutated (Fig. 10E). Thus, we conclude that Mkrn1 binds to pAbp via the PAM2 motif although its sequence differs from the mammalian core. Altogether, our findings hint to an important regulatory role of pAbp towards Mkrn1.

3.2.4. The RING domain and PAM2 motif are essential for the function of Mkrn1

Intrigued by the findings that Mkrn1 associates with many factors required for oogenesis, we aimed to analyze the function of Mkrn1 in this process. We first generated transgenic lines carrying different versions of Mkrn1, similar to the constructs used for S2R+ cells (Fig. S3A). These include $Mkrn1^{\Delta ZnF1}$, $Mkrn1^{RING}$, $Mkrn1^{PAM2}$ and human MKRN1 (5.2.2.4 and Table 1).

In addition, we created a double mutant for the ZnF1 and RING domain (Mkrn1$^{\Delta ZnF1+RING}$). Overexpression in ovaries and subsequent western blot analysis revealed that Mkrn1 was expressed at low levels compared to Mkrn1^{RING}, similar to the results obtained in cell culture (Fig. 11A). However, human MKRN1 was hardly detected, which was not observed in cell culture (Fig. M2 and data not shown). Thus, it is possible that the construct is either not properly expressed or the protein more rapidly degraded in ovaries. Due to this observation, we did not further investigate this line.

To test the different mutant versions *in vivo*, we first assayed their ability to interact with pAbp. To this end, either wild-type or mutant Mkrn1 was overexpressed in ovaries and immunoprecipitated using the FLAG tag. In line with previous results, the binding of Mkrn1 to pAbp was strongly reduced when the PAM2 motif was mutated (Fig. 11A). In contrast, the ZnF1 and RING domain are not essential for the interaction with pAbp, although the binding was mildly reduced in these mutants compared to wild-type Mkrn1 (Fig. 11A). Surprisingly, the Mkrn1$^{\Delta ZnF1+RING}$ mutant was not able to interact with pAbp (Fig. S6A). Since the ZnF1 and RING mutations alone have no effect on pAbp binding, we hypothesize that the double mutation might affect either folding or function of Mkrn1. We therefore did not proceed with this mutant.

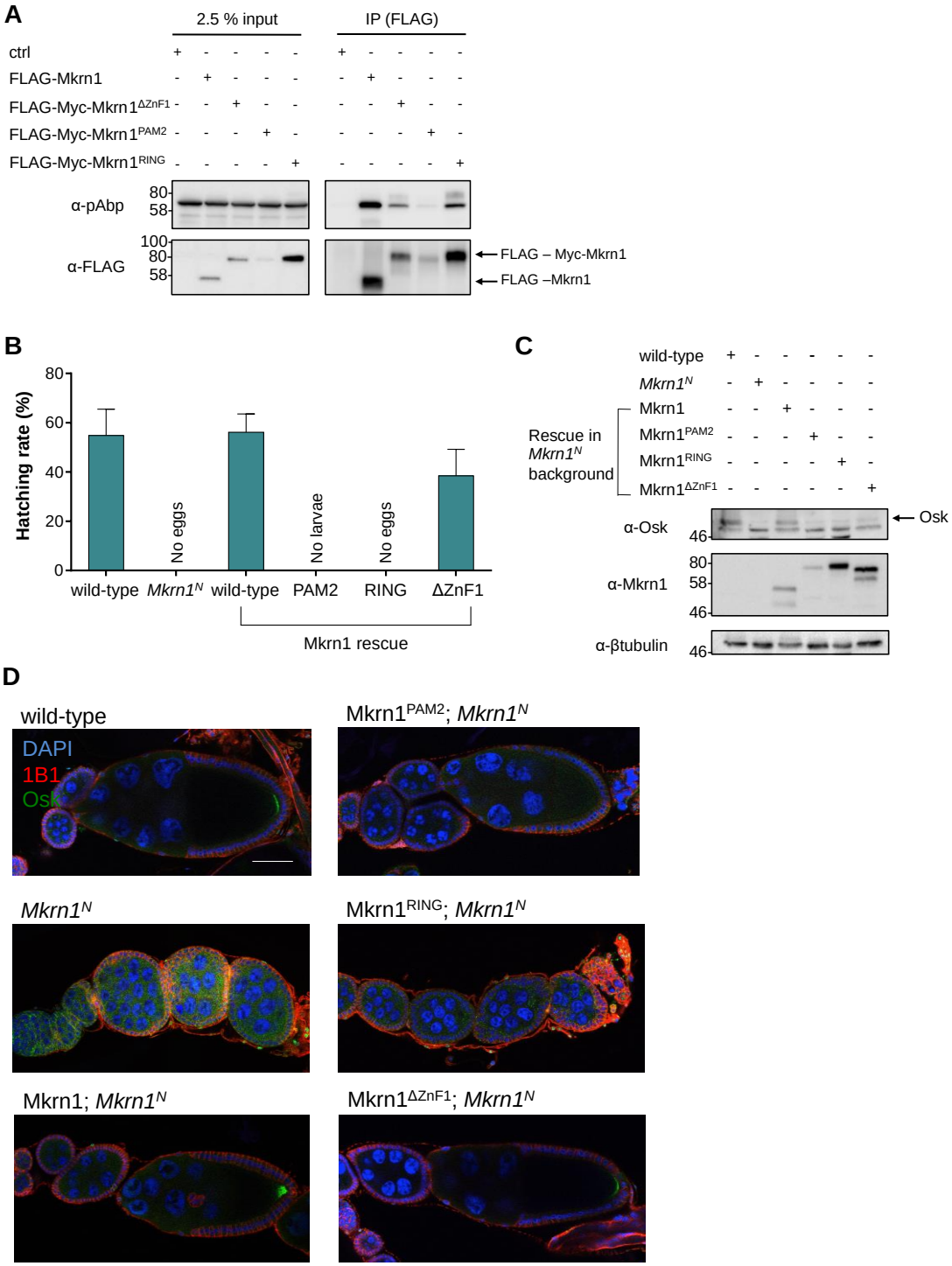

Figure 11. Impact of different domains on Mkrn1 rescuing ability.

(A) co-IP experiments between various FLAG-tagged Mkrn1 proteins and pAbp were analyzed by western blotting. Wild-type or mutant Mkrn1 were overexpressed via a *nos>Gal4* driver in ovaries. Binding of pAbp to Mkrn1 is compromised when the PAM2 motif is mutated. **(B)** Hatching rates of progeny from flies with overexpressed Mkrn1 mutants in the *Mkrn1*^{N} background were analyzed. Females were crossed with wild-type males and hatching rates of the progeny was analyzed. Error bars depict SEM from at least 6 different biological replicates. **(C)** Ovarian lysates from females in (B) were analyzed by western blotting. Osk protein levels are restored when overexpressing wild-type Mkrn1 but not when the PAM2 motif, the RING domain or the ZnF1 are mutated. **(D)** Rescue experiments of wild-type or mutant Mkrn1 in *Mkrn1*^{N} ovaries. FLAG-tagged Mkrn1 was overexpressed in ovaries using a *nos>Gal4* driver line. Ovaries were stained with α-1B1 (cytoskeleton-specific, red) and α-Osk (green). DNA was visualized using DAPI (blue). Although overexpression of wild-type Mkrn1 could restore Osk protein at the posterior, Mkrn1^{PAM2} and Mkrn1^{RING} could not. Scale bar indicate 50 µm.

Given the mislocalization of *osk* mRNA observed in *Mkrn1*^{W} mutants, we wondered whether Mkrn1 travels to the posterior pole maybe even as part of an *osk* mRNP complex [346]. Consistent with this possibility, pAbp was already shown to localize to the posterior [110]. To assess this hypothesis, we analyzed the localization of wild-type and mutant Mkrn1 proteins in ovaries by immunostainings against their FLAG tag. Except for Mkrn1^{PAM2}, a distinct signal at the posterior pole was observed for all mutants tested (Fig. S6B). Thus, we conclude that the interaction with pAbp might be essential for the localization of Mkrn1 to the posterior pole.

To elucidate the role of the PAM2 domain *in vivo*, we performed rescue experiments. We hypothesized, that if the localization of Mkrn1 to the posterior pole is important for its function, then overexpressing Mkrn1^{PAM2} in the *Mkrn1*^{N} background should not rescue the ovarian phenotype. This was only partially the case as many egg chambers could now develop into mature eggs (Fig. S6C). However, none of the laid eggs hatched into larvae (Fig. 11B). Furthermore, immunostainings revealed that Osk protein was not visible at the posterior pole of the oocytes and its protein levels are dramatically reduced (Fig. 11C, 11D). This resembles the phenotypical defects of the *Mkrn1*^{W} allele. Together, these results indicate that the PAM2 motif is not essential for the early function of Mkrn1 in egg maturation but is required for proper assembly of the germ plasm by promoting *osk* translation.

We also analyzed the importance of the RING and ZnF1 domains of Mkrn1 using similar rescue experiments. Interestingly, mutation of the RING domain did not lead to any mature eggs, resembling the *Mkrn1*^{N} phenotype (Fig. 11B-11D, S6C). Thus, the E3 ligase activity of Mkrn1 is essential for its function, probably leading to ubiquitination of critical targets at the posterior pole. In contrast, Mkrn1$^{\Delta ZnF1}$ could rescue the *Mkrn1*^{N} mutants to an extend comparable to wild-type (Fig. 11B-11D, S6C). Although some of the ovaries contained degenerated egg chambers, the majority developed mature eggs with proper localization of Osk at the posterior (Fig. 11D). However, the level of Osk protein was slightly lower compared to wild-type which might explain the minor reduction in embryonic viability (Fig. 11C).

3.3. Mkrn1 competes with Bru1 for binding to *osk* 3' UTR

3.3.1. Mkrn1 associates specifically with *osk* 3' UTR

Due to the pivotal role of pAbp and many other binding partners of Mkrn1 in translation and the reduced levels of Osk protein in *Mkrn1* mutants, we wondered if Mkrn1 is involved in translation of *osk*. If this is the case, then Mkrn1 may bind directly to the mRNA. Mammalian MKRN1 has been shown to be an RBP, but the domain that mediates the association with RNA has not been identified [173, 185]. To analyze if *Drosophila* Mkrn1 can also bind RNA, FLAG-tagged Mkrn1 was isolated via IP in S2R+ cells. Prior to harvesting, the cells were crosslinked introducing covalent bounds between proteins and their bound RNAs. Next, Mkrn1 protein-RNA complexes were isolated via IP using high stringency conditions. The stringent IP conditions exclude the presence of other proteins in the IP fraction. Following IP, the bound RNAs are were trimmed to the desired size with RNase 1. By applying distinct dilutions of the RNase, the RNA-protein complexes exhibit specific sizes due to the different length of the digested RNAs [356]. Radioactive labelling of the RNA can permit to visualize the size shift of the complexes and thus inform about the RNA-binding ability of the isolated protein. Indeed, IP of FLAG-Mkrn1 resulted in a distributed shift when using a low concentration of RNase 1 (1/5000 dilution, Fig. 12A) compared to a focused band at a high concentration (1/50 dilution). Strikingly, mutations in the RING and ZnF2 domains did not interfere with the RNA-binding ability, while deletion of the ZnF1 displayed a reduced signal (Fig. 12A). Thus, we conclude that *Drosophila* Mkrn1 is able to bind RNA and the ZnF1 domain is necessary to mediate this interaction.

Since the experiment above only informs about the RNA-binding behavior of a protein, RNA-IP (RIP) experiments were conducted to identify mRNA targets of Mkrn1. To this end, either FLAG-tagged Mkrn1 or Mkrn1$^{\Delta ZnF1}$ was overexpressed in *Mkrn1*^{N} ovaries. The proteins were isolated via an IP against the FLAG tag and the associated RNA was isolated. To analyze the binding of Mkrn1 to individual mRNAs, the enriched RNA of the IP fractions was examined by RT-qPCR. To monitor the enrichment of specific mRNAs, primers that bind to the respective

3’ UTRs were used. Compared to *grk* and *bcd* mRNA, *osk* mRNA was significantly enriched when using wild-type Mkrn1 as bait (Fig. 12B). Consistent with our previous findings, the interaction was reduced in the Mkrn1$^{\Delta ZnF1}$ RIP highlighting the importance of this domain for binding to RNA.

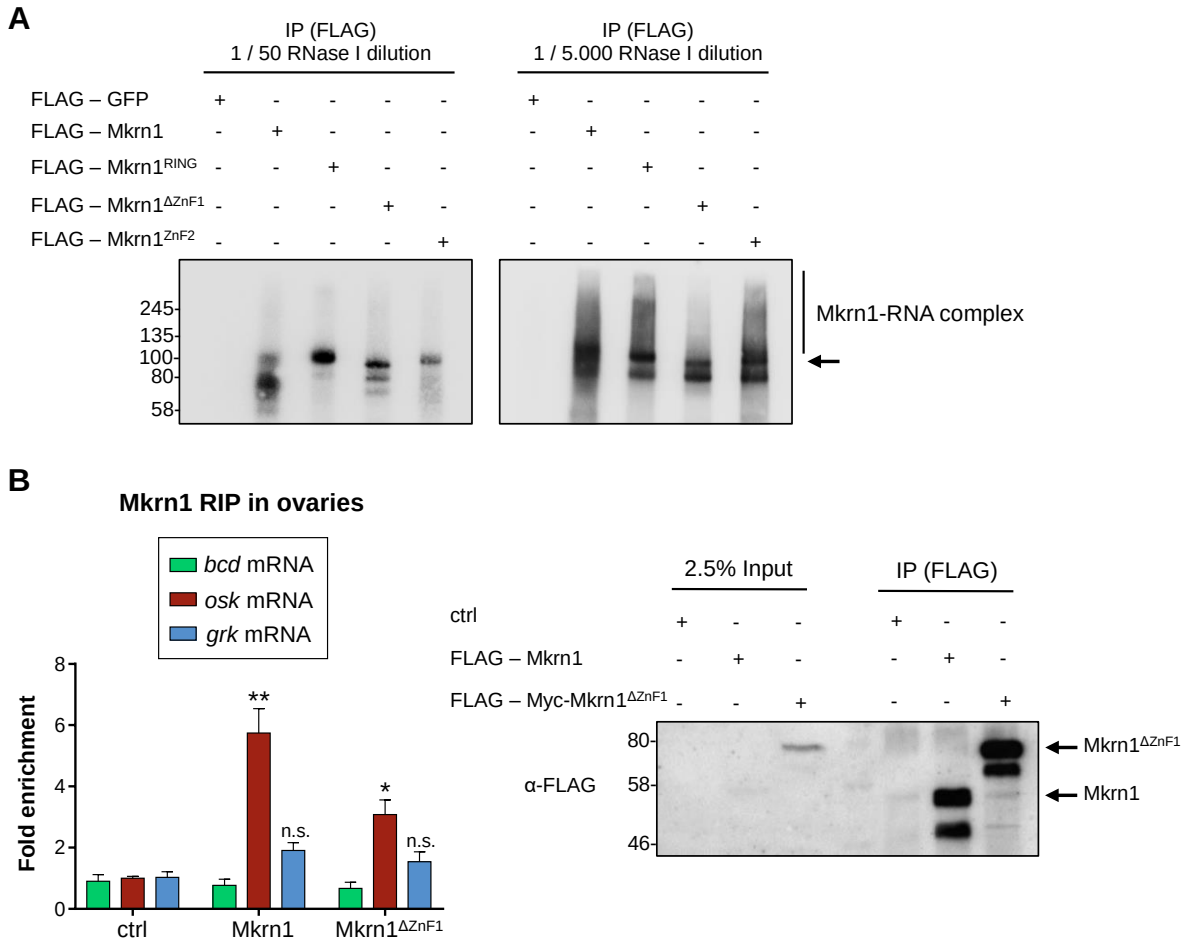

Figure 12. Analysis of the RNA-binding ability of Mkrn1.
(A) Autoradiography experiments to examine the RNA-binding activity of Mkrn1. Different forms of FLAG-tagged Mkrn1 were overexpressed in S2R+ cells and crosslinked to RNA. The RNA-protein complexes were immunoprecipitated and treated with different distinct of RNase I (left: 1/50, right: 1/5000). RNA was radiolabelled and the RNA-protein complexes were separated by SDS-PAGE. The sharp band corresponds to the size of FLAG-Mkrn1 (arrow) while a smear indicates RNA of different sizes bound by Mkrn1. FLAG-tagged GFP was used as control. **(B)** RIP experiments in ovaries. Either FLAG-tagged Mkrn1 or Mkrn1$^{\Delta ZnF1}$ were overexpressed in ovaries using a *nos>Gal4* driver. Left: RNA enriched in the IP fractions was analyzed by RT-qPCR using primers of the respective 3‘ UTRs. As control, ovarian lysate of the *nos>Gal4* driver alone was used. Error bars depict SEM, n = 3, n.s. $p > 0.05$, * ≤ 0.05, ** $p \leq 0.01$ (multiple t-test). Right: Representative western blot of a FLAG-RIP in ovaries. Note that the Mkrn1$^{\Delta ZnF1}$ runs higher due to the additional Myc tag that is not present in the *Mkrn1* transgene.

Intrigued by the RNA-binding ability of Mkrn1, we aimed to analyze the specific binding site on *osk* mRNA. Therefore, iCLIP experiments for Mkrn1 were conducted in cultured cells. As *osk* is hardly expressed in S2R+ cells, a reporter containing the *osk* genomic region under the

control of an *actin* promoter was co-transfected with FLAG-tagged Mkrn1. Similar to autoradiography experiments, the RNA-protein complexes were covalently bound by crosslinking and isolated by FLAG-IP. Sequencing of the bound RNA further allows a nucleotide resolution of the crosslinking events between protein and RNA [256, 356, 357]. We identified 46 mRNAs specifically bound by Mkrn1. Among them was *osk* mRNA, depicting distinct binding sites in the 3' UTR at the BRE-C (Fig. 13A). Interestingly, the binding sites are in close proximity to the polyA tail and upstream of an A-rich sequence (AR) bound by pAbp [110]. In addition, the Mkrn1 binding sites partially overlap with a *cis*-element that is bound by Bru1, the BRE-C. Bru1 is a well-studied translational repressor of *osk* that is known to bind to the BREs located in the *osk* 3' UTR [318, 319]. However, the BRE-C region is also involved in translational activation of *osk* [320].

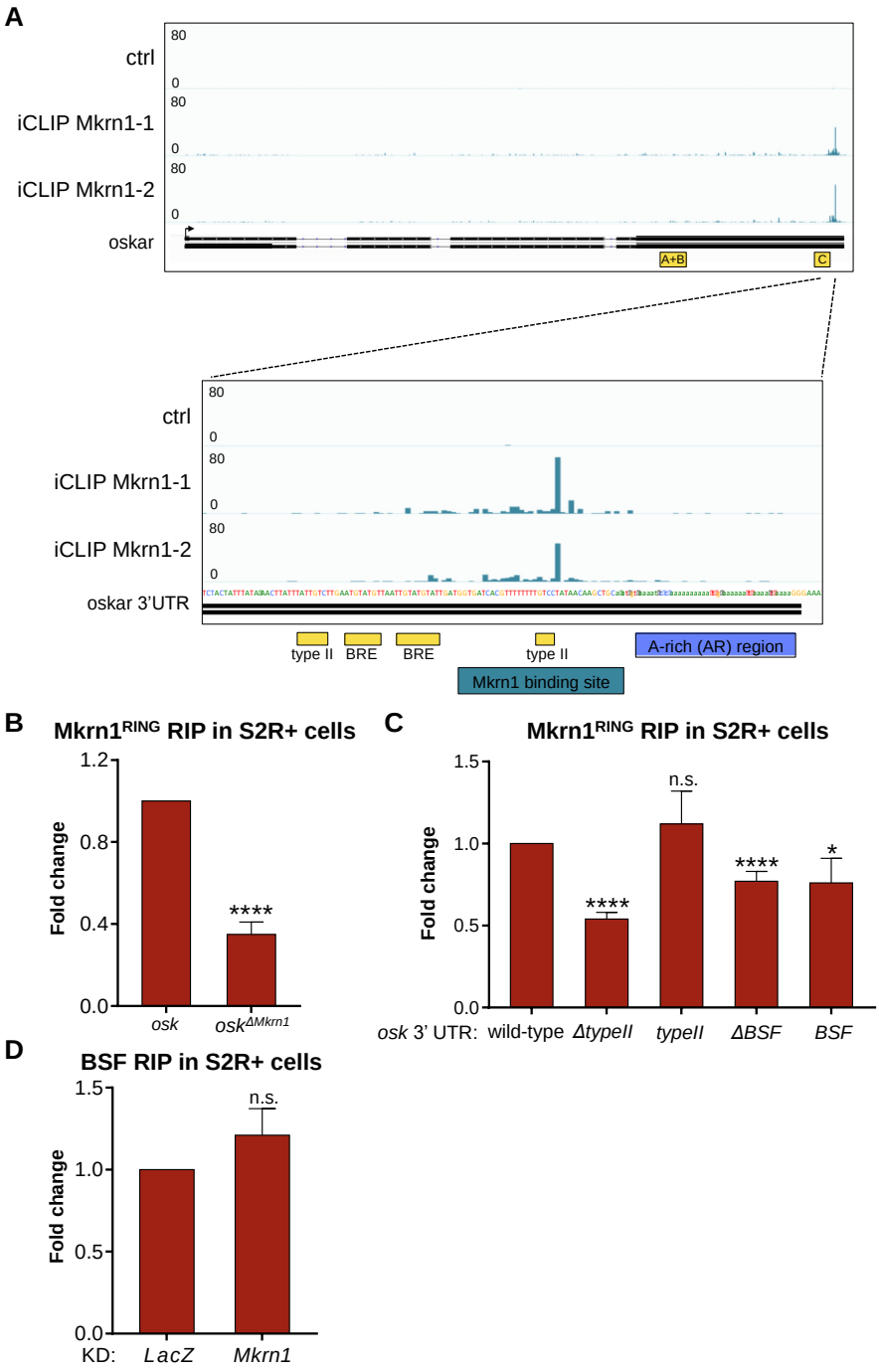

Figure 13. Mkrn1 specifically binds to *osk* 3‘ UTR.
(A) iCLIP experiment of Mkrn1 in S2R+ cells. Above: gene browser view of *osk* depicts crosslinking events of either FLAG-tagged GFP (ctrl) or Mkrn1 (two technical replicates). Mkrn1 binds to the BRE-C region (yellow). Below: close up of the *osk* 3’ UTR indicates that the Mkrn1 binding site (turquois) partially overlaps with the BRE-C region upstream of an AR region (blue). Different *cis*-elements of the BRE-C region are indicated (yellow). **(B and C)** RIP experiments of FLAG-Mkrn1^{RING} in S2R+ cells. Fold enrichment of the *luciferase-osk*-3’UTR reporter was analyzed by RT-qPCR. Fold change is illustrated relative to wild-type *osk* 3’ UTR reporter. **(B)** To validate the binding site of Mkrn1, this site was deleted (*osk*$^{\Delta Mkrn1}$, deletion of nucleotides 955-978 of *osk* 3’ UTR). Error bars depict SEM, n = 4. **(C)** The 3’ type II Bru1-binding site (nucleotides 968-973 of *osk* 3’ UTR) and BSF binding site (nucleotides 976-980 of *osk* 3’ UTR) were either deleted or mutated to analyze the association of Mkrn1 to the reporter constructs in S2R+ cells. Error bars depict SEM, n = 4. **(D)** BSF RIP was performed in either control (*LacZ*) or *Mkrn1* knockdown S2R+ cells. Depicted is the relative change in binding to *luciferase-osk*-3’UTR. Error bars depict SEM, n = 3. (B-D) Data information: n.s. $p > 0.05$, * ≤ 0.05, **** $p \leq 0.0001$ (one sample t-test).

The binding sites identified by iCLIP were further verified using RIP experiments. For this, the 3' UTRs of either *osk* or *grk* were cloned downstream of the *firefly luciferase* coding sequence. The constructs were co-transfected in cells together with either FLAG-tagged GFP (ctrl) or Mkrn1^{RING}. Similar to experiments performed in ovaries, the *osk* 3' UTR displayed a significant enrichment in the Mkrn1 RIP compared to the *grk* 3' UTR (Fig. S7A). Consistently, the binding to the *osk* 3' UTR was reduced when using Mkrn1$^{\Delta ZnF1}$. Furthermore, deletion of the binding site identified by iCLIP (nucleotides 955-978 of *osk* 3' UTR; *osk*$^{\Delta Mkrn1}$, Fig. S7B) diminished the association of Mkrn1^{RING} to the reporter construct (Figs. 13B and S8A).

We next wondered whether Mkrn1 might bind to the 3' type II Bru1-binding site (nucleotides 968-973 of *osk* 3' UTR, Fig. 13A). Interestingly, the group of Paul Macdonald observed that mutation of this sequence abrogates translational activation of *osk* [321]. To test binding of Mkrn1, the distal type II Bru1-binding site was either mutated (nucleotides 968-973 (TGTCC) mutated to CGCTT; *osk*^{typeII}, Fig. S7B) or deleted (nucleotides 968-973 of *osk* 3' UTR; *osk*$^{\Delta typeII}$, Fig. S7B). RIP experiments in S2R+ cells using FLAG-Mkrn1^{RING} revealed that the association with *osk* 3' UTR did not change when mutating the 3' type II Bru1-binding site (Fig. 13C, S8B). However, deletion of the element reduced the binding of Mkrn1^{RING} with *osk* by around half. Collectively, these results confirmed that Mkrn1 binds specifically to the 3' UTR of *osk* via the ZnF1 domain and that its binding site partially overlaps with the Bru1 binding site.

Another factor that has been shown to activate *osk* is BSF. Knockdown of *BSF* impairs *osk* translation during late oogenesis [321]. Interestingly, the binding site of BSF at *osk* overlaps with the Mkrn1 binding site [321]. Therefore, we asked if Mkrn1 and BSF may act in concert to regulate *osk* translation. To this end, we first assessed a possible interaction between the two proteins by co-IP experiments. Interestingly, we observed that BSF binds to Mkrn1^{RING} in an RNA-independent manner (Fig. S8C). Next, generated a *luciferase-osk*-3'UTR reporter harboring a mutation in the BSF binding site (nucleotides 976-980 (TAACA) of *osk* 3' UTR mutated to ATTGT; *osk*^{BSF}, Fig. S7B) or a deletion. Interestingly, a mild but reproducible effect on Mkrn1 binding was observed with both mutant reporters (Fig. 13C, S8D). Given that the absence of Mkrn1 impaired *osk* translation in earlier stages than observed for *BSF* knockdown, we speculate that Mkrn1 might recruit BSF to *osk* 3' UTR [321]. To examine this hypothesis, RIP experiments of FLAG-tagged BSF were performed in S2R+ cells subsequently to knockdown of *Mkrn1* mRNA. However, the binding of BSF was unchanged compared to control cells (Fig. 13D, S8E). Therefore, we conclude that Mkrn1 does not affect the interaction of BSF with *osk* 3' UTR in S2R+ cells.

3.3.2. The interaction of Mkrn1 to *osk* 3' UTR depends on pAbp

Due to our observations of pAbp interacting and stabilizing Mkrn1, we hypothesized that the protein might facilitate the binding of Mkrn1 to *osk* 3' UTR. This argument is supported by the fact that pAbp binds in close proximity to the Mkrn1 binding site at the AR region of *osk* [110]. To test if pAbp has indeed a regulatory role on Mkrn1 binding, the AR region was deleted in the *luciferase-osk*-3'UT*R* reporter (nucleotides 987-1019 of *osk* 3' UTR; $osk^{\Delta AR}$, Fig. S7B). Intriguingly, RIP experiments in S2R+ cells revealed a reduction in $Mkrn1^{RING}$ binding to the reporter when the AR is absent (Fig. 14A, S9A). Moreover, the observed reduction is of similar extent as the deletion of the Mkrn1 binding site ($osk^{\Delta Mkrn1}$, Fig. 13B), suggesting that the AR sequence has an important function in the association of Mkrn1 to *osk*. The close proximity of the AR to the Mkrn1 binding site might enhance the probability of pAbp to interact with Mkrn1, which in turn leads to the increased stability of Mkrn1. Consistently, we observed a decreased enrichment of *osk* 3' UTR in the $Mkrn1^{RING}$ RIP upon knockdown of *pAbp* in S2R+ cells (Fig. 14B, S9B). Since the knockdown of another interaction partner, *Imp*, did not result in a change of Mkrn1 binding, we conclude that this effect is specific for pAbp (Fig. 14B, S9C).

If the diminished association of Mkrn1 to *osk* is indeed dependent on the interaction with pAbp, mutation of the PAM2 motif should interfere with the binding to *osk* as well. Therefore, the interaction of $Mkrn1^{PAM2}$ with *osk* was assessed in S2R+ cells. In line with RIP experiments in ovaries, we observed a reduced binding of Mkrn1 to *osk* when the ZnF1 domain is deleted (Fig. 14C, S9D). Interestingly, a similar reduction was observed when mutating the PAM2 domain. Furthermore, a double mutant comprising the deletion of the ZnF1 as well as a mutation of the PAM2 motif ($Mkrn1^{\Delta ZnF1+PAM2}$) strongly impaired the association between Mkrn1 and *osk* (Fig. 14C, S9D). Thus, Mkrn1 binds directly to *osk* 3' UTR upstream of an AR region and this binding is facilitated or stabilized by the interaction with pAbp. Mkrn1 interacts with *osk* via its ZnF1 domain that does not interfere with the binding to pAbp.

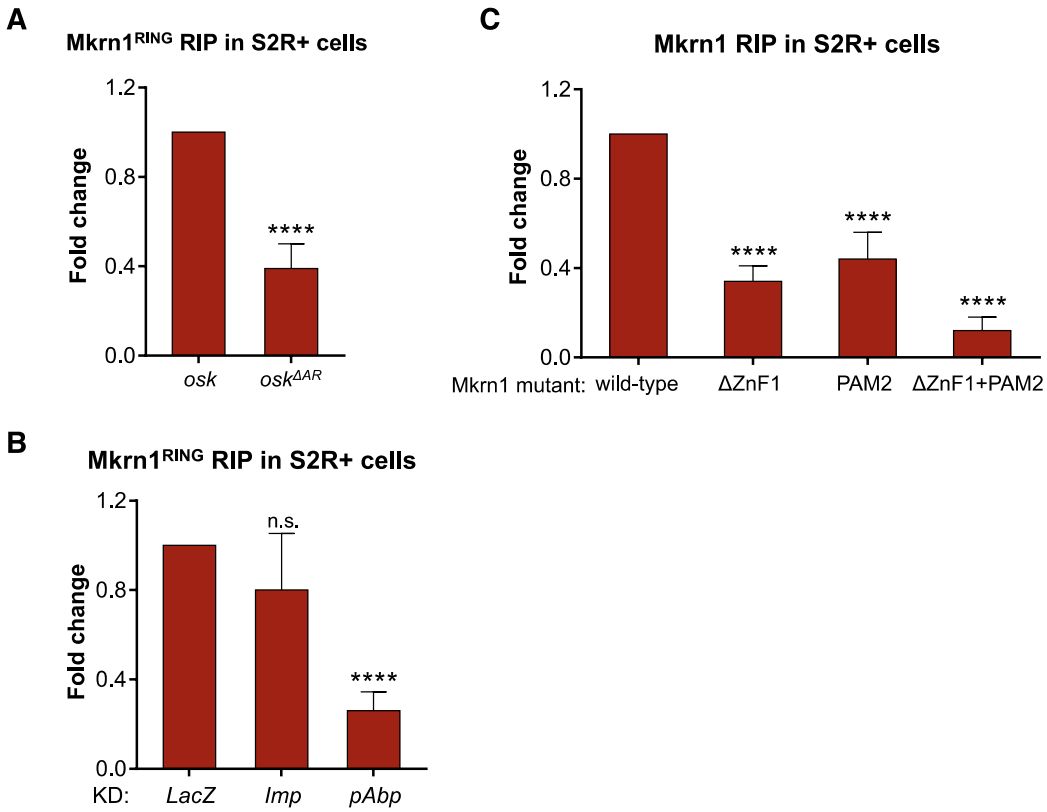

Figure 14. Binding of Mkrn1 to *osk* 3‘ UTR depends on pAbp.
(A-C) RIP experiments of FLAG-Mkrn1 to the *luciferase-osk*-3’UTR reporter in S2R+ cells. Error bars depict SEM. n.s. $p > 0.05$, **** $p \leq 0.0001$ (one sample t-test). **(A)** A deletion of the A-rich region of *osk* 3’ UTR ($osk^{\Delta AR}$, deletion of nucleotides 987-1019 of *osk* 3’ UTR) was introduced to examine the binding of $Mkrn1^{RING}$. Fold enrichment displays the difference of immunoprecipitated $osk^{\Delta AR}$ reporter compared to IP with wild-type *osk* 3’ UTR. n = 4. **(B)** RIP experiments were performed in either control (*LacZ*), *Imp* or *pAbp* knockdown cells. Fold change of $Mkrn1^{RING}$ compared to the *LacZ* knockdown is displayed. n=3. **(C)** RIP experiments of different versions of FLAG-Mkrn1 binding to *luciferase-osk*-3’UTR. Fold change of binding to *osk* 3’ UTR is depicted compared to wild-type Mkrn1. Binding of Mkrn1 depends on the ZnF1 domain as well as the PAM2 motif. $n \geq 3$.

3.3.3. Mkrn1 antagonizes the binding of Bru1 to *osk* 3’ UTR

As mentioned above, the Mkrn1 binding site at *osk* 3’ UTR partially overlaps with the BRE-C. Given the positive role of Mkrn1 on *osk* translation and the fact that interaction with *osk* occurs at a region bound by the translational repressor Bru1, it is possible that Mkrn1 and Bru1 compete for binding to *osk*. To gain insights into this possible scenario, the interaction of both proteins and the well-studied binding partner of Bru1, Cup, was examined. Intriguingly, co-IP experiments in S2R+ cells showed that $Mkrn1^{RING}$ binds to both, Bru1 and Cup independently of RNA (Fig. S10A, S10B).

To next address whether Mkrn1 influences Bru1 binding to *osk* mRNA, we performed RIP experiments upon depletion of *Mkrn1*. We found that knockdown of *Mkrn1* lead to an increased association of Bru1 with *osk* (Fig. 15A, S10C). In contrast, the interaction with other factors involved in *osk* regulation such as pAbp, Sqd and Imp was not affected (Fig. 15A, S10D, S10E). To confirm that Mkrn1 indeed influences the binding of Bru1 to *osk*, we repeated the RIP experiment in the absence of *pAbp*. Consistently, the *luciferase-osk*-3'UTR reporter was enriched in RIPs of GFP-Bru1 when *pAbp* was depleted (Fig. 15B, S11A). We also tested the association of Bru1 to the *osk* reporter deleted for the AR region. RIP experiments revealed a mild increase in Bru1 binding when using the $osk^{\Delta AR}$ reporter (Fig. S11B).

As the experiments above were performed in *Drosophila* cultured cells, we aimed to confirm our findings *in vivo* as well. To this end, RIP experiments were conducted in ovaries using endogenous Bru1 antibody. Since $Mkrn1^{N}$ ovaries do not develop to late-stage egg chambers, ovarian extract from $Mkrn1^{W}$ flies was used. Heterozygous $Mkrn1^{W}$ ovaries were prepared in a similar manner as control. Consistent with the experiments in S2R+ cells, the interaction between Bru1 and *osk* mRNA increased in $Mkrn1^{W}$ mutant ovaries (Fig. 15C, S11C). Together, these results suggest that Mkrn1 competes with Bru1 for binding to the *osk* 3' UTR.

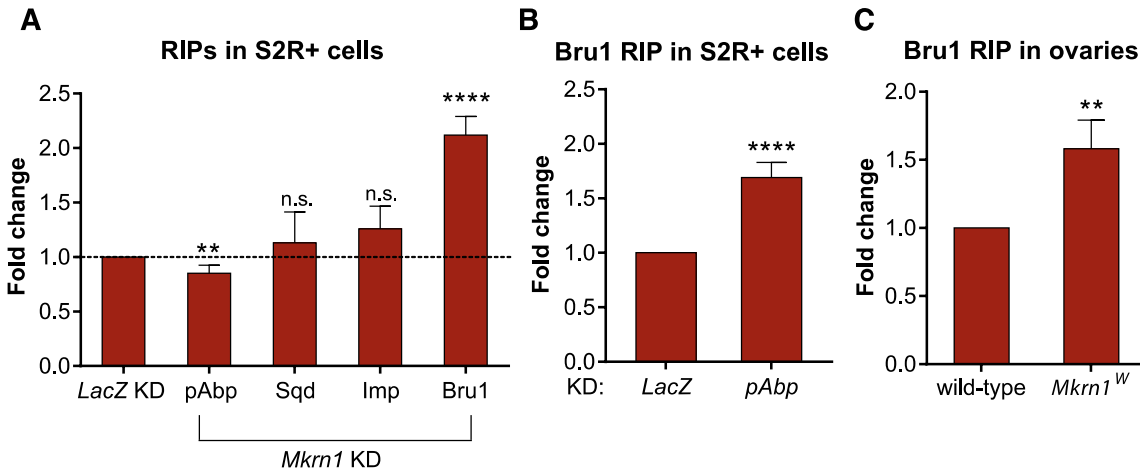

Figure 15. Mkrn1 competes with Bru1 for binding to *osk* mRNA.
(A) RIP experiments of different proteins in either *LacZ* (control) or *Mkrn1* knockdown condition in S2R+ cells. Fold change represents the difference in enrichment to *osk* 3' UTR compared to control knockdown. Error bars depict SEM, n ≥ 4. **(B)** RIP experiments of GFP-tagged Bru1 in S2R+ cells either depleted for *LacZ* or *pAbp* mRNA. Fold change of *osk* 3' UTR upon *pAbp* knockdown is depicted. Error bars depict SEM, n = 3. (C) RIP experiments in ovaries for endogenous Bru1. Fold change depicts enrichment of endogenous *osk* in heterozygous (wild-type) compared to homozygous $Mkrn1^{W}$ ovaries. Error bars indicate SEM, n = 4. (A-C) Data information: n.s. $p > 0.05$, ** ≤ 0.01, **** $p \leq 0.0001$ (one sample t-test).

3.3.4. Mkrn1 does not influence Bru1 dimerization nor its interaction with Cup

Bru1 was recently shown to be phosphorylated resulting in its homodimerization [358]. The phosphorylation relieves the repressive effect of Bru1 and stimulates *osk* translation. We thus wondered whether Mkrn1 mediates *osk* translation by affecting Bru1 phosphorylation or homodimerization. To test this possibility, co-IP experiments were performed in S2R+ cells. Using two differently tagged versions of Bru1, the homodimerization can be examined by western blotting. We did, however, not observe a change in Bru1 dimerization upon knockdown of *Mkrn1* (Fig. S12A).

Apart from the dimerization, the function of Bru1 is regulated via its interaction with Cup [60]. To elucidate a possible role of Mkrn1 in regulating the interaction between Bru1 and Cup, co-IP experiments were conducted in cultured cells. Compared to the control, depletion of *Mkrn1* did not affect the interaction of Bru1 with Cup (Fig. S12B). This finding suggests that in $Mkrn1^{W}$ ovaries, Cup should also associate stronger with *osk* mRNA via its interaction to Bru1. Therefore, we performed RIP experiments using an endogenous Cup antibody with ovarian extracts from $Mkrn1^{W}$ flies. Surprisingly, the interaction of Cup with *osk* was not altered in the $Mkrn1^{W}$ mutant (Fig. S12C). These results indicate that Mkrn1 targets specifically Bru1 but does not interfere with Cup.

Since Mkrn1 is an E3 ligase, it is possible that it exerts its function via ubiquitination of Bru1. To test this hypothesis, we performed a ubiquitination assay in S2R+ cells: Bru1, Cup and Imp were overexpressed in either control or *Mkrn1* depleted cells and subsequently isolated by IP. The stringent conditions employed during the IP allowed isolation of the respective protein without other interaction partners (5.2.6.5). The ubiquitination was further tested by western blotting using an antibody against endogenous Ub. However, neither Bru1, Cup nor Imp displayed ubiquitination in any of the conditions tested (Fig. S13A, S13B), suggesting that Mkrn1 does not ubiquitinate either of the proteins.
Interestingly, pAbp depicted a polyubiquitin signal in control conditions, which was clearly lost upon *Mkrn1* depletion (Fig. S13B). This indicates that pAbp is targeted for ubiquitination, perhaps directly via Mkrn1.

3.3.5. Mkrn1 has no global effect on translational regulation

Human MKRN1 has been recently identified to regulate aberrant translation of A-rich sequences [173]. Readthroughs of the ribosome into polyA stretches results in recruitment of MKRN1 and ZNF598. The two proteins subsequently induce RQC by ubiquitination of ribosomal proteins and PABP [161, 162, 173]. In *Drosophila*, Mkrn1 binds upstream of an A-rich sequence at the *osk* 3' UTR and this association strongly depends on pAbp. Moreover, Mkrn1 influences the ubiquitination of pAbp. Thus, we wondered if *Drosophila* Mkrn1 might have a similar effect on RQC. To test this possibility, we took advantage of a flow cytometry-based assay that has been used before to study RQC in human cells [161]. This assay employs a reporter consisting of *GFP* and *RFP* that are separated by viral *P2A* sequences (Fig. S14A). The *P2A* element leads to skipping of the peptide bond formation without terminating translation [359-361]. A FLAG-tagged stalling reporter (SR) is inserted between the *GFP* and *RFP* coding sequences, which contains a stretch of adenosine triplets encoding for lysine $(K^{AAA})_N$ [161]. If the SR does not contain lysine codons translation is not affected. This $(K^{AAA})_0$ SR leads to GFP and RFP being equally translated (Fig. S14A). However, if the SR consists of a longer stretch of adenosine triplets as for instance in $(K^{AAA})_{20}$, the ribosome stalls and translation abrogates resulting in a shifted ratio towards GFP (Fig. S14A) [161].
In human cells, knockdown of either *ZNF598* or *MKRN1* rescues this ratio by increasing translation of RFP due to suppression of ribosome stalling [161, 173]. Employing the same reporter in *Drosophila* S2R+ cells revealed a similar shift towards GFP when using an high number of lysine codons (Fig S14B). In line with observations in humans, this shift was not visible when using a nucleotide stretch encoding for arginines $(R^{CGA})_{10}$ [161]. However, knockdown of either *Mkrn1* nor the ortholog of human ZNF598, *CG11414*, did not rescue translation of RFP (Fig. S14B). This result suggests that the RQC pathway in *Drosophila* is not regulated by Mkrn1.

As many of the Mkrn1 interactors are involved in translation, we argued that Mkrn1 might have a global effect on protein synthesis. To test this, mass spectrometry-based proteome analysis of S2R+ cells was performed in different conditions. However, neither knockdown nor the overexpression of Mkrn1 did interfere with protein synthesis on a global scale (Fig. S15A, S15B). Thus, these results suggest that the function of Mkrn1 on translation is highly specific.

3.4. The regulation of Mkrn1

3.4.1. The function of Mkrn1 is not regulated by phosphorylation

As *osk* expression undergoes a high degree of regulation, Mkrn1 itself might be tightly regulated to ensure a spatial and temporal activation of translation. One possible way to regulate the activity, localization and stability of a protein is by phosphorylation. Employing the online prediction tool PTMcode2 for possible phosphorylation sites in Mkrn1 identified only one residue, serine 343 (Fig. S16A) [362]. To analyze if Mkrn1 is regulated via phosphorylation of this serine, two different point mutations were introduced that either inhibit the usage of the amino acid for phosphorylation (mutation of serine to alanine, $Mkrn1^{S343A}$) or mimic phosphorylation (mutation of serine to aspartic acid, $Mkrn1^{S343D}$). Together with wild-type Mkrn1, the mutants were overexpressed in S2R+ cells and binding to *osk* 3' UTR was assessed by RIP experiments. Neither the phosphosilant nor the phosphomimetic mutant had an impact on binding to the *luciferase-osk*-3'UTR reporter (Fig. S16B). Similarly, we did not observe a change in the interaction with pAbp for any of the mutants (Fig. S16C), suggesting that Mkrn1 might not be regulated by phosphorylation.

3.4.2. Mkrn1 autoregulates itself via the RING domain

Mammalian MKRN1 has been shown to autoubiquitinate itself resulting in its own degradation by the proteasome [173, 181, 184]. A mutation of the RING domain abolishes this autoregulation leading to elevated protein levels. Since we observed a similar effect in *Drosophila*, we hypothesized that this autoregulation might be conserved. To test this, FLAG-tagged versions of the different Mkrn1 mutants were overexpressed in S2R+ cells. As described before, an IP against the FLAG tag was performed in order to isolate Mkrn1 applying stringent conditions (5.2.6.4.1). Western blot analysis revealed that Mkrn1 depicts a polyubiquitination pattern similar to its human ortholog (Fig. 16A) [173, 181, 183, 340]. Intriguingly, this signal

is present in all mutants except for Mkrn1^{RING}, indicating that the RING domain mediates polyubiquitination of Mkrn1.

If Mkrn1 directly mediates its own polyubiquitination, the E3 ligase should be able to homodimerize. To this end, Mkrn1 proteins containing different tags were overexpressed in S2R+ cells and isolated by IP. The co-IP experiments revealed that Mkrn1 is indeed able to bind to itself (Fig. 16B). Furthermore, we also observed that the Mkrn1^{RING} mutant can bind to itself (data not shown). Thus, our data suggests that Mkrn1 binds and polyubiquitinates itself, probably to autoregulate its protein levels within the cell.

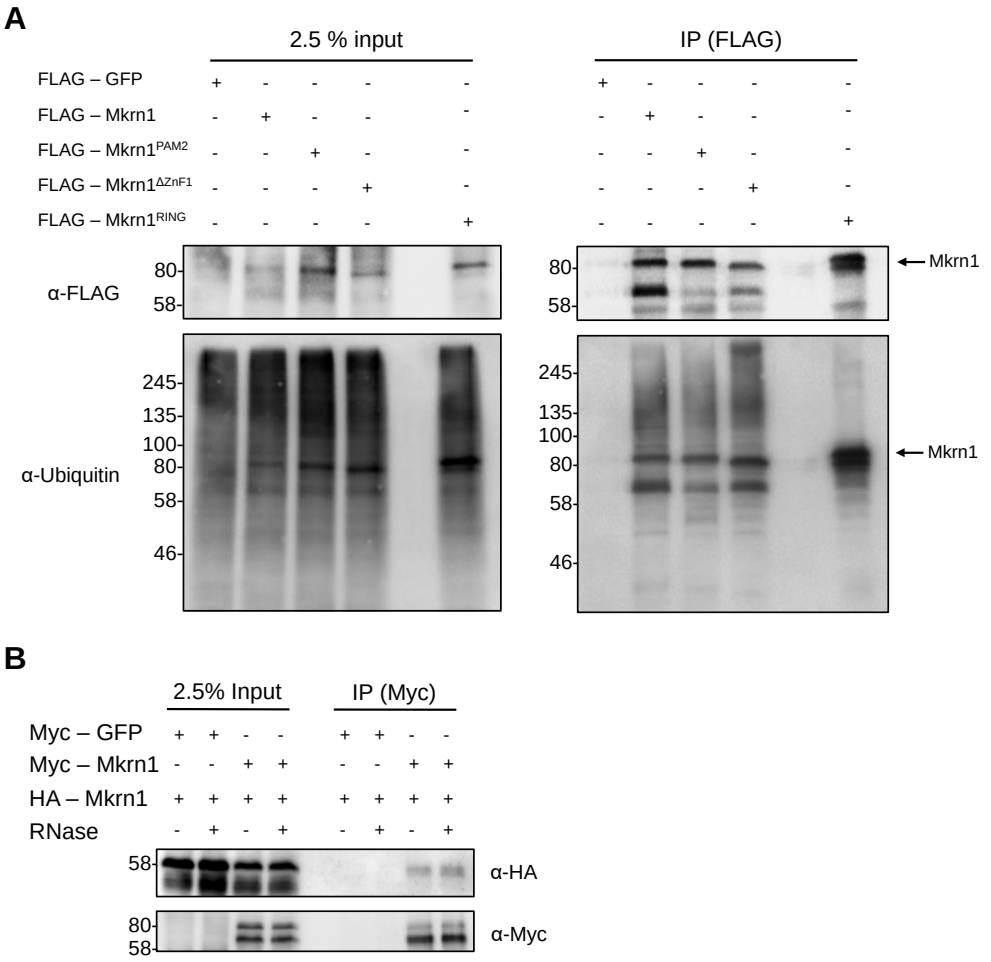

Figure 16. Mkrn1 ubiquitinates itself.
(A) Ubiquitination assay of different Mkrn1 mutants in S2R+ cells. FLAG-tagged GFP or different Mkrn1 mutants were overexpressed and immunoprecipitated. IP efficiency and ubiquitination pattern were analyzed by western blotting. Ubiquitination is diminished in the Mkrn1^{RING} mutant. **(B)** Western blot depicting co-IP experiments of differently tagged versions of Mkrn1. HA-Mkrn1 was overexpressed co-expressed with Myc-tagged GFP or Mkrn1. Myc-IP was performed in the presence or absence of RNase T1.

DISCUSSION

4.1. Mkrn1 is a new regulator of oogenesis

With this study, the function of the RBP Mkrn1 was characterized using *Drosophila* as a model system. Strikingly, knockout of *Mkrn1* results in female sterility (Fig. 6C), identifying the conserved E3 ligase as a novel regulator of oogenesis. In line with the specific expression of *Mkrn1* in ovaries (Fig. 5), the knockout displays a female-specific phenotype. Moreover, overexpressing Mkrn1 in the germline, but not in follicle cells rescued the complete knockout of *Mkrn1* (*Mkrn1*^{N}, Fig. S1). To further analyze the function of Mkrn1 during oogenesis, the rescue potential of different Mkrn1 mutant constructs was examined. These experiments highlighted that the RING domain and PAM2 motif are essential for the function of Mkrn1 (further discussed in 4.1.2 and 4.2).

In collaboration with the group of Paul Lasko, different mutations within the *Mkrn1* gene were introduced. For instance, the *Mkrn1*^{S} allele only expresses a truncated version of Mkrn1 and displays a similar phenotype as *Mkrn1*$^{N.}$ On the other hand, the *Mkrn1*^{W} mutation consists of a small deletion of the ZnF1 that disrupts the RNA-binding ability of the protein (Fig. 12A). This allele has a weaker phenotype: ovaries can partially develop to eggs. However, the *Mkrn1*^{W} allele is embryonic lethal as none of the laid eggs further develop to larvae. Together, these observations imply that Mkrn1 is essential for oogenesis.

Interestingly, the E3 ligase is dispensable for other tissues and developmental stages. Consistently, another study reported similar findings: female *Mkrn1* null mutants are sterile and this phenotype can be rescued by germline-specific overexpression of Mkrn1 [186]. However, the authors showed that Mkrn1 has an important role in the regulation of the insulin pathway. This is in contrast to our work implicating Mkrn1 as a novel regulator of *osk* translation. It might be possible that Mkrn1 has diverse functions during oogenesis. In line with this, another study in mice also identified MKRN1 as a regulator of the insulin pathway, suggesting that the function of Mkrn1 is conserved throughout different species [340]. As the *Mkrn1*^{W} allele gives rise to a weaker phenotype, another domain that is functional in this mutant might be required to regulate insulin signaling.

Apart from *Mkrn1*, three other related genes (*CG12477*, *CG5334* and *CG5347*) are present in *Drosophila*. Interestingly, these three genes exhibit an expression pattern that greatly differs from *Mkrn1* with high levels in males and during pupation (Fig. 5). The differential expression

might indicate that the *Mkrn1*-related genes have an independent function, maybe in testis. This hypothesis is supported by observations in mice where knockout of *MKRN2* leads to complete sterility of males, but not in females [195]. Furthermore, the study found a positive association of mutations in the human *MKRN2* gene and male sterility.
Intriguingly, *MKRN2* knockout in mice led to increased apoptosis in testis [197]. Similarly, we observed apoptosis in *Mkrn1* mutant ovaries (Fig. 7B). This suggests that murine MKRN2 and *Drosophila* Mkrn1 might act by a similar mechanism. To test if the *Mkrn1*-related genes display a similar phenotype as reported in mice, knockout of *CG12477* was performed and a potential effect on fertility was examined. However, both females and males were fertile and produced viable progeny (Fig. 6C). This result indicates that *CG12477* might encode a non-functional retrocopy. Indeed, retroposition of *Mkrn* genes is frequent across evolution, resulting in duplicated genes that are not functional [170]. On the other hand, it is possible that *CG12477*, *CG5334* and *CG5347* have a redundant role in males. To test this possibility, triple knockouts should be examined for effects on fertility and spermatogenesis.

4.1.1. Mkrn1 specifically regulates *osk* translation

Translational activation of *osk* was suggested to be induced by active derepression once the mRNA reaches the posterior pole of the oocyte [327]. Several lines of evidence support Mkrn1 as a novel derepressor of *osk*. First, Mkrn1 is a cytoplasmic protein that localizes to the posterior within the oocyte (Fig. S3B, S6B). Second, it interacts with many known RBPs that regulate *osk* expression (Fig. 9, S4). Third, Mkrn1 binds directly and with high specificity to *osk* 3’ UTR (Fig. 12B, 13A). Moreover, Mkrn1 associates with *osk* at the BRE-C known to be bound by the translational repressor Bru1 and the interaction of Mkrn1 with *osk* has an antagonistic effect on Bru1 binding (Fig. 12B, 15, S10). Finally, in the absence of Mkrn1, Osk protein levels are dramatically reduced (Fig. 8A, 11C). Together, these observations support the hypothesis that Mkrn1 is a component of the *osk* mRNP, which is required for activation of *osk* translation.

Curiously, knockdown or overexpression of Mkrn1 in cultured cells had only a mild effect on the proteome (Fig. S15). The small changes observed suggest that Mkrn1 does not have a global role on translation but regulates only a specific set of mRNAs. Nevertheless, it would be

important to examine changes on the proteome in *Mkrn1* mutant ovaries as this is the place where loss of Mkrn1 produces a strong phenotype.

4.1.1.1. Mkrn1 is part of the *osk* mRNP

Our mass spectrometry experiments revealed that Mkrn1 interacts with several proteins involved in *osk* expression (Fig. 9). As many of the binding partners of Mkrn1 are known to associate with *osk* mRNA, it is likely that Mkrn1 is part of a multiprotein complex regulating the transcript. This is supported by various studies examining the association of Mkrn1's interactors with each other. For instance, Sqd is known to bind to Imp, Hrb27C, and Cup [289, 290, 294]. Furthermore, Hrb27C and Me31B both bind to Cup, and Imp interacts with Hrb27C [60, 290, 294]. All of these interactions are mediated by RNA. Moreover, Me31B and Sqd interact with Bru1 [60, 285]. Together, these observations demonstrate that the regulators of *osk* bind to each other – either directly or mediated by the mRNA itself. Due to the RNA-independent association of Mkrn1 with its binding partners, Mkrn1 might be part of different *osk* mRNPs regulating distinct processes.

As stated above, many Mkrn1-interacting partners are known regulators of translation. This includes the initiation factors eIF4G and pAbp [15]. Moreover, Imp, Me31B, larp, Sqd, Hrb27C, and the human orthologs of Larp4B and Upf1 associate with pAbp to regulate translation [74, 294, 351-353, 363].

In mammals, IGF2BP represses translation of *β-actin* mRNAs during its axonal transport [48-50]. Interestingly, *Drosophila* Imp has been implicated in translational control of localized mRNAs during neurogenesis and oogenesis [290, 330, 364, 365]. Furthermore, PABP stabilizes the RNA-binding ability of IGF2BP [366]. Given that pAbp acts on Mkrn1 in a similar manner, it is tempting to speculate that, when binding together to mRNA, Imp, Mkrn1 and pAbp stabilize one another. In support of this hypothesis, the interaction of pAbp with Imp is reduced in *Mkrn1* depleted cells (data not shown).

In addition, IGF2BP remodels the structure of its bound RNA [367]. This remodeling step was suggested to be required for other factors to bind to the same transcript. Since Imp binds to the

osk 3’ UTR as well, one could argue that the protein modulates the accessibility of *osk* mRNAs for Mkrn1 and other factors [330]. However, for Mkrn1, binding to *osk* does not depend on Imp nor does Mkrn1 affect the interaction of Imp with *osk* 3’ UTR in S2R+ cells (Fig. 14B, 15A, S9C, 10D). Still, it would be compelling to repeat these experiments in ovaries where an effect could be more pronounced.

Me31B on the other hand has an established role in repressing translation. The yeast and human orthologs initiate mRNA decay by recruiting the decapping complex and CCR4-NOT1 [66-68]. Interestingly, although the interaction between the two proteins was relatively weak, Mkrn1 protein levels were greatly reduced in *Me31B* depleted cells (data not shown). It is plausible, that Me31B affects the mRNA or protein stability of Mkrn1. Moreover, the RNA helicase activity of Me31B might be required for the accessibility of *osk* for Mkrn1. In this case, we expect that knockdown of *Me31B* would affect the binding of Mkrn1 to *osk* 3’ UTR which could be measure by RIP experiments.

The functions of larp and Larp4B on translation are more elusive as they depend on the bound mRNA and interacting proteins [72]. Consequently, human LARP1 was shown to both repress and activate translation when binding to 5’ TOP mRNAs [71, 73]. Moreover, in *C. elegans*, larp regulates translation during oogenesis via mRNA decay [70]. Similarly, human LARP4 also binds A-rich sequences together with PABP [363]. However, *Drosophila* Larp4B appears to negatively influence translation [355, 363]. We did not test the genetic or physical association of larp nor Larp4B to Mkrn1, but such experiments would be helpful to analyze the dependencies of the proteins with each other.

Together, the findings reveal that Mkrn1 exists as part of one – or several – mRNP complexes that regulate *osk* translation. This implies that most likely, Mkrn1 acts in synergy with other regulatory proteins to fulfill its job. Further experiments are needed to clarify their interplay.

4.1.1.2. Mkrn1 activates translation by competing with Bru1 for binding to *osk*

The BRE-C region was shown to be required for both repression and activation of *osk* translation [296, 320]. Deletion of this sequence results in severe patterning defects due to the absence of Osk protein. Our demonstration that Mkrn1 associates with the BRE-C to activate translation of *osk* by competing with Bru1, answered a long-standing question about the dual activity of this *cis*-regulatory sequence.

We tested the antagonizing function of Mkrn1 via different approaches. For instance, knockdown of either *Mkrn1* or *pAbp* in S2R+ cells increased the association of Bru1 to *osk* 3' UTR (Fig. 15A, 15B, S10C, S11A). A similar result was observed in $Mkrn1^{W}$ ovaries (Fig. 15C, S11C). Surprisingly, while deletion of the AR region reduces the interaction of Mkrn1 to *osk*, it only had a minor impact on Bru1 binding (Fig. 14A, S11B). An earlier study reported a similar observation of Bru1 binding being unaffected when the AR region of *osk* 3' UTR was deleted [110]. Given that the binding of Mkrn1 to $osk^{\Delta AR}$ is only reduced to around 40%, it could be that the residual Mkrn1 proteins interacting with *osk* are sufficient to antagonize Bru1 binding. Also, the increased association of Bru1 to *osk* in $Mkrn1^{W}$ ovaries was weaker than the increase observed in cultured cells. Since the main fraction of *osk* is not localized to the posterior and is translationally silent, it might overshadow the effect seen for the *Mkrn1* mutant. In the future, *in vitro* binding assays using the *osk* 3' UTR with different deletions including the AR region could help to decipher the competitive behavior of Mkrn1 to Bru1.

In support of the competitive binding of the two proteins at *osk* 3' UTR, we found that they also interact genetically: a partial rescue of *osk* translation was observed when removing one copy of *Bru1* in the $Mkrn1^{W}$ mutant [346]. This partial rescue, however, suggests that additional mechanisms are involved to relieve the repression by Bru1. Perhaps a similar competitive mode of binding between Bru1 and BSF occurs at a later stage (see also below). Another important question to address will be to identify the signal that releases Bru1 repressive function towards *osk* translation only when the transcript reaches the posterior pole. Why the competition between Mkrn1 and Bru1 occurs only at the posterior? Perhaps the polyA tail of *osk* mRNA increases in size at this location, allowing stronger binding of pAbp, and therefore the stabilization of Mkrn1 and its interaction with *osk*. More experiments would be required to test

this hypothesis, including *in vitro* binding assays with *osk* containing different polyA tail lengths in the absence or presence of pAbp.

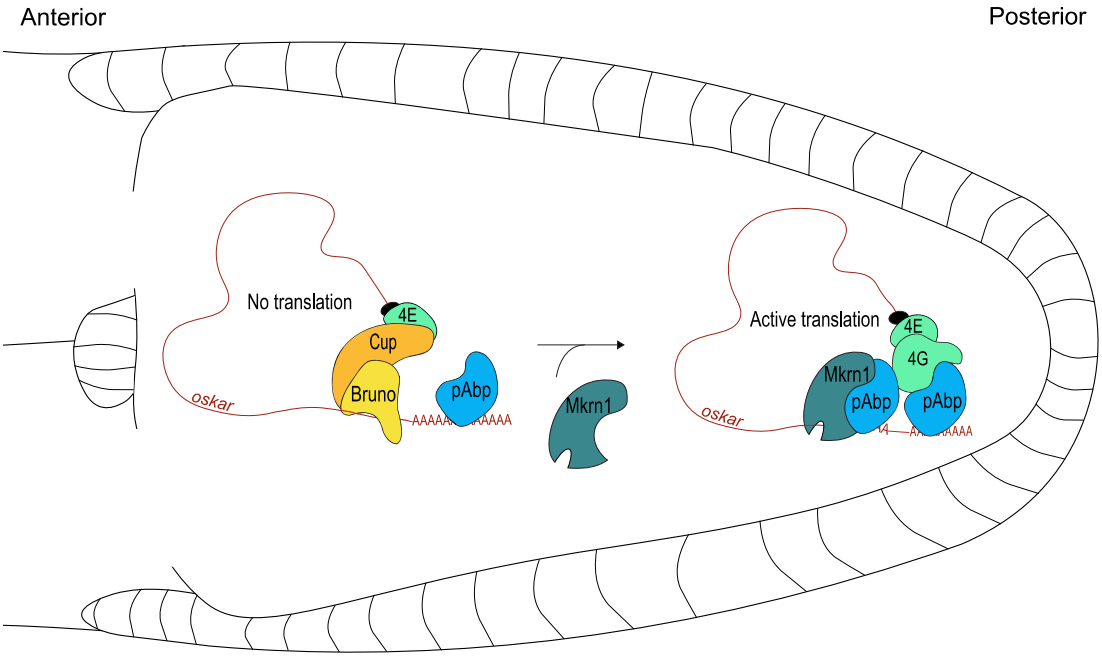

Figure 17. Model of Mkrn1 regulating translation of *osk* mRNA.
During transport of *osk*, Bru1 and Cup associate with the mRNA and repress its translation. At the posterior of the oocyte *osk* translation is activated. One factor involved in this derepression is Mkrn1 that is recruited to the *osk* 3' UTR and stabilized by pAbp. The interaction with Mkrn1 leads to the displacement of Bru1 from the BRE-C, promoting *osk* translation.

Another open question raised from our work is to understand how precisely Mkrn1 interplays with Bru1. Bru1 represses translation by interacting with Cup, a 4E-BP that competes with eIF4G for binding to eIF4E [59-61]. Moreover, repression can be achieved by Bru1 homodimerization [358]. Surprisingly, neither the interaction of Bru1 to Cup nor its dimerization was affected in *Mkrn1* depleted cells (Fig. S12A, S12B). Similarly, Cup binding to *osk* was hardly affected in $Mkrn1^{W}$ ovaries (Fig. S12C). This might be due to the fact that the majority of *osk* mRNA is in a repressive state, making it difficult to dissect changes occurring only at the posterior pole. However, our findings could also indicate that Mkrn1 activates translation by a mechanism that does not involve Cup. In line with this observation, Mkrn1 interacts with eIF4G but not with eIF4E, which is bound by Cup (Fig. S4G).

Another possibility could be that, by repelling the binding of Bru1, Mkrn1 reduces the RNA-RNA dimerization of *osk* transcripts. The mRNAs might thus be less associated with each other

enabling the binding of translation factors and ribosomes. Such a mechanism has been proposed for *osk* mRNA to occur independently of Cup and the 5' cap [322, 323].
Also, for *nos* mRNA, an analogous mechanism was suggested to repress its translation during embryogenesis [368]. Intriguingly, Me31B was identified as one factor that interacts with *nos* mRNA with a high stoichiometry [368]. The binding of Me31B might in turn prevent recruitment of the ribosome to *nos* mRNA. Thus, it would be intriguing to analyze the interplay of Mkrn1 and Me31B on *osk* in more detail.

BSF was also recently identified as a positive regulator of *osk* translation [321]. The binding site of BSF was reported to have a strong influence on embryonic patterning similar to the phenotype observed for *Mkrn1* mutants [273, 321]. The Mkrn1 binding site overlaps with the distal type II Bru1-binding site, which is also bound by BSF, and deletion of this sequence affects the association of Mkrn1 to *osk* (Fig. 13A, 13C, S8B). However, a mutation that affects BSF binding did not change the interaction of Mkrn1 with *osk*. Moreover, mutating or deleting the main BSF binding site had only a mild effect on Mkrn1. Therefore, BSF might influence the binding of Mkrn1 only to some extent. Also, we did not observe a change in binding of BSF when *Mkrn1* was depleted (Fig. 13D, S8E). Nevertheless, since Bru1 is not expressed in S2R+ cells, it is possible that our results obtained in cultured cells do not reflect the *in vivo* situation. For instance, additional factors only present at the posterior of the oocyte might be required for this regulation.

An elegant way to regulate translation of *osk* would be by Mkrn1 and BSF acting in synergy. BSF is required for *osk* translation only at stage 10 onwards indicating that another factor is necessary to activate translation during mid-oogenesis [321]. During mid-oogenesis, the effect of Mkrn1 on Bru1 binding might be required to derepress a subset of *osk* transcripts. This initial activation might be further enhanced by BSF in late oogenesis. Such a stepwise activation might be required to ensure correct *osk* expression and would explain why Mkrn1 has a relatively mild effect on Bru1 binding.
Interestingly, for the accurate translational control of *polar granule component* (*pgc*) mRNA, a cascade of different regulatory factors acting at specific stages of oogenesis was proposed [369]. The restrictive manner by which individual factors regulate *pgc* is necessary to establish a distinct expression pattern. Furthermore, the study predicts that such complex mechanisms are used for many different mRNAs during oogenesis. Due to the plurality of regulators required

for *osk* expression, it is reasonable to assume that *osk* translation could be activated by a similar stepwise mechanism.

4.1.2. The function of Mkrn1 is regulated by pAbp

Using different approaches, we identified pAbp as crucial interactor of Mkrn1 in *Drosophila*. The interaction was confirmed by various mass spectrometry approaches (Fig. 9, 10B) as well as by co-IPs in S2R+ cells and ovaries (Fig. 10A, S4A). Moreover, we identified the PAM2 motif in *Drosophila* Mkrn1 as the region required for the binding to pAbp (Fig. 10E, 11A, see also 4.1.2.1). The increased stability of Mkrn1 in the presence of pAbp (Fig. 10C) and the reduced protein level of Mkrn1^{PAM2} in ovaries (Fig. 11A, 11C) further demonstrate the importance of this interaction to stabilize the E3 ligase. Consequently, if pAbp is depleted or the PAM2 motif mutated, the association of Mkrn1 to *osk* 3' UTR is impaired (Fig. 14).

Consistent with the functionality of this interaction, overexpression of Mkrn1^{PAM2} in the null allele led to the production of a certain number of eggs but none of them hatched (Fig. 11B). Moreover, Osk protein level was reduced and not localized to the posterior (Fig. 11C, 11D). In contrast, this effect was not observed when using Mkrn1 with a deletion of the ZnF1 domain. Instead, rescue with Mkrn1$^{\Delta ZnF1}$ displayed a phenotype more similar to wild-type ovaries, producing viable embryos. This result was not anticipated as the deletion of the ZnF1 in the *Mkrn1*^{W} mutant leads to embryonic lethality. We suspect that the protein level of Mkrn1$^{\Delta ZnF1}$ in the rescue experiment might increase the probability of the mutant to associate with pAbp, and therefore bypass the need to directly interact with *osk* mRNA. Consequently, Mkrn1$^{\Delta ZnF1}$ still localized to the posterior pole, which was not observed when the PAM2 motif was mutated (Fig. S6B). Hence, although the RNA-binding ability is to some extent dispensable, the interaction with pAbp is essential for the function of Mkrn1.

For human MKRN1, a similar dependency on pAbp was observed, as MKRN1 binds less efficiently to RNA when the PAM2 motif is mutated [173]. Interestingly, the same study found that MKRN1 binds to mRNAs predominantly upstream of A-rich stretches, as we observed for Mkrn1 binding to *osk*. Therefore, the presence of A-rich sequences could be a conserved prerequisite for Mkrn1 binding. We could not address this on a global scale in *Drosophila* as

our iCLIP approach was suboptimal and only a few targets were identified. It would be compelling to repeat this experiment in ovaries, to identify the full set of physiological targets and to analyze their nucleotide sequences downstream of Mkrn1 binding sites.

4.1.2.1. Mkrn1 interacts with pAbp via a non-conserved PAM2 motif

In the course of this study, we identified a non-conserved PAM2 motif in Mkrn1 which contains a glutamic acid to valine substitution (Fig. 10D). Despite this mutation, the interaction with pAbp is intact (Fig. 10D, 11A). The interaction between Mkrn1 and pAbp is also conserved in other species including *C. elegans* where mkrn1 contains a PAM2 with the EFxP consensus sequence (Almeida and Ketting, personal communication). In contrast, Mkrn4 in *Danio rerio* lacks this motif and does not bind to Pabp (Wittkopp and Ketting, personal communication). Together, these observations suggest that the PAM2 motif has a conserved and essential function in Mkrn1 to mediate the interaction with pAbp.

Compared to other PABP-interacting proteins like Paip1 and Paip2, MKRN1 only shares the essential EFxP motif [173]. Although this finding is surprising, it seems very common for the motif to diverge: for other proteins containing PAM2 motifs that differ from the consensus site, the interaction with PABP was also shown to be maintained [370]. For instance, the PAM2 of LARP4 does not possess the EFxP core but still associates with PABP [363].

It is then clear that the PAM2 motif of MKRN1 has partially evolved but the structure still allows binding to PABP. Usually, the PAM2 motif recognizes the MLLE domain [111, 174]. However, rat MKRN1 mainly interacts with PABP via the RRM1 and RRM2 domains [212]. Interestingly, the RRM2 domain also interacts with eIF4G [371]. An altered PAM2 motif that binds to RRM1 and RRM2 could potentially enhance the interaction with eIF4G and other members of the PIC. This in turn would increase translation efficiency, which was reported for rat MKRN1 [212]. It would be interesting to investigate if a similar binding preference exists for *Drosophila* Mkrn1. To address this, binding assays of Mkrn1 with different truncated versions of pAbp could be examined.

In addition to PAM2, MKRN1 contains a PAM2L motif. Recently, a study in *Ustilago maydis* focused on the protein Upa1 that possesses such a PAM2L motif [175]. Interestingly, the authors showed that this PAM2L motif was able to interact with the MLLE domain of Rrm4 and is required for the recruitment to endosomal mRNPs. This MLLE domain however displays a distinct sequence that differs from the PABP MLLE domain.
In *Drosophila*, the PAM2L motif comprises a mutation within the consensus site (DFVCP instead of EFxxP). Similar to the PAM2 motif, this mutation is conserved among close relatives of *Drosophila* including *Anopheles* (Rücklé and Zarnack, personal communication). Likewise, this amino acid substitution might not interfere with the interaction to a certain binding partner. Currently, the relevance of this motif for Mkrn1 function is unknown. Mutational analysis and mass spectrometry approaches could help to elucidate this question and identify potential factors that require this motif for interacting with Mkrn1.

4.1.3. Other possible functions of Mkrn1 during oogenesis

We identified a role for Mkrn1 on translational activation of *osk*. Nevertheless, due to its essential function during oogenesis, the question arises if Mkrn1 possesses other roles within the oocyte besides mediating *osk* translation.

Since many interaction partners of Mkrn1 regulate mRNA stability, it is tempting to speculate that Mkrn1 could regulate this process as well. For instance, pAbp has a distinct role in stabilizing *osk* mRNA by binding to the AR region in its 3' UTR [110]. Cup on the other hand can recruit the deadenylase complex to repress translation [317]. Moreover, in *Cup* mutants *osk* mRNA levels are reduced [372]. Mutating the binding site of BSF negatively affects the stability of *osk* mRNA as well [273]. Also for *bcd*, BSF has a positive influence on its stability [373]. In addition, Imp was shown to stabilize its bound mRNAs in human cell culture as well as in *Drosophila* neurons [374, 375]. Furthermore, Me31B and larp negatively affect the stability of their mRNA targets [68, 69, 74].
Nevertheless, using RNA-seq and RT-qPCR we did not detect a global effect on RNA stability in $Mkrn1^{W}$ ovaries (Fig. 8B, S2). Consistently, Mkrn1 does not interact with the decapping enzyme Dcp1 (Fig. S4F). These findings are further supported by observations in mouse ESCs

where MKRN1 is not required for the stability of its mRNA targets [185]. Therefore, despite the association of Mkrn1 with several factors involved in mRNA stability, our results indicate that Mkrn1 does not carry out such a function.

Similarly, it is unlikely that Mkrn1 regulates the localization of *osk* mRNA to the posterior. In *Mkrn1*^{W} ovaries, a clear localization of *osk* to the posterior was visible at stages 7/8 [346]. Starting at stage 10B, *osk* mRNA was detached from the posterior due to a lack of Osk protein, which is required for anchoring of its own transcript [248, 249]. Moreover, deletion of the BRE-C region at the *osk* 3' UTR did not interfere with its early posterior localization [296, 320]. Thus, the results of our study together with those of other groups suggest that Mkrn1 is not involved in the localization of *osk* mRNA. We cannot rule out, however, that Mkrn1 mediates the localization of other mRNAs. *In situ* hybridizations of different mRNAs in *Mkrn1*^{W} ovaries could help to identify such a function.

4.1.3.1. Mkrn1 as a regulator of the polyA tail length

Many reports highlighted the role of polyA tail lengthening in translational activation of maternal mRNAs [97]. This is also the case for *osk* as its polyA tail requires at least 150 adenosines to be translated [335]. Interestingly, a recent study demonstrated that Bru1 negatively influences the polyA tail length of *osk* [105]. Moreover, Bru1 shows homologies to the EDEN-binding protein that induces deadenylation in *Xenopus* embryos [319, 376]. It is thus possible that Bru1 is able to act as translational repressor by maintaining a short polyA tail.

However, lengthening of the polyA tail itself cannot overcome Bru1-mediated repression indicating that additional regulators are required [335]. Since Mkrn1 binds in close proximity to the polyA tail, interacts with pAbp and displaces Bru1 from *osk*, it is a good candidate to additionally relieve *osk* repression. Consistent with such a role, knockdown of *Mkrn1* led to a slight but significant decrease of pAbp binding to *osk* 3' UTR (Fig. 15A). This reduced enrichment of *osk* might be due to a shorter polyA tail length. Alternatively, Mkrn1 may have a mild stabilizing effect on pAbp. In our interactome experiments, we did not find evidence for an association of Mkrn1 with polyA polymerases. However, Bru1 interacts with Orb, which positively regulates the polyA tail length of *osk* [335]. Further experiments assessing the polyA

tail length of *osk* in *Mkrn1*^{W} ovaries and a potential interaction with Orb could tell us whether Mkrn1 is involved in this function.

4.1.3.2. Mkrn1 as a possible new m^{6}A reader

A layer of gene regulation that recently gained strong interest is the modification of distinct nucleotides on mRNAs. One prominent modification that has been extensively studied is N^6-methyladenosine (m^{6}A). Intriguingly, m^{6}A deposited on mRNA can enhance translation of the targets [377]. Moreover, during oogenesis and embryogenesis, the modification is used to regulate the levels of maternal mRNAs [378, 379].
Overall, the impact of m^{6}A greatly depends on reader proteins that recognize and bind to the modified base. The number of identified m^{6}A readers is constantly growing revealing the complex regulation of methylated mRNAs. For instance, in human cell culture, IGF2BP proteins, Fragile X Mental Retardation Protein 1 (FMR1) and YBX1 were recently classified as such novel m^{6}A reader proteins [374, 377, 380].

Strikingly, mass spectrometry experiments revealed that human, mouse and *Drosophila* MKRN1 interact with IGF2BP1, FMR1 and YBX1 [173, 185, 346]. In addition, these proteins are expressed during *Drosophila* oogenesis where m^{6}A levels are high [290, 330, 381-383]. Thus, it is possible that the modification has a function in regulating maternal mRNAs during *Drosophila* oogenesis, and Mkrn1 could be involved in this process. Consistently, our group has preliminary data suggesting that indeed Mkrn1 binding is enriched on methylated mRNA in S2R+ cells (Stock and Roignant, unpublished). Thus, one potential novel reader protein could be Mkrn1 that would exert its function in translational activation after binding to m^{6}A-modified mRNA.
While a direct binding of Mkrn1 to Imp was confirmed, the interaction with FMR1 and Yps still needs to be addressed. We could imagine a scenario where the modification would be added at the posterior site of the oocyte, leading to enhanced binding of Mkrn1 to *osk* mRNA, either directly or indirectly via its interaction with Imp, and perhaps others like Fmr1 and Yps. This would explain why *osk* is only translated when reaching the posterior pole. Further experiments are needed to test this hypothesis. For instance, the binding of Mkrn1 to *osk* could be examined in ovaries depleted for the functional m^{6}A writer complex [381]. Also, localization and protein

levels of Osk in these mutants would give insights into a potential role of m^6A on *osk* expression.

4.2. The E3 ligase activity of Mkrn1 is essential for its function

In our work, the importance of the E3 ligase activity of *Drosophila* Mkrn1 was determined. Similar to mammalian MKRN1, the RING domain is essential for the function of the RBP since a mutation that removes the domain gives rise to an early arrest during oogenesis (Fig. 6, 7). Furthermore, overexpression of Mkrn1 with a mutation in the RING domain could not rescue the $Mkrn1^N$ phenotype (Fig. 11C, 11D, S6C). This indicated that Mkrn1 has other targets than *osk*, but the ubiquitination substrates of Mkrn1 still remain to be identified. It is possible that Mkrn1 is selective towards a few substrates rather than ubiquitinating many different targets. This would be consistent with the specific function of Mkrn1 on *osk* translation.

Using ubiquitination assays, the E3 ligase activity of Mkrn1 in S2R+ cells was assessed. Neither Bru1, Cup nor Imp display any ubiquitination pattern in wild-type conditions (Fig. S13). Due to the fact that Bru1 is not expressed in S2R+ cells, this observation does not necessarily indicate that it is not ubiquitinated in a more physiological context. Since *Mkrn1* levels are especially high in ovaries (Fig. 5), its E2 enzyme might show a similar expression pattern. In line with this possibility, we did not identify an E2 enzyme by interactome analysis of Mkrn1 in S2R+ cells.

Furthermore, the binding to *osk* mRNA might be necessary to activate the ubiquitinating activity. This is the case for other E3 ligases, like TRIM25, where the binding to RNA is required for its enzymatic activity [384]. On the other hand, a Bru1-Ub signal might have been missed due to a limited sensitivity of the approach. Interestingly, Bru1 protein levels were mildly upregulated in $Mkrn1^W$ ovaries (Fig. S11C), indicating a negative regulation by Mkrn1. A global ubiquitylome analysis in ovaries might give more insight into the possible targets of Mkrn1.

Strikingly, pAbp is of polyubiquitinated in cultured cells, and this signal is reduced when Mkrn1 is depleted (Fig. S13B). This finding indicates that Mkrn1 – either directly or indirectly – regulates the ubiquitination of pAbp. Human PABP was also shown to be ubiquitinated by MKRN1, but without effect on protein stability [173]. Thus, perhaps the ubiquitination does not induce pAbp degradation but modulates the binding to another protein or the polyA tail. Interestingly, the main ubiquitination site of PABP regulated by MKRN1 is positioned at the RRM1. Since this domain is required for the binding to the polyA tail, the PTM might modulate the binding affinity of PABP [86]. This in turn would regulate translation initiation. It would be interesting to further examine the effect of ubiquitination on pAbp as well as the role of Mkrn1 in this process. To this end, effects on translation and RNA binding for a Ub mutant version of pAbp could be analyzed. Also, *in vitro* ubiquitination assays between pAbp and Mkrn1 could verify a direct role of the E3 ligase.

Human MKRN1 was additionally found to ubiquitinate the ribosomal proteins RPS10 and RPS20 [173]. Both ribosomal proteins were also found in the interactome of $Mkrn1^{RING}$. Therefore, it could be interesting to test if the function of Mkrn1 in ubiquitinating these ribosomal proteins is conserved in *Drosophila*.

4.2.1. Mkrn1 autoregulates itself

PTMs are powerful means to regulate protein stability, localization, folding, interactions and activity. Among all PTMs, phosphorylation is the most prevalent one [385]. For instance, pAbp was shown to be phosphorylated in plants, yeast and sea urchins [386]. When phosphorylated, the binding of pAbp to polyA mRNA is enhanced. For RING ligases, phosphorylation is also a common regulatory layer to influence their activity and localization [385]. However, the predicted modification site, when altered, does not affect Mkrn1 binding to pAbp nor to *osk* 3’ UTR (Fig. S16). While this experiment suggests that phosphorylation does not regulate Mkrn1 function, one cannot exclude that the software we used to identify the PTM failed to identify relevant sites. Thus, analysis of the global interactome of phosphomutants of Mkrn1 could help to identify a possible regulatory role of this PTM.

In mammals, the only identified PTM having a regulatory influence on MKRN1 is Ub [181]. Interestingly, MKRN1 is able to autoubiquitinate itself using K48-linked chains [173, 181, 340]. This autoubiquitination results in decreased stability of the E3 ligase due to its degradation by the proteasome. Consistently with these observations, a positive stability effect for the RING mutant was also observed in *Drosophila* (Fig. 11A, 11C, S3C). Moreover, the ubiquitination pattern of Mkrn1 is strongly reduced when the RING domain is not functional (Fig. 16A) and increasing the amount of transfected Mkrn1 reduces its own protein stability (Fig. 16B). Furthermore, treatment with a proteasome inhibitor stabilizes Mkrn1 (data not shown). Together, these results suggest that *Drosophila* Mkrn1 autoregulates itself similar to the human ortholog. This autoregulatory function has already been reported for other RING E3 ligases [385]. Given that the observed effect of the RING mutant could also imply an indirect role of Mkrn1, this needs to be further assessed using *in vitro* ubiquitination assays with purified protein.

MATERIALS AND METHODS

5.1. Materials

5.1.1. Cell and fly lines

5.1.1.1. Cell line

Drosophila S2R+ are embryonic derived cells obtained from Drosophila Genomics Resource Center (DGRC, Flybase ID: FBtc0000150).

5.1.1.2. Fly lines

Table 1. List of fly lines used in this study.

Name	Genotype	Source
wild-type	w^{1118}	Bloomington *Drosophila* Stock Center
Balancer line	*Sp/Cyo; Prnt/Tm6B*	Roignant lab
TBX-0002	*y1 v1 P(nos-phiC31\int.NLS)X; attP40*	National Insitute of Genetics (NIG)
TBX-0008	*y2 cho2 v1/Yhs-hid; Sp/CyO*	National Insitute of Genetics (NIG)
Cas-0001	*y2 cho2 v1; attP40(nos-Cas9)/CyO*	National Insitute of Genetics (NIG)
attP40	*yw (nanos:integrase); attP40*	Perrimon lab
$Mkrn1^{Def}$	*w1118; Df(3L)BSC418/TM6C, Sb1 cu1*	Bloomington *Drosophila* Stock Center
$CG12477^{Def}$	*w[1118]; Df(3L)BSC832, P+PBac(w[+mC]=XP3.RB5)BSC832/ TM6C, Sb[1] cu[1]*	Bloomington *Drosophila* Stock Center
$Mkrn1^{W}$	$Mkrn1^{W}$*/Tm3*	Lasko lab
$Mkrn1^{S}$	$Mkrn1^{S}$*/Tm3*	Lasko lab
$Mkrn1^{N}$	$Mkrn1^{N}$*/Tm6B*	This study
$CG12477^{N}$	$CG12477^{N}$*/Tm6B*	This study
nos>Gal4 driver line	*Nanos>Gal4/CyO;* $Mkrn1^{N}$*/Tm3*	Lasko lab
Tj>Gal4 driver line	*Tj>GAL4/CyO; UAS-3HA-piwi/Tm3*	Roignant lab
UASp-FLAG-Mkrn1	*w; UASp-FLAG-Mkrn1/CyO*	Lasko lab

UASp-FLAG-Myc-Mkrn1$^{\Delta ZnF1}$	*w; UASp-FLAG-Myc-Mkrn1$^{\Delta ZnF1}$/CyO*	This study
UASp-FLAG-Myc-Mkrn1^{PAM2}	*w; UASp-FLAG-Myc-Mkrn1^{PAM2}/CyO*	This study
UASp-FLAG-Myc-Mkrn1^{RING}	*w; UASp-FLAG-Myc-Mkrn1^{RING}/CyO*	This study
UASp-FLAG-Myc-Mkrn1$^{\Delta ZnF1+RING}$	*w; UASp-FLAG-Myc-Mkrn1$^{\Delta ZnF1+RING}$/ CyO*	This study
UASp-FLAG-Myc-huMKRN1	*w; UASp-huMKRN1/CyO*	This study

5.1.2. Plasmids

5.1.2.1. Plasmids of different Mkrn1 constructs

Table 2. List of plasmids used in this study encoding different Mkrn1 constructs.

Name	Promoter	Tag	Insertion	Source
pAFW_Mkrn1	*actin5*	FLAG	Mkrn1	This study
pAFW_Mkrn1_H239E	*actin5*	FLAG	Mkrn1^{RING}	This study
pAHW_Mkrn1_H239E	*actin5*	HA	Mkrn1^{RING}	This study
pPFW_attB_Mkrn1	*UASp*	FLAG, Myc	Mkrn1	This study
pPFW_attB_Mkrn1_H239E	*UASp*	FLAG, Myc	Mkrn1^{RING}	This study
pPFMW_attB_Mkrn1_ΔZnF1	*UASp*	FLAG, Myc	Mkrn1$^{\Delta ZnF1}$	This study
pPFMW_attB_Mkrn1_ZnF2	*UASp*	FLAG, Myc	Mkrn1^{ZnF2}	This study
pPFMW_attB_Mkrn1_PAM2	*UASp*	FLAG, Myc	Mkrn1^{PAM2}	This study
pPFMW_attB_Mkrn1_S343A	*UASp*	FLAG, Myc	Mkrn1^{S343A}	This study
pPFMW_attB_Mkrn1_S343D	*UASp*	FLAG, Myc	Mkrn1^{S343D}	This study
pPFM_attB_Mkrn1_ΔZnF1+ RING	*UASp*	FLAG, Myc	Mkrn1$^{\Delta ZnF1+RING}$	This study
pPFMW_attB_human_Mkrn1	*UASp*	FLAG, Myc	human MKRN1	This study

5.1.2.2. Plasmids created of binding partners of Mkrn1

Table 3. List of plasmids used in this study encoding binding partners of Mkrn1.

Name	Promoter	Tag	Insertion	Source
pAWG_pAbp	*actin5*	GFP	pAbp	This study
pAWG_Imp	*actin5*	GFP	Imp	This study
pAWG_Bruno	*actin5*	GFP	Bruno	This study
pAWG_Squid	*actin5*	GFP	Squid	This study
pPFMW_attB_pAbp	*UASp*	FLAG, Myc	pAbp	This study
pPFMW_attB_Squid	*UASp*	FLAG, Myc	Squid	This study
pPFMW_attB_me31B	*UASp*	FLAG, Myc	me31B	This study
pPFMW_attB_eIF4G	*UASp*	FLAG, Myc	eIF4G	This study
pPFMW_attB_Cup	*UASp*	FLAG, Myc	Cup	This study
pPFMW_attB_BSF	*UASp*	FLAG, Myc	BSF	This study
pPFMW_attB_Dcp1	*UASp*	FLAG, Myc	Dcp1	This study

5.1.2.3. Plasmids used to analyze Mkrn1 binding to RNA

Table 4. Plasmids used to analyze Mkrn1 binding to RNA.

Name	Promoter	Insertion	Source
pAct5-osk_gene	*actin5*	*oskar* gene	This study
pAct_FL_EcoRV	*actin5*	*firefly luciferase*	This study
pAct_FL_grk_3'UTR	*actin5*	*grk* 3' UTR	This study
pAct_FL_osk_3'UTR	*actin5*	*osk* 3' UTR	This study
pAct_FL_osk_3'UTR-ΔAR	*actin5*	$osk^{\Delta AR}$ 3' UTR	This study
pAct_FL_osk_3'UTR-ΔMkrn1	*actin5*	$osk^{\Delta Mkrn1}$ 3' UTR	This study
pAct_FL_osk_3'UTR-typeII-2	*actin5*	osk^{typeII} 3' UTR	This study
pAct_FL_osk_3'UTR-ΔtypeII-2	*actin5*	$osk^{\Delta typeII}$ 3' UTR	This study
pAct_FL_osk_3'UTR-BSF	*actin5*	osk^{BSF} 3' UTR	This study
pAct_FL_osk_3'UTR-ΔBSF	*actin5*	$osk^{\Delta BSF}$ 3' UTR	This study

5.1.2.4. Plasmids used for flow cytometry

Table 5. Plasmids used for flow cytometry.

Name	Promoter	Source
act5_GFP-RFP_R10	*actin5*	Hegde lab, modified in this study
act5_GFP-RFP_K0	*actin5*	Hegde lab, modified in this study
act5_GFP-RFP_K12	*actin5*	Hegde lab, modified in this study
act5_GFP-RFP_K20	*actin5*	Hegde lab, modified in this study

5.1.2.5. Others

Table 6. Additional plasmids used in this study.

Name	Promoter	Tag	Position of tag	Source
act5_GFP	*actin5*	GFP	N/A	Roignant lab
act5_Myc-GFP	*actin5*	Myc	GFP	Roignant lab
act5_HA-Flag-GFP	*actin5*	FLAG, HA	GFP	This study
act5_Gal4	*actin5*	N/A	N/A	Roignant lab
pAFW	*actin5*	FLAG	N-terminal	Drosophila Gateway Vector Collection
pAHW	*actin5*	HA	N-terminal	Drosophila Gateway collection
pAWG	*actin5*	GFP	C-terminal	Drosophila Gateway Vector Collection
pPFMW_attB	*UASp*	FLAG, Myc	N-terminal	Drosophila Gateway Vector Collection, modified in this study

5.1.3. Oligonucleotides

5.1.3.1. Oligonucleotides used to prepare dsRNAs

Table 7. Oligonucleotides used to prepare dsRNAs.

Name	Sequence
RNAi-LacZ-F	TAATACGACTCACTATAGGGCAGGCTTTCTTTCACAGATG
RNAi-LacZ-R	TAATACGACTCACTATAGCTGATGTTGAACTGGAAGTC
RNAi_Mkrn1_F	TAATACGACTCACTATAGGGTCTCCAGTCAGCAGAGGAAC
RNAi_Mkrn1_R	TAATACGACTCACTATAGCGTTGAGCAATTTGTCCTTT
RNAi_PABPC1_F	TAATACGACTCACTATAGGGTCAGGCTCTCAATGGCAAGG
RNAi_PABPC1_R	TAATACGACTCACTATAGTGATTTGACGGAAGGGTCGG
RNAi_IMP_F	TAATACGACTCACTATAGGGGGTCTGAACGGTGTCGAGTT
RNAi_IMP_R	TAATACGACTCACTATAGGTGTCGACATCATTGCCATC
RNAi_Mkrn1_F2	TAATACGACTCACTATAGGGTGTTGGCCACAAGCGTAATA
RNAi_Mkrn1_R2	TAATACGACTCACTATAGTCCTACGAGGGTCCTCAATG
RNAi_CG11414_F	TAATACGACTCACTATAGGGGAGCAACCAGGAGAATCAGC
RNAi_CG11414_R	TAATACGACTCACTATAGGCTGGTGGCTCTTTAAGTCG

5.1.3.2. Oligonucleotides to generate *Mkrn1* mutants

Table 8. Oligonucleotides used to create *Mkrn1* mutants.

Name	Sequence
Mkrn1_sgRNA_left_sense	CTTCGAATCTGCGTATGTACGCAG
Mkrn1_sgRNA_left_as	AAACCTGCGTACATACGCAGATTC
Mkrn1_sgRNA_right_sense	CTTCGACTAAGCTTCTGAAGCAGA
Mkrn1_sgRNA_right_as	AAACTCTGCTTCAGAAGCTTAGTC
sgRNA_CG12477_left_sense	CTTCGGGCTGTTCGTGCTGGGCAC
sgRNA_CG12477_left_as	AAACGTGCCCAGCACGAACAGCCC
sgRNA_CG12477_right_sense	CTTCGTAAACTAGTCTGACGAAAC
sgRNA_CG12477_right_as	AAACGTTTCGTCAGACTAGTTTAC

Table 9. Oligonucleotides used to screen for *Mkrn1* mutants.

Name	Sequence
Mkrn1_gDNA_F	CGAACAACTGTGGTTTAAGGGT
Mkrn1_gDNA_R2	GGATTGGTGTGTGCGTTTCA
CG12477_gDNA_F	CAGGTAATTGTCCGCACCTT
CG12477_gDNA_R	CATGCAAAAAGTGTCCCAAA

5.1.3.3. Oligonucleotides used for cloning

5.1.3.3.1. Cloning of coding sequences

Table 10. Oligonucleotides used for cloning of coding sequences.

Name	Sequence
Mkrn1_wt_KpnI_F	CACCGGTACCATGAGTGCCGTCACCAG
Mkrn1_wt_XbaI_R	TCTAGAGTCTTCATCCGAGTAATCTGA
hMkrn1_Kpn1_F	AAAAGGTACCATGGCGGAGGCTGCAAC
hMkrn1_XbaI_R	AAAATCTAGATAGATCCAAGTCATAAAAATCTTCCA
Mkrn1_H239E_F	TGCAACGAAATATTCTGCTTGGAGTGCAT
Mkrn1_H239E_R	CAGAATATTTCGTTGCAGTTGGGGAGAATGC
Mkrn1_PAM2_mut_F	CCCTGTGGCCGTGGCCAGCCAAAAGCGCTATACTGC
Mkrn1_PAM2_mut_R	TTGGCTGGCCACGGCCACAGGGGCGTTCGCCCAGT
Mkrn1_ZnF1_del_F	GGAGCCAGACCATCTGCCGCTTTGGGGAACTTTG CCGC
Mkrn1_ZnF1_del_R	GTTCCCCAAAGCGGCAGATGGTCTGGCTCC
Mkrn1_Znf2_F	AGGACGCCAAATACTTTAAAAAAGGAGAGGGCAAG GCCCCCTTTGGTAACAAGGCCTTCTACAAGCACGCTC TGCCCAA
Mkrn1_Znf2_R	TGTAGAAGGCCTTGTTACCAAAGGGGGCCTTGCCCT CTCCTTTTTTAAAGTATTTGGCGTCCTTTGCTCCCAAA GCGG
Mkrn1_S343A_F	GTTACAGGCGCAGAATGAAATAATCGATTTA
Mkrn1_S343A_R	TCATTCTGCGCCTGTAACTTTCGGGTGCGCTT
Mkrn1_S343D_F	GTTACAGGACCAGAATGAAATAATCGATTTA
Mkrn1_S343D_R	TCATTCTGGTCCTGTAACTTTCGGGTGCGCTT
Imp_KpnI_F	AAAAGGTACCATGCACAGCAACAATAATAGCA
Imp_XbaI_R	AAAATCTAGACTGTTGTGAGCTCGCCAG
eif4G-PB_NotI_F	AAAGCGGCCGCCATGCAACAGGCTATACCAAC
eif4G-PB_AscI_R	AAAGGCGCGCCCGTTGGCATCATCGTTTAACA
me31B-RA_NotI_F	AAAGCGGCCGCCATGATGACTGAAAAGTTAAATTC
me31B-RA_AscI_R	AAAGGCGCGCCCTTTGCTAACGTTGCCCTC

Sqd_NotI_F	AAAGCGGCCGCCATGGCCGAGAACAAGCAA
Sqd_AscI_R	AAAGGCGCGCCCGAACTGCTGATAGTTGTTGCT
cup_RB_NotI_F	AAAGCGGCCGCCATGCAAATGGCCGAAGCTGA
cup_RB_KpnI_F	AAAAGGTACCATGCAAATGGCCGAAGCTGA
cup_RB_AscI_R	AAAGGCGCGCCCATGAAACTCATCCCCGCTGT
cup_RB_XbaI_R	AAAATCTAGAATGAAACTCATCCCCGCTGT
bruno_RA_KpnI_F	AAAAGGTACCATGTTCACCAGCCGCGCTT
bruno_RA_AscI_R	AAAGGCGCGCCCGTAGGGCTTCGAGTCCTTGGG
bruno_RA_XbaI_R	AAATCTAGAGTAGGGCTTCGAGTCCTTGGG
Sqd_KpnI_F	AAAAGGTACCATGGCCGAGAACAAGCAA
Sqd_XbaI_R	AAAATCTAGAGAACTGCTGATAGTTGTTGCT
BSF_Notl F	AAAGCGGCCGCCATGGCATCCATCCTGAGGAC
BSF_AscI_R	AAAGGCGCGCCCGGCCTTGCTGTCCGGTTT
Dcp1_NotI_F	AAAGCGGCCGCCATGGCCGACGAGAGCATC
Dcp1_AscI_R	AAAGGCGCGCCCTTGATATGTGGAGCTGGAGTCC
eiF4E_NotI_F	AAAGCGGCCGCCATGCAGAGCGACTTTCACA
eiF4E_AscI_R	AAAGGCGCGCCCCAAAGTGTAGATCGATTTCACG

5.1.3.3.2. Cloning of reporter constructs

Table 11. Oligonucleotides used for cloning of reporter constructs.

Name	**Sequence**
osk_KpnI_F	AAAAGGTACCGGATCACTTTCCTCCAAGC
osk_SalI_R	AAAAGTCGACTAATGCAAGGTTGGAAACTG
osk_3UTR_EcoRV_F	AAAAGATATCGTTGGGTTCTTAATCAAGAT
osk_3UTR_SalI_R	AAAAGTCGACTAGCAAAGATTCAAGCCAAT
grk_3UTR_EcoRI_F	AAAAGAATTCGATTTAGAATTTGATTTGGA
grk_3UTR_SalI_R	AAAAGTCGACAAATGATGAAAGTGAGGAGA
osk_delta_AR_F	TTTGTCCTATAACAAGCTGCAATAAAAGGGA AATCAATGA
osk_delta_AR_R	TCATTGATTTCCCTTTTATTGCAGCTTGTTAT AGGACAAA
osk_delta_Mkrn1_F	AATTGTATGTATTGATGGTGCAAGCTGCAAT GTAAAATCC
osk_delta_Mkrn1_R	GGATTTTACATTGCAGCTTGCACCATCAATA CATACAATT
osk_typeII_2_F	TGATGGTGATCACGTTTTTTTCGCTTTATAAC AAGCTGCAATGTAA
osk_typeII_2_R	TTACATTGCAGCTTGTTATAAAGCGAAAAAA ACGTGATCACCATCA
osk_delta_typeII_2_F	TGATGGTGATCACGTTTTTTTATAACAAGCTG CAATGTAA

osk_delta_typeII_2_R	TTACATTGCAGCTTGTTATAAAAAAACGTGATCACCATCA
Osk_977-981_mut_F	ATCACGTTTTTTTTGTCCTAATTGTAGCTGCAATGTAAAATCCAA
Osk_977-981_mut_R	TTGGATTTTACATTGCAGCTACAATTAGGACAAAAAAAACGTGAT
Osk_977-981_del_F	ATCACGTTTTTTTTGTCCTAAGCTGCAATGTAA AATCCAA
Osk_977-981_del_R	TTGGATTTTACATTGCAGCTTAGGACAAAAAAAACGTGAT

5.1.3.3.3. Others

Table 12. Additional oligonucleotides used for cloning in this study.

Name	Sequence
attB_F	TCGACATGCCCGCCGTGA
attB_R	GACGATGTAGGTCACGGTCTCGA
Act5_prom_AseI_F	CCCCATTAATCACAAATGATACTTCTAAAA
Act5_prom_NheI_R	CCCCGCTAGCGTCTCTGGATTAGACGACT

5.1.3.4. Oligonucleotides used for RT-qPCR

Table 13. Oligonucleotides used for RT-qPCR.

Name	Sequence
rpl15_F	AGGATGCACTTATGGCAAGC
rpl15_R	GCGCAATCCAATACGAGTTC
18S_F	CTGAGAAACGGCTACCACATC
18S_R	ACCAGACTTGCCCTCCAAT
Fluc_F	CCAGGGATTTCAGTCGATGT
Fluc_R	AATCTGACGCAGGCAGTTCT
osk_mRNA_F2	TTCGCTTGCACAAAATCAAC
osk_mRNA_R2	TTTGCAAACGGAAACAGAAA
grk_mRNA_F2	AGCTTTCGTTGGAGCTTTTG
grk_mRNA_R2	TCGAGTCCCAATCCTCTTCT
bcd_mRNA_F2	AACATTTGCGCATTCTTTGA
bcd_mRNA_R2	AGTTATTCCGTTTGGCAGCA
Mkrn1_mRNA_qPCR_F2	CCCAACGGAGATATCGTCGA

Mkrn1_mRNA_qPCR_R2	AGCTTAGTCTTCATCCGAGTAATCT
CG12477_mRNA_qPCR_F1	AACCAATCCAATAGAGCAG
CG12477_mRNA_qPCR_R1	TTCACTATGTCGGCAGAG
CG5334_mRNA_qPCR_F2	GTTGCTAAGCGAATATCGCG
CG5334_mRNA_qPCR_R2	TAAAAGTCGTCATCCTCCATTG
CG5347_mRNA_qPCR_F2	CGTGAACGTCGCTTTGGCAT
CG5347_mRNA_qPCR_R2	CCCATTGCCGCGCGATATTC
dPABP_cDNA_F	CCAGCAGCGTACTTCCAACT
dPABP_cDNA_R	CCCAGGATCTGTTTCTGCTC
Imp_mRNA_F	TCCGGTGGAGATGAAGAGAC
Imp_mRNA_R	TGTTCTTTGGCAGCTTTCTG
CG11414_mRNA_F	GCGAACTGGAGGCAAATAAC
CG11414_mRNA_R	TCTCGACGCATAGGTCACAG

5.1.4. Antibodies and beads

5.1.4.1. Antibodies used for western blotting

Table 14. List of primary antibodies used for western blotting.

Antibody	Dilution	Source/ Supplier
α-β-Tubulin MMS-410P mouse	1:5.000	Covance
α-Bru1 rabbit	1:1.000	Ephrussi lab
α-Cup rat	1:1.000	Lasko lab
α-FLAG M2 mouse	1:1.000	Sigma-Aldrich
α-GFP TP401 rabbit	1:5.000	Acris Antibodies
α-HA F7 mouse	1:1.000	Santa Cruz
α-HA mouse	1:1.000	IMB CF, Protein Production
α-HA rabbit	1:1.000	Santa Cruz
α-HA 3F10 rat	1:1.000	Roche
α-Myc 9E10 mouse	1:2.000	Enzo Life Sciences
α-Myc 9B11 mouse	1:2.000	Cell Signaling
α-Osk rabbit	1:1.000	Ephrussi lab
α-pAbp rabbit	1:3.000	Lasko lab
α-Ubiquitin sc-8017 mouse	1:1.000	Santa Cruz

Table 15. List of secondary antibodies used for western blotting.

Antibody	Dilution	Source/ Supplier
α-mouse HRP (L)	1:10.000	Dianova
α-mouse HRP (H+L)	1:10.000	Dianova
α-rabbit HRP (H+L)	1:10.000	Dianova
α-rat HRP (H+L)	1:10.000	Dianova

5.1.4.2. Antibodies used for immunostaining experiments

Table 16. List of primary antibodies used for immunostaining.

Antibody	Dilution	Source
α-1B1 1ea mouse	1:20	DSHB
α-Dcp1, cleaved 9578 rabbit	1:200	Cell Signaling
α-FLAG M2 mouse	1:500	Sigma-Aldrich
α-Osk rabbit	1:1.000	Ephrussi lab
α-Orb 4H8 mouse	1:20	DSHB
DAPI	1:1.000	Sigma-Aldrich

Table 17. List of secondary antibodies used for immunostaining.

Antibody	Dilution	Source
α-mouse Alexa Flour 488	1:500	Dianova
α-mouse TRITC	1:250	Dianova
α-rabbit Alexa Flour 488	1:500	Dianova

5.1.4.3. Antibodies used for IPs

Table 18. List of antibodies used for IPs.

Antibody	Dilution	Source
α-Bru1 rabbit	1:1.000	Ephrussi lab
α-Cup mouse	1:1.000	Lasko lab
α-FLAG M2 mouse	1:1.000	Sigma
α-mouse IgG 12-371	1:500	Merck
α-Myc 9E10 mouse	1:500	Enzo Life Sciences
α-Myc 9B11 mouse	1:1.000	Cell Signaling
α-rabbit IgG 12-370	1:500	Merck

5.1.4.4. Beads used for IPs

Table 19. Beads used for IP experiments.

Beads	Source
Dynabeads® Protein G	Thermo Fisher
GFP binder beads, magnetic agarose	IMB CF, Protein Production
GFP-Trap, magnetic agarose	Chromotek
Myc-Trap, magnetic agarose	Chromotek
Pierce™ α-Myc magnetic beads	Thermo Fisher

5.1.5. Enzymes, reagents and commercially available kits

Table 20. List of enzymes used in this study.

Enzyme	Supplier
AscI	NEB
AseI	NEB
DNaseI	NEB
EcoRI	NEB
EcoRV	NEB
KpnI	NEB
M-MLV Reverse Transcriptase	Promega
NheI	NEB
NotI	NEB
OneTaq	NEB
Phusion	NEB
Polynucleotide Kinase (PNK)	NEB
Power SYBR® Green PCR Master Mix	ThermoFisher
Proteinase K	Sigma-Aldrich
RNaseI	Thermo Fisher
RNase A	Sigma-Aldrich
RNase T1	ThermoFisher
SalI	NEB
T4 DNA Ligase	NEB
Turbo DNase	Thermo Fisher
XbaI	NEB

Table 21. List of reagents used in this study.

Reagent	Supplier
1 kb ladder	NEB
4x LDS buffer	Life Technologies
5x OneTaq quick load buffer	NEB
5x Phusion HF buffer	NEB
10x Cutsmart buffer	NEB
10x PBS	IMB CF, Media Lab
10x PNK buffer	NEB
10x Running buffer	IMB CF, Media Lab
10x T4 DNA Ligase	NEB
10x Transfer buffer	IMB CF, Media Lab
30% Acrylamide/Bis Solution	BioRad
50x TAE butter	IMB CF, Media Lab
100 bp ladder	NEB
µ-Slide containing 8 well	ibidi
Agarose	Sigma-Aldrich
Ambion nuclease-free water	Thermo Fisher
Ambion GlycoBlue™	Thermo Fisher
Ambion 3M Sodium acetate (NaAc)	Thermo Fisher
Ampicillin	Sigma-Aldrich
Ampure XP beads	Beckman Coulter
Ammonium Persulfate (APS)	BioRad
Apoprotinin	Roth
Bleach/ Sodium hypochlorite	Roth
Blotting Paper	Neolab
Bradford reagent	BioRad
Bromphenol Blue	Sigma-Aldrich
Chloroform/ Trichlormethan	Roth
Colloidal Blue Staining Kit	Life Technologies
Cycloheximide (CHX)	Sigma-Aldrich
Donkey serum	Sigma-Aldrich
Dry milk powder, non-fat	Cell Signaling
DL-Dithiothreitol (DTT)	Sigma-Aldrich
EDTA	IMB CF, Media lab
Ethanol (EtOH)	Thermo Fisher
Ethidium Bromide (EtBr)	Applichem
FBS	Sigma-Aldrich
Formaldehyde	Sigma-Aldrich
Glycerol	Sigma-Aldrich
Glycine	Sigma-Aldrich
Isopropanol	Honeywell Research Chemicals
Kanamycine	IMB CF, Media lab

LB media	IMB CF, Media lab
Leupeptin	Roth
Lithium chloride (LiCl)	Sigma-Aldrich
low molecular weight marker	NEB
Magnesium chloride, 2M	IMB CF, Media lab
Methanol	Roth
MG-132	Sigma-Aldrich
N-Ethylmaleimide (NEM)	Sigma-Aldrich
Nitrocellulose membrane	Neolab
Nonfat Dry Milk	Cell Signaling
Nonidet P 40 (NP-40)	Sigma-Aldrich
NuPAGE 5x TBE buffer	Thermo Fisher
NuPAGE 6% TBE-Urea gel	Thermo Fisher
NuPAGE 20x MOPS buffer	Thermo Fisher
NuPAGE 20x Transfer buffer	Thermo Fisher
NuPAGE Antioxidant	Thermo Fisher
NuPAGE Tris-Bis gel 4-12%	Thermo Fisher
Oligo d(T)25 magnetic beads	NEB
Orange G	Merck
Paraformaldehyde 95%	Sigma-Aldrich
Patent blue V	Sigma-Aldrich
Penicillin-Streptomycin	Sigma-Aldrich
Pepstatin	Roth
Phenol - chloroform - isoamyl alcohol mixture	Sigma-Aldrich
Phenylmethanesulfonyl fluoride (PMSF)	Sigma-Aldrich
Polylysine	Sigma-Aldrich
Potassium chloride (KCl)	Roth
Prestained Protein Marker	NEB
PVDF membrane, Immobilon®-P	Merck
Schneider’s Drosophila Medium, w: L-Glutamine, w: 0.4 g/L NaHCO3	PAN Biotech
Schneider's medium without lysine and arginine, Custom Medium Manufacturing	AthenaES
SDS running solution	IMB CF, Media lab
SDS stacking solution	IMB CF, Media lab
Sodium acetate (NaAc)	Thermo Fisher
Sodium chloride (NaCl), 5 M	IMB CF, Media lab
Sodium phosphate monobasic (NaH2PO4)	Sigma-Aldrich
Sodium deoxycholate (Na-DOC)	Sigma-Aldrich
Sodium dodecyl sulfate (SDS)	Sigma-Aldrich
Sodium hydroxide (NaOH)	Sigma-Aldrich
SuperSignal™ West Femto Chemiluminescent Substrate	Thermo Fisher
SuperSignal™ West Pico Chemiluminescent Substrate	Thermo Fisher

Tetramethylethylenediamine (TEMED)	Roth
Tris, 1M, pH 7.5	IMB CF, Media lab
Tris, 1M, pH 8	IMB CF, Media lab
Triton-X 100	Sigma-Aldrich
TRIzol	Thermo Fisher
Tween-20	Sigma-Aldrich
Urea	Sigma-Aldrich
Vectashield with DAPI	Linaris
Voltaleff Oil 3S	Lehmann & Voss
Voltaleff Oil 10S	VWR
Water, ultra pure	IMB CF, Media lab
Water, nuclease free	Qiagen

Table 22. List of commercial kits used in this study.

Kit	Supplier
Effectene	Quiagen
Gateway kit	ThermoFisher
Gel extraction Kit	Eurogentec
GeneJet Plasmid Mini Kit	Thermo Scientific
High Sensitivity DNA Kit	Aglient
HiScribe T7 Kit	NEB
NEBNext Ultra II Directional RNA Kit	NEB
pENTR/D-TOPO cloning kit	ThermoFisher
QIAprep Spin Midiprep Kit	Quiagen
QIAprep Spin Miniprep Kit	Quiagen
RNA 6000 Nano Kit	Aglient
SmartPure Gel Kit	Eurogentec

5.1.6. Electronic devices and software

Table 23. List of electronic devices used in this study.

Electronic device	Supplier
Bioanalyzer 2100	Aglient
Bioruptor	Diagenode
Gel Doc™ XR+ Gel Documentation System	BioRad
LSRFortessa SORP analyzer	BD Biosciences
Microscope M80 (Brightfied)	Leica
MiSeq sequencing system	Illumina

NanoDrop 2000	Thermo Fisher
NextSeq500 sequencing system	Illumina
TCS SP5 (inverted)	Leica
Phosphoimager Typhoon FLA9500	GE Healthcare Life Sciences
ViiA7 real-time PCR system	Applied Biosystems

Table 24. List of software used in this study.

Software	**Supplier**
bcl2fastq conversion software v2.19.1	Illumina
Bioanalyzer 2100 Expert Software	Aglient
FastQC v0.11.5	Babraham Bioinformatics
FlowJo™	BD Biosciences
Image Lab v2.0	BioRad
MaxQuant v1.5.28	Max Planck Institute of Biochemistry
NanoDrop™ 2000	Thermo Fisher
Leica Application Suite (LAS)	Leica
QuantStudio Real-Time PCR Software	Thermo Fisher
SerialCloner v2.6	Serial Basics

5.2. Methods

5.2.1. Cell culture

5.2.1.1. Cell culture maintenance

Drosophila S2R+ cells were grown in Schneider's medium supplemented with 10% FBS and 1% Penicillin-Streptomycin.

5.2.1.2. Knockdown and transfection

For knockdown experiments, S2R+ cells were seeded at the density of 106 cells/ml in serum-free medium and 15 µg/ml of dsRNA (5.2.5.2) was added to the cells. After 6 h of cell starvation, serum supplemented medium was added to the cells. dsRNA treatment was repeated after 48 h and cells were collected 24 h after the last treatment. A list of primers used to create dsRNA templates by PCR is appended (Table 7). Effectene® was used to transfect vector constructs in all overexpression experiments following the manufacturer's protocol.

5.2.1.3. Cycloheximide treatment

For cycloheximide (CHX) treatments, 10 mM of CHX was added to S2R+ cells prior to harvesting for 4, 8 or 24 hrs.

5.2.1.4. Protein lysate preparation

Proteins from S2R+ cells seeded in 6-well formate were extracted using 100 µl of RIPA buffer (Table 25) containing protease inhibitors (1 µg/mL Leupeptin, 1 µg/mL Pepstatin, 1 µg/mL Aprotinin and 1 mM PMSF) by incubating at 4°C for 10 min. Cells were subsequently subjected to 2 cycles of sonication on a bioruptor with 30 seconds "ON"/ "OFF" at low setting. Remaining

cell debris was removed by centrifugation at 21.000 g for 10 min at 4°C and protein content was measured using Bradford reagent.

Table 25. Buffer used for protein lysate preparation.

Name	Composition
RIPA buffer	140 mM NaCl, 50 mM Tris pH 7.5, 1 mM EDTA pH 8, 1% Triton X-100, 0.1% SDS, 0.1% sodium deoxycholate

5.2.1.5. Western Blotting

For Western blot analysis, proteins were separated on an 8% SDS-PAGE gel and transferred on Immobilon-P PVDF membrane according to the manufacturer's instruction. After blocking for 1 h at RT, the membrane was incubated with primary antibody in blocking solution O/N at 4°C. The membrane was washed 3x in PBST for 10 min and incubated 1 h a RT with 1:10.000 dilution of HRP secondary antibody in blocking solution. Protein bands were detected using SuperSignal™ West Pico Chemiluminescent Substrate in a Gel Doc station. A list of antibodies used in this study can be found in Table 16 and Table 17.
For restaining, the membrane was incubated for 10 min with mild stripping buffer, washed twice with PBS and PBST and blocked again. Incubation of primary and secondary antibodies was performed as described above. Buffer compositions are displayed in Table 26.

Table 26. Buffers used for western blotting.

Name	Composition
Blocking solution	5 % (w/v) skim milk powder in PBST
Mild stripping buffer	100 mM Glycine, 1% SDS, 10% Tween 20, adjust pH to 2.2
PBST	0.1% Tween-20 in PBS
SDS buffer	50 mM Tris pH 6.8, 2% SDS, 10% glycerol, 100 mM DTT, 0.05% Bromphenol Blue

5.2.2. Fly work

5.2.2.1. Genomic DNA preparation from flies

To isolate gDNA, flies were collected in tubes and smashed in 100 µl Fly lysis buffer (Table 27) and incubated at 37°C for 1 hr. Proteinase K and RNase A were subsequently inhibited at 95°C for 5 min and the DNA containing supernatant was stored at 4°C.

Table 27. Buffer composition used for DNA preparation from flies.

Name	Composition
Fly lysis buffer	150 mM NaCl, 100 mM Tris pH 8, 10 mM EDTA pH 8, 200 µg/ ml Proteinase K, 10 µg/ ml RNase A

5.2.2.2. Protein lysate preparation

To isolate proteins from ovaries, the protocol was applied as for S2R+ cells (5.2.1.4) with small adjustments: The ovaries were smashed in RIPA buffer using pistils and sonicated twice with 10 min incubation at 4°C in between. To remove remaining lipids from ovaries, the centrifugation step was repeated 3 times.

5.2.2.3. Generation of *Mkrn1* mutants using CRISPR/ Cas9

The guide RNAs used were cloned into expression vectors pBFv-U6.2 and pBFv-U6.2B [387]. To this end, two guide RNAs were used in combination (gRNA_left starting at 387 nt of *Mkrn1* gene and gRNA_right starting at position 2239 nt and for deletion of *CG12477* gRNA_left starting at 196 nt and gRNA_right starting at 934 nt). TBX-0002 embryos were injected with the purified plasmids containing the gRNA (250 ng/µl in injection buffer, Table 28). When reaching adulthood, the injected embryos were crossed with TBX-0008 flies to analyze the integration of the gRNAs by the expression of the *vermillion* gene in the progeny [387]. Flies carrying the integrated gRNAs were crossed with Cas-0001 flies expressing Cas9 under the control of a *nos* promoter [387]. Subsequently, the progeny was crossed with a balancer line and screened for successful deletion. To this end, genomic PCR from single flies was prepared

and tested for CRISPR/ Cas9 induced mutations by PCR using primers that bind in proximity to the gRNA targeting site. Successful deletion was indicated by a reduced size of the amplicon (Fig. M1). To verify the deletion the amplicon was subsequently sequenced. A list of gRNAs and primers to verify the knockout can be found in Table 8 and Table 9.

Table 28. Buffer used for DNA injection into *Drosophila* embryos.

Name	Composition
Injection buffer	0.1 mM NaH_2PO_4, 5 mM KCl, adjusted to pH 6.8

Flies containing the deletion of the Mkrn1 gene (*Mkrn1*^{N}) were isogeniezed before using for experiments. To this end, the *Mkrn1*^{N} flies were crossed four times with *w1118* wild-type flies to remove potential off-target mutations induced by CRISPR/ Cas9. To ensure the presence of the deletions, flies were screened by PCR. After isogenization, flies were crossed with a balancer line to establish a stable stock.

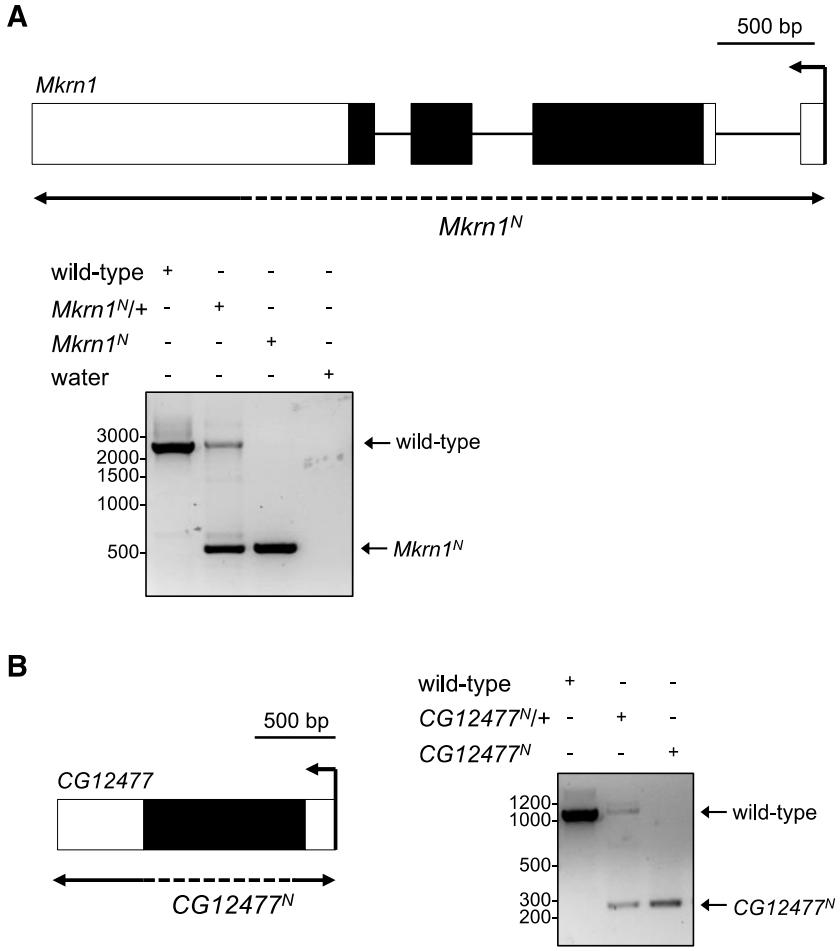

Figure M1. Generation of *Mkrn1* mutants in *Drosophila*.
Mutations of the (A) *Mkrn1* and (B) *CG12477* genes were generated using CRISPR/ Cas9. The genes are schematically presented with the coding sequence indicated in black and introns as lanes. The deletions introduced by CRISPR/ Cas9 are indicated with dashed lines below. Scale bars depict 500 bp. For both genes, the deletion was verified by semi-quantitative PCR indicated by a drop visualized with agarose gels. **(A)** Below: Deletion of the *Mkrn1* gene resulting in $Mkrn1^{N}$ allele was verified by PCR and is indicated with a fragment size of 565 bp instead of 2388 bp. **(B)** Right: A Deletion of the *CG12477* gene leading to the $CG12477^{N}$ allele was analyzed by PCR and depicted with a fragment size of 247 bp instead of 1005 bp.

5.2.2.4. Generation of transgenic flies

The *Mkrn1* constructs were prepared using the Gateway™ pPFMW vector containing an inserted *attB* sequence (5.2.3). Constructs containing either huMKRN1, $Mkrn1^{\Delta ZnF1}$, $Mkrn1^{RING}$, $Mkrn1^{\Delta ZnF1+RING}$ or $Mkrn1^{PAM2}$ were verified by sequencing and injected into attP40 embryos (250 ng/µl in injection buffer) either in-house or via BestGene Inc. Progeny harboring the transgenes were crossed with balancer flies to establish the individual lines. Mkrn1 expression was driven by crossing the transgenic flies with a *nos>Gal4* driver. Expression of Mkrn1 transgenes was verified by western blotting (Fig. M2). As control, flies with integrated wild-type Mkrn1 were used [346].

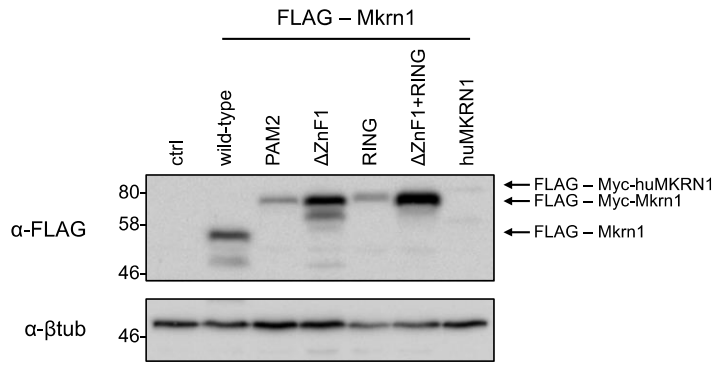

Figure M2. Validation of *Mkrn1* transgenes in *Drosophila*.
pPFMW constructs with *Mkrn1* coding sequence containing mutations of either the PAM2 motif, ZnF1, ZnF2 or RING domain were introduced in the *Drosophila* genome. In addition, a construct encoding a double mutant of the ZnF1 deletion and the mutation within the RING domain (ΔZnF1+RING) was generated. Human *MKRN1* was integrated as well. The expression of all transgenes was examined using a *nos>Gal4* driver. Ovarian protein lysates were analyzed for their expression using an immunoblot against the FLAG tag. As loading control, protein levels of β-tubulin were analyzed. To verify the expression, wild-type Mkrn1 was used as control. Note that the wild-type Mkrn1 runs faster as it does not possess an additional Myc tag.

5.2.2.5. Rescue experiments

Flies carrying wild-type, human or mutant *Mkrn1* transgenes on the second chromosome were crossed with the *nos>Gal4* driver in the $Mkrn1^{N}$ mutant background. For wildtype Mkrn1, transgenic flies carrying *pPFW-Mkrn1* were used [346]. For all other Mkrn1 constructs, *pPFMW-Mkrn1* transgenes with the respective mutations were used (5.2.2.4). The progeny was collected and analyzed together with heterozygous and homozygous $Mkrn1^{N}$ mutants as controls (Fig. M3). To examine the degree of each rescue, hatching rate (5.2.2.6) was measured and immunostaining (5.2.4.2) as well as western blotting (5.2.1.5) of the ovaries was performed.

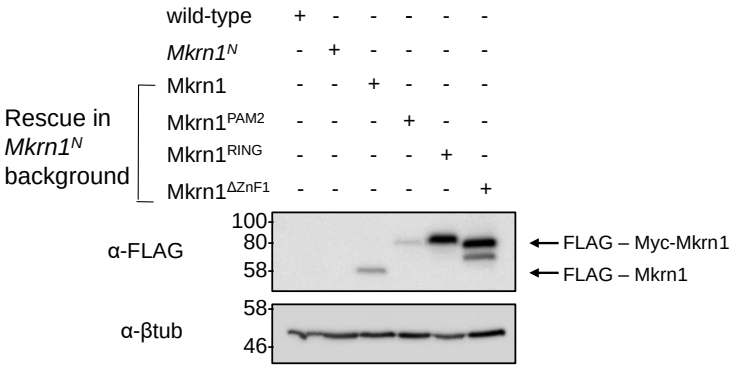

Figure M3. Analysis of rescue experiments performed in *Drosophila*.
Different transgenes encoding wild-type or mutant Mkrn1 were overexpressed in the *Mkrn1*^{N} background. Overexpression was induced via a *nos>Gal4* driver. Expression of the transgenes was analyzed by western blotting against the FLAG tag. As loading control, protein levels of β-tubulin were analyzed. Note that wild-type Mkrn1 runs faster due to a missing Myc tag present in the other transgenes.

5.2.2.6. Hatching rate

Flies were incubated on apple juice plates for 6-10 h. The laid eggs were collected and incubated at 25°C for 36 h to allow completion of hatching. Hatched and non-hatched embryos were counted with a M80 brightfield microscope, and the hatching rate was calculated. For every genotype at least three individual tests were performed.

5.2.2.7. Staging

Staging experiment was performed as described using *Drosophila* wild-type flies [381]. For all stages, RNA was isolated and cDNA prepared.

5.2.3. Gene cloning

5.2.3.1. Polymerase chain reaction

Amplifications of DNA for cloning and colony PCR (5.2.3.4), to create dsRNA templates (5.2.1.2) as well as to screen for *Makorin* mutants (5.2.2.3) were performed using PCR. To this end, either OneTaq® DNA Polymerase or Phusion® High-Fidelity DNA Polymerase was

used according to the manufacturer's instructions. The produced amplicons were examined using agarose gel electrophoresis (5.2.3.2).

5.2.3.2. Agarose gel electrophoresis and gel elution

Analysis of PCR products and plasmids incubated with restriction endonucleases was performed using agarose gel electrophoresis. Dependent on the size, 1-1.7% agarose gels were prepared using 1x TAE buffer. DNA fragments were loaded on the gels with 1x DNA loading buffer (Table 29), separated by size and detected using Ethidium Bromide staining in a Gel Doc™ station.

To purify specific DNA fragments, the responding band was cut out of the agarose gel and purified using SmartPure gel extraction kit according to the manufacturer's instruction.

Table 29. Buffer used to separate DNA fragments via agarose gel electrophoresis.

Name	Composition
6 x DNA loading buffer	15 % Ficoll, 10 mM EDTA pH 8.0, Orange G

5.2.3.3. Digestion, ligation and transformation

The produced PCR amplicons were incubated with the indicated restriction endonucleases according to the manufacturer's instructions. Digested DNA fragments were purified and subsequently ligated to the digested vector in a molar vector / insert ratio of 3 / 1 using T4 DNA Ligase.

The ligated plasmids were transformed into chemically competent DH5α cells. In brief, ligation mix was added to 10-fold volume of cells and incubated for 10 min on ice. Heat shock was performed at 42°C for 45 sec and 10 volumes of LB medium was added. After incubation at 37°C for 45 min, cells were plated on LB agar plates either containing ampicillin (100 mg/l) or kanamycine (50 mg/l) and kept at 37°C O/N.

5.2.3.4. Cloning analysis

To validate the successful cloning, colony PCR (5.2.3.1) or restriction digestion was performed. To analyze the restriction pattern, plasmid DNA was isolated using a conventional DNA mini prep protocol. Bacterial cells were pelleted at 12.000 g for 30 sec and resuspended in 250 µl Solution P1, mixed with 250 µl Solution P2 and subsequently with 350 µl Solution P3 by inversion. Cell debris were pelleted at 20.000 g for 10 min and the supernatant was mixed with 1 volume of Solution P4. The DNA was precipitated at 20.000 g for 10 min, washed with Solution P5 and air dried before resuspending in 50 µl water. Buffer compositions are listed in Table 30.

For transfections in cell culture and injections in flies, plasmid DNA was isolated using the GeneJet Plasmid Mini Kit and QIAprep Spin Miniprep Kit, respectively. All plasmids were additionally verified by DNA sequencing using GATC lightrun (Eurofins Genomics).

Table 30. Buffers used for plasmid DNA isolation using mini prep.

Name	Composition
Solution P1	50 mM Tris-HCl, 10 mM EDTA pH 8.0, 0.1 mg/ml RNase A
Solution P2	200 mM NaOH, 1% SDS.
Solution P3	3 M potassium acetate pH 5.5.
Solution P4	Isopropanol
Solution P5	70% Ethanol

5.2.3.5. Strategies used for cloned plasmids

Full-length wild-type *Mkrn1* coding sequence was cloned into the pENTR entry vector using the pENTR/D-TOPO cloning kit. For further cloning, *KpnI* and *XbaI* restriction sites were introduced flanking the coding sequence. The insert was subcloned into Gateway™ expression vectors containing the *actin5* promoter with different tags by LR in vitro recombination (The Drosophila Gateway™ Vector Collection) [347, 350, 388]. A list of plasmids with their respective promoter and tags can be found in Table 2 and Table 3. To introduce mutations or different coding sequences into the same vectors, the *KpnI* and *XbaI* restriction sites were subsequently used. To overexpress proteins under the control of a UASp promoter, the respective coding sequence was inserted into the Gateway™ pPFMW vector using *AscI* and *NotI* restriction sites. A list of primers used to introduce the coding sequences as well as to

introduce mutations in the *Mkrn1* coding sequence is appended (Table 10). To use the Gateway™ pPFMW vector for attB/ attP recombination, an *attB* sequence was introduced into the vector backbone using *ZraI* restriction site (primers sequence see Table 12). All plasmids produced in this study contain the *attB* sequence in the pPFMW vector.

To analyze the binding of Mkrn1 to *osk* by iCLIP, the *osk* gene was cloned in the vector backbone of pAc5.1B-EGFP (gift from Elisa Izaurralde, Addgene plasmid #21181) using restriction sites *KpnI* and *SalI*. The binding of Mkrn1 to the 3' UTR of *osk* and *grk* was examined by insertion of the respective 3' UTR downstream of firefly luciferase coding sequence. To this end, firefly luciferase coding sequence was introduced into the pAc5.1B-EGFP backbone using *KpnI* and *EcoRI* restriction sites. In addition, the coding sequence contained an *EcoRV* restriction site at its 3' end. The 3' UTRs of (wild-type and mutant) *osk* and *grk* were introduced using *EcoRV* and *SalI* or *EcoRI* and *SalI* restriction patterns, respectively. To ensure the proper usage of the endogenous polyA signal the 3' UTRs included 220 and 229 nucleotides of sequence downstream of the 3' UTR. All plasmids used to analyze the RNA-binding ability of Mkrn1 are listed in Table 4. Primers used for cloning of the respective plasmids are listed in Table 11.

The dual fluorescence reporter plasmids (pmGFP-P2A-K0-P2A-RFP, pmGFP-P2A-$(KAAA)_{12}$-P2A-RFP, pmGFP-P2A-$(KAAA)_{20}$-P2A-RFP and pmGFP-P2A-$(RCGA)_{10}$-P2A-RFP) were generously provided by Ramanujan S. Hegde [161]. To ensure the expression in *Drosophila* S2R+ cell culture the promoter was replaced by the *actin5* promoter using *AseI* and *NheI* restriction patterns (Primer sequences see Table 12). A list of the reporter plasmids is appended in Table 5.

5.2.4. Immunostaining

5.2.4.1. Immunostaining of S2R+ cells

Immunostaining was performed using µ-Slide 8 well microscopy chambers and S2R+ cells transfected 72 h prior to the experiments. The chambers were treated with polylysine for 30 min, washed once with PBS and around 10^6 cells were seeded in *Drosophila's* Schneider medium. Cells were allowed to attach for 1 h at RT and then washed with PBS. Fixation was

performed using 4 % formaldehyde in PBS for 10 min at RT. Subsequently, cells were washed with PBST0.1 for 10 min and blocked using PBST0.1 supplemented with 10 % donkey serum for 1 h at RT. Primary antibodies were diluted in PBST0.1 supplemented with 10 % donkey serum in the respective dilutions (Table 16) and incubated with the cells O/N at 4°C. Cells were washed three times with PBST0.1 and the secondary antibodies together with DAPI were added diluted in PBST0.1 supplemented with 10 % donkey serum (Table 17) for 2 h at 4°C. After the incubation cells were washed again three times with PBST0.1 and imaged using a TCS SP5 (inverted) confocal microscope using 40 x oil lens by laser scanning and processed with ImageJ. Buffer compositions are displayed in Table 31.

Table 31. Buffers used for immunostainings in S2R+ cells.

Name	Composition
PBST0.1	0.1% Triton-X100 in 1x PBS
PBST0.2	0.2% Triton-X100 in 1x PBS

5.2.4.2. Immunostaining of ovaries

Ovaries were dissected and fixed in 4% paraformaldehyde in PBS for 20 min at RT. Ovaries were washed three times in PBST0.2, washed once with PBST1 and permeabilized for 2 h at RT in PBST1. Subsequently, the ovaries were blocked in PBTB for 1 h at RT and incubated with the primary antibodies diluted in PBTB at 4°C overnight. The respective dilution of the antibodies can be found in Table 16. The ovaries were washed twice for 30 min with PBTB and blocked again using PBTB containing 5% donkey serum for 1 h at RT. Incubation with the conjugated secondary antibodies was performed in PBTB with 5% donkey serum for 2 h at RT. After 5 washes for 15 min with PBST0.2 egg chambers were dissected and mounted in DAPI containing Vectashield®. Buffer compositions are displayed in Table 32.
Stained egg chambers were examined using a TCS SP5 (inverted) confocal microscope. Images were taken using 40 x oil lens by laser scanning and processed with ImageJ.

Table 32. Buffers used for immunostainings in ovaries.

Name	Composition
PBTB	0.2% Triton X-100 and 1 % BSA (neutral pH) in 1x PBS
PBST0.2	0.2% Triton-X100 in 1x PBS
PBST 1	1% Triton-X100 in 1x PBS

5.2.5. RNA work

5.2.5.1. RNA isolation and measurement of RNA levels

Cells or tissues were harvested in TRIzol Reagent, RNA was extracted using Chloroform and precipitated with Isopropanol according to the manufacturer's instructions. For input and IP samples of RIP experiments, precipitation was performed in the presence of 0.5 µl of Ambion GlycoBlue™.

Prior to RT, possible DNA contaminants were removed with a DNaseI treatment at 37°C for 20 min. DNaseI was subsequently inhibited by adding 5 mM EDTA and incubating at 75°C for 10 min. cDNA was prepared from 500 ng - 2 µg of RNA with M-MLV Reverse Transcriptase and random primer according to the manufacturer's instructions.

The transcript levels were quantified by qPCR with Power SYBR® Green PCR Master Mix using the indicated primer (Table 13) and a ViiA7 real-time PCR system.

5.2.5.2. *In vitro* transcription and purification of ds RNAs

For preparation of dsRNAs, in vitro transcription was performed using the HiScribe® T7 Kit according to the manufacturer's instructions. To this end, 500 ng of DNA template containing T7 overhangs were used in 20 µl reaction volume. The produced dsRNAs were purified using 2.5 M Lithium Chloride and washed with 70% Ethanol. Subsequently, the dsRNA was dissolved in nuclease free water at 65°C for 10 min and allowed to slowly cooled down to RT to assure correct annealing.

5.2.5.3. RNA sequencing

5.2.5.3.1. Sample and library preparation

Ovaries of 6-7 days old flies were isolated and lysed in TRIzol Reagent. RNA was isolated (5.2.5.15.2.5.1) and the integrity of the RNA samples was analyzed using an RNA nano 6000 Chip.

2 µg of the obtained RNA was subjected to DNaseI treatment in 100 µl reaction volume according to the manufacturer's instruction. The mRNA was subsequently isolated in two rounds of PolyA extraction with oligo $d(T)_{25}$ magnetic beads following the manufacturer's instruction. Four individual libraries for homozygous *Mkrn1*^{W} and three for heterozygous *Mkrn1*^{W} ovary samples were prepared using NEBNext Ultra II Directional RNA Kit according to the manufacturer's instructions. To this end, 10 cycles were used to amplify each library. Libraries were subsequently purified from remnant oligo-dimers twice using Ampure XP beads. Concentration and profiles of the libraries were analyzed with an Agilent High Sensitivity DNA Kit. The libraries were pooled to a final concentration of 4 nM and submitted to sequenced using Illumina NextSeq500 with a read length of 2x42 bp paired-end (NextSeq Control Software v. 2.2.0.4).

5.2.5.3.2. Sequencing analysis

The subsequent steps were performed by N. Kreim (IMB CF, Bioinformatics).

The samples were demultiplexed using bcl2fastq and the fastq files downsampled to 21 million read pairs. The paired end fastq files were mapped against BDGP6 Ensembl release 91 [389] using STAR [390]. Gene expression was quantified using featureCounts from the subread package taking only uniquely mapping reads into account [391]. Bigwig coverage tracks were generated using deepTools2 [392]. Differential expression analysis was performed using R/Bioconductor and DESeq2 [393, 394]. Genes were deemed significantly differently expressed for an FDR < 1%. GO-term and pathway analysis was performed using ClusterProfiler and ReactomePA [395, 396].

5.2.6. Immunoprecipitation (IP)

5.2.6.1. IP

Methods are described after [346].

For IPs, S2R+ cells were harvested, washed with PBS and lysed in IP buffer (Table 33) supplemented with proteinase inhibitors (1 µg/mL Leupeptin, 1 µg/mL Pepstatin, 1 µg/mL Aprotinin and 1 mM PMSF) for 30 min at 4°C. Cells were subjected to 2 cycles of sonication on a Bioruptor® with 30 seconds "ON"/ "OFF" at low setting and the remaining cell debris was removed by centrifugation at 21.000 g for 10 min at 4°C. Protein concentrations were determined using Bradford reagent.
2 mg of the protein lysates was incubated for 3 h with 2 µg of α-Myc or α-FLAG antibody pre-coupled to 15 µl of protein G Dynabeads® or 10 µl GFP-Trap® magnetic agarose beads with head-over-tail at 4°C. Beads were washed 4x for 10 min in IP buffer and eluted in 1x SDS buffer 95°C for 10 min. Eluted IP proteins were removed from the beads and analyzed by Western blot together with input samples.
To determine the dependence of interactions on RNA, 50 Units of RNaseT1 were added to the respective IP. To ensure the activity of RNase T1, lysates were incubated 10 min at room temperature prior to the incubation of lysate with antibody.

Table 33. Buffer used for IP experiments.

Name	Composition
IP buffer	150 mM NaCl, 50 mM Tris-HCl pH 7.5, 0.5% NP-40

5.2.6.2. Liquid chromatography-tandem mass spectrometry LC-MS/MS

Methods are described after [346].

5.2.6.2.1. Experimental setup and IP

To identify binding partners of Mkrn1, either Myc-GFP as control or Myc-Mkrn1 were ectopically expressed in S2R+ cells. Upon lysis, Myc-GFP or Myc-Mkrn1 were immunoprecipitated as described above (5.2.6.1). To ensure efficient IP, 15 µl of Pierce™ α-Myc magnetic beads were incubated for 2 h with the lysate at 4°C. In addition, the IP buffer was supplemented with 10 mM N-ethylmaleimide, 1 mM sodium orthovandate, 5 mM β-glycerophophoate and 5 mM sodium flouride to avoid degradation of target proteins. After IP, samples were eluted in 2x LDS buffer supplemented with 1 mM Dithiothreitol for 10 min at 70°C and incubated with 5.5 mM 2-chloracetamide (CAA) for 30 min at RT in the dark. All conditions were prepared in technical triplicates and performed in parallel.
For SILAC experiments, IP was performed similar as above containing the following additions: Cells were grown in Schneider's medium supplemented with 600 mg/ mL arginine and 1,650 mg/ mL lysine. The supplementation allows the metabolic incorporation of either "light" or "heavy" labelled amino acids. Whereas the natural containing amino acids are referred to as "light" (Arg0 and Lys0), "heavy" labelled amino acids contain the isotopes $^{15}N_2{}^{13}C_6$-lysine (Lys8) and $^{15}N_4{}^{13}C_6$-arginine [Arg10, 354]. The "light" cells were transfected with Myc-GFP whereas "heavy" cells expressed Myc-Mkrn1^{RING}. IP was performed as for the label-free quantification method described above. To analyze the strength of interaction, different NaCl concentrations (150 mM or 500 mM) were used in the washing buffer. After the third wash, "light" and "heavy" samples were combined and washed once more prior to elution and CAA treatment.

5.2.6.2.2. LC-MS/MS analysis

The subsequent steps were performed by A. Hildebrandt (P. Beli group, IMB) and A. Busch (IMB CF, Bioinformatics).

Conventional interactome analysis of the IP samples was performed as described before [164] with following changes: The enriched proteins were separated by SDS-PAGE with a 4-12% Bis-Tris protein gel and stained with Colloidal Blue Staining Kit. Subsequently, proteins were in-gel digested using trypsin and digested peptides were then extracted from the gel. Concentration, clearance and acidification of peptides, mass spectrometry analysis, and peptide identification were performed as described before [164]. For the SILAC quantification, samples were prepared using the conventional SILAC workflow [164].
For peptide identification in MaxQuant, the DROME database from UniProtKB (release May 2016) was used. For label-free quantification (LFQ) at least 2 LFQ ratio counts (without fast LFQ) were activated.

The data table of LFQ values resulting from MaxQuant was filtered for potential contaminants, reverse binders and protein groups only identified by site. Furthermore, protein groups with less than two peptides and less than 1 unique peptide were also removed from further analysis. After log-transforming all remaining LFQ values, missing values were imputed by beta distributed random numbers between 0.1% and 1.5% of the lowest measured values. As a final filtering step, only protein groups having measured values for at least two replicates of at least one experimental condition were kept for further analysis. All filter and imputing steps were done with an in-house R script.
Differential protein abundance analysis was performed on log-transformed LFQ values between two conditions at the time using the R package limma [397]. For each such comparison, only protein groups found in at least two replicates of at least one condition were kept and used. To visualize the interactome, the R package ggplot2 was used [398]. All protein groups with an FDR ≤ 0.05 and a $\log_2$ fold change of ≥ 2 were considered significantly changed.

5.2.6.3. RNA-Immunoprecipitation (RIP)

Methods are described after [346].

For RIP, S2R+ cells or ovaries were harvested and lysed in RIP buffer (Table 34) supplemented with proteinase inhibitors (1.5 µg/ml Leupeptin, 1.5 µg/ml Pepstatin, 1.5 µg/ml Aprotinin and 1.5 mM PMSF) and RNase inhibitors (20 U/µl). S2R+ cells were lysed for 20 min at 4°C, subtracted to 2 cycles of sonication on a Bioruptor® with 30 sec “ON”/“OFF” at low setting and

the remaining cell debris was removed by centrifugation at 21,000 g for 10 min at 4°C. To remove lipids and cell debris, ovary lysates were centrifuged 4 times. Protein concentrations were determined using Bradford reagent. 2 mg of protein lysate were incubated for 3 h with 2 µg of α-FLAG M2® antibody pre-coupled to 20 µl of rotein G Dynabeads® head-over-tail at 4°C. For RIP experiments analyzing binding of Bru1 or Cup in ovaries, either 1 µl of rabbit α-Bru1 or 1 µl of mouse α-Cup were incubated with ovarian lysate over night (15 h) at 4°C. As controls, either 2 µg of normal rabbit IgG or 2 µg of normal mouse IgG were used. 20 µl of protein G Dynabeads® were added for 2 h after the incubation. For every RIP experiment, beads were washed 4 x for 10 min in RIP buffer at 4°C.

For immunoprecipitation of GFP-tagged Imp and Bru1 15 µl of GFP-Trap® were used. Lysates were prepared similar as above using RIPA buffer (Table 34) supplemented with proteinase and RNase inhibitors. IP was performed for 2 h at 4°C and subsequently washed 4 x for 10 min with RIPA buffer.

Table 34. Buffers used for RIP experiments.

Name	Composition
RIPA buffer	140 mM NaCl, 50 mM Tris pH 7.5, 1 mM EDTA pH 8, 1% Triton X-100, 0.1% SDS, 0.1% sodium deoxycholate
RIP buffer	150 mM NaCl, 50 mM Tris-HCl pH 7.5, 0.5% NP-40, 1 mM EDTA

5.2.6.4. Individual-nucleotide resolution UV CrossLinking and ImmunoPrecipitation (iCLIP) and autoradiography

Methods are described after [346].

5.2.6.4.1. Experimental setup of iCLIP experiments

The iCLIP protocol was performed as in [256] with the following adaptations: S2R+ cells were crosslinked with 150 mJ/cm2 of UV light and subsequently harvested. Cells were lysed in urea cracking buffer and sonicated using 2 cycles with 30 sec “ON”/“OFF” at low setting. Remaining cell debris was removed by centrifugation at 21,000 x g for 10 min at 4°C. For ovaries, the centrifugation step was repeated twice. Lysate was diluted 1:5 in IP buffer and incubated with 4 µg of anti-FLAG M2® antibody pre-coupled to 100 µl of protein G

Dynabeads® for 2 h at 4°C. After IP, the pulled-down RNA-protein complexes were washed 3x with high salt buffer and 3x with PNK buffer. To trim the length of the crosslinked RNA, on-bead digestion using Turbo DNase and RNase I was performed. Subsequently, the beads were washed again 3x with high salt buffer and 3x with PNK buffer. Buffer compositions are displayed in Table 35.

Table 35. Buffers used for iCLIP experiments.

Name	Composition
High salt buffer	1 M NaCl, 50 mM Tris pH 7.4, 1 mM EDTA, 1% NP-40, 0.1% SDS, 0.5% Na-DOC
IP buffer	150 mM NaCl, 50 mM Tris pH 7.5, 0.5% Tween-20, 0.1 mM EDTA
PNK buffer	10 mM MgCl2, 20 mM Tris pH 7.6, 0.2% Tween-20
Urea cracking buffer	50 mM Tris pH 7.5, 6 M urea, 1% SDS, 25% PBS

5.2.6.4.2. Library preparation

The following steps were performed by A. Hildebrandt (J. König group, IMB)

For high-throughput sequencing of S2R+ cells, libraries of 6 technical replicates for FLAG-Mkrn1 and 1 replicate for FLAG-GFP (ctrl) were prepared as described [256].
Multiplexed iCLIP libraries were sequenced as 75-nt single-end reads on an Illumina MiSeq sequencing system.

5.2.6.4.3. Sequencing analysis

The following steps were performed by A. Busch (IMB CF, Bioinformatics).

Sequencing qualities were checked for all reads using FastQC. Afterwards, reads were filtered based on sequencing qualities (Phred score) of the barcode region. Reads with more than one position with a Phred score < 20 in the experimental barcode (positions 4 to 7 of the reads) or any position with a Phred score < 17 in the random barcode (positions 1 to 3 and 8 to 9) were excluded from subsequent analysis. Remaining reads were de-multiplexed based on the experimental barcode (positions 4 to 7) using Flexbar without allowing any mismatch [399].

All following steps of the analysis were performed on the individual samples after de-multiplexing. Remaining adapter sequences were removed from the read ends using Flexbar (version 3.0.0) with a maximal error rate of 0.1 and a minimal overlap of 1 nt between the beginning of the adapter and the end of the read. Following adapter trimming, the first 9 nt of each read containing the experimental and random barcodes were trimmed off and added to the read name in the fastq files in order to keep this information for downstream analysis. Reads shorter than 15 nt were removed from further analysis. Trimmed and filtered reads were mapped to the *Drosophila* genome (Ensembl genome assembly version BDGP6) and its annotation using STAR [390, 400]. When running STAR, up to two mismatches were allowed, soft-clipping was prohibited at the 5' ends of reads and only uniquely mapping reads were kept for further analysis. For further analysis, only unspliced reads were kept and analyzed.
Following mapping, duplicate reads were marked using the dedup function of bamUtil (version 1.0.13), which defines duplicates as reads whose 5' ends map to the same position in the genome (https://github.com/statgen/bamUtil). Subsequently, marked duplicates with identical random barcodes were removed since they are considered technical duplicates, while biological duplicates showing unequal random barcodes were kept.
Resulting bam files were sorted and indexed using SAMtools [401]. Afterwards, bedgraph files were created based on bam files, using bamToBed of the BEDTools, considering only the position upstream of the 5' mapping position of the read, since this nucleotide is considered as the crosslinked nucleotide [402]. Using bedGraphToBigWig of the UCSC tool suite, all bedgraph files were converted into bigWig files [403].

5.2.6.5. Ubiquitination assay

Ubiquitination assay was performed as described previously [194, 404] with the following adaptations: Cells were transfected with GFP alone or GFP-tagged protein of interest and treated for 6 h with 10 µM MG-132 prior to harvesting. Cells were lysed using 500 µl lysis buffer supplemented with protease inhibitors, PMSF and 10 mM NEM. IP was performed using 20 µl of GFP-Trap® beads for 90 min at 4°C. Subsequently, beads were washed once with dilution buffer, 3 times with stringent washing buffer and once with mild washing buffer. Buffer compositions are displayed in Table 36.
For analysis of proteins with a FLAG tag, IP conditions of iCLIP were used (5.2.6.4.1) with the following changes: Cells were treated for 6 h with 10 µM MG-132 prior to harvesting. The

Urea cracking buffer as well as IP buffer contained 10 mM NEM in addition to protease inhibitors. IP was washed 4 times with high salt buffer and 3 times with PNK buffer.
In both assays described above beads were boiled in 1x SDS buffer at 95°C for 10 min. Ubiquitination of the eluted proteins was analyzed by western blotting together with input samples using 50% of IP samples. The other half was analyzed for its IP efficiency on a different blot.

Table 36. Buffers used for UB assays.

Name	Composition
Dilution buffer	150 mM NaCl, 10 mM Tris pH 7.5, 0.5 mM EDTA
Lysis buffer	150 mM NaCl, 50 mM Tris pH 7.5, 1 mM EDTA, 0.5% Triton X-100
Mild washing buffer	1% SDS in PBS
Stringent washing buffer	8 M Urea, 1% SDS in PBS

5.2.7. Dual fluorescence translation stall assay by flow cytometry

To analyze the effect of Mkrn1 on RQC, a translation stall assay was performed as described before [161, 173]. In short, knockdowns in S2R+ cells were performed in 6 well format against *LacZ* (ctrl), *Mkrn1* and *CG11414* mRNA (5.2.1.2). Cells were washed and harvested in cold PBS (1x). Subsequently, cells were resuspended in 300 µl FACS buffer (Table 37).
The cellular expression of GFP and RFP was measured by flow cytometry using LSRFortessa SORP analyzer. For every experiment, 30.000 viable and transfected cells were analyzed. The data was analyzed using FlowJo and the ratio of RFP to GFP expression was calculated.

Table 37. Buffer used for flow cytometry experiments.

Name	Composition
FACS buffer	3 mM EDTA, 5% FBS in 1x PBS

SUPPLEMENTS

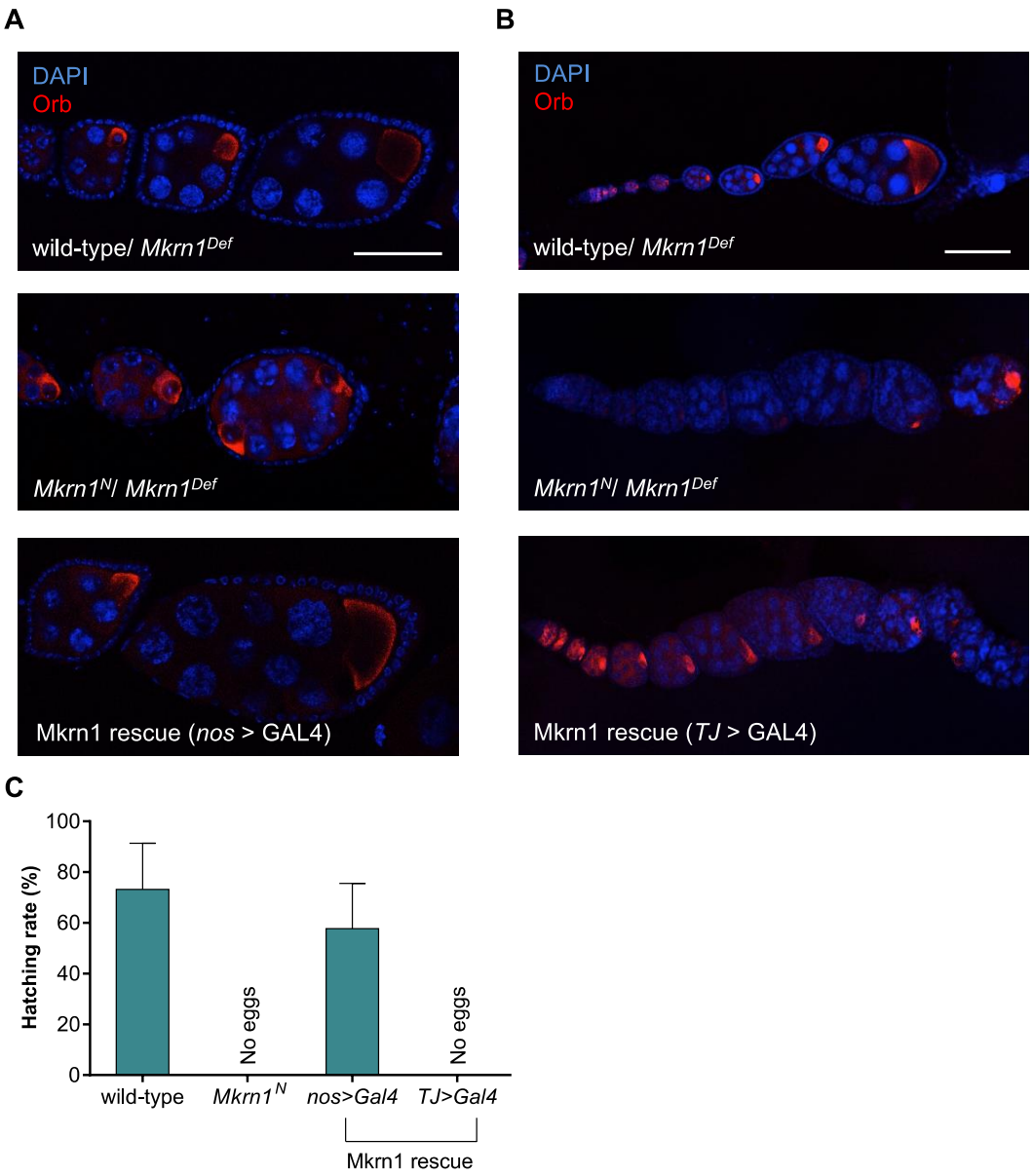

Figure S1. *Mkrn1* is required in germ cells but not in follicle cells.
Rescue experiments in *Mkrn1*^{N} ovaries were conducted. **(A, B)** Wild-type Mkrn1 was overexpressed using (A) a *nos>Gal4* or (B) a *Tj>Gal4* driver line. Ovaries were analyzed by immunostaining against α-Orb (oocyte specific; red) and DAPI (DNA; blue). Scale bars indicate 50 µm. **(C)** Fertility of *Mkrn1* females was analyzed via a hatching assay. The number of laid eggs was compared to the number of larvae hatched from females overexpressing Mkrn1 in the germline (*nos>Gal4*) or in the follicle cells (*Tj>Gal4*) in a *Mkrn1*^{N} background. Error bars depict Stdev of three technical replicates.

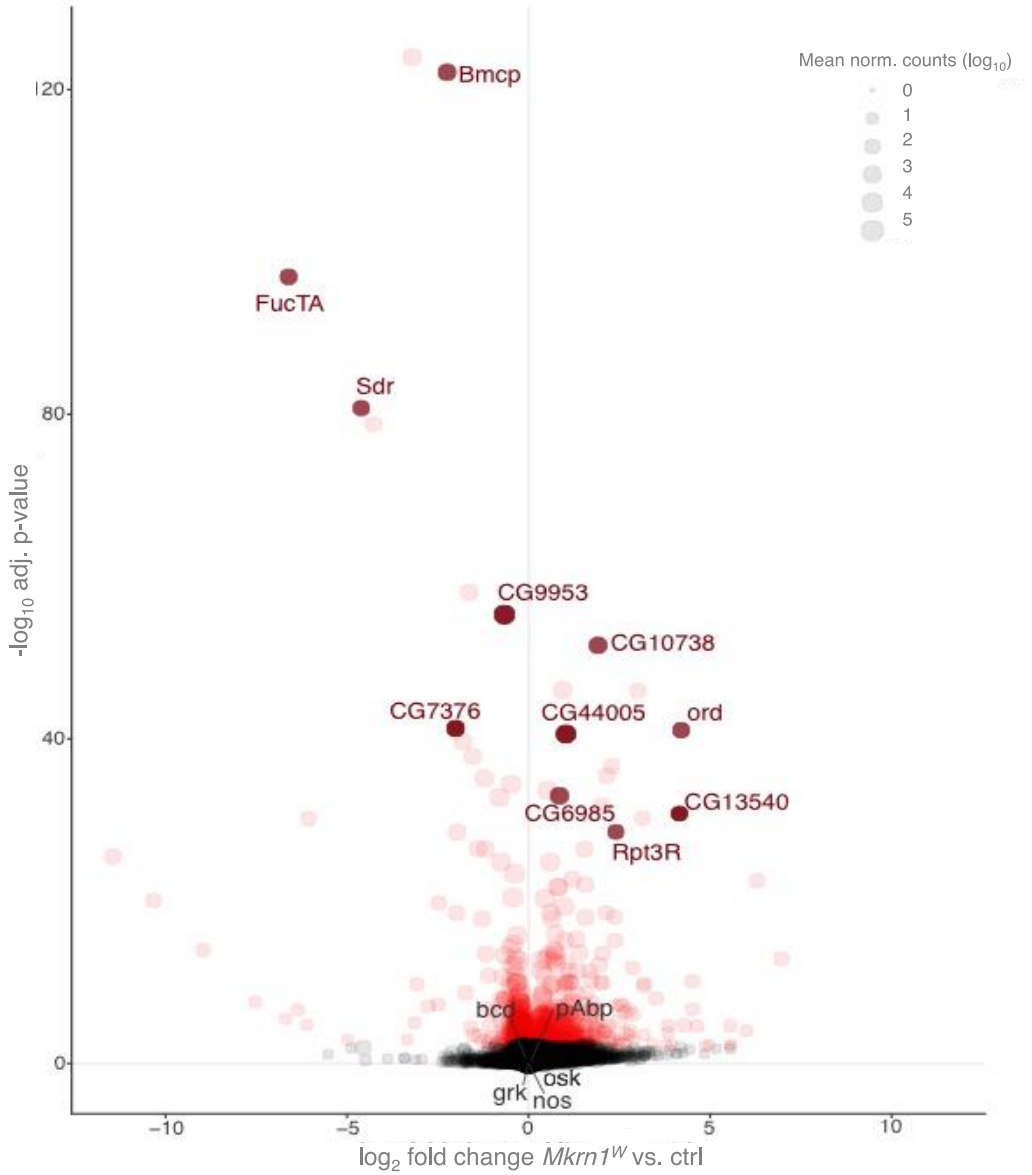

Figure S2. Transcriptome of *Mkrn1*^{W} ovaries hardly differs from wild-type condition.
RNA-seq analysis of polyA-enriched RNA in either heterozygous (ctrl) or homozygous *Mkrn1*^{W} ovaries was compared. Genes with an FDR ≤ 1% are marked in red as significantly differentially expressed. Selected genes, which are differentially expressed are highlighted. Also, *pAbp* as well as maternal effect genes including *osk*, *bcd* and *grk* are highlighted.

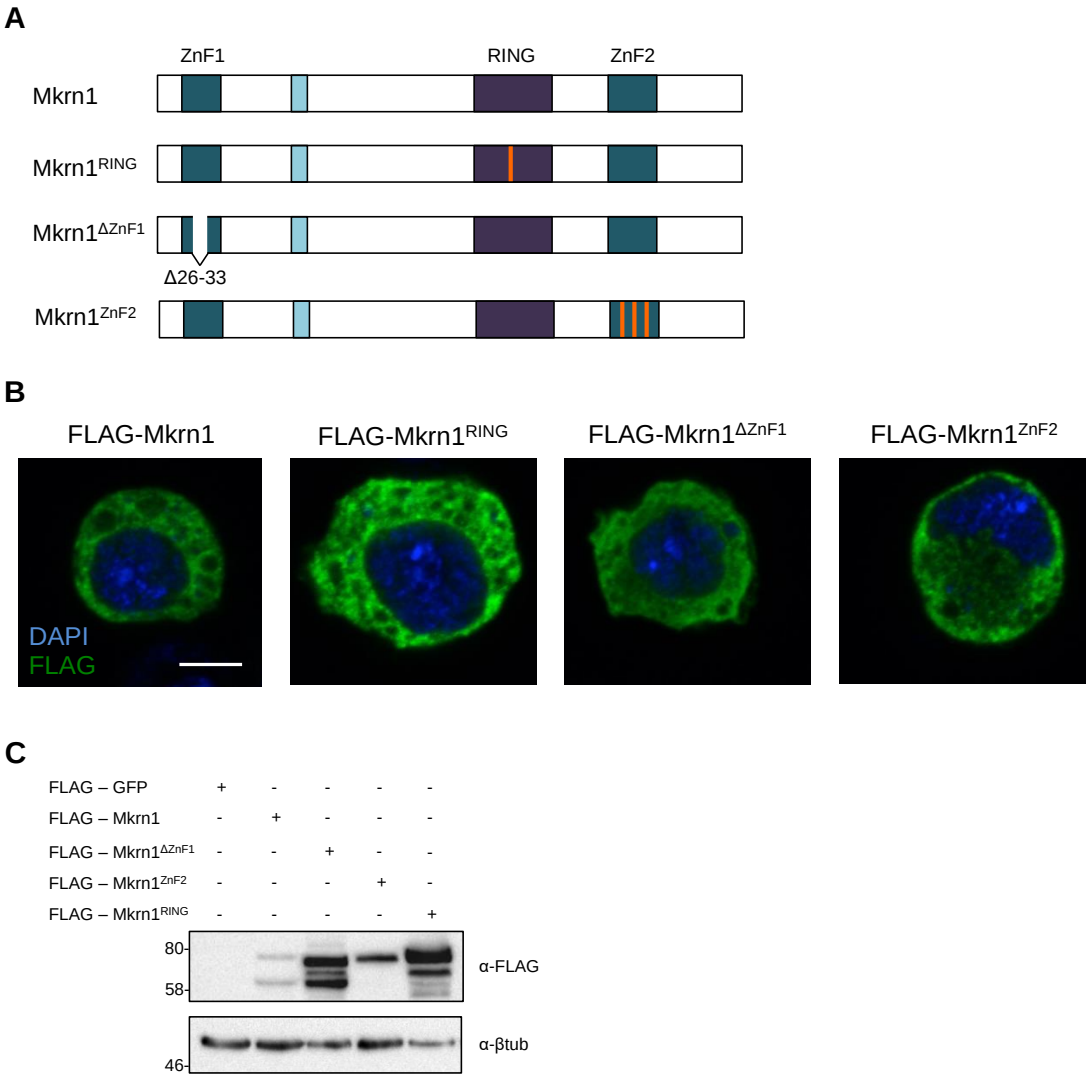

Figure S3. Generation of different *Mkrn1* mutants in S2R+ cells.
(A) Schematic diagram of various Mkrn1 protein mutants. Different mutations were introduced to analyze the distinct domains: Mkrn1^{RING} carries a point mutation that substitutes histidine 239 with glutamic acid (H239E). Mkrn1$^{\Delta ZnF1}$ contains a deletion of amino acids 26 to 33 similar to the *Mkrn1^{W}* allele. The ZnF2 domain was mutated with amino acid substitutions of the cysteines at positions 302, 312 and 318 to alanines (C302A, C312A and C318A; Mkrn1^{ZnF2}). **(B)** Immunostaining of the different Mkrn1 mutants indicated in (A). The proteins were overexpressed in S2R+ cells and immunostained against the FLAG-tag (green). To visualize the nucleus, DAPI staining (blue) was performed as well. Scale bar indicates 5 µm. **(C)** Western blotting of the individual Mkrn1 mutants indicated in (A). To normalize the protein levels, β-tubulin was analyzed.

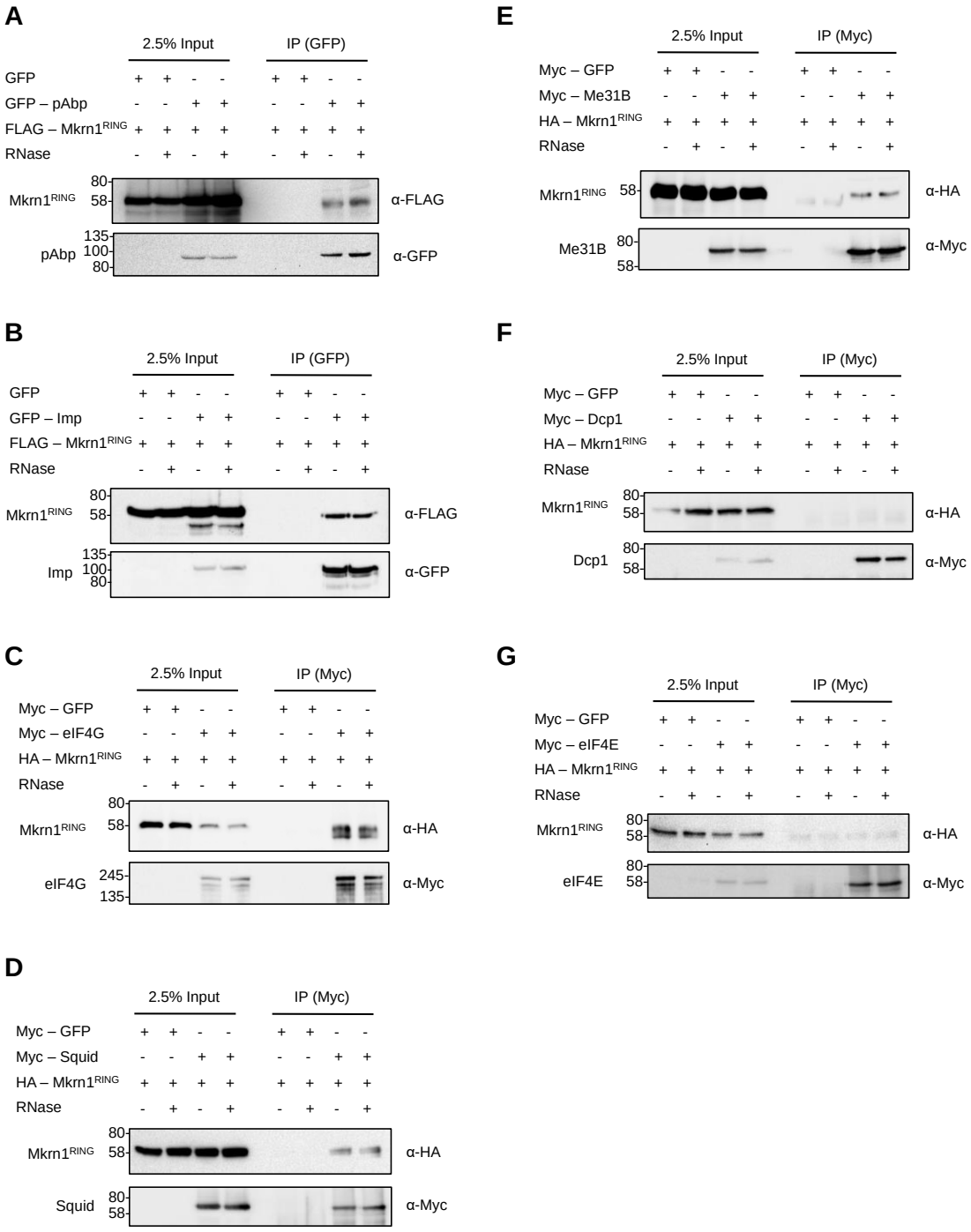

Figure S4. Validation of the Mkrn1 interactome.

Pulldown experiments to validate the associations of tagged Mkrn1^{RING} with (A) GFP-pAbp, (B) GFP-Imp, (C) Myc-eIF4G (D) Myc-Sqd, (E) Myc-Me31B (F) Myc-Dcp1 and (G) Myc-eIF4E. GFP and Myc IPs were performed in the absence or presence of RNase T1 and enrichment of the proteins was analyzed by western blotting. As control, GFP alone or Myc-GFP were used. All co-IP experiments were performed in S2R+ cells.

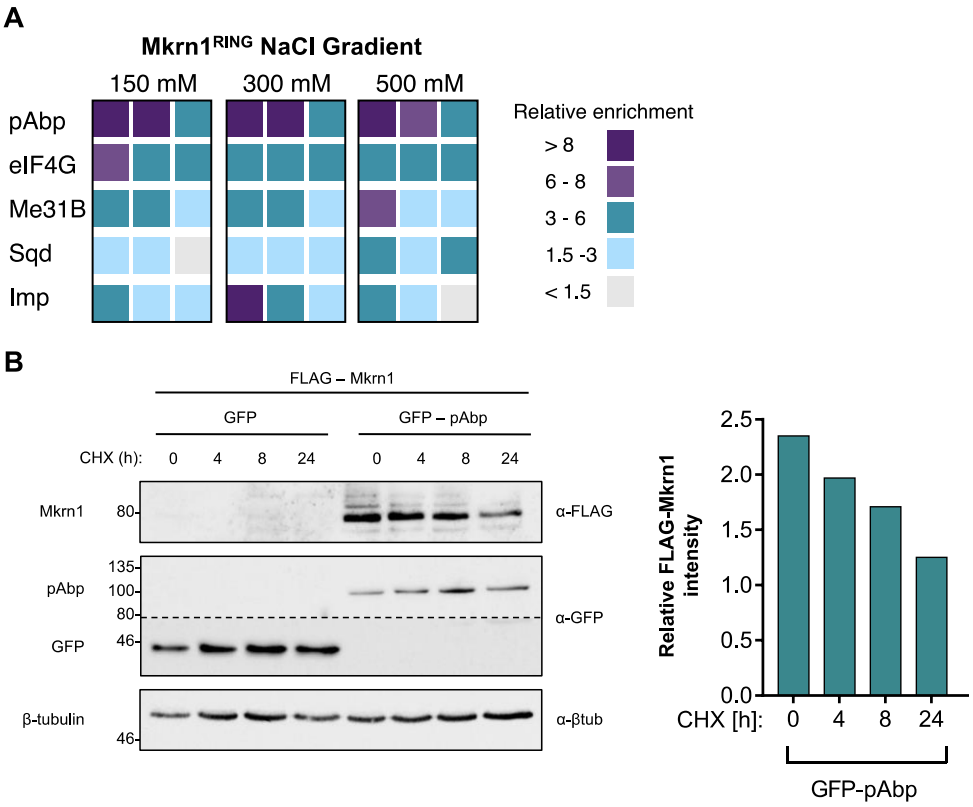

Figure S5. Analysis of the interaction of Mkrn1 with pAbp.
(A) Summary of co-IP experiments between Myc- or GFP-tagged interacting proteins and Mkrn1^{RING}. IP experiments were performed in the presence of RNase T1 using 150, 300 or 500 mM NaCl for washing. The relative enrichment of Mkrn1^{RING} signal in each IP compared to the GFP controls is depicted for three individual experiments. **(B)** Cycloheximide (CHX) treatments of cells to analyze the protein stability of Mkrn1. FLAG-Mkrn1 was co-expressed with either GFP or GFP-pAbp in S2R+ cells. Cells were treated with CHX for different times and subsequently analyzed. Left: protein levels of Mkrn1 were analyzed by western blotting. Mkrn1 protein levels are increased in the presence of pAbp. Right: Protein levels of Mkrn1 in the presence of pAbp were quantified and normalized to intensities of β-tubulin.

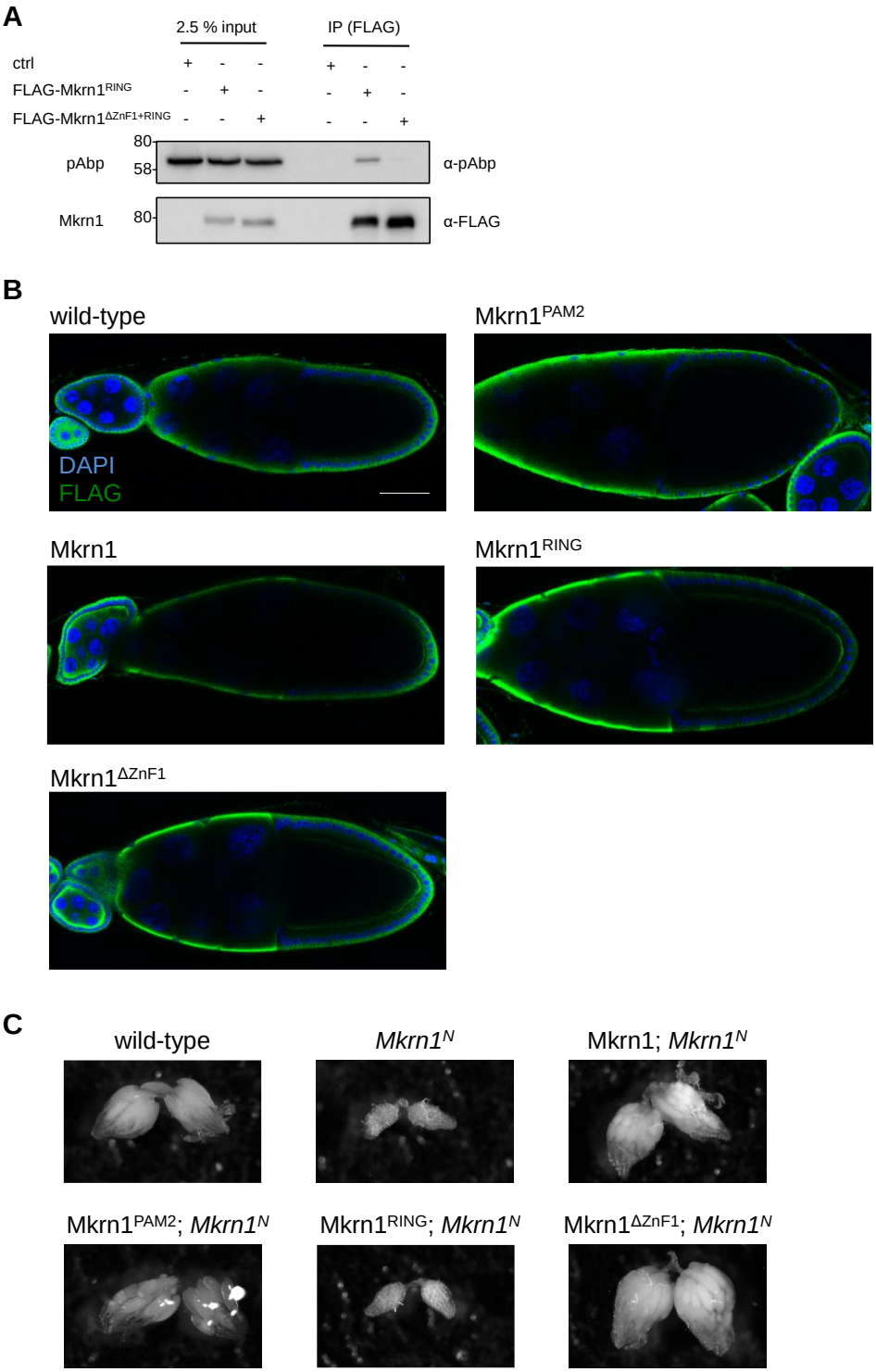

Figure S6. Analysis of different *Mkrn1* mutants in ovaries.
(A) IPs of either Mkrn1^{RING} or Mkrn1$^{\Delta ZnF1+RING}$ in ovaries. The Mkrn1 mutants were overexpressed using a *nos>Gal4* driver and immunoprecipitated with an α-FLAG antibody. IP was analyzed by western blotting to examine the interaction with pAbp. **(B)** Different versions of Mkrn1 were overexpressed in ovaries and immunostaining was performed to assess their localization within the oocyte. Wild-type or mutant Mkrn1 was stained using α-FLAG (green) and nuclei were stained using DAPI (blue). Scale bar indicates 50 µm. **(C)** Brightfield images of ovaries from different mutant flies. Either wild-type Mkrn1, Mkrn1^{PAM2}, Mkrn1^{RING} or Mkrn1$^{\Delta ZnF1}$ were overexpressed in the *Mkrn1*^{N} background.

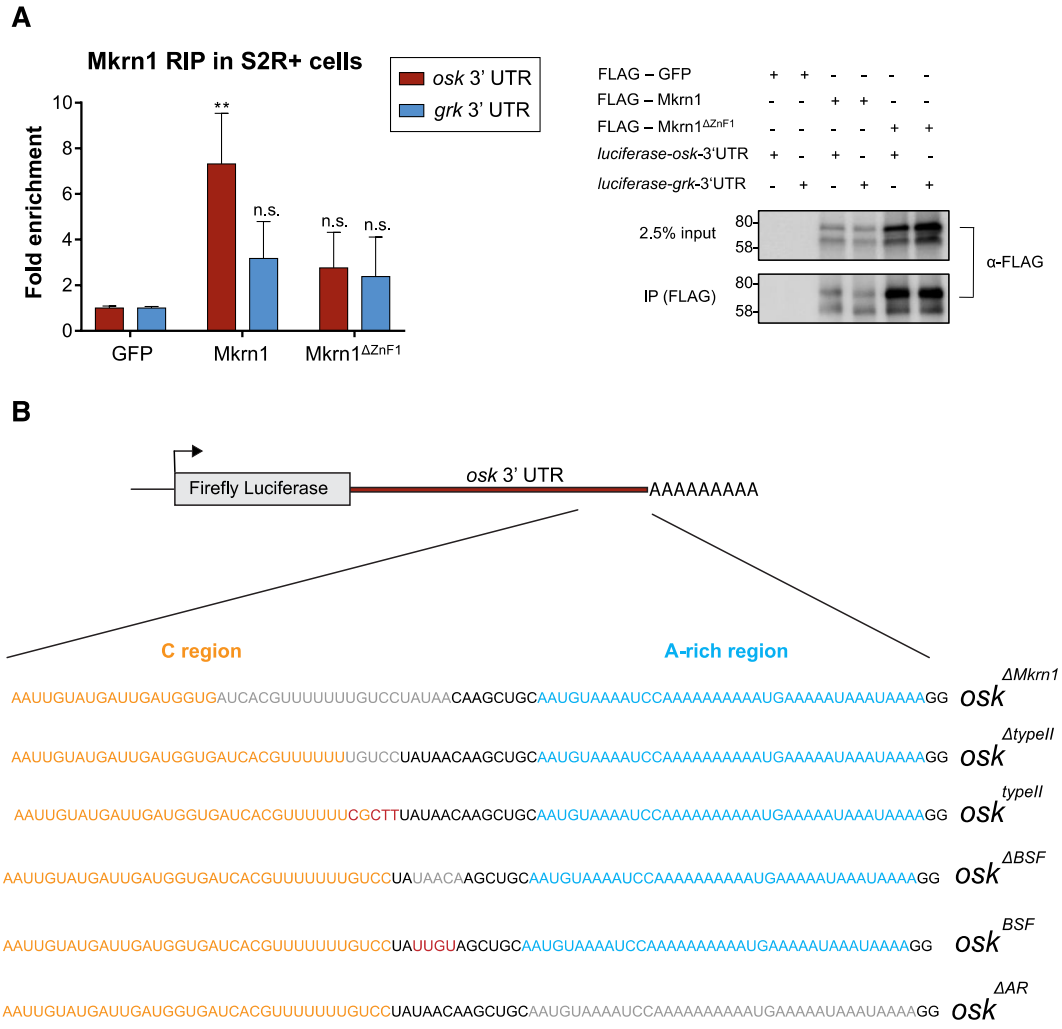

Figure S7. Application of different reporter constructs to assess the RNA-binding activity of Mkrn1. **(A)** RIP experiments of FLAG-tagged Mkrn1 or Mkrn1$^{\Delta ZnF1}$ in S2R+ cells. Proteins were co-expressed with either *luciferase-osk*-3'UTR (red) or *luciferase-grk*-3'UTR (blue). Left: enrichment of the different *luciferase* transcripts was analyzed by RT-qPCR. Fold enrichment is illustrated relative to the control RIP using FLAG-GFP. Error bars illustrate SEM, n = 3, n.s. $p > 0.05$, ** $p \leq 0.01$ (one sample t-test). Right: representative western blot of the FLAG-RIP performed in S2R+ cells. **(B)** Schematic presentation of the *luciferase-osk*-3'UTR reporters created and utilized in this study. The BRE-C region bound by Bru1 is indicated in yellow while the AR region is annotated with blue letters. The different deletions (gray) and mutations (red) introduced in the *osk* 3' UTR are indicated.

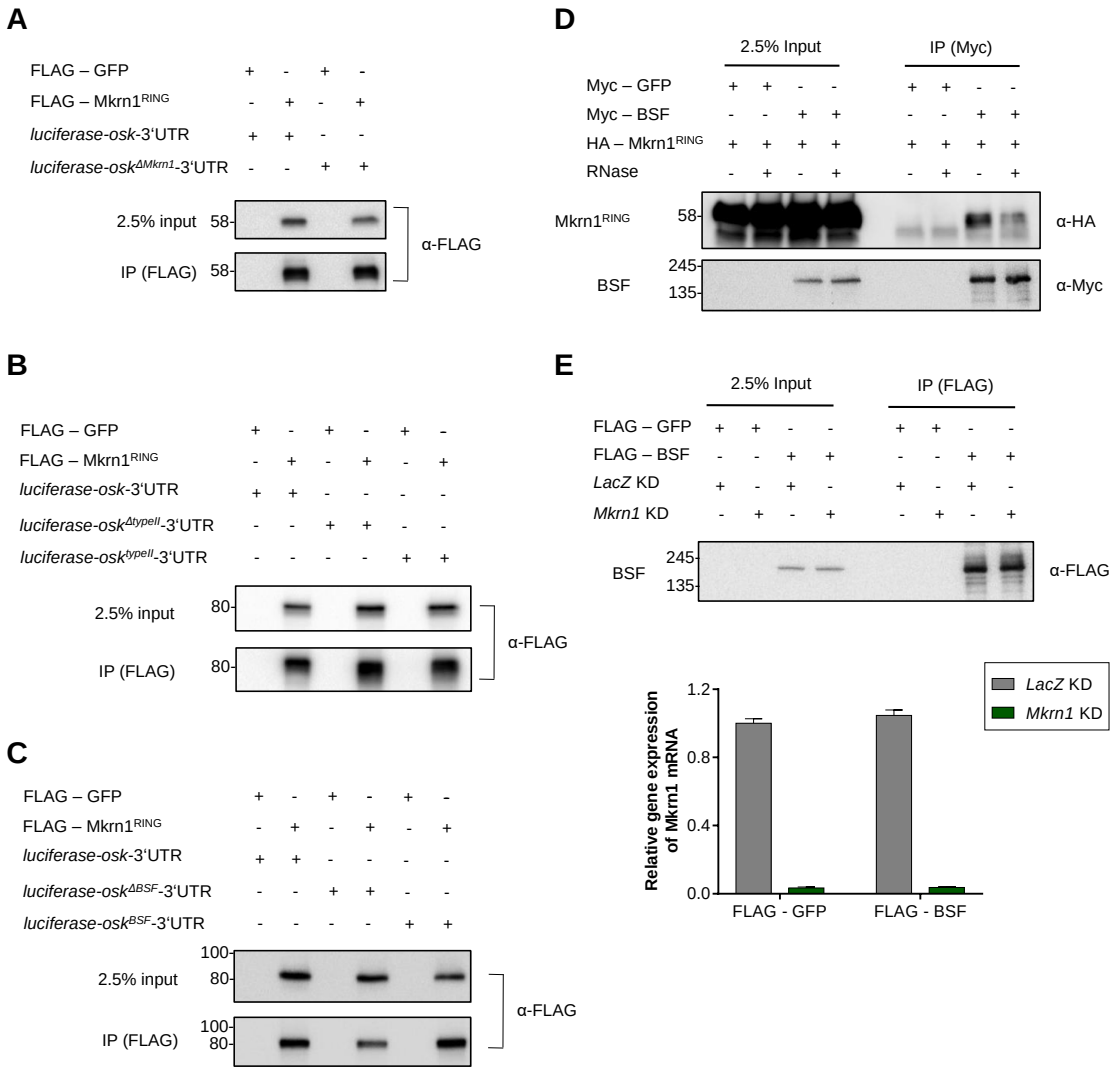

Figure S8. Mkrn1 specifically binds to the *osk* 3‘ UTR.
(A-C) Representative western blot depicting a RIP experiment of FLAG-Mkrn1^{RING} in S2R+ cells illustrated in Fig. 13B and 13C. FLAG-RIP of the *osk* 3’ UTR reporter was compared to either (A) *osk*$^{\Delta Mkrn1}$ (B) *osk*$^{\Delta typeII}$ and *osk*^{typeII} or (C) *osk*$^{\Delta BSF}$ and *osk*^{BSF}. **(D)** IP experiment of Mkrn1^{RING} with Myc-tagged BSF in S2R+ cells. As control, Myc-GFP was used. The Myc-IP was performed in the absence or presence of RNase T1. **(E)** FLAG-RIP of BSF was performed in either *LacZ* or *Mkrn1* knockdown cells. FLAG-GFP used as a control. Above: representative western blot depicting a RIP experiment illustrated in Fig. 13D. Below: RT-qPCR analysis of a representative RIP to validate knockdown efficiency of *Mkrn1* mRNA. The mRNA levels were normalized to *Rpl15* mRNA. Error bars depict Stdev of 3 technical replicates.

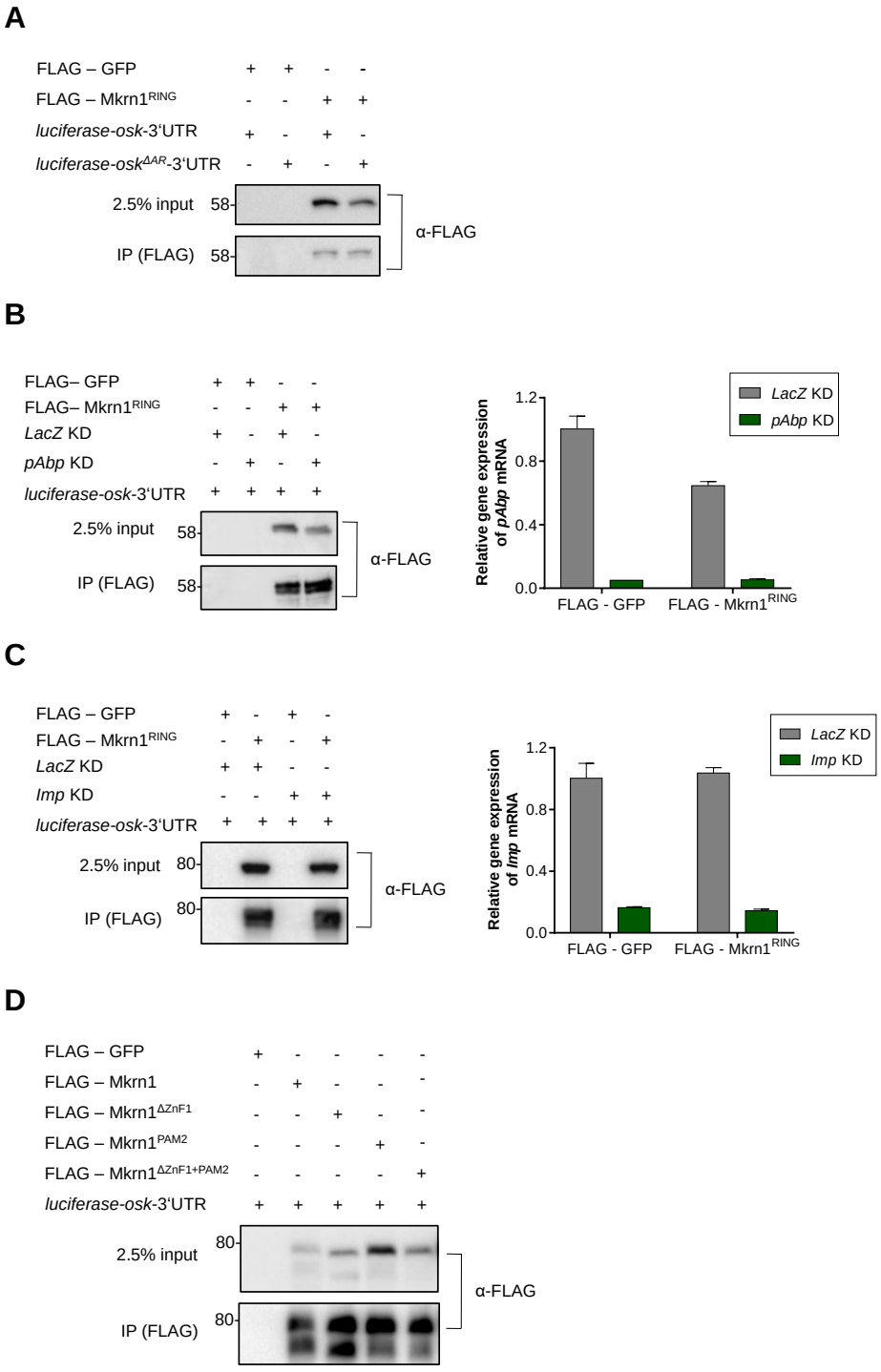

Figure S9. Binding of Mkrn1 to *osk* 3‘ UTR is dependent on pAbp.
(A-D) Representative western blots of FLAG-RIP experiments performed in S2R+ cells displayed in Fig. 14 A-14C. (A) RIP experiment of Mkrn1^{RING} comparing binding of a reporter containing wild-type *osk* 3’ UTR or *osk*$^{\Delta AR}$. (B and C) Left: western blots of FLAG-RIPs of Mkrn1^{RING} in control, (B) *Imp* and (C) *pAbp* knockdown cells. Right: RT-qPCR validation of the knockdown efficiency for a representative RIP experiment. The mRNA levels were normalized to *Rpl15* mRNA. Error bars depict Stdev of 3 technical replicates. (D) Western blot of FLAG-RIP experiments in S2R+ cells analyzing the binding of wild-type and mutant Mkrn1 to *luciferase-osk*-3’UTR reporter.

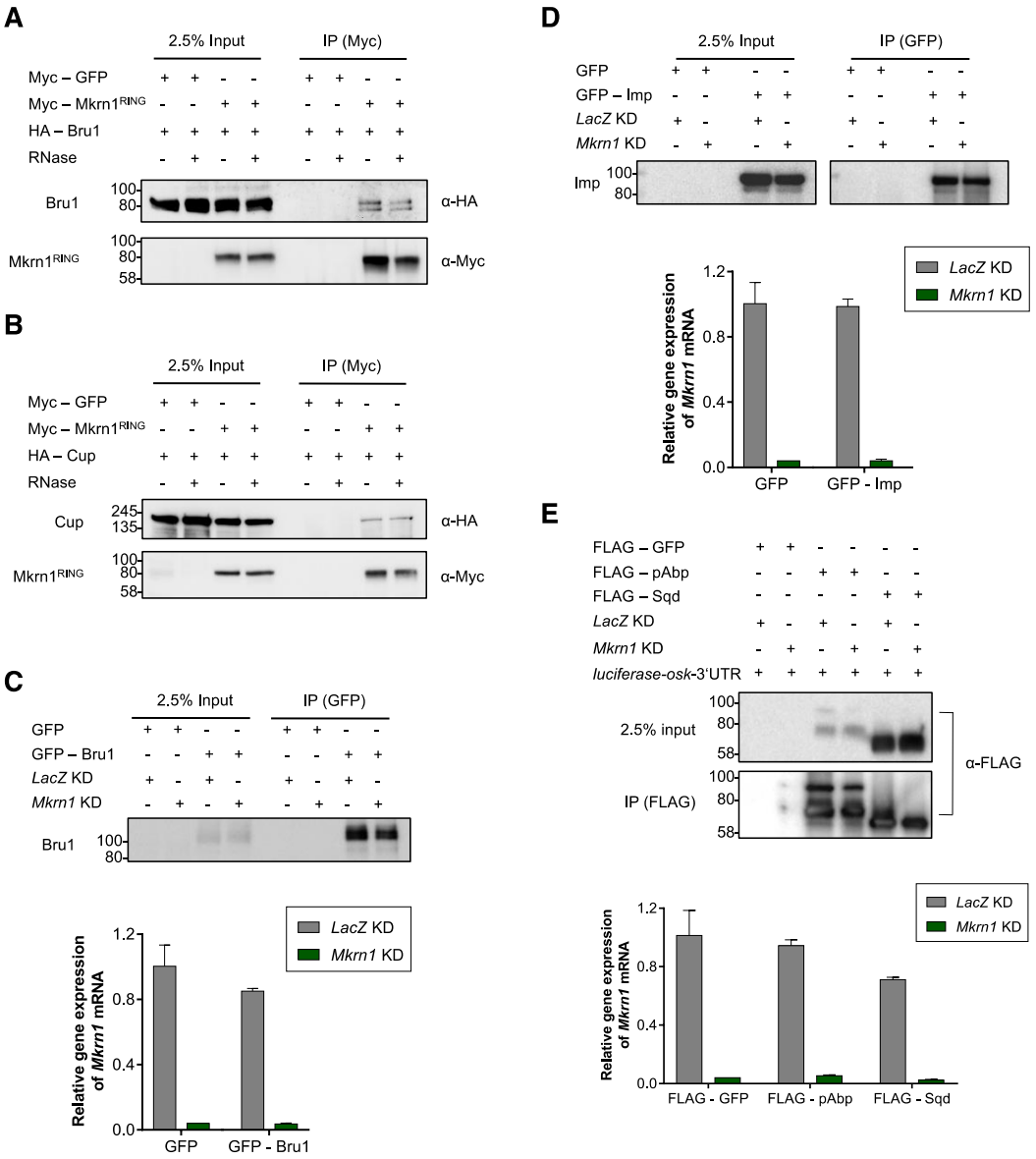

Figure S10. Mkrn1 antagonizes binding of Bru1 to *osk* 3‘ UTR.
(A and B) Western blots depicting co-IP experiments of Myc-tagged Mkrn1^{RING} with either (A) Bru1 or (B) Cup. Proteins were overexpressed in S2R+ cells and Myc-IP was performed in the absence or presence of RNase T1. **(C-E)** Above: western blots of representative RIP experiments displayed in Fig. 15A. RIPs were performed in either *LacZ* or *Mkrn1* knockdown condition in S2R+ cells to analyze changes in *luciferase-osk*-3’UTR enriched when performing an IP with (C) Bru1, (D) Imp (E) pAbp and Sqd. Below: RT-qPCR analysis to validate the efficiency of the *Mkrn1* knockdown. The mRNA levels were normalized to *Rpl15* mRNA. Error bars depict Stdev of 3 technical replicates.

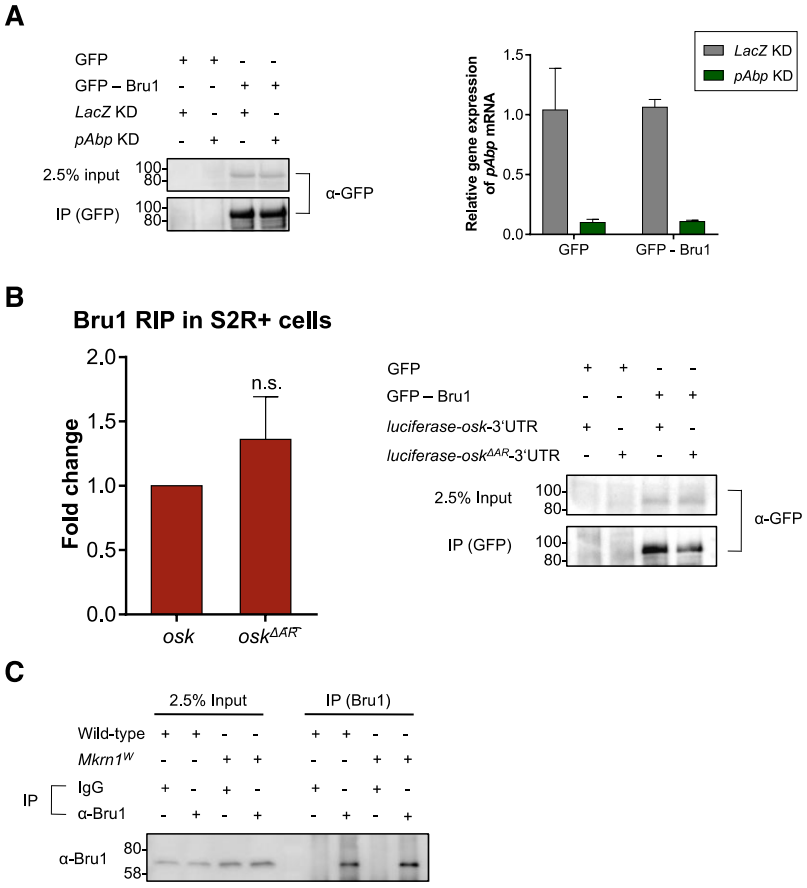

Figure S11. Mkrn1 antagonizes the binding of Bru1 to *osk* 3‘ UTR.
(A) Left: representative western blot of a GFP-RIP in either control (*LacZ*) or *pAbp* depleted S2R+ cells illustrated in Fig. 15B. Right: RT-qPCR of a RIP experiment measuring knockdown efficiency of *pAbp* mRNA. The mRNA levels were normalized to *Rpl15* mRNA. Error bars depict Stdev of 3 technical replicates. **(B)** RIP experiments of GFP-tagged Bru1 in S2R+ cells using either wild-type *osk* or $osk^{\Delta AR}$ reporter. Left: fold change of *osk* 3‘ UTR compared to $osk^{\Delta AR}$ was analyzed by RT-qPCR. Error bars depict SEM, n = 3, n.s. $p > 0.05$ (one sample t-test). Right: representative immunoblot. **(C)** Western blot of Bru1-RIP experiment displayed in Fig. 15C. Endogenous Bru1 was immunoprecipitated in either heterozygous (wild-type) or homozygous $Mkrn1^{W}$ ovaries. For the control IP, normal IgG was used.

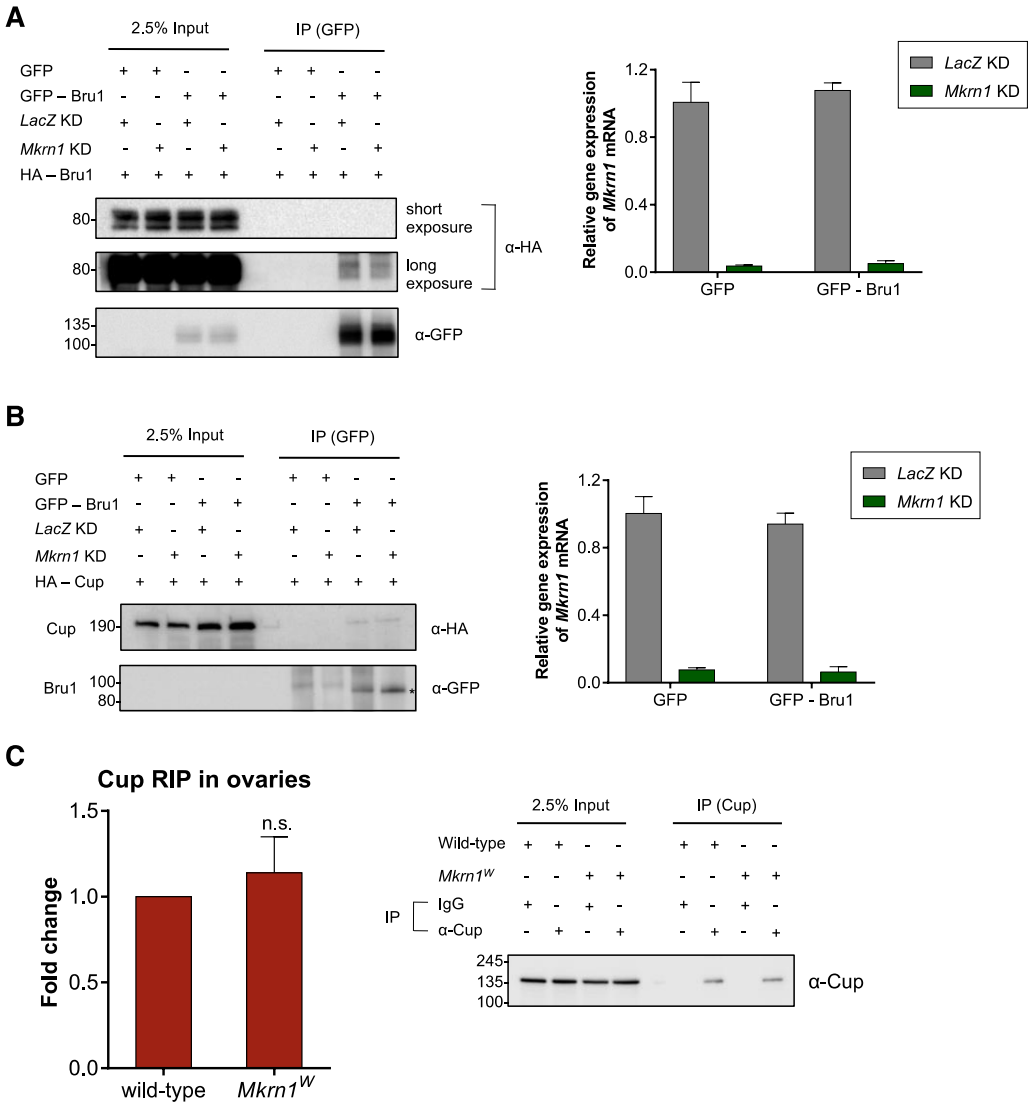

Figure S12. Mkrn1 does not influence Bru1 binding to Cup.
(A and B) Left: western blots of co-IP experiments in either *LacZ* or *Mkrn1* knockdown condition. GFP-IP was performed to analyze the binding of Bru1 to (A) Bru1 and (B) Cup. Right: RT-qPCR validation of *Mkrn1* knockdown efficiency in S2R+ cells. The mRNA levels were normalized to *Rpl15* mRNA. Error bars depict Stdev of 3 technical replicates. **(C)** Cup-RIP experiments in ovaries. IP was conducted using an α-Cup antibody. Left: enrichment of endogenous *osk* mRNA was analyzed by RT-qPCR. The fold change of RIP experiments in homozygous $Mkrn1^{W}$ ovaries compared to heterozygous (wild-type) ones is depicted. For the control IP, normal IgG was used. Error bars indicate SEM, n = 4, n.s. $p > 0.05$ (one sample t-test). Right: representative immunoblot of a Cup-RIP in $Mkrn1^{W}$ ovaries.

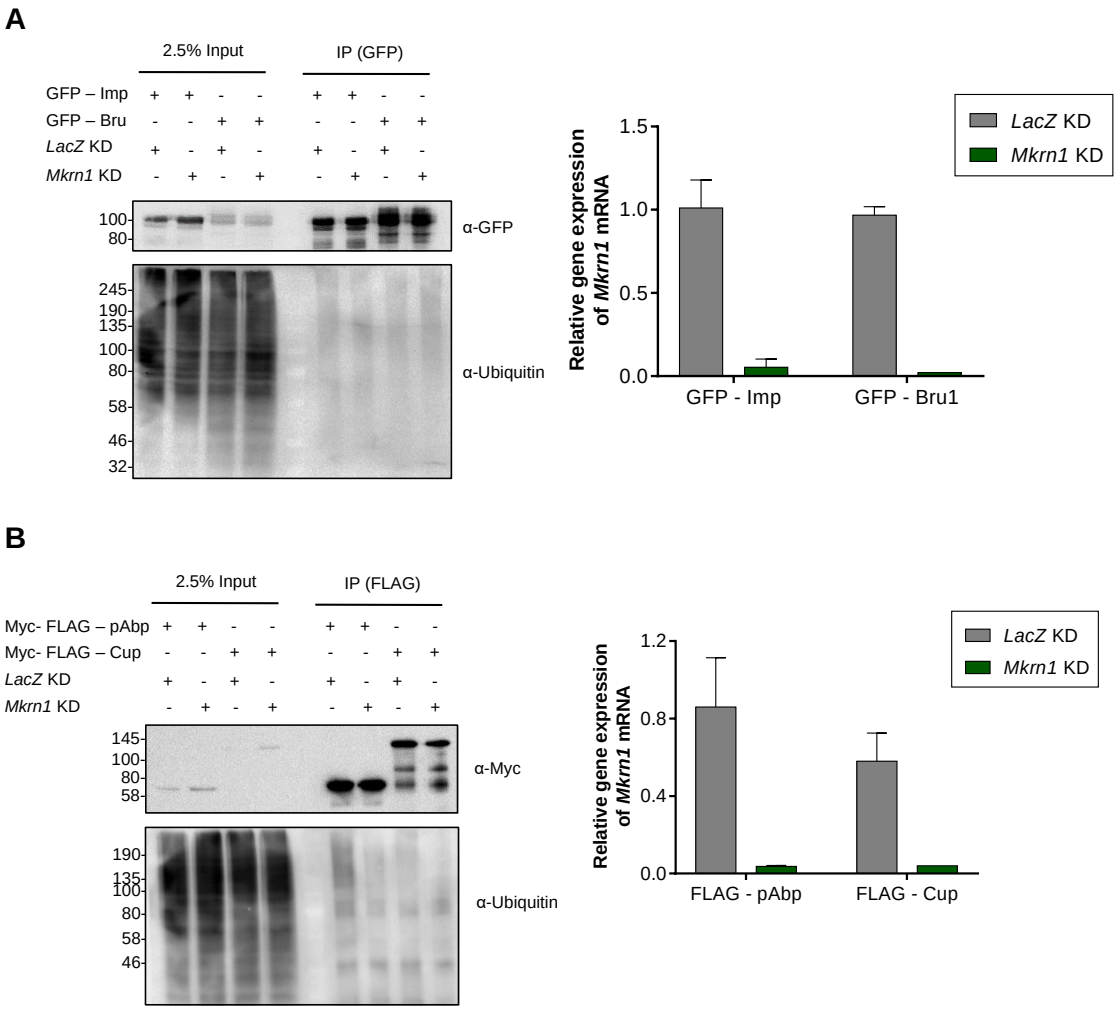

Figure S13. Mkrn1 ubiquitinates pAbp.
Ub assay of either (A) GFP-tagged Imp and Bru1 or (B) FLAG-tagged pAbp and Cup in control (*LacZ*) compared to *Mkrn1* knockdown condition. Left: IP efficiency and ubiquitination pattern were analyzed by western blotting. Right: RT-qPCR analysis to measure efficiency of the *Mkrn1* knockdown is displayed. The mRNA levels were normalized to *Rpl15* mRNA. Error bars depict Stdev of 3 technical replicates.

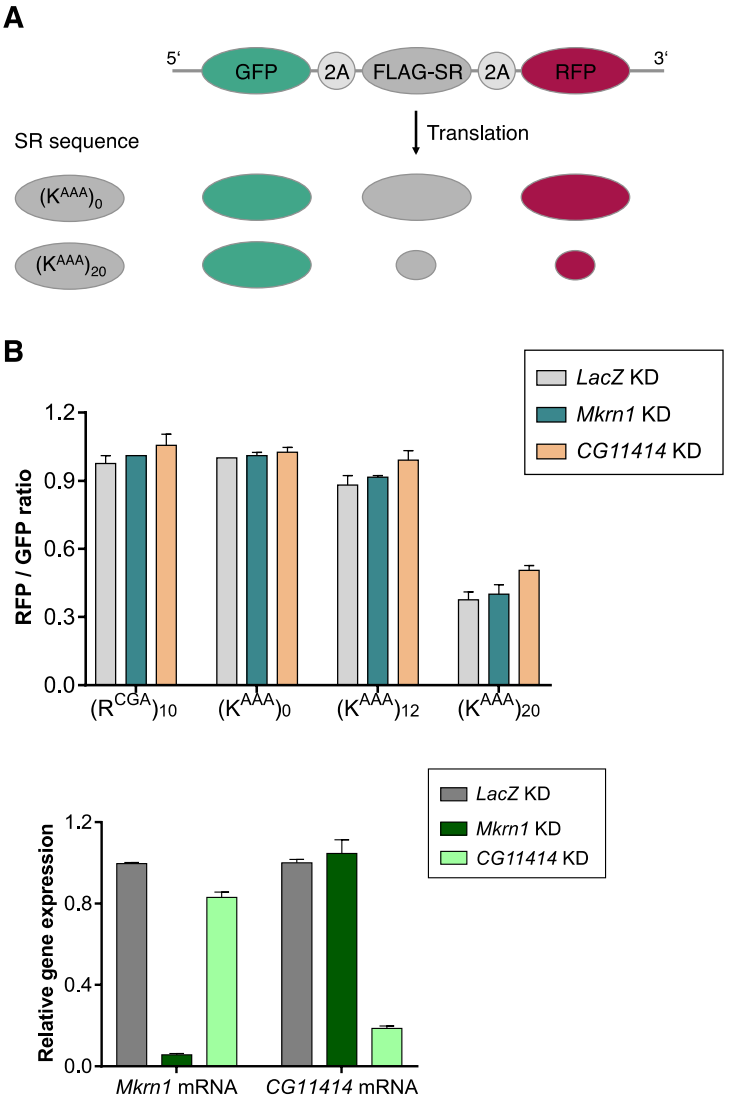

Figure S14. Analysis of the role of Mkrn1 in RQC.
(A) Schematic representation of the reporter assay used to analyze translation stalling via flow cytometry. The reporter construct encodes for GFP (green) and RFP (red). Both coding sequences are separated by viral *P2A* sequences (light grey). Within these P2A sequences, a stalling reporter (grey) is present that contains different codon sequences encoding for lysines (AAA triplets with various repeats) or arginines (CGA triplet of 10 repeats). Depending on the inserted stalling reporter, the ratio of GFP to RFP present in the cell differs. **(B)** Flow cytometry analysis of translation stall assay in S2R+ cells. Above: cells were either depleted for *LacZ*, *Mkrn1* or *CG11414* and the median of GFP and RFP-positive cells was calculated. For every experiment, 30.000 cells were analyzed. The ratio of GFP to RFP is displayed for every reporter. Error bars depict Stdev, n = 2. Below: RT-qPCR analysis of knockdown efficiencies of a representative experiment.

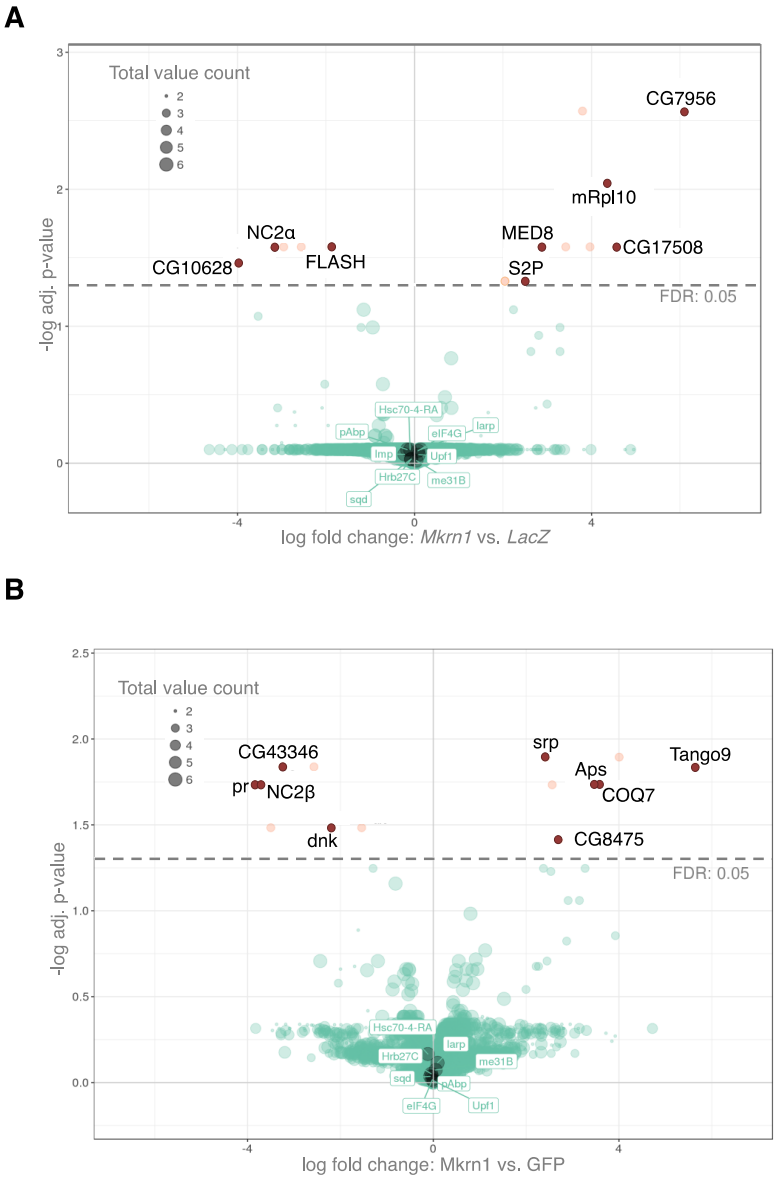

Figure S15. Proteome analysis in S2R+ cells.
Mass spectrometry analysis of SILAC-treated cells comparing either (A) *LacZ* with *Mkrn1* knockdown or (B) FLAG-tagged GFP with Mkrn1 overexpression. Proteins with an FDR of ≤ 0.5 % are indicated as significantly differentially expressed (red). Interaction candidates of Mkrn1 (turquoise) were not affected.

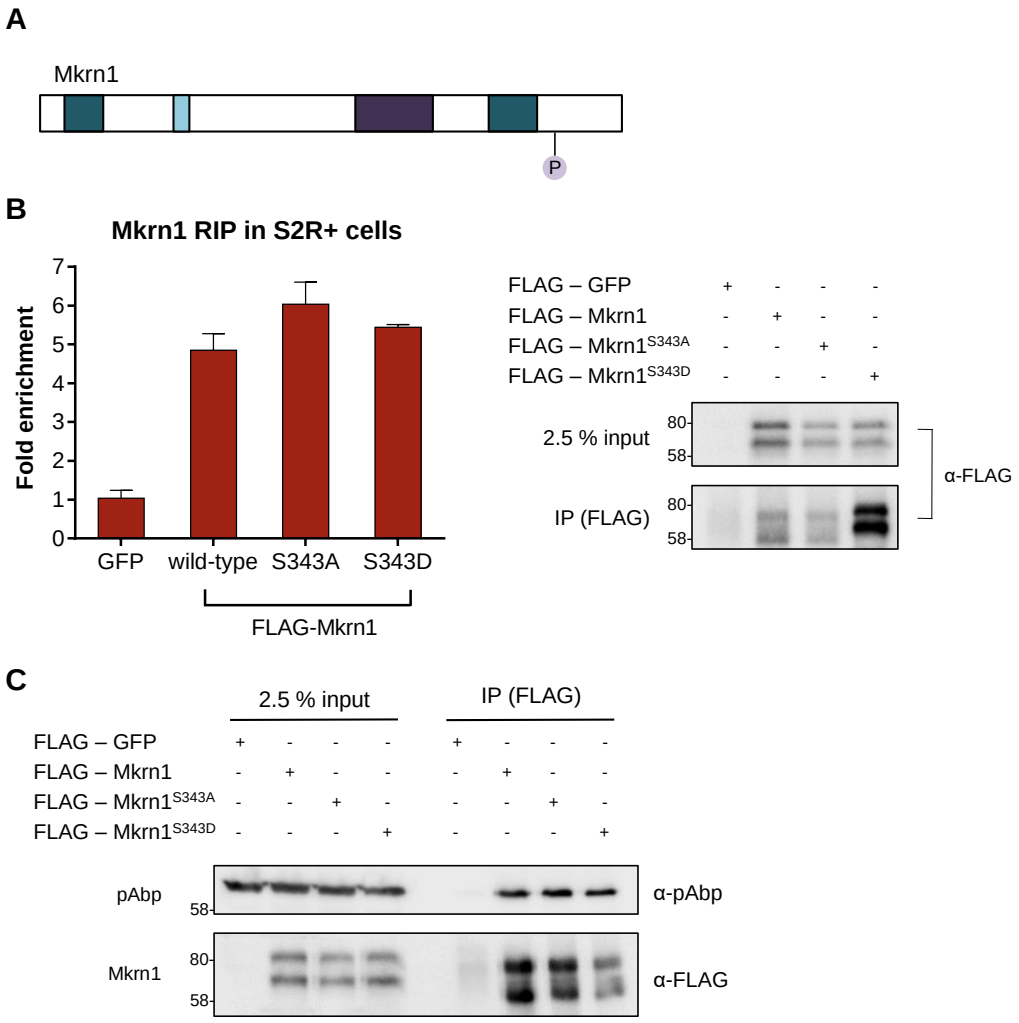

Figure S16. Analysis of the effect of phosphorylation on Mkrn1.
(A) Schematic indication of Mkrn1 and the position of its potential phosphorylation site identified by PTMcode2 [362]. **(B)** FLAG-RIP experiments of phosphomutants of Mkrn1 in S2R+ cells. Left: the enrichment of the *osk* 3' UTR reporter is displayed compared to RIP with FLAG-GFP. Error bars depict Stdev. Right: western blot analysis of FLAG-RIP experiment. (C) Western blot illustrating co-IP experiments between Mkrn1 phosphomutants and pAbp in S2R+ cells. FLAG-tagged Mkrn1 was immunoprecipitated and the interaction compared to FLAG-GFP as negative control.

REFERENCES

1. Moore, M.J., *From birth to death: the complex lives of eukaryotic mRNAs.* Science, 2005. **309**(5740): p. 1514-8.
2. Wilson, D.N., et al., *Initiation of Protein Synthesis*, in *Protein Synthesis and Ribosome Structure*. 2005: Wiley Online Library. p. 219-322.
3. Jackson, R.J., C.U. Hellen, and T.V. Pestova, *The mechanism of eukaryotic translation initiation and principles of its regulation.* Nat Rev Mol Cell Biol, 2010. **11**(2): p. 113-27.
4. Hinnebusch, A.G. and J.R. Lorsch, *The mechanism of eukaryotic translation initiation: new insights and challenges.* Cold Spring Harb Perspect Biol, 2012. **4**(10).
5. Haghighat, A., et al., *Repression of cap-dependent translation by 4E-binding protein 1: competition with p220 for binding to eukaryotic initiation factor-4E.* EMBO J, 1995. **14**(22): p. 5701-9.
6. Ptushkina, M., et al., *Cooperative modulation by eIF4G of eIF4E-binding to the mRNA 5' cap in yeast involves a site partially shared by p20.* EMBO J, 1998. **17**(16): p. 4798-808.
7. Oberer, M., A. Marintchev, and G. Wagner, *Structural basis for the enhancement of eIF4A helicase activity by eIF4G.* Genes Dev, 2005. **19**(18): p. 2212-23.
8. Schutz, P., et al., *Crystal structure of the yeast eIF4A-eIF4G complex: an RNA-helicase controlled by protein-protein interactions.* Proc Natl Acad Sci U S A, 2008. **105**(28): p. 9564-9.
9. Marintchev, A., et al., *Topology and regulation of the human eIF4A/4G/4H helicase complex in translation initiation.* Cell, 2009. **136**(3): p. 447-60.
10. Feoktistova, K., et al., *Human eIF4E promotes mRNA restructuring by stimulating eIF4A helicase activity.* Proc Natl Acad Sci U S A, 2013. **110**(33): p. 13339-44.
11. LeFebvre, A.K., et al., *Translation initiation factor eIF4G-1 binds to eIF3 through the eIF3e subunit.* J Biol Chem, 2006. **281**(32): p. 22917-32.
12. Villa, N., et al., *Human eukaryotic initiation factor 4G (eIF4G) protein binds to eIF3c, -d, and -e to promote mRNA recruitment to the ribosome.* J Biol Chem, 2013. **288**(46): p. 32932-40.
13. Baer, B.W. and R.D. Kornberg, *Repeating structure of cytoplasmic poly(A)-ribonucleoprotein.* Proc Natl Acad Sci U S A, 1980. **77**(4): p. 1890-2.
14. Baer, B.W. and R.D. Kornberg, *The protein responsible for the repeating structure of cytoplasmic poly(A)-ribonucleoprotein.* J Cell Biol, 1983. **96**(3): p. 717-21.
15. Tarun, S.Z., Jr. and A.B. Sachs, *Association of the yeast poly(A) tail binding protein with translation initiation factor eIF-4G.* EMBO J, 1996. **15**(24): p. 7168-77.
16. Tarun, S.Z., Jr. and A.B. Sachs, *A common function for mRNA 5' and 3' ends in translation initiation in yeast.* Genes Dev, 1995. **9**(23): p. 2997-3007.
17. Kahvejian, A., et al., *Mammalian poly(A)-binding protein is a eukaryotic translation initiation factor, which acts via multiple mechanisms.* Genes Dev, 2005. **19**(1): p. 104-13.
18. Hinnebusch, A.G., *The scanning mechanism of eukaryotic translation initiation.* Annu Rev Biochem, 2014. **83**: p. 779-812.
19. Passmore, L.A., et al., *The eukaryotic translation initiation factors eIF1 and eIF1A induce an open conformation of the 40S ribosome.* Mol Cell, 2007. **26**(1): p. 41-50.
20. Unbehaun, A., et al., *Release of initiation factors from 48S complexes during ribosomal subunit joining and the link between establishment of codon-anticodon base-pairing and hydrolysis of eIF2-bound GTP.* Genes Dev, 2004. **18**(24): p. 3078-93.
21. Maag, D., et al., *A conformational change in the eukaryotic translation preinitiation complex and release of eIF1 signal recognition of the start codon.* Mol Cell, 2005. **17**(2): p. 265-75.

22. Algire, M.A., D. Maag, and J.R. Lorsch, *Pi release from eIF2, not GTP hydrolysis, is the step controlled by start-site selection during eukaryotic translation initiation.* Mol Cell, 2005. **20**(2): p. 251-62.
23. Jennings, M.D. and G.D. Pavitt, *eIF5 has GDI activity necessary for translational control by eIF2 phosphorylation.* Nature, 2010. **465**(7296): p. 378-81.
24. Pestova, T.V., et al., *The joining of ribosomal subunits in eukaryotes requires eIF5B.* Nature, 2000. **403**(6767): p. 332-5.
25. Pisareva, V.P. and A.V. Pisarev, *eIF5 and eIF5B together stimulate 48S initiation complex formation during ribosomal scanning.* Nucleic Acids Res, 2014. **42**(19): p. 12052-69.
26. Fringer, J.M., et al., *Coupled release of eukaryotic translation initiation factors 5B and 1A from 80S ribosomes following subunit joining.* Mol Cell Biol, 2007. **27**(6): p. 2384-97.
27. Voorhees, R.M. and V. Ramakrishnan, *Structural basis of the translational elongation cycle.* Annu Rev Biochem, 2013. **82**: p. 203-36.
28. Ling, C. and D.N. Ermolenko, *Structural insights into ribosome translocation.* Wiley Interdiscip Rev RNA, 2016. **7**(5): p. 620-36.
29. Varenne, S., et al., *Translation is a non-uniform process. Effect of tRNA availability on the rate of elongation of nascent polypeptide chains.* J Mol Biol, 1984. **180**(3): p. 549-76.
30. Sorensen, M.A., C.G. Kurland, and S. Pedersen, *Codon usage determines translation rate in Escherichia coli.* J Mol Biol, 1989. **207**(2): p. 365-77.
31. Dong, H., L. Nilsson, and C.G. Kurland, *Co-variation of tRNA abundance and codon usage in Escherichia coli at different growth rates.* J Mol Biol, 1996. **260**(5): p. 649-63.
32. Tuller, T., et al., *An evolutionarily conserved mechanism for controlling the efficiency of protein translation.* Cell, 2010. **141**(2): p. 344-54.
33. Matlack, K.E. and P. Walter, *The 70 carboxyl-terminal amino acids of nascent secretory proteins are protected from proteolysis by the ribosome and the protein translocation apparatus of the endoplasmic reticulum membrane.* J Biol Chem, 1995. **270**(11): p. 6170-80.
34. Kosolapov, A., et al., *Structure acquisition of the T1 domain of Kv1.3 during biogenesis.* Neuron, 2004. **44**(2): p. 295-307.
35. Woolhead, C.A., P.J. McCormick, and A.E. Johnson, *Nascent membrane and secretory proteins differ in FRET-detected folding far inside the ribosome and in their exposure to ribosomal proteins.* Cell, 2004. **116**(5): p. 725-36.
36. Nissen, P., et al., *The structural basis of ribosome activity in peptide bond synthesis.* Science, 2000. **289**(5481): p. 920-30.
37. Lu, J. and C. Deutsch, *Electrostatics in the ribosomal tunnel modulate chain elongation rates.* J Mol Biol, 2008. **384**(1): p. 73-86.
38. Ferbitz, L., et al., *Trigger factor in complex with the ribosome forms a molecular cradle for nascent proteins.* Nature, 2004. **431**(7008): p. 590-6.
39. Hoffmann, A., et al., *Trigger factor forms a protective shield for nascent polypeptides at the ribosome.* J Biol Chem, 2006. **281**(10): p. 6539-45.
40. Song, H., et al., *The crystal structure of human eukaryotic release factor eRF1--mechanism of stop codon recognition and peptidyl-tRNA hydrolysis.* Cell, 2000. **100**(3): p. 311-21.
41. Alkalaeva, E.Z., et al., *In vitro reconstitution of eukaryotic translation reveals cooperativity between release factors eRF1 and eRF3.* Cell, 2006. **125**(6): p. 1125-36.
42. Hellen, C.U.T., *Translation Termination and Ribosome Recycling in Eukaryotes.* Cold Spring Harb Perspect Biol, 2018. **10**(10).

43. Thomson, A.M., J.T. Rogers, and P.J. Leedman, *Iron-regulatory proteins, iron-responsive elements and ferritin mRNA translation.* Int J Biochem Cell Biol, 1999. **31**(10): p. 1139-52.
44. Castelo-Szekely, V., et al., *Translational contributions to tissue specificity in rhythmic and constitutive gene expression.* Genome Biol, 2017. **18**(1): p. 116.
45. Jung, Y., et al., *The RNA-binding protein hnRNP Q represses translation of the clock gene Bmal1 in murine cells.* J Biol Chem, 2019. **294**(19): p. 7682-7691.
46. Bassell, G.J., et al., *Sorting of beta-actin mRNA and protein to neurites and growth cones in culture.* J Neurosci, 1998. **18**(1): p. 251-65.
47. Zhang, H.L., et al., *Neurotrophin-induced transport of a beta-actin mRNP complex increases beta-actin levels and stimulates growth cone motility.* Neuron, 2001. **31**(2): p. 261-75.
48. Huttelmaier, S., et al., *Spatial regulation of beta-actin translation by Src-dependent phosphorylation of ZBP1.* Nature, 2005. **438**(7067): p. 512-5.
49. Sasaki, Y., et al., *Phosphorylation of zipcode binding protein 1 is required for brain-derived neurotrophic factor signaling of local beta-actin synthesis and growth cone turning.* J Neurosci, 2010. **30**(28): p. 9349-58.
50. Gaynes, J.A., et al., *The RNA Binding Protein Igf2bp1 Is Required for Zebrafish RGC Axon Outgrowth In Vivo.* PLoS One, 2015. **10**(9): p. e0134751.
51. Martineau, Y., et al., *Anti-oncogenic potential of the eIF4E-binding proteins.* Oncogene, 2013. **32**(6): p. 671-7.
52. Murata, T. and K. Shimotohno, *Ubiquitination and proteasome-dependent degradation of human eukaryotic translation initiation factor 4E.* J Biol Chem, 2006. **281**(30): p. 20788-800.
53. Marcotrigiano, J., et al., *Cap-dependent translation initiation in eukaryotes is regulated by a molecular mimic of eIF4G.* Mol Cell, 1999. **3**(6): p. 707-16.
54. Gruner, S., et al., *The Structures of eIF4E-eIF4G Complexes Reveal an Extended Interface to Regulate Translation Initiation.* Mol Cell, 2016. **64**(3): p. 467-479.
55. Lin, T.A., et al., *PHAS-I as a link between mitogen-activated protein kinase and translation initiation.* Science, 1994. **266**(5185): p. 653-6.
56. Pause, A., et al., *Insulin-dependent stimulation of protein synthesis by phosphorylation of a regulator of 5'-cap function.* Nature, 1994. **371**(6500): p. 762-7.
57. Minshall, N., et al., *CPEB interacts with an ovary-specific eIF4E and 4E-T in early Xenopus oocytes.* J Biol Chem, 2007. **282**(52): p. 37389-401.
58. Standart, N. and N. Minshall, *Translational control in early development: CPEB, P-bodies and germinal granules.* Biochem Soc Trans, 2008. **36**(Pt 4): p. 671-6.
59. Wilhelm, J.E., et al., *Cup is an eIF4E binding protein required for both the translational repression of oskar and the recruitment of Barentsz.* J Cell Biol, 2003. **163**(6): p. 1197-204.
60. Nakamura, A., K. Sato, and K. Hanyu-Nakamura, *Drosophila cup is an eIF4E binding protein that associates with Bruno and regulates oskar mRNA translation in oogenesis.* Dev Cell, 2004. **6**(1): p. 69-78.
61. Nelson, M.R., A.M. Leidal, and C.A. Smibert, *Drosophila Cup is an eIF4E-binding protein that functions in Smaug-mediated translational repression.* The EMBO Journal, 2004. **23**(1): p. 150-159.
62. Rom, E., et al., *Cloning and characterization of 4EHP, a novel mammalian eIF4E-related cap-binding protein.* J Biol Chem, 1998. **273**(21): p. 13104-9.
63. Cho, P.F., et al., *Cap-dependent translational inhibition establishes two opposing morphogen gradients in Drosophila embryos.* Curr Biol, 2006. **16**(20): p. 2035-41.
64. Cho, P.F., et al., *A new paradigm for translational control: inhibition via 5'-3' mRNA tethering by Bicoid and the eIF4E cognate 4EHP.* Cell, 2005. **121**(3): p. 411-23.

65. Morita, M., et al., *A novel 4EHP-GIGYF2 translational repressor complex is essential for mammalian development.* Mol Cell Biol, 2012. **32**(17): p. 3585-93.
66. Peter, D., et al., *Molecular basis for GIGYF-Me31B complex assembly in 4EHP-mediated translational repression.* Genes Dev, 2019. **33**(19-20): p. 1355-1360.
67. Ruscica, V., et al., *Direct role for the Drosophila GIGYF protein in 4EHP-mediated mRNA repression.* Nucleic Acids Res, 2019. **47**(13): p. 7035-7048.
68. Coller, J.M., et al., *The DEAD box helicase, Dhh1p, functions in mRNA decapping and interacts with both the decapping and deadenylase complexes.* RNA, 2001. **7**(12): p. 1717-27.
69. Radhakrishnan, A., et al., *The DEAD-Box Protein Dhh1p Couples mRNA Decay and Translation by Monitoring Codon Optimality.* Cell, 2016. **167**(1): p. 122-132 e9.
70. Nykamp, K., M.H. Lee, and J. Kimble, *C. elegans La-related protein, LARP-1, localizes to germline P bodies and attenuates Ras-MAPK signaling during oogenesis.* RNA, 2008. **14**(7): p. 1378-89.
71. Lahr, R.M., et al., *La-related protein 1 (LARP1) binds the mRNA cap, blocking eIF4F assembly on TOP mRNAs.* Elife, 2017. **6**.
72. Maraia, R.J., et al., *The La and related RNA-binding proteins (LARPs): structures, functions, and evolving perspectives.* Wiley Interdiscip Rev RNA, 2017. **8**(6).
73. Tcherkezian, J., et al., *Proteomic analysis of cap-dependent translation identifies LARP1 as a key regulator of 5'TOP mRNA translation.* Genes Dev, 2014. **28**(4): p. 357-71.
74. Blagden, S.P., et al., *Drosophila Larp associates with poly(A)-binding protein and is required for male fertility and syncytial embryo development.* Dev Biol, 2009. **334**(1): p. 186-97.
75. Tuazon, P.T., W.C. Merrick, and J.A. Traugh, *Comparative analysis of phosphorylation of translational initiation and elongation factors by seven protein kinases.* J Biol Chem, 1989. **264**(5): p. 2773-7.
76. Morley, S.J. and J.A. Traugh, *Differential stimulation of phosphorylation of initiation factors eIF-4F, eIF-4B, eIF-3, and ribosomal protein S6 by insulin and phorbol esters.* J Biol Chem, 1990. **265**(18): p. 10611-6.
77. Qin, H., et al., *Phosphorylation screening identifies translational initiation factor 4GII as an intracellular target of Ca(2+)/calmodulin-dependent protein kinase I.* J Biol Chem, 2003. **278**(49): p. 48570-9.
78. Raught, B., et al., *Serum-stimulated, rapamycin-sensitive phosphorylation sites in the eukaryotic translation initiation factor 4GI.* EMBO J, 2000. **19**(3): p. 434-44.
79. Ling, J., S.J. Morley, and J.A. Traugh, *Inhibition of cap-dependent translation via phosphorylation of eIF4G by protein kinase Pak2.* EMBO J, 2005. **24**(23): p. 4094-105.
80. Dobrikov, M., et al., *Phosphorylation of eukaryotic translation initiation factor 4G1 (eIF4G1) by protein kinase C{alpha} regulates eIF4G1 binding to Mnk1.* Mol Cell Biol, 2011. **31**(14): p. 2947-59.
81. Pyronnet, S., et al., *Human eukaryotic translation initiation factor 4G (eIF4G) recruits mnk1 to phosphorylate eIF4E.* EMBO J, 1999. **18**(1): p. 270-9.
82. Lykke-Andersen, S. and T.H. Jensen, *Nonsense-mediated mRNA decay: an intricate machinery that shapes transcriptomes.* Nat Rev Mol Cell Biol, 2015. **16**(11): p. 665-77.
83. Ivanov, P.V., et al., *Interactions between UPF1, eRFs, PABP and the exon junction complex suggest an integrated model for mammalian NMD pathways.* EMBO J, 2008. **27**(5): p. 736-47.
84. Kim, Y.K. and L.E. Maquat, *UPFront and center in RNA decay: UPF1 in nonsense-mediated mRNA decay and beyond.* RNA, 2019. **25**(4): p. 407-422.
85. Chritton, J.J. and M. Wickens, *A role for the poly(A)-binding protein Pab1p in PUF protein-mediated repression.* J Biol Chem, 2011. **286**(38): p. 33268-78.

86. Deo, R.C., et al., *Recognition of polyadenylate RNA by the poly(A)-binding protein.* Cell, 1999. **98**(6): p. 835-45.
87. Nicholson, A.L. and A.E. Pasquinelli, *Tales of Detailed Poly(A) Tails.* Trends Cell Biol, 2019. **29**(3): p. 191-200.
88. Yang, F., et al., *Genome-wide analysis identifies cis-acting elements regulating mRNA polyadenylation and translation during vertebrate oocyte maturation.* bioRxiv, 2019: p. 712695.
89. Subtelny, A.O., et al., *Poly(A)-tail profiling reveals an embryonic switch in translational control.* Nature, 2014. **508**(7494): p. 66-71.
90. Lim, J., et al., *mTAIL-seq reveals dynamic poly(A) tail regulation in oocyte-to-embryo development.* Genes Dev, 2016. **30**(14): p. 1671-82.
91. Wahle, E. and G.S. Winkler, *RNA decay machines: deadenylation by the Ccr4-not and Pan2-Pan3 complexes.* Biochim Biophys Acta, 2013. **1829**(6-7): p. 561-70.
92. Hsu, C.L. and A. Stevens, *Yeast cells lacking 5'-->3' exoribonuclease 1 contain mRNA species that are poly(A) deficient and partially lack the 5' cap structure.* Mol Cell Biol, 1993. **13**(8): p. 4826-35.
93. Eisen, T.J., et al., *The Dynamics of Cytoplasmic mRNA Metabolism.* bioRxiv, 2019: p. 763599.
94. Blanchette, M., et al., *Genome-wide analysis of alternative pre-mRNA splicing and RNA-binding specificities of the Drosophila hnRNP A/B family members.* Mol Cell, 2009. **33**(4): p. 438-49.
95. Muhlrad, D., C.J. Decker, and R. Parker, *Deadenylation of the unstable mRNA encoded by the yeast MFA2 gene leads to decapping followed by 5'-->3' digestion of the transcript.* Genes Dev, 1994. **8**(7): p. 855-66.
96. Shyu, A.B., M.F. Wilkinson, and A. van Hoof, *Messenger RNA regulation: to translate or to degrade.* EMBO J, 2008. **27**(3): p. 471-81.
97. Weill, L., et al., *Translational control by changes in poly(A) tail length: recycling mRNAs.* Nat Struct Mol Biol, 2012. **19**(6): p. 577-85.
98. Semotok, J.L., et al., *Smaug recruits the CCR4/POP2/NOT deadenylase complex to trigger maternal transcript localization in the early Drosophila embryo.* Curr Biol, 2005. **15**(4): p. 284-94.
99. Zaessinger, S., I. Busseau, and M. Simonelig, *Oskar allows nanos mRNA translation in Drosophila embryos by preventing its deadenylation by Smaug/CCR4.* Development, 2006. **133**(22): p. 4573-83.
100. Zhang, B., et al., *A conserved RNA-binding protein that regulates sexual fates in the C. elegans hermaphrodite germ line.* Nature, 1997. **390**(6659): p. 477-84.
101. Kadyrova, L.Y., et al., *Translational control of maternal Cyclin B mRNA by Nanos in the Drosophila germline.* Development, 2007. **134**(8): p. 1519-27.
102. Leeb, M., et al., *Genetic exploration of the exit from self-renewal using haploid embryonic stem cells.* Cell Stem Cell, 2014. **14**(3): p. 385-93.
103. Weidmann, C.A., et al., *The RNA binding domain of Pumilio antagonizes poly-adenosine binding protein and accelerates deadenylation.* RNA, 2014. **20**(8): p. 1298-319.
104. Rabani, M., et al., *A Massively Parallel Reporter Assay of 3' UTR Sequences Identifies In Vivo Rules for mRNA Degradation.* Mol Cell, 2017. **68**(6): p. 1083-1094 e5.
105. Flora, P., et al., *Transient transcriptional silencing alters the cell cycle to promote germline stem cell differentiation in Drosophila.* Dev Biol, 2018. **434**(1): p. 84-95.
106. Goldstrohm, A.C., T.M.T. Hall, and K.M. McKenney, *Post-transcriptional Regulatory Functions of Mammalian Pumilio Proteins.* Trends Genet, 2018. **34**(12): p. 972-990.
107. Arvola, R.M., et al., *Unique repression domains of Pumilio utilize deadenylation and decapping factors to accelerate destruction of target mRNAs.* bioRxiv, 2019: p. 802835.

108. Yi, H., et al., *PABP Cooperates with the CCR4-NOT Complex to Promote mRNA Deadenylation and Block Precocious Decay.* Mol Cell, 2018. **70**(6): p. 1081-1088 e5.
109. Webster, M.W., et al., *mRNA Deadenylation Is Coupled to Translation Rates by the Differential Activities of Ccr4-Not Nucleases.* Mol Cell, 2018. **70**(6): p. 1089-1100 e8.
110. Vazquez-Pianzola, P., H. Urlaub, and B. Suter, *Pabp binds to the osk 3'UTR and specifically contributes to osk mRNA stability and oocyte accumulation.* Dev Biol, 2011. **357**(2): p. 404-18.
111. Kozlov, G., et al., *Structure and function of the C-terminal PABC domain of human poly(A)-binding protein.* Proc Natl Acad Sci U S A, 2001. **98**(8): p. 4409-13.
112. Martineau, Y., et al., *Poly(A)-binding protein-interacting protein 1 binds to eukaryotic translation initiation factor 3 to stimulate translation.* Mol Cell Biol, 2008. **28**(21): p. 6658-67.
113. Khaleghpour, K., et al., *Dual interactions of the translational repressor Paip2 with poly(A) binding protein.* Mol Cell Biol, 2001. **21**(15): p. 5200-13.
114. Khaleghpour, K., et al., *Translational repression by a novel partner of human poly(A) binding protein, Paip2.* Mol Cell, 2001. **7**(1): p. 205-16.
115. Pique, M., et al., *A combinatorial code for CPE-mediated translational control.* Cell, 2008. **132**(3): p. 434-48.
116. Richter, J.D. and P. Lasko, *Translational control in oocyte development.* Cold Spring Harb Perspect Biol, 2011. **3**(9): p. a002758.
117. Juge, F., et al., *Control of poly(A) polymerase level is essential to cytoplasmic polyadenylation and early development in Drosophila.* EMBO J, 2002. **21**(23): p. 6603-13.
118. Benoit, P., et al., *PAP- and GLD-2-type poly(A) polymerases are required sequentially in cytoplasmic polyadenylation and oogenesis in Drosophila.* Development, 2008. **135**(11): p. 1969-79.
119. Cui, J., et al., *Wispy, the Drosophila homolog of GLD-2, is required during oogenesis and egg activation.* Genetics, 2008. **178**(4): p. 2017-29.
120. Cui, J., et al., *Cytoplasmic polyadenylation is a major mRNA regulator during oogenesis and egg activation in Drosophila.* Dev Biol, 2013. **383**(1): p. 121-31.
121. Zheng, N. and N. Shabek, *Ubiquitin Ligases: Structure, Function, and Regulation.* Annual Review of Biochemistry, 2017. **86**(1): p. 129-157.
122. Jiang, J., et al., *MKRN2 inhibits migration and invasion of non-small-cell lung cancer by negatively regulating the PI3K/Akt pathway.* J Exp Clin Cancer Res, 2018. **37**(1): p. 189.
123. Buetow, L. and D.T. Huang, *Structural insights into the catalysis and regulation of E3 ubiquitin ligases.* Nat Rev Mol Cell Biol, 2016. **17**(10): p. 626-42.
124. Haas, A.L. and I.A. Rose, *The mechanism of ubiquitin activating enzyme. A kinetic and equilibrium analysis.* J Biol Chem, 1982. **257**(17): p. 10329-37.
125. Haas, A.L., et al., *Ubiquitin-activating enzyme. Mechanism and role in protein-ubiquitin conjugation.* J Biol Chem, 1982. **257**(5): p. 2543-8.
126. Hershko, A., et al., *Immunochemical analysis of the turnover of ubiquitin-protein conjugates in intact cells. Relationship to the breakdown of abnormal proteins.* J Biol Chem, 1982. **257**(23): p. 13964-70.
127. Jin, J., et al., *Dual E1 activation systems for ubiquitin differentially regulate E2 enzyme charging.* Nature, 2007. **447**(7148): p. 1135-8.
128. Chang, M., et al., *Region-specific RNA m(6)A methylation represents a new layer of control in the gene regulatory network in the mouse brain.* Open Biol, 2017. **7**(9).
129. Markson, G., et al., *Analysis of the human E2 ubiquitin conjugating enzyme protein interaction network.* Genome Res, 2009. **19**(10): p. 1905-11.

130. Michelle, C., et al., *What was the set of ubiquitin and ubiquitin-like conjugating enzymes in the eukaryote common ancestor?* J Mol Evol, 2009. **68**(6): p. 616-28.
131. George, A.J., et al., *A Comprehensive Atlas of E3 Ubiquitin Ligase Mutations in Neurological Disorders.* Front Genet, 2018. **9**: p. 29.
132. Dove, K.K. and R.E. Klevit, *RING-Between-RING E3 Ligases: Emerging Themes amid the Variations.* J Mol Biol, 2017. **429**(22): p. 3363-3375.
133. Sarikas, A., T. Hartmann, and Z.Q. Pan, *The cullin protein family.* Genome Biol, 2011. **12**(4): p. 220.
134. Li, W., et al., *Genome-wide and functional annotation of human E3 ubiquitin ligases identifies MULAN, a mitochondrial E3 that regulates the organelle's dynamics and signaling.* PLoS One, 2008. **3**(1): p. e1487.
135. Freemont, A.J., et al., *Diagnostic value of synovial fluid microscopy: a reassessment and rationalisation.* Ann Rheum Dis, 1991. **50**(2): p. 101-7.
136. Kamura, T., et al., *Rbx1, a component of the VHL tumor suppressor complex and SCF ubiquitin ligase.* Science, 1999. **284**(5414): p. 657-61.
137. Lorick, K.L., et al., *RING fingers mediate ubiquitin-conjugating enzyme (E2)-dependent ubiquitination.* Proc Natl Acad Sci U S A, 1999. **96**(20): p. 11364-9.
138. Ohta, T., et al., *ROC1, a homolog of APC11, represents a family of cullin partners with an associated ubiquitin ligase activity.* Mol Cell, 1999. **3**(4): p. 535-41.
139. Seol, J.H., et al., *Cdc53/cullin and the essential Hrt1 RING-H2 subunit of SCF define a ubiquitin ligase module that activates the E2 enzyme Cdc34.* Genes Dev, 1999. **13**(12): p. 1614-26.
140. Yokouchi, M., et al., *Ligand-induced ubiquitination of the epidermal growth factor receptor involves the interaction of the c-Cbl RING finger and UbcH7.* J Biol Chem, 1999. **274**(44): p. 31707-12.
141. Hicke, L., H.L. Schubert, and C.P. Hill, *Ubiquitin-binding domains.* Nat Rev Mol Cell Biol, 2005. **6**(8): p. 610-21.
142. Garcia-Higuera, I., et al., *Interaction of the Fanconi anemia proteins and BRCA1 in a common pathway.* Mol Cell, 2001. **7**(2): p. 249-62.
143. Wang, H., et al., *Role of histone H2A ubiquitination in Polycomb silencing.* Nature, 2004. **431**(7010): p. 873-8.
144. Metzger, E., et al., *KMT9 monomethylates histone H4 lysine 12 and controls proliferation of prostate cancer cells.* Nature Structural & Molecular Biology, 2019. **26**(5): p. 361-371.
145. Cooray, S.N., L. Guasti, and A.J. Clark, *The E3 ubiquitin ligase Mahogunin ubiquitinates the melanocortin 2 receptor.* Endocrinology, 2011. **152**(11): p. 4224-31.
146. Yin, H., et al., *Dependence of phospholipase D1 multi-monoubiquitination on its enzymatic activity and palmitoylation.* J Biol Chem, 2010. **285**(18): p. 13580-8.
147. Alfano, C., S. Faggiano, and A. Pastore, *The Ball and Chain of Polyubiquitin Structures.* Trends Biochem Sci, 2016. **41**(4): p. 371-385.
148. Komander, D. and M. Rape, *The ubiquitin code.* Annu Rev Biochem, 2012. **81**: p. 203-29.
149. Chau, V., et al., *A multiubiquitin chain is confined to specific lysine in a targeted short-lived protein.* Science, 1989. **243**(4898): p. 1576-83.
150. Deng, L., et al., *Activation of the IkappaB kinase complex by TRAF6 requires a dimeric ubiquitin-conjugating enzyme complex and a unique polyubiquitin chain.* Cell, 2000. **103**(2): p. 351-61.
151. Kovalenko, A., et al., *The tumour suppressor CYLD negatively regulates NF-kappaB signalling by deubiquitination.* Nature, 2003. **424**(6950): p. 801-5.
152. Trompouki, E., et al., *CYLD is a deubiquitinating enzyme that negatively regulates NF-kappaB activation by TNFR family members.* Nature, 2003. **424**(6950): p. 793-6.

153. Nucifora, F.C., Jr., et al., *Ubiqutination via K27 and K29 chains signals aggregation and neuronal protection of LRRK2 by WSB1.* Nat Commun, 2016. **7**: p. 11792.
154. Haakonsen, D.L. and M. Rape, *Branching Out: Improved Signaling by Heterotypic Ubiquitin Chains.* Trends Cell Biol, 2019. **29**(9): p. 704-716.
155. Mevissen, T.E.T. and D. Komander, *Mechanisms of Deubiquitinase Specificity and Regulation.* Annu Rev Biochem, 2017. **86**: p. 159-192.
156. Takahashi, S., et al., *Upf1 potentially serves as a RING-related E3 ubiquitin ligase via its association with Upf3 in yeast.* RNA, 2008. **14**(9): p. 1950-8.
157. Kuroha, K., T. Tatematsu, and T. Inada, *Upf1 stimulates degradation of the product derived from aberrant messenger RNA containing a specific nonsense mutation by the proteasome.* EMBO Rep, 2009. **10**(11): p. 1265-71.
158. Ito-Harashima, S., et al., *Translation of the poly(A) tail plays crucial roles in nonstop mRNA surveillance via translation repression and protein destabilization by proteasome in yeast.* Genes Dev, 2007. **21**(5): p. 519-24.
159. Brandman, O., et al., *A Ribosome-Bound Quality Control Complex Triggers Degradation of Nascent Peptides and Signals Translation Stress.* Cell, 2012. **151**(5): p. 1042-1054.
160. Bengtson, M.H. and C.A.P. Joazeiro, *Role of a ribosome-associated E3 ubiquitin ligase in protein quality control.* Nature, 2010. **467**(7314): p. 470-473.
161. Juszkiewicz, S. and R.S. Hegde, *Initiation of Quality Control during Poly(A) Translation Requires Site-Specific Ribosome Ubiquitination.* Mol Cell, 2017. **65**(4): p. 743-750 e4.
162. Garzia, A., et al., *The E3 ubiquitin ligase and RNA-binding protein ZNF598 orchestrates ribosome quality control of premature polyadenylated mRNAs.* Nat Commun, 2017. **8**: p. 16056.
163. Cano, F., D. Miranda-Saavedra, and P.J. Lehner, *RNA-binding E3 ubiquitin ligases: novel players in nucleic acid regulation.* Biochem Soc Trans, 2010. **38**(6): p. 1621-6.
164. Hildebrandt, A., et al., *Interaction profiling of RNA-binding ubiquitin ligases reveals a link between posttranscriptional regulation and the ubiquitin system.* Sci Rep, 2017. **7**(1): p. 16582.
165. Vinuesa, C.G., et al., *A RING-type ubiquitin ligase family member required to repress follicular helper T cells and autoimmunity.* Nature, 2005. **435**(7041): p. 452-8.
166. Yu, D., et al., *Roquin represses autoimmunity by limiting inducible T-cell co-stimulator messenger RNA.* Nature, 2007. **450**(7167): p. 299-303.
167. Leppek, K., et al., *Roquin promotes constitutive mRNA decay via a conserved class of stem-loop recognition motifs.* Cell, 2013. **153**(4): p. 869-81.
168. Buchet-Poyau, K., et al., *Identification and characterization of human Mex-3 proteins, a novel family of evolutionarily conserved RNA-binding proteins differentially localized to processing bodies.* Nucleic Acids Res, 2007. **35**(4): p. 1289-300.
169. Cano, F., et al., *A non-proteolytic role for ubiquitin in deadenylation of MHC-I mRNA by the RNA-binding E3-ligase MEX-3C.* Nat Commun, 2015. **6**: p. 8670.
170. Bohne, A., et al., *The vertebrate makorin ubiquitin ligase gene family has been shaped by large-scale duplication and retroposition from an ancestral gonad-specific, maternal-effect gene.* BMC Genomics, 2010. **11**: p. 721.
171. Lunde, B.M., C. Moore, and G. Varani, *RNA-binding proteins: modular design for efficient function.* Nature Reviews Molecular Cell Biology, 2007. **8**(6): p. 479-490.
172. Gray, T.A., et al., *The ancient source of a distinct gene family encoding proteins featuring RING and C(3)H zinc-finger motifs with abundant expression in developing brain and nervous system.* Genomics, 2000. **66**(1): p. 76-86.

173. Hildebrandt, A., et al., *The RNA-binding ubiquitin ligase MKRN1 functions in ribosome-associated quality control of poly(A) translation.* Genome Biology, 2019. **20**(1): p. 216.
174. Kozlov, G., et al., *Molecular determinants of PAM2 recognition by the MLLE domain of poly(A)-binding protein.* J Mol Biol, 2010. **397**(2): p. 397-407.
175. Pohlmann, T., et al., *A FYVE zinc finger domain protein specifically links mRNA transport to endosome trafficking.* Elife, 2015. **4**.
176. Kessel, M. and P. Gruss, *Murine developmental control genes.* Science, 1990. **249**(4967): p. 374-9.
177. Wadekar, H.B., et al., *MKRN expression pattern during embryonic and post-embryonic organogenesis in rice (Oryza sativa L. var. Nipponbare).* Planta, 2013. **237**(4): p. 1083-95.
178. Li, H., et al., *TreeFam: a curated database of phylogenetic trees of animal gene families.* Nucleic Acids Research, 2006. **34**(suppl_1): p. D572-D580.
179. Schreiber, F., et al., *TreeFam v9: a new website, more species and orthology-on-the-fly.* Nucleic Acids Research, 2013. **42**(D1): p. D922-D925.
180. Gray, T.A., et al., *Phylogenetic conservation of the makorin-2 gene, encoding a multiple zinc-finger protein, antisense to the RAF1 proto-oncogene.* Genomics, 2001. **77**(3): p. 119-26.
181. Kim, J.H., et al., *Ubiquitin ligase MKRN1 modulates telomere length homeostasis through a proteolysis of hTERT.* Genes Dev, 2005. **19**(7): p. 776-81.
182. Ko, A., et al., *Acceleration of gastric tumorigenesis through MKRN1-mediated posttranslational regulation of p14ARF.* J Natl Cancer Inst, 2012. **104**(21): p. 1660-72.
183. Lee, E.W., et al., *Differential regulation of p53 and p21 by MKRN1 E3 ligase controls cell cycle arrest and apoptosis.* EMBO J, 2009. **28**(14): p. 2100-13.
184. Lee, M.S., et al., *Loss of the E3 ubiquitin ligase MKRN1 represses diet-induced metabolic syndrome through AMPK activation.* Nat Commun, 2018. **9**(1): p. 3404.
185. Cassar, P.A., et al., *Integrative genomics positions MKRN1 as a novel ribonucleoprotein within the embryonic stem cell gene regulatory network.* EMBO Rep, 2015. **16**(10): p. 1334-57.
186. Jeong, E.B., et al., *Makorin 1 is required for Drosophila oogenesis by regulating insulin/Tor signaling.* PLoS One, 2019. **14**(4): p. e0215688.
187. Salvatico, J., et al., *Differentiation linked regulation of telomerase activity by Makorin-1.* Mol Cell Biochem, 2010. **342**(1-2): p. 241-50.
188. O'Malley, J., et al., *High-resolution analysis with novel cell-surface markers identifies routes to iPS cells.* Nature, 2013. **499**(7456): p. 88-91.
189. Gray, T.A., et al., *The putatively functional Mkrn1-p1 pseudogene is neither expressed nor imprinted, nor does it regulate its source gene in trans.* Proc Natl Acad Sci U S A, 2006. **103**(32): p. 12039-44.
190. Hirotsune, S., et al., *An expressed pseudogene regulates the messenger-RNA stability of its homologous coding gene.* Nature, 2003. **423**(6935): p. 91-6.
191. Liu, N. and P. Lasko, *Analysis of RNA Interference Lines Identifies New Functions of Maternally-Expressed Genes Involved in Embryonic Patterning in Drosophila melanogaster.* G3 (Bethesda), 2015. **5**(6): p. 1025-34.
192. Altschul, S.F., *A protein alignment scoring system sensitive at all evolutionary distances.* J Mol Evol, 1993. **36**(3): p. 290-300.
193. Altschul, S.F., et al., *Gapped BLAST and PSI-BLAST: a new generation of protein database search programs.* Nucleic Acids Research, 1997. **25**(17): p. 3389-3402.
194. Lee, K.Y., et al., *Ubiquitous expression of MAKORIN-2 in normal and malignant hematopoietic cells and its growth promoting activity.* PLoS One, 2014. **9**(3): p. e92706.

195. Qian, X., et al., *Deficiency of Mkrn2 causes abnormal spermiogenesis and spermiation, and impairs male fertility.* Sci Rep, 2016. **6**: p. 39318.
196. Zhang, Q.H., et al., *Cloning and functional analysis of cDNAs with open reading frames for 300 previously undefined genes expressed in CD34+ hematopoietic stem/progenitor cells.* Genome Res, 2000. **10**(10): p. 1546-60.
197. Qian, Y.C., et al., *Mkrn2 deficiency induces teratozoospermia and male infertility through p53/PERP-mediated apoptosis in testis.* Asian J Androl, 2019.
198. Herrera, R.A., K. Kiontke, and D.H. Fitch, *Makorin ortholog LEP-2 regulates LIN-28 stability to promote the juvenile-to-adult transition in Caenorhabditis elegans.* Development, 2016. **143**(5): p. 799-809.
199. Yang, P.H., et al., *Makorin-2 is a neurogenesis inhibitor downstream of phosphatidylinositol 3-kinase/Akt (PI3K/Akt) signal.* J Biol Chem, 2008. **283**(13): p. 8486-95.
200. Cheung, W.K., et al., *Identification of protein domains required for makorin-2-mediated neurogenesis inhibition in Xenopus embryos.* Biochem Biophys Res Commun, 2010. **394**(1): p. 18-23.
201. Shin, C., et al., *MKRN2 is a novel ubiquitin E3 ligase for the p65 subunit of NF-kappaB and negatively regulates inflammatory responses.* Sci Rep, 2017. **7**: p. 46097.
202. Jong, M.T., et al., *Imprinting of a RING zinc-finger encoding gene in the mouse chromosome region homologous to the Prader-Willi syndrome genetic region.* Hum Mol Genet, 1999. **8**(5): p. 795-803.
203. Butler, M.G., *Prader-Willi Syndrome: Obesity due to Genomic Imprinting.* Curr Genomics, 2011. **12**(3): p. 204-15.
204. Abreu, A.P., et al., *A new pathway in the control of the initiation of puberty: the MKRN3 gene.* J Mol Endocrinol, 2015. **54**(3): p. R131-9.
205. Grandone, A., et al., *MKRN3 levels in girls with central precocious puberty and correlation with sexual hormone levels: a pilot study.* Endocrine, 2018. **59**(1): p. 203-208.
206. Jeong, H.R., et al., *Serum Makorin ring finger protein 3 values for predicting Central precocious puberty in girls.* Gynecol Endocrinol, 2019. **35**(8): p. 732-736.
207. Yi, B.R., et al., *Association between MKRN3 and LIN28B polymorphisms and precocious puberty.* BMC Genet, 2018. **19**(1): p. 47.
208. Liu, H., X. Kong, and F. Chen, *Mkrn3 functions as a novel ubiquitin E3 ligase to inhibit Nptx1 during puberty initiation.* Oncotarget, 2017. **8**(49): p. 85102-85109.
209. Lawson, H., et al., *The Makorin lep-2 and the lncRNA lep-5 regulate lin-28 to schedule sexual maturation of the C. elegans nervous system.* Elife, 2019. **8**.
210. Pauli, A., et al., *Systematic identification of long noncoding RNAs expressed during zebrafish embryogenesis.* Genome Res, 2012. **22**(3): p. 577-91.
211. Baltz, A.G., et al., *The mRNA-bound proteome and its global occupancy profile on protein-coding transcripts.* Mol Cell, 2012. **46**(5): p. 674-90.
212. Miroci, H., et al., *Makorin ring zinc finger protein 1 (MKRN1), a novel poly(A)-binding protein-interacting protein, stimulates translation in nerve cells.* J Biol Chem, 2012. **287**(2): p. 1322-34.
213. Hudson, A.M. and L. Cooley, *Methods for studying oogenesis.* Methods, 2014. **68**(1): p. 207-17.
214. McLaughlin, J.M. and D.P. Bratu, *Drosophila melanogaster Oogenesis: An Overview.* Methods Mol Biol, 2015. **1328**: p. 1-20.
215. Spradling, A.C., *Germline cysts: communes that work.* Cell, 1993. **72**(5): p. 649-51.
216. Ables, E.T., *Drosophila oocytes as a model for understanding meiosis: an educational primer to accompany "corolla is a novel protein that contributes to the architecture of the synaptonemal complex of Drosophila".* Genetics, 2015. **199**(1): p. 17-23.

217. Gutzeit, H., *The role of microtubules in the differentiation of ovarian follicles during vitellogenesis inDrosophila.* Roux Arch Dev Biol, 1986. **195**(3): p. 173-181.
218. Robinson, D.N., K. Cant, and L. Cooley, *Morphogenesis of Drosophila ovarian ring canals.* Development, 1994. **120**(7): p. 2015-25.
219. Warn, R.M., et al., *F-actin rings are associated with the ring canals of the Drosophila egg chamber.* Exp Cell Res, 1985. **157**(2): p. 355-63.
220. Palacios, I.M. and D. St Johnston, *Kinesin light chain-independent function of the Kinesin heavy chain in cytoplasmic streaming and posterior localisation in the Drosophila oocyte.* Development, 2002. **129**(23): p. 5473-85.
221. Pokrywka, N.J. and E.C. Stephenson, *Microtubules are a general component of mRNA localization systems in Drosophila oocytes.* Dev Biol, 1995. **167**(1): p. 363-70.
222. Ran, B., R. Bopp, and B. Suter, *Null alleles reveal novel requirements for Bic-D during Drosophila oogenesis and zygotic development.* Development, 1994. **120**(5): p. 1233-42.
223. Bolivar, J., et al., *Centrosome migration into the Drosophila oocyte is independent of BicD and egl, and of the organisation of the microtubule cytoskeleton.* Development, 2001. **128**(10): p. 1889-97.
224. Mach, J.M. and R. Lehmann, *An Egalitarian-BicaudalD complex is essential for oocyte specification and axis determination in Drosophila.* Genes Dev, 1997. **11**(4): p. 423-35.
225. Navarro, C., et al., *Egalitarian binds dynein light chain to establish oocyte polarity and maintain oocyte fate.* Nat Cell Biol, 2004. **6**(5): p. 427-35.
226. Sladewski, T.E., et al., *Recruitment of two dyneins to an mRNA-dependent Bicaudal D transport complex.* Elife, 2018. **7**.
227. McClintock, M.A., et al., *RNA-directed activation of cytoplasmic dynein-1 in reconstituted transport RNPs.* Elife, 2018. **7**.
228. Gonzalez-Reyes, A., H. Elliott, and D. St Johnston, *Polarization of both major body axes in Drosophila by gurken-torpedo signalling.* Nature, 1995. **375**(6533): p. 654-8.
229. Gonzalez-Reyes, A. and D. St Johnston, *Patterning of the follicle cell epithelium along the anterior-posterior axis during Drosophila oogenesis.* Development, 1998. **125**(15): p. 2837-46.
230. Roth, S. and J.A. Lynch, *Symmetry breaking during Drosophila oogenesis.* Cold Spring Harb Perspect Biol, 2009. **1**(2): p. a001891.
231. Neuman-Silberberg, F.S. and T. Schupbach, *The Drosophila dorsoventral patterning gene gurken produces a dorsally localized RNA and encodes a TGF alpha-like protein.* Cell, 1993. **75**(1): p. 165-74.
232. Peri, F., C. Bokel, and S. Roth, *Local Gurken signaling and dynamic MAPK activation during Drosophila oogenesis.* Mech Dev, 1999. **81**(1-2): p. 75-88.
233. MacDougall, N., et al., *Drosophila gurken (TGFalpha) mRNA localizes as particles that move within the oocyte in two dynein-dependent steps.* Dev Cell, 2003. **4**(3): p. 307-19.
234. Zhao, T., et al., *Growing microtubules push the oocyte nucleus to polarize the Drosophila dorsal-ventral axis.* Science, 2012. **336**(6084): p. 999-1003.
235. Nilson, L.A. and T. Schupbach, *EGF receptor signaling in Drosophila oogenesis.* Curr Top Dev Biol, 1999. **44**: p. 203-43.
236. Van Buskirk, C. and T. Schupbach, *Versatility in signalling: multiple responses to EGF receptor activation during Drosophila oogenesis.* Trends Cell Biol, 1999. **9**(1): p. 1-4.
237. Cha, B.J., et al., *Kinesin I-dependent cortical exclusion restricts pole plasm to the oocyte posterior.* Nat Cell Biol, 2002. **4**(8): p. 592-8.
238. Januschke, J., et al., *Polar transport in the Drosophila oocyte requires Dynein and Kinesin I cooperation.* Curr Biol, 2002. **12**(23): p. 1971-81.
239. Januschke, J., et al., *The centrosome-nucleus complex and microtubule organization in the Drosophila oocyte.* Development, 2006. **133**(1): p. 129-39.

240. Parton, R.M., et al., *A PAR-1-dependent orientation gradient of dynamic microtubules directs posterior cargo transport in the Drosophila oocyte.* J Cell Biol, 2011. **194**(1): p. 121-35.
241. Brendza, R.P., et al., *A function for kinesin I in the posterior transport of oskar mRNA and Staufen protein.* Science, 2000. **289**(5487): p. 2120-2.
242. Clark, I., et al., *Transient posterior localization of a kinesin fusion protein reflects anteroposterior polarity of the Drosophila oocyte.* Curr Biol, 1994. **4**(4): p. 289-300.
243. Duncan, J.E. and R. Warrior, *The cytoplasmic dynein and kinesin motors have interdependent roles in patterning the Drosophila oocyte.* Curr Biol, 2002. **12**(23): p. 1982-91.
244. Schnorrer, F., K. Bohmann, and C. Nusslein-Volhard, *The molecular motor dynein is involved in targeting swallow and bicoid RNA to the anterior pole of Drosophila oocytes.* Nat Cell Biol, 2000. **2**(4): p. 185-90.
245. Quinlan, M.E., *Cytoplasmic Streaming in the Drosophila Oocyte.* Annu Rev Cell Dev Biol, 2016. **32**: p. 173-195.
246. Babu, K., et al., *Roles of Bifocal, Homer, and F-actin in anchoring Oskar to the posterior cortex of Drosophila oocytes.* Genes Dev, 2004. **18**(2): p. 138-43.
247. Jankovics, F., et al., *MOESIN crosslinks actin and cell membrane in Drosophila oocytes and is required for OSKAR anchoring.* Curr Biol, 2002. **12**(23): p. 2060-5.
248. Kim-Ha, J., J.L. Smith, and P.M. Macdonald, *oskar mRNA is localized to the posterior pole of the Drosophila oocyte.* Cell, 1991. **66**(1): p. 23-35.
249. Rongo, C., E.R. Gavis, and R. Lehmann, *Localization of oskar RNA regulates oskar translation and requires Oskar protein.* Development, 1995. **121**(9): p. 2737-46.
250. Wang, Y. and V. Riechmann, *Microtubule anchoring by cortical actin bundles prevents streaming of the oocyte cytoplasm.* Mech Dev, 2008. **125**(1-2): p. 142-52.
251. Forrest, K.M. and E.R. Gavis, *Live imaging of endogenous RNA reveals a diffusion and entrapment mechanism for nanos mRNA localization in Drosophila.* Curr Biol, 2003. **13**(14): p. 1159-68.
252. Pritchett, T.L., E.A. Tanner, and K. McCall, *Cracking open cell death in the Drosophila ovary.* Apoptosis, 2009. **14**(8): p. 969-79.
253. Horner, V.L. and M.F. Wolfner, *Mechanical stimulation by osmotic and hydrostatic pressure activates Drosophila oocytes in vitro in a calcium-dependent manner.* Dev Biol, 2008. **316**(1): p. 100-9.
254. Sysoev, V.O., et al., *Global changes of the RNA-bound proteome during the maternal-to-zygotic transition in Drosophila.* Nat Commun, 2016. **7**: p. 12128.
255. Wessels, H.H., et al., *The mRNA-bound proteome of the early fly embryo.* Genome Res, 2016. **26**(7): p. 1000-9.
256. Sutandy, F.X., A. Hildebrandt, and J. Konig, *Profiling the Binding Sites of RNA-Binding Proteins with Nucleotide Resolution Using iCLIP.* Methods Mol Biol, 2016. **1358**: p. 175-95.
257. Garcia-Bellido, A. and L.G. Robbins, *Viability of Female Germ-Line Cells Homozygous for Zygotic Lethals in DROSOPHILA MELANOGASTER.* Genetics, 1983. **103**(2): p. 235-47.
258. Schupbach, T. and E. Wieschaus, *Maternal-effect mutations altering the anterior-posterior pattern of the Drosophila embryo.* Roux Arch Dev Biol, 1986. **195**(5): p. 302-317.
259. Perrimon, N., L. Engstrom, and A.P. Mahowald, *The effects of zygotic lethal mutations on female germ-line functions in Drosophila.* Dev Biol, 1984. **105**(2): p. 404-14.
260. Lehmann, R. and C. Nusslein-Volhard, *Abdominal segmentation, pole cell formation, and embryonic polarity require the localized activity of oskar, a maternal gene in Drosophila.* Cell, 1986. **47**(1): p. 141-52.

261. Driever, W. and C. Nusslein-Volhard, *The bicoid protein determines position in the Drosophila embryo in a concentration-dependent manner.* Cell, 1988. **54**(1): p. 95-104.
262. Schupbach, T., *Germ line and soma cooperate during oogenesis to establish the dorsoventral pattern of egg shell and embryo in Drosophila melanogaster.* Cell, 1987. **49**(5): p. 699-707.
263. Driever, W. and C. Nusslein-Volhard, *The bicoid protein is a positive regulator of hunchback transcription in the early Drosophila embryo.* Nature, 1989. **337**(6203): p. 138-43.
264. Dubnau, J. and G. Struhl, *RNA recognition and translational regulation by a homeodomain protein.* Nature, 1996. **379**(6567): p. 694-9.
265. Rivera-Pomar, R., et al., *RNA binding and translational suppression by bicoid.* Nature, 1996. **379**(6567): p. 746-9.
266. Jaramillo, A.M., et al., *The dynamics of fluorescently labeled endogenous gurken mRNA in Drosophila.* J Cell Sci, 2008. **121**(Pt 6): p. 887-94.
267. Caceres, L. and L.A. Nilson, *Translational repression of gurken mRNA in the Drosophila oocyte requires the hnRNP Squid in the nurse cells.* Dev Biol, 2009. **326**(2): p. 327-34.
268. Thio, G.L., et al., *Localization of gurken RNA in Drosophila oogenesis requires elements in the 5' and 3' regions of the transcript.* Dev Biol, 2000. **221**(2): p. 435-46.
269. Ephrussi, A., L.K. Dickinson, and R. Lehmann, *Oskar organizes the germ plasm and directs localization of the posterior determinant nanos.* Cell, 1991. **66**(1): p. 37-50.
270. Ephrussi, A. and R. Lehmann, *Induction of germ cell formation by oskar.* Nature, 1992. **358**(6385): p. 387-92.
271. Markussen, F.H., et al., *Translational control of oskar generates short OSK, the isoform that induces pole plasma assembly.* Development, 1995. **121**(11): p. 3723-32.
272. Jenny, A., et al., *A translation-independent role of oskar RNA in early Drosophila oogenesis.* Development, 2006. **133**(15): p. 2827-33.
273. Kanke, M., et al., *oskar RNA plays multiple noncoding roles to support oogenesis and maintain integrity of the germline/soma distinction.* RNA, 2015. **21**(6): p. 1096-109.
274. Zimyanin, V., N. Lowe, and D. St Johnston, *An oskar-dependent positive feedback loop maintains the polarity of the Drosophila oocyte.* Curr Biol, 2007. **17**(4): p. 353-9.
275. Vanzo, N.F. and A. Ephrussi, *Oskar anchoring restricts pole plasm formation to the posterior of the Drosophila oocyte.* Development, 2002. **129**(15): p. 3705-14.
276. Kistler, K.E., et al., *Phase transitioned nuclear Oskar promotes cell division of Drosophila primordial germ cells.* Elife, 2018. **7**.
277. Little, S.C., et al., *Independent and coordinate trafficking of single Drosophila germ plasm mRNAs.* Nat Cell Biol, 2015. **17**(5): p. 558-68.
278. Trcek, T., et al., *Drosophila germ granules are structured and contain homotypic mRNA clusters.* Nat Commun, 2015. **6**: p. 7962.
279. Styhler, S., et al., *vasa is required for GURKEN accumulation in the oocyte, and is involved in oocyte differentiation and germline cyst development.* Development, 1998. **125**(9): p. 1569-78.
280. Tomancak, P., et al., *Oocyte polarity depends on regulation of gurken by Vasa.* Development, 1998. **125**(9): p. 1723-32.
281. Carrera, P., et al., *VASA mediates translation through interaction with a Drosophila yIF2 homolog.* Mol Cell, 2000. **5**(1): p. 181-7.
282. Johnstone, O. and P. Lasko, *Interaction with eIF5B is essential for Vasa function during development.* Development, 2004. **131**(17): p. 4167-78.
283. Saunders, C. and R.S. Cohen, *The role of oocyte transcription, the 5'UTR, and translation repression and derepression in Drosophila gurken mRNA and protein localization.* Mol Cell, 1999. **3**(1): p. 43-54.

284. Delanoue, R., et al., *Drosophila Squid/hnRNP helps Dynein switch from a gurken mRNA transport motor to an ultrastructural static anchor in sponge bodies.* Dev Cell, 2007. **13**(4): p. 523-38.
285. Norvell, A., et al., *Specific isoforms of squid, a Drosophila hnRNP, perform distinct roles in Gurken localization during oogenesis.* Genes Dev, 1999. **13**(7): p. 864-76.
286. Kelley, R.L., *Initial organization of the Drosophila dorsoventral axis depends on an RNA-binding protein encoded by the squid gene.* Genes Dev, 1993. **7**(6): p. 948-60.
287. Wieschaus, E. and R. Riggleman, *Autonomous requirements for the segment polarity gene armadillo during Drosophila embryogenesis.* Cell, 1987. **49**(2): p. 177-84.
288. Filardo, P. and A. Ephrussi, *Bruno regulates gurken during Drosophila oogenesis.* Mech Dev, 2003. **120**(3): p. 289-97.
289. Goodrich, J.S., K.N. Clouse, and T. Schupbach, *Hrb27C, Sqd and Otu cooperatively regulate gurken RNA localization and mediate nurse cell chromosome dispersion in Drosophila oogenesis.* Development, 2004. **131**(9): p. 1949-58.
290. Geng, C. and P.M. Macdonald, *Imp associates with squid and Hrp48 and contributes to localized expression of gurken in the oocyte.* Mol Cell Biol, 2006. **26**(24): p. 9508-16.
291. Chang, J.S., et al., *Functioning of the Drosophila orb gene in gurken mRNA localization and translation.* Development, 2001. **128**(16): p. 3169-77.
292. Norvell, A., et al., *Squid is required for efficient posterior localization of oskar mRNA during Drosophila oogenesis.* Dev Genes Evol, 2005. **215**(7): p. 340-9.
293. Hawkins, N.C., et al., *Post-transcriptional regulation of gurken by encore is required for axis determination in Drosophila.* Development, 1997. **124**(23): p. 4801-10.
294. Clouse, K.N., S.B. Ferguson, and T. Schupbach, *Squid, Cup, and PABP55B function together to regulate gurken translation in Drosophila.* Dev Biol, 2008. **313**(2): p. 713-24.
295. Van Buskirk, C., N.C. Hawkins, and T. Schupbach, *Encore is a member of a novel family of proteins and affects multiple processes in Drosophila oogenesis.* Development, 2000. **127**(22): p. 4753-62.
296. Kim-Ha, J., et al., *Multiple RNA regulatory elements mediate distinct steps in localization of oskar mRNA.* Development, 1993. **119**(1): p. 169-78.
297. Suter, B. and R. Steward, *Requirement for phosphorylation and localization of the Bicaudal-D protein in Drosophila oocyte differentiation.* Cell, 1991. **67**(5): p. 917-26.
298. Jambor, H., et al., *A stem-loop structure directs oskar mRNA to microtubule minus ends.* RNA, 2014. **20**(4): p. 429-39.
299. Ryu, Y.H., et al., *Multiple cis-acting signals, some weak by necessity, collectively direct robust transport of oskar mRNA to the oocyte.* J Cell Sci, 2017. **130**(18): p. 3060-3071.
300. Zimyanin, V.L., et al., *In vivo imaging of oskar mRNA transport reveals the mechanism of posterior localization.* Cell, 2008. **134**(5): p. 843-53.
301. Nieuwburg, R., et al., *Localised dynactin protects growing microtubules to deliver oskar mRNA to the posterior cortex of the Drosophila oocyte.* Elife, 2017. **6**.
302. Hachet, O. and A. Ephrussi, *Drosophila Y14 shuttles to the posterior of the oocyte and is required for oskar mRNA transport.* Curr Biol, 2001. **11**(21): p. 1666-74.
303. Ghosh, S., et al., *Control of RNP motility and localization by a splicing-dependent structure in oskar mRNA.* Nat Struct Mol Biol, 2012. **19**(4): p. 441-9.
304. Newmark, P.A. and R.E. Boswell, *The mago nashi locus encodes an essential product required for germ plasm assembly in Drosophila.* Development, 1994. **120**(5): p. 1303-13.
305. Palacios, I.M., et al., *An eIF4AIII-containing complex required for mRNA localization and nonsense-mediated mRNA decay.* Nature, 2004. **427**(6976): p. 753-7.

306. van Eeden, F.J., et al., *Barentsz is essential for the posterior localization of oskar mRNA and colocalizes with it to the posterior pole.* J Cell Biol, 2001. **154**(3): p. 511-23.
307. Jambor, H., C. Brunel, and A. Ephrussi, *Dimerization of oskar 3′ UTRs promotes hitchhiking for RNA localization in the Drosophila oocyte.* RNA, 2011. **17**(12): p. 2049-57.
308. Steinhauer, J. and D. Kalderon, *The RNA-binding protein Squid is required for the establishment of anteroposterior polarity in the Drosophila oocyte.* Development, 2005. **132**(24): p. 5515-25.
309. Krauss, J., et al., *Myosin-V regulates oskar mRNA localization in the Drosophila oocyte.* Curr Biol, 2009. **19**(12): p. 1058-63.
310. Erdelyi, M., et al., *Requirement for Drosophila cytoplasmic tropomyosin in oskar mRNA localization.* Nature, 1995. **377**(6549): p. 524-7.
311. Gaspar, I., et al., *An RNA-binding atypical tropomyosin recruits kinesin-1 dynamically to oskar mRNPs.* EMBO J, 2017. **36**(3): p. 319-333.
312. Veeranan-Karmegam, R., et al., *A new isoform of Drosophila non-muscle Tropomyosin 1 interacts with Kinesin-1 and functions in oskar mRNA localization.* J Cell Sci, 2016. **129**(22): p. 4252-4264.
313. Jeske, M., et al., *The Crystal Structure of the Drosophila Germline Inducer Oskar Identifies Two Domains with Distinct Vasa Helicase- and RNA-Binding Activities.* Cell Rep, 2015. **12**(4): p. 587-98.
314. Jeske, M., C.W. Muller, and A. Ephrussi, *The LOTUS domain is a conserved DEAD-box RNA helicase regulator essential for the recruitment of Vasa to the germ plasm and nuage.* Genes Dev, 2017. **31**(9): p. 939-952.
315. Yang, N., et al., *Structure of Drosophila Oskar reveals a novel RNA binding protein.* Proc Natl Acad Sci U S A, 2015. **112**(37): p. 11541-6.
316. Morais-de-Sa, E., et al., *Oskar is targeted for degradation by the sequential action of Par-1, GSK-3, and the SCF(-)Slimb ubiquitin ligase.* Dev Cell, 2013. **26**(3): p. 303-14.
317. Igreja, C. and E. Izaurralde, *CUP promotes deadenylation and inhibits decapping of mRNA targets.* Genes Dev, 2011. **25**(18): p. 1955-67.
318. Kim-Ha, J., K. Kerr, and P.M. Macdonald, *Translational regulation of oskar mRNA by bruno, an ovarian RNA-binding protein, is essential.* Cell, 1995. **81**(3): p. 403-12.
319. Webster, P.J., et al., *Translational repressor bruno plays multiple roles in development and is widely conserved.* Genes Dev, 1997. **11**(19): p. 2510-21.
320. Reveal, B., et al., *BREs mediate both repression and activation of oskar mRNA translation and act in trans.* Dev Cell, 2010. **18**(3): p. 496-502.
321. Ryu, Y.H. and P.M. Macdonald, *RNA sequences required for the noncoding function of oskar RNA also mediate regulation of Oskar protein expression by Bicoid Stability Factor.* Dev Biol, 2015. **407**(2): p. 211-23.
322. Chekulaeva, M., M.W. Hentze, and A. Ephrussi, *Bruno acts as a dual repressor of oskar translation, promoting mRNA oligomerization and formation of silencing particles.* Cell, 2006. **124**(3): p. 521-33.
323. Lie, Y.S. and P.M. Macdonald, *Translational regulation of oskar mRNA occurs independent of the cap and poly(A) tail in Drosophila ovarian extracts.* Development, 1999. **126**(22): p. 4989-96.
324. Besse, F., et al., *Drosophila PTB promotes formation of high-order RNP particles and represses oskar translation.* Genes Dev, 2009. **23**(2): p. 195-207.
325. Macdonald, P.M., M. Kanke, and A. Kenny, *Community effects in regulation of translation.* Elife, 2016. **5**: p. e10965.
326. Nakamura, A., et al., *Me31B silences translation of oocyte-localizing RNAs through the formation of cytoplasmic RNP complex during Drosophila oogenesis.* Development, 2001. **128**(17): p. 3233-42.

327. Gunkel, N., et al., *Localization-dependent translation requires a functional interaction between the 5' and 3' ends of oskar mRNA.* Genes Dev, 1998. **12**(11): p. 1652-64.
328. Huynh, J.R., et al., *The Drosophila hnRNPA/B homolog, Hrp48, is specifically required for a distinct step in osk mRNA localization.* Dev Cell, 2004. **6**(5): p. 625-35.
329. Yano, T., et al., *Hrp48, a Drosophila hnRNPA/B homolog, binds and regulates translation of oskar mRNA.* Dev Cell, 2004. **6**(5): p. 637-48.
330. Munro, T.P., et al., *A repeated IMP-binding motif controls oskar mRNA translation and anchoring independently of Drosophila melanogaster IMP.* J Cell Biol, 2006. **172**(4): p. 577-88.
331. Micklem, D.R., et al., *Distinct roles of two conserved Staufen domains in oskar mRNA localization and translation.* EMBO J, 2000. **19**(6): p. 1366-77.
332. Ramos, A., et al., *RNA recognition by a Staufen double-stranded RNA-binding domain.* EMBO J, 2000. **19**(5): p. 997-1009.
333. Ferrandon, D., et al., *Staufen protein associates with the 3'UTR of bicoid mRNA to form particles that move in a microtubule-dependent manner.* Cell, 1994. **79**(7): p. 1221-32.
334. Chang, J.S., L. Tan, and P. Schedl, *The Drosophila CPEB homolog, orb, is required for oskar protein expression in oocytes.* Dev Biol, 1999. **215**(1): p. 91-106.
335. Castagnetti, S. and A. Ephrussi, *Orb and a long poly(A) tail are required for efficient oskar translation at the posterior pole of the Drosophila oocyte.* Development, 2003. **130**(5): p. 835-43.
336. Weil, T.T., *mRNA localization in the Drosophila germline.* RNA Biology, 2014. **11**(8): p. 1010-1018.
337. Becalska, A.N. and E.R. Gavis, *Lighting up mRNA localization in Drosophila oogenesis.* Development, 2009. **136**(15): p. 2493-503.
338. Wippich, F. and A. Ephrussi, *Transcript specific mRNP capture from Drosophila egg-chambers for proteomic analysis.* Methods, 2019.
339. Mukherjee, N., et al., *Deciphering human ribonucleoprotein regulatory networks.* Nucleic Acids Res., 2019. **47**(2): p. 570–581.
340. Lee, H.K., et al., *Ubiquitylation and degradation of adenomatous polyposis coli by MKRN1 enhances Wnt/beta-catenin signaling.* Oncogene, 2018. **37**(31): p. 4273-4286.
341. Farrell, J.A. and P.H. O'Farrell, *From egg to gastrula: how the cell cycle is remodeled during the Drosophila mid-blastula transition.* Annu Rev Genet, 2014. **48**: p. 269-94.
342. Hamm, D.C. and M.M. Harrison, *Regulatory principles governing the maternal-to-zygotic transition: insights from Drosophila melanogaster.* Open Biol, 2018. **8**(12): p. 180183.
343. Molla, K.A. and Y. Yang, *CRISPR/Cas-Mediated Base Editing: Technical Considerations and Practical Applications.* Trends Biotechnol, 2019. **37**(10): p. 1121-1142.
344. Cong, L., et al., *Multiplex genome engineering using CRISPR/Cas systems.* Science, 2013. **339**(6121): p. 819-23.
345. Mali, P., et al., *RNA-guided human genome engineering via Cas9.* Science, 2013. **339**(6121): p. 823-6.
346. Dold, A., et al., *Makorin 1 controls embryonic patterning by alleviating Bruno1-mediated repression of oskar translation.* bioRxiv, 2019: p. 501643.
347. Brand, A.H. and N. Perrimon, *Targeted gene expression as a means of altering cell fates and generating dominant phenotypes.* Development, 1993. **118**(2): p. 401-15.
348. Fischer, J.A., et al., *GAL4 activates transcription in Drosophila.* Nature, 1988. **332**(6167): p. 853-6.
349. Tracey, W.D., Jr., et al., *Quantitative analysis of gene function in the Drosophila embryo.* Genetics, 2000. **154**(1): p. 273-84.
350. Rorth, P., *Gal4 in the Drosophila female germline.* Mech Dev, 1998. **78**(1-2): p. 113-8.

351. Lee, J., et al., *LSM12 and ME31B/DDX6 Define Distinct Modes of Posttranscriptional Regulation by ATAXIN-2 Protein Complex in Drosophila Circadian Pacemaker Neurons.* Mol Cell, 2017. **66**(1): p. 129-140 e7.
352. Patel, G.P. and J. Bag, *IMP1 interacts with poly(A)-binding protein (PABP) and the autoregulatory translational control element of PABP-mRNA through the KH III-IV domain.* FEBS J, 2006. **273**(24): p. 5678-90.
353. Wang, M., et al., *ME31B globally represses maternal mRNAs by two distinct mechanisms during the Drosophila maternal-to-zygotic transition.* Elife, 2017. **6**.
354. Ong, S.E. and M. Mann, *A practical recipe for stable isotope labeling by amino acids in cell culture (SILAC).* Nat Protoc, 2006. **1**(6): p. 2650-60.
355. Funakoshi, M., et al., *Overexpression of Larp4B downregulates dMyc and reduces cell and organ sizes in Drosophila.* Biochem Biophys Res Commun, 2018. **497**(2): p. 762-768.
356. Huppertz, I., et al., *iCLIP: protein-RNA interactions at nucleotide resolution.* Methods, 2014. **65**(3): p. 274-87.
357. Konig, J., et al., *iCLIP reveals the function of hnRNP particles in splicing at individual nucleotide resolution.* Nat Struct Mol Biol, 2010. **17**(7): p. 909-15.
358. Kim, G., et al., *Region-specific activation of oskar mRNA translation by inhibition of Bruno-mediated repression.* PLoS Genet, 2015. **11**(2): p. e1004992.
359. Ryan, M.D., A.M.Q. King, and G.P. Thomas, *Cleavage of foot-and-mouth disease virus polyprotein is mediated by residues located within a 19 amino acid sequence.* Journal of General Virology, 1991. **72**(11): p. 2727-2732.
360. Kim, J.H., et al., *High cleavage efficiency of a 2A peptide derived from porcine teschovirus-1 in human cell lines, zebrafish and mice.* PLoS One, 2011. **6**(4): p. e18556.
361. Shao, S., et al., *Decoding Mammalian Ribosome-mRNA States by Translational GTPase Complexes.* Cell, 2016. **167**(5): p. 1229-1240 e15.
362. Minguez, P., et al., *PTMcode: a database of known and predicted functional associations between post-translational modifications in proteins.* Nucleic Acids Res, 2013. **41**(Database issue): p. D306-11.
363. Yang, R., et al., *La-related protein 4 binds poly(A), interacts with the poly(A)-binding protein MLLE domain via a variant PAM2w motif, and can promote mRNA stability.* Mol Cell Biol, 2011. **31**(3): p. 542-56.
364. Hansen, H.T., et al., *Drosophila Imp iCLIP identifies an RNA assemblage coordinating F-actin formation.* Genome Biol, 2015. **16**: p. 123.
365. Boylan, K.L., et al., *Motility screen identifies Drosophila IGF-II mRNA-binding protein--zipcode-binding protein acting in oogenesis and synaptogenesis.* PLoS Genet, 2008. **4**(2): p. e36.
366. Patel, G.P., S. Ma, and J. Bag, *The autoregulatory translational control element of poly(A)-binding protein mRNA forms a heteromeric ribonucleoprotein complex.* Nucleic Acids Res, 2005. **33**(22): p. 7074-89.
367. Chao, J.A., et al., *ZBP1 recognition of beta-actin zipcode induces RNA looping.* Genes Dev, 2010. **24**(2): p. 148-58.
368. Gotze, M., et al., *Translational repression of the Drosophila nanos mRNA involves the RNA helicase Belle and RNA coating by Me31B and Trailer hitch.* RNA, 2017. **23**(10): p. 1552-1568.
369. Flora, P., et al., *Sequential Regulation of Maternal mRNAs through a Conserved cis-Acting Element in Their 3' UTRs.* Cell Rep, 2018. **25**(13): p. 3828-3843 e9.
370. Munoz-Escobar, J., et al., *The MLLE domain of the ubiquitin ligase UBR5 binds to its catalytic domain to regulate substrate binding.* J Biol Chem, 2015. **290**(37): p. 22841-50.

371. Kessler, S.H. and A.B. Sachs, *RNA recognition motif 2 of yeast Pab1p is required for its functional interaction with eukaryotic translation initiation factor 4G.* Mol Cell Biol, 1998. **18**(1): p. 51-7.
372. Broyer, R.M., E. Monfort, and J.E. Wilhelm, *Cup regulates oskar mRNA stability during oogenesis.* Dev Biol, 2017. **421**(1): p. 77-85.
373. Mancebo, R., et al., *BSF binds specifically to the bicoid mRNA 3' untranslated region and contributes to stabilization of bicoid mRNA.* Mol Cell Biol, 2001. **21**(10): p. 3462-71.
374. Huang, H., et al., *Recognition of RNA N(6)-methyladenosine by IGF2BP proteins enhances mRNA stability and translation.* Nat Cell Biol, 2018. **20**(3): p. 285-295.
375. Samuels, T.J., et al., *Imp/IGF2BP levels modulate individual neural stem cell growth and division through myc mRNA stability.* bioRxiv, 2019: p. 754382.
376. Graindorge, A., et al., *Identification of CUG-BP1/EDEN-BP target mRNAs in Xenopus tropicalis.* Nucleic Acids Res, 2008. **36**(6): p. 1861-70.
377. Wang, X., et al., *N(6)-methyladenosine Modulates Messenger RNA Translation Efficiency.* Cell, 2015. **161**(6): p. 1388-99.
378. Zhao, B.S., et al., *m(6)A-dependent maternal mRNA clearance facilitates zebrafish maternal-to-zygotic transition.* Nature, 2017. **542**(7642): p. 475-478.
379. Ivanova, I., et al., *The RNA m(6)A Reader YTHDF2 Is Essential for the Post-transcriptional Regulation of the Maternal Transcriptome and Oocyte Competence.* Mol Cell, 2017. **67**(6): p. 1059-1067 e4.
380. Edupuganti, R.R., et al., *N(6)-methyladenosine (m(6)A) recruits and repels proteins to regulate mRNA homeostasis.* Nat Struct Mol Biol, 2017. **24**(10): p. 870-878.
381. Lence, T., et al., *m(6)A modulates neuronal functions and sex determination in Drosophila.* Nature, 2016. **540**(7632): p. 242-247.
382. Greenblatt, E.J. and A.C. Spradling, *Fragile X mental retardation 1 gene enhances the translation of large autism-related proteins.* Science, 2018. **361**(6403): p. 709-712.
383. Wilhelm, J.E., et al., *Isolation of a ribonucleoprotein complex involved in mRNA localization in Drosophila oocytes.* J Cell Biol, 2000. **148**(3): p. 427-40.
384. Choudhury, N.R., et al., *RNA-binding activity of TRIM25 is mediated by its PRY/SPRY domain and is required for ubiquitination.* BMC Biol, 2017. **15**(1): p. 105.
385. Deshaies, R.J. and C.A. Joazeiro, *RING domain E3 ubiquitin ligases.* Annu Rev Biochem, 2009. **78**: p. 399-434.
386. Gorgoni, B. and N.K. Gray, *The roles of cytoplasmic poly(A)-binding proteins in regulating gene expression: a developmental perspective.* Brief Funct Genomic Proteomic, 2004. **3**(2): p. 125-41.
387. Kondo, S. and R. Ueda, *Highly improved gene targeting by germline-specific Cas9 expression in Drosophila.* Genetics, 2013. **195**(3): p. 715-21.
388. Huynh, C.Q. and H. Zieler, *Construction of modular and versatile plasmid vectors for the high-level expression of single or multiple genes in insects and insect cell lines.* J Mol Biol, 1999. **288**(1): p. 13-20.
389. Zerbino, D.R., et al., *Ensembl 2018.* Nucleic Acids Res, 2018. **46**(D1): p. D754-D761.
390. Dobin, A., et al., *STAR: ultrafast universal RNA-seq aligner.* Bioinformatics, 2013. **29**(1): p. 15-21.
391. Liao, Y., G.K. Smyth, and W. Shi, *featureCounts: an efficient general purpose program for assigning sequence reads to genomic features.* Bioinformatics, 2014. **30**(7): p. 923-30.
392. Ramirez, F., et al., *deepTools2: a next generation web server for deep-sequencing data analysis.* Nucleic Acids Res, 2016. **44**(W1): p. W160-5.
393. Love, M.I., W. Huber, and S. Anders, *Moderated estimation of fold change and dispersion for RNA-seq data with DESeq2.* Genome Biol, 2014. **15**(12): p. 550.

394. Huber, W., et al., *Orchestrating high-throughput genomic analysis with Bioconductor.* Nat Methods, 2015. **12**(2): p. 115-21.
395. Yu, G., et al., *clusterProfiler: an R package for comparing biological themes among gene clusters.* OMICS, 2012. **16**(5): p. 284-7.
396. Yu, G. and Q.Y. He, *ReactomePA: an R/Bioconductor package for reactome pathway analysis and visualization.* Mol Biosyst, 2016. **12**(2): p. 477-9.
397. Ritchie, M.E., et al., *limma powers differential expression analyses for RNA-sequencing and microarray studies.* Nucleic Acids Res, 2015. **43**(7): p. e47.
398. Wickham, H., *Toolbox*, in *ggplot2: Elegant Graphics for Data Analysis*. 2016, Springer International Publishing: Cham. p. 33-74.
399. Dodt, M., et al., *FLEXBAR-Flexible Barcode and Adapter Processing for Next-Generation Sequencing Platforms.* Biology (Basel), 2012. **1**(3): p. 895-905.
400. Aken, B.L., et al., *Ensembl 2017.* Nucleic Acids Res, 2017. **45**(D1): p. D635-D642.
401. Li, H., et al., *The Sequence Alignment/Map format and SAMtools.* Bioinformatics, 2009. **25**(16): p. 2078-9.
402. Quinlan, A.R. and I.M. Hall, *BEDTools: a flexible suite of utilities for comparing genomic features.* Bioinformatics, 2010. **26**(6): p. 841-2.
403. Kent, W.J., et al., *BigWig and BigBed: enabling browsing of large distributed datasets.* Bioinformatics, 2010. **26**(17): p. 2204-7.
404. Heidelberger, J.B., et al., *Proteomic profiling of VCP substrates links VCP to K6-linked ubiquitylation and c-Myc function.* EMBO Rep, 2018. **19**(4).

ACKNOWLEDGMENTS

Aus Datenschutzgründen entfernt.

CURRICULUM VITAE

Aus Datenschutzgründen entfernt.